ACID GAS INJECTION AND CARBON DIOXIDE SEQUESTRATION

John J. Carroll

WILEY

Scrivener

This Page Intentionally Left Blank

Acid Gas Injection and Carbon Dioxide Sequestration

Scrivener Publishing
3 Winter Street, Suite 3
Salem, MA 01970

Acid Gas Injection and Carbon Dioxide Sequestration

John J. Carroll
Gas Liquids Engineering, Ltd.

Scrivener

WILEY

Co-published by John Wiley & Sons, Inc. Hoboken, New Jersey, and Scrivener Publishing LLC, Salem, Massachusetts.
Published simultaneously in Canada.

Cover design by Russell Richardson.

Library of Congress Cataloging-in-Publication Data:

ISBN 978-0-470-62593-4

Printed in the United States of America

10 9 8 7 6 5 4 3 2 1

This book is dedicated to Wu Ying, my loving wife.
She is the love of my life and a constant source of inspiration.

This Page Intentionally Left Blank

Contents

Preface

Acid gas injection (AGI) has become a mature technology for disposing of acid gas, a mixture of CO_2 and H_2S. AGI is particularly useful for small producers who have few options for dealing with the H_2S. Larger producers, however, have seen the value in AGI as well and the industry has discovered that AGI is an environmentally friendly solution to a difficult problem.

This book presents the art, the science, and the engineering aspects of AGI, and to present it in a manner that is accessible to the average engineer. It begins with a discussion of the basic data and models for designing an injection scheme. In particular it is important that those working in the field have a good understanding of the phase equilibria involved. Most of the operational problems are related to the formation of an unwanted phase. Admittedly, some of these concepts are a little complicated, and it is a challenge to present them in a form that is comprehensible to a wide audience.

Next the engineering aspects are presented. These include the design of the compressor and pipeline and in particular what makes them different from standard designs. Finally, some of the subsurface aspects are reviewed. Admittedly, the focus of this book is the surface aspects of AGI, but the subsurface aspects cannot be overlooked, even by the process engineer.

Hopefully, those involved in the emerging field of CO_2 sequestration will note the similarities and take the information presented here and apply it to their projects. Lessons learned in AGI can be exported to the technology of carbon sequestration.

This Page Intentionally Left Blank

Acknowledgements

There are many people to thank when one writes a book. The first, and certainly the most important, is my employer Gas Liquids Engineering, and in particular the company principals Doug MacKenzie and Jim Maddocks but also my colleague Peter Griffin. They provided me the opportunity to present the course and much of the time to write the manuscript.

In addition, through my job at Gas Liquids Engineering, I have had the chance to work on many acid gas injection projects throughout the world. Some of these were just studies that have not yet come to fruition, but others have been operating for many years. Much of what is presented in this book has come from lessons learned from working on those projects.

Alan Mather has been my long time friend and mentor. He is an important source of information, often from obscure sources. Plus his lab is the source of much of the useful information in this field. The research studies of his group are vital to the advancement of many fields in the gas processing.

This book is based on a course on acid gas injection that I have presented throughout the world. Feedback from the attendees over the years has greatly improved the quality and content of both the course and this book. The acid gas injection course has also been presented in Chinese and Polish. I have received excellent feedback from Eugene Grynia, my Polish translator, and Ying Wu, my Chinese translator.

This Page Intentionally Left Blank

1

Introduction

Although many gases are natural (air, for example), the term "natural gas" refers to the hydrocarbon-rich gas that is found in underground formations. These gases are organic in origin, and thus along with oil, coal, and peat are called "fossil fuels." Time and the effects of pressure and temperature have converted the originally living matter into hydrocarbon gases that we call natural gas.

Natural gas is largely made up of methane but also contains other light hydrocarbons, typically ethane through hexane. In addition, natural gas contains inorganic contaminants – notably hydrogen sulfide and carbon dioxide, but also nitrogen and trace amounts of helium and hydrogen.

The formations and the gas contained therein are almost always associated with water, and thus the gas is usually water-saturated. The water concentration depends on the temperature and pressure of the reservoir and to some extent on the composition of the gas.

Natural gas that contains hydrogen sulfide is referred to as "sour." Gas that does not contain hydrogen sulfide, or at least contains hydrogen sulfide but in very small amounts, is called "sweet."

Contaminants in natural gas, like hydrogen sulfide and carbon dioxide, are usually removed from the gas in order to produce a

sales gas. Hydrogen sulfide and carbon dioxide are called "acid gases" because when dissolved in water they form weak acids.

Hydrogen sulfide must be removed because of its high toxicity and strong, offensive odor. Carbon dioxide is removed because it has no heating value. Another reason these gases must be removed is because they are corrosive. In Alberta, sales gas must typically contain less than 16 ppm[1] hydrogen sulfide and less than 2% carbon dioxide. However, different jurisdictions have different standards.

Once removed from the raw gas, the question arises as to what should be done with the acid gas. If there is a large amount of acid gas, it may be economical to build a Claus-type sulfur plant to convert the hydrogen sulfide into the more benign elemental sulfur. Once the H_2S has been converted to sulfur, the leftover carbon dioxide is emitted to the atmosphere. Claus plants can be quite efficient, but even so, they also emit significant amounts of sulfur compounds. For example, a Claus plant processing 10 MMSCFD of H_2S and converting 99.9% of the H_2S into elemental sulfur (which is only possible with the addition of a tail gas clean up unit) emits the equivalent of 0.01 MMSCFD or approximately 0.4 ton/day of sulfur into the atmosphere. Note that there is more discussion of standard volumes and sulfur equivalents later in this chapter.

For small acid gas streams, Claus-type sulfur plants are not feasible. In the past, it was permissible to flare small amounts of acid gas. However, with growing environmental concerns, such practices are being legislated out of existence.

In the natural gas business, acid gas injection has quickly become the method of choice for the disposal of such gases. Larger producers are also considering injection because of the volatility of the sulfur markets.

1.1 Acid Gas

As noted earlier, hydrogen sulfide and carbon dioxide are called acid gases. When dissolved in water they react to form weak acids.

The formation of acid in water is another reason that acid gases are often removed from natural gas. The acidic solutions are very corrosive and require special materials to handle them.

---

1. For H_2S 16 ppm is equal to 1 grain per 100 SCF, which is an older unit for expressing H_2S content of a gas.

On the other hand, the acidity of the acid gases is used to our advantage in processes for their removal.

1.1.1 Hydrogen Sulfide

Hydrogen sulfide is a weak, diprotic acid (i.e., it undergoes two acid reactions). The ionization reactions are as follows:

$$H_2S_{(aq)} \leftrightarrow HS^-_{(aq)} + H^+_{(aq)} \tag{1.1}$$

$$HS^-_{(aq)} \leftrightarrow S^{2-}_{(aq)} + H^+_{(aq)} \tag{1.2}$$

The subscript (aq) indicates that the reaction takes place in the aqueous (water-rich) phase.

It is the H^+ ion that makes the solution acidic. Hydrogen sulfide is diprotic because it has two reactions that both form the hydrogen ion. Furthermore, when hydrogen sulfide is dissolved in water it exists as three species – the molecular form (H_2S) and the two ionic forms: the bisulfide ion (HS^-) and the sulfide ion (S^{2-}).

The measure of how far these reactions proceed is the equilibrium ratios. For our purposes, these ratios are as follows:

$$K_{1,H_2S} = \frac{\left[H^+_{(aq)}\right]\left[HS^-_{(aq)}\right]}{\left[H_2S_{(aq)}\right]} = 1.0\times10^{-7} \text{ at } 25°C$$

$$K_{2,H_2S} = \frac{\left[H^+_{(aq)}\right]\left[S^{-2}_{(aq)}\right]}{\left[HS^-_{(aq)}\right]} = 6\times10^{-16} \text{ at } 25°C$$

where the square brackets indicate the concentration of each species. These relations are valid only if the concentration is small. The fact that these ratios are so small indicates that these reactions do not proceed very far, and thus, in an otherwise neutral solution, most of the hydrogen sulfide is found in the solution in the molecular form. The concentration of the ionic species is greatly affected by the presence of an alkaline and to some extend the presence of an acid. And since hydrogen sulfide is an acid, the effect of an alkaline is very significant.

At 25°C and 101.325 kPa (1 atm) the distribution of the various species in the aqueous solution can be calculated from the solubility and the equilibrium ratios. The distribution is:

$[H_2S] = 0.1$ mol/kg
$[HS^-] = 1.0 \times 10^{-4}$ mol/kg
$[S^{-2}] = 6.4 \times 10^{-16}$ mol/kg
$[H^+] = 1.0 \times 10^{-4}$ mol/kg
$pH^2 = 4.0$

The units of concentration used here are molality or moles of species per kg of solvent (water).

1.1.2 Carbon Dioxide

Carbon dioxide is also a weak diprotic acid, but the reactions for CO_2 are slightly different. The first reaction is a hydrolysis (a reaction with water):

$$CO_{2(aq)} + H_2O \leftrightarrow H^+_{(aq)} + HCO^-_{3(aq)} \tag{1.3}$$

The second is a simple acid formation reaction:

$$HCO^-_{3(aq)} \leftrightarrow H^+_{(aq)} + CO^{2-}_{3(aq)} \tag{1.4}$$

Again, these reactions take place in the aqueous phase. The carbon dioxide exists in three species in the aqueous phase – the molecular form CO_2, and two ionic forms: the bicarbonate ion, also call the hydrogen carbonate ion (HCO_3^-), and the carbonate ion (CO_3^{2-}).

The equilibrium ratios for these reactions are:

$$K_{1,CO_2} = \frac{\left[H^+_{(aq)}\right]\left[HCO^-_{3\,(aq)}\right]}{\left[CO_{2\,(aq)}\right]} = 4.5 \times 10^{-7} \text{ at } 25°C$$

$$K_{2,CO_2} = \frac{\left[H^+_{(aq)}\right]\left[CO^{-2}_{3\,(aq)}\right]}{\left[HCO^-_{3\,(aq)}\right]} = 4.7 \times 10^{-11} \text{ at } 25°C$$

2. $pH = -\log[H^+]$ and usually the concentration, $[H^+]$ is expressed in moles of solute per kg of water (molality), but for aqueous solutions at low concentration mol/kg of water is approximately equal to moles per litre of solution (molarity).

Again, the square brackets are used to indicate the concentration of the various species. As with hydrogen sulfide, these ratios are very small, and thus in an otherwise neutral solution most of the carbon dioxide exist in the molecular form. At 25°C and 101.325 kPa (1 atm) the distribution of the various species in the aqueous solution is:

$[CO_2]$ = 0.033 mol/kg
$[HCO_3^-]$ = 1.2×10^{-4} mol/kg
$[CO_3^{-2}]$ = 4.7×10^{-11} mol/kg
$[H^+]$ = 1.2×10^{-4} mol/kg
pH = 3.9

The pH of the CO_2 solution is slightly less than that for H_2S even though the solubility of CO_2 is significantly less. This is because more of the carbon dioxide ionizes, which in turn produces more of the H^+ ion – the acid ion.

1.2 Anthropogenic CO_2

The disposal of man-made carbon dioxide into the atmosphere is becoming an undesirable practice. Whether or not one believes that CO_2 is harmful to the environment has almost become a moot point. The general consensus is that CO_2 is contributing to global climate change. Furthermore, it is clear that legislators all around the world believe that it is a problem. In some countries there is a carbon tax applied to such disposal. Engineers will increasingly be faced with the problem of disposing of CO_2.

Some of the technologies for dealing with this CO_2 are the same as acid gas injection, and thus they will be discussed here as well.

1.3 Flue Gas

Flue gas, as used here, is the byproduct of the combustion of fuels. Typically the fuels of concern here are natural gas, oil (and distillates from oil such as gasoline), coal, wood, etc.

Combustion is a process involving oxygen. However, air is composed of only 21% oxygen, which is required for combustion, and 79% inerts, mostly nitrogen. Thus for every mole of oxygen consumed in the combustion of a paraffin hydrocarbon, more than 9.5 moles of air must be supplied.

The combustion of a carbon-based fuel (coal, natural gas, or oil) produces a gaseous byproduct called flue gas. First consider the combustion of a paraffin hydrocarbon.

$$2\,C_nH_{2n+2} + (3n + 1)\,O_2 \rightarrow 2n\,CO_2 + 2(n+1)\,H_2O \qquad (1.5)$$

For example, the reaction for the combustion of methane is:

$$CH_4 + 2\,O_2 \rightarrow CO_2 + 2\,H_2O \qquad (1.6)$$

So the combustion of a hydrocarbon releases carbon dioxide and water. In addition, the combustion of one mole of methane consumes 2 moles of oxygen.

Table 1.1 summarizes the amount of oxygen and air required for the combustion of several light paraffin hydrocarbons. It is interesting to note that as the hydrocarbon becomes larger, the amount of carbon dioxide produced by the combustion process also increases.

Table 1.1 Air requirements for the combustion of one mole of various paraffin fuels.

Fuel	Moles of Oxygen Consumed	Moles of Air Required (0% Excess)	Moles of Air Required (15% Excess)	Moles of CO_2 Produced
Methane	2.0	9.52	10.95	2.00
Ethane	3.5	16.67	19.17	4.00
Propane	5.0	23.81	23.81	6.00
i-Butane	6.5	30.95	35.60	8.00
n-Butane	6.5	30.95	35.60	8.00
i-Pentane	8.0	38.10	43.81	10.00
n-Pentane	8.0	38.10	43.81	10.00

Table 1.2 Approximate flue gas composition from the combustion of various paraffin hydrocarbon fuels (water-free basis).

	0% Excess Air		15% Excess Air		
Fuel	**Nitrogen**	**CO_2**	**Nitrogen**	**CO_2**	**Oxygen**
Methane	79.00	21.00	79.00	18.26	2.74
Ethane	76.70	23.30	76.99	20.34	2.67
Propane	75.82	24.18	76.22	21.14	2.64
i-Butane	75.35	24.65	75.81	21.57	2.63
n-Butane	75.35	24.65	75.81	21.57	2.63
i-Pentane	75.06	24.94	75.55	21.83	2.62
n-Pentane	75.06	24.94	75.55	21.83	2.62

From table 1.2 we can see that the flues gas is more than three quarters nitrogen and only about 20% carbon dioxide. In addition, when 15% excess air is used in the combustion process, then the flue gas also includes slightly more than 2.5% oxygen. As noted below, the flue gas will also include small amounts of oxides of nitrogen and oxides of sulfur.

It is probably undesirable to attempt to inject the entire flue gas stream. As we shall see, the cost of a disposal stream is directly related to the volume of gas injected.

In some cases, there is insufficient oxygen and one gets incomplete combustion to form carbon monoxide:

$$C_nH_{2n+2} + (3n + 1)\, O_2 \rightarrow n\, CO + (n+1)\, H_2O \qquad (1.7)$$

Carbon monoxide is a very dangerous chemical. It is gaseous at room conditions, and it is colorless, odorless, and highly toxic. It is often referred to as the "silent killer."

1.3.1 Sulfur Oxides

Most of the fuels we use contain some sulfur compounds. Even "sweet" natural gas has some sulfur in it. These sulfur compounds burn to form the so-called sulfur oxides – SO_x : sulfur dioxide (SO_2) and sulfur trioxide (SO_3). At room conditions, pure SO_2 is a gas but pure

SO_3 is a liquid (boiling pt 45°C). Like carbon dioxide and hydrogen sulfide, these compounds form acids when dissolved in water.

More properties of the sulfur oxides are provided in the appendix.

1.3.2 Nitrogen Oxides

There are two sources of nitrogen in the combustion process. Some fuels, notably coal and heavier oil, contain nitrogen compounds. When these fuels are burned they release oxides of nitrogen. The other source of nitrogen is the high temperature reaction of atmospheric oxygen and nitrogen.

More properties of the oxides of nitrogen are given in the appendix.

1.4 Standard Volumes

In the petroleum business it is common to report flow rates in standard volumes per unit time.

1.4.1 Gas Volumes

The common units for the flow rate of a gas stream are MMSCFD, Sm^3/d or Nm^3/d. These are equivalent to the following number of moles of gas:

1 MMSCF = 2635 lb-mol $= 1.195 \times 10^6$ mol
10^3 Sm^3 = 42 210 mol
10^3 Nm^3 = 40 874 mol[3]

The use of the prefix symbol M is a cause of much confusion in the natural gas business. In standard *SI Units*, M means mega and

3. The S indicates *standard conditions*, as used in the petroleum industry, which are 15.56°C (60°F) and 101.325 kPa (14.696 psia, 1 atm), whereas N is *normal conditions* 20°C and 101.325 kPa. In chemistry it is common to refer to *Standard Temperature and Pressure* (*STP*), which is 0°C and 1 atm, but this is not the standard used in the petroleum business.

The following are the conversion factors from standard volumes to moles:

379.5 std. ft^3 = 1 lbmol
0.023 690 Sm^3 = 1 mol
0.024 465 Nm^3 = 1 mol

has the multiplier 10^6. Therefore, in *SI Units*, 1 MJ is one megajoule or one million Joules. In American Engineering Units, the M is taken from Roman numerals, where M means one thousand. Thus 1 MSCF is one thousand standard cubic feet and not one million standard cubic feet. To indicate one million, two M's are used (1,000 × 1,000 = 1,000,000), so one million standard cubic feet is denoted 1 MMSCF. In spite of the confusion, this notation will be used in this work.

1.4.2 Liquid Volumes

In the oil business, a barrel is a volume exactly 42 USgal, which is equivalent to 5.61458 ft^3 or 158.99 L. The density of a liquid is affected by the temperature, not as significantly as a gas, but it changes nonetheless. Therefore, a standard barrel is the volume occupied at 60°F (15.56°C).

By definition (GPA, 1996) we have:

1 bbl of H_2S = 280.6 ib = 127.3 kg
1 bbl of CO_2 = 286.4 lb = 129.9 kg

So one standard barrel (usually referred to as a barrel) of liquefied acid gas has a mass of about 280 lb or 127 kg. It will weigh slightly less due to the presence of light hydrocarbon in the mixture. The conversion from standard barrels to standard meters is 1 bbl = 0.158 987 Sm^3 or 6.2898 bbl = 1 Sm^3.

Furthermore, as was given earlier, 1 MMSCF is 1.195×10^6 mol, so 1 MMSCFD of compressed H_2S is equal to 40 728 kg/d, which equals 320 bpd. Similarly for CO_2 1 MMSFD is 405 bpd. Although 1 barrel of H_2S has approximately the same mass as 1 bbl of CO_2, there is a significant difference when converting from standard cubic feet. This is because the molecular mass of CO_2 is significantly larger than that of H_2S. So as an approximation, 1 MMSCFD of acid gas is equal to approximately 350 bbl of liquefied acid gas.

1.5 Sulfur Equivalent

It is common to express the sulfur content of a stream in terms of sulfur equivalent. This assumes that all of the hydrogen

sulfide in a gas stream is converted to elemental sulfur via the reaction:

$$H_2S \rightarrow H_2 + S \tag{1.8}$$

According to this reaction, 1 mole of hydrogen sulfide is converted to one mole of S.

First you must determine the number of moles of hydrogen sulfide in the gas stream, as discussed earlier. Therefore to obtain the molar flow rate of H_2S in the gas stream, multiply the flow rate by the molar equivalent given above and then multiply by the mole fraction H_2S in the stream.

$$\dot{n}_{H_2S} = F\,Q\,y_{H_2S} \tag{1.9}$$

where: $\dot{n}_{H_2S}$ – molar flow rate of H_2S in mol/day
Q – flow rate at standard or normal conditions
F – the factor given earlier to convert the standard flow rate into a molar flow rate
y_{H_2S} – mole fraction H_2S in the gas

From the chemical reaction, one mole of H_2S produces one mole of S. Therefore:

$$\dot{n}_S = F\,Q\,y_{H_2S} \tag{1.10}$$

where: $\dot{n}_s$ – molar flow rate of S in mol/day

Finally, use the molar mass of sulfur, 32.066 g/mol, to convert to a molar flow rate in g/day. This is converted to tonne/day using the conversion factor 10^6 g = 1 t.

$$\dot{m}_S = 32.066 \times 10^{-6}\,F\,Q\,y_{H_2S} \tag{1.11}$$

where: $\dot{m}_s$ – mass flow rate of sulfur in t/day

The more common form of sulfur is actually S_8. Therefore the chemically more correct version of the reaction is:

$$8\,H_2S \rightarrow 8\,H_2 + S_8 \tag{1.12}$$

However, when we express the flow rate on a mass basis it is independent of the form of the elemental sulfur. Other species of

elemental sulfur also exist, but if the sulfur rate is expressed on a mass basis, it does not matter which species you assume for the elemental sulfur.

Examples

1.1 An acid gas stream of 1 MMCSFD is 75% H_2S. What is the sulfur equivalent for this stream?

Answer: Using equation (1.11) yields:

$$\begin{aligned}\dot{m}_S &= 32.066\times10^{-6}\ F\,Q\,y_{H2S}\\ &= 32.066\times10^{-6}(1.195\times10^{6})(1)(0.75)\\ &= 28.7\ \text{tonne/day}\end{aligned}$$

This is equivalent to 31.6 ton/day[4].

1.2 An acid gas stream of 20×10^3 Sm^3/day is 5% H_2S. What is the sulfur equivalent for this stream?

Answer: Again using equation (1.11) yields:

$$\begin{aligned}\dot{m}_S &= 32.066\times10^{-6}\ F\,Q\,y_{H2S}\\ &= 32.066\times10^{-6}(42210)(20)(0.05)\\ &= 1.35\ \text{tonne/day}\end{aligned}$$

1.6 Sweetening Natural Gas

Although many processes are available to sweeten natural gas – that is to remove the acid gases – those based on alkanolamines are the most common.

Alkanolamines are ammonia-like organic compounds. When dissolved in water they form weak bases. The bases react with the acids formed when H_2S and CO_2 dissolve in water. This acid-base reaction greatly enhances the solubility of the acid gases. Because the alkanolamines are weak bases, the process can be reversed. When the solutions are heated, the acid gases are liberated and the solvent regenerated.

---

4. By definition 1 tonne = 1000 kg
   and 1 ton = 2000 lb
   therefore: 1 tonne = 1.102 ton

The process for absorbing acid gas takes place in two stages: (1) absorption and (2) regeneration. The absorption takes place in a column where the sour gas is contacted with the lean solvent. The rich solvent is sent to a second column where the solvent is regenerated. Heat is applied to the system via a reboiler and the overheads are condensed, typically in an aerial cooler. The solvent regeneration is done not only at higher temperature, but also at lower pressure. Figure 1.1 is a schematic of the process.

Other processes are available for sweetening natural gas, but the alkanolamine systems are by far the most common. More discussion about processes for sweetening natural gas can be found in Kohl and Nielsen (1997).

1.6.1 Combustion Process Gas

In the carbon capture world there are two approaches to capturing the carbon dioxide: 1. post-combustion and 2. pre-combustion.The post-combustion approach is to take the CO_2 from the combustion process, purify it, and then inject it. In the pre-combustion approach, the carbon is removed from the fuel before combustion. These two approaches are discussed in the following sections.

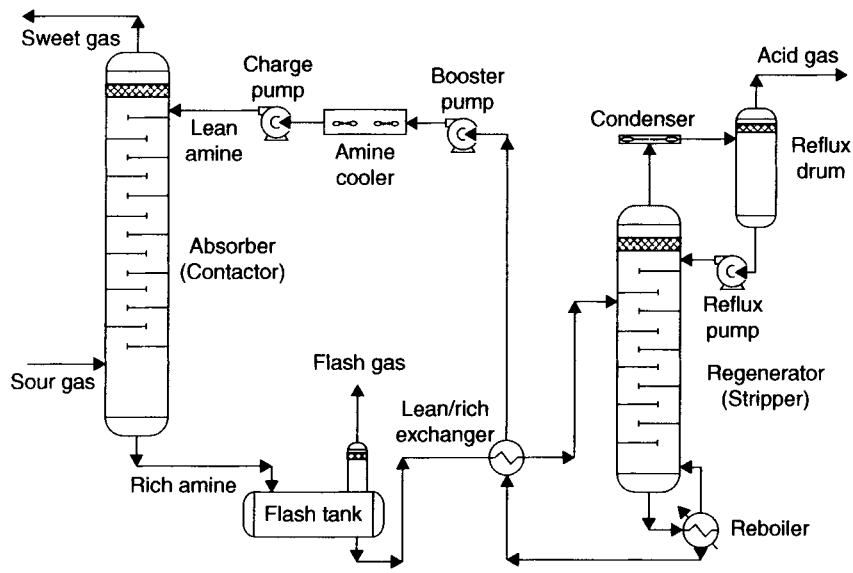

Figure 1.1 A simplified schematic diagram of the process for removing acid gas from natural gas.

1.6.1.1 *Post-Combustion*

As was mentioned earlier, it is probably wise to separate the carbon dioxide from the flue gas and inject only a CO_2-rich stream. This is the so-call "capture" part of the carbon capture and storage.

At first look, we should be able to achieve this using a process similar to those used for sweetening natural gas. However, there are several factors that complicate this.

1. High Temperature – Since the source of the stream is a combustion process, this stream will be at high temperature. It may be necessary to cool the flue gas stream before sending it to the treating process.
2. Low Pressure – The flue gas stream is produced at near atmospheric pressure. At a minimum, blower will probably have to be used to raise the pressure of the gas to a sufficient level such that it can flow through the process equipment.

   In addition, and perhaps more importantly, the absorption process is favored by higher pressure.

   The low pressure also means that there is a very high actual flow rate. This means that larger diameter towers are required for the absorption process.
3. Solvent Losses – The combination of the high temperature and low pressure noted above result in significant solvent losses. Some extra process, such as a residue gas scrubber, is needed to reduce these losses.
4. Impurities – There are two key impurities in the flue gas: oxygen and oxides of sulfur.
   a. Sulfur Oxides – Sulfur oxides are also acid gases in as much as they form acidic solution in water. However they are much stronger acids than H_2S or CO_2 and for this reason they react irreversibly with most bases, including the alkanolamines commonly used to sweeten natural gas streams.
   b. Oxygen – Oxygen is also known to cause problems in the alkanolamine process.

Chemical vendors and engineering companiesare working diligently to overcome these and other problems associated with the decarbonation of flue gas.

1.6.1.2 Pre-Combustion

The hydrocarbon can be converted to hydrogen and carbon monoxide using the steam reforming reaction.

$$CH_4 + H_2O \rightarrow CO + 3\,H_2 \tag{1.13}$$

Although the reaction given is for methane, other hydrocarbons can be substituted instead and the products remain hydrogen and carbon monoxide. The carbon monoxide can be further reacted with water via the water-shift reaction:

$$CO + H_2O \rightarrow CO_2 + H_2 \tag{1.14}$$

which produces additional hydrogen. The net result of these two reactions is a stream that contains hydrogen and carbon dioxide. The hydrogen and carbon dioxide are separated, and one obtains a high-pressure carbon dioxide stream and a hydrogen stream that can be used as a fuel. The combustion of hydrogen is a relatively clean process producing only water as a by-product.

The reactions given above are not new technology. This is the most commonly used process for producing hydrogen and is used in most petroleum refineries that require hydrogen.

The carbon dioxide from this process can then be injected. Since this is a high pressure stream, it requires only a fraction of the power to compress the low pressure stream that results from the post-combustion separation.

A project like this was proposed by a company lead by BP in Peterhead, Scotland. The CO_2 was to be injected into the offshore Miller field, which had reached the end of its productive life. However, it was canceled largely due to delays by the government regarding incentives.

Another project of this type lead by Shell and Statoil in Tjeldbergodden, Norway, was also abandoned because it was deemed uneconomic.

1.7 Acid Gas Injection

With growing environmental concerns, the disposal of small quantities of acid gas is a problem. In the past, producers could flare these acid gases; however, in many jurisdictions this is no longer

the case. New and stricter regulations are curbing the disposal of sulfur compounds into the atmosphere. Usually a sulfur plant is not an option for these small producers. Thus, other methods must be developed to deal with the unwanted acid gas.

Acid gas injection is quickly becoming the method of choice for disposing of these gases. The acid gas is compressed and injected, usually into a non-producing formation. Recently though, some have investigated the value of using the compressed acid gas as a part of a miscible flood scheme. Such a scheme is usually not recommended because it will lead to a build-up of acid gas and ultimately an increased the load on the amine unit. The goal is to dispose of the acid gas, not necessarily to recycle it.

In addition, with the current depressed market for sulfur, some larger producers are considering acid gas injection as an alternative for dealing with unwanted sulfur.

Injection of the acid gas also eliminates the release of carbon dioxide and sulfur oxides to the atmosphere. Sulfur plants emit all of the CO_2 to the atmosphere and even the most efficient emit small amounts of SO_x.

Acid-gas injection basically involves taking the acid gas from the amine regeneration column (the stripper), compressing it to a sufficient pressure, and injecting it into a suitable underground formation. Acid-gas injection is essentially a zero-emission process. During normal operation, "all" of the hydrogen sulfide from the produced gas is re-injected. Only during upsets, when the acid gas is sent to flare, or if there are leaks in the system, which must be attended to, are sulfur compounds emitted into the atmosphere. Of course, there are other locations in the plant where hydrogen sulfide may be emitted, but the acid gas from the regenerator accounts for the vast majority of the produced hydrogen sulfide.

Figure 1.2 shows the basic block diagram for the acid-gas injection process, including a block for the natural gas sweetening unit. For CCS, the sweetening block is replaced by a carbon capture block, but the rest of the process is unchanged. The four main components of the injection scheme are: 1. compression, 2. pipeline, 3. injection well, and 4. reservoir. Each of these will be discussed in some detail in this book.

Both a pump and a dehydration unit are required in only a few cases. A pump may be required if the injection pressure cannot be achieved by compression alone. As will be demonstrated in chapter 6, it is often possible to dehydrate the acid gas using compression and cooling alone.

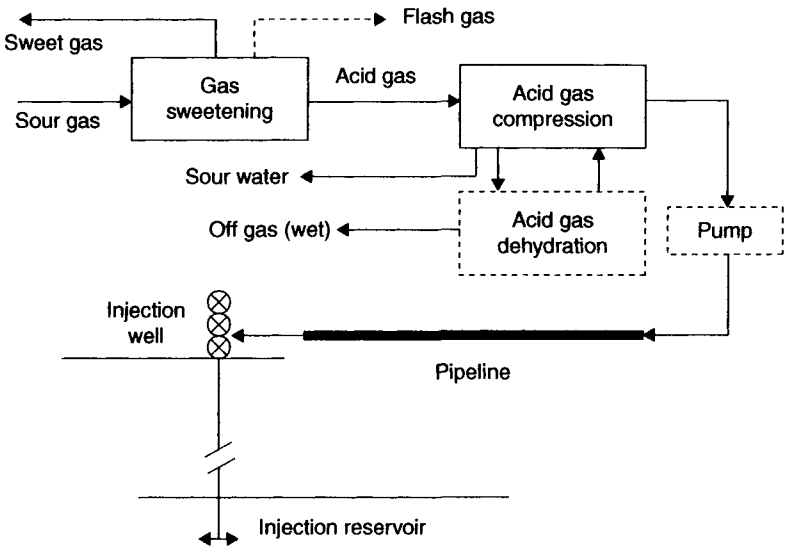

Figure 1.2 Block diagram of an acid gas injection scheme.

However, in some cases additional dehydration is required. Some of the complexities of dehydrating acid gas are discussed in Chapter 7.

1.8 Who Uses Acid Gas Injection?

As was mentioned, acid-gas injection has become a viable option for the disposal of unwanted acid gas.

1.8.1 Western Canada

In Western Canada there are more than 40 injection schemes. The first of these, the Chevron Acheson, near Edmonton, Alberta, began in 1989 and continues in operation today (Lock, 1997). Most of these injection schemes are quite small. About 80% are less than 5 MMSCFD. However, the largest is licensed to inject about 30 MMCFD. The composition of the injected gas ranges from essentially pure CO_2 to essentially pure H_2S and most everything in between. Injection pressures (the pressure at the wellhead) range from 4 000 to 13 000 kPa (600 to 1900 psia). Well depths are typically between 1000 and 3000 m (3,300 and 9,800 ft), with the deepest at about 3500 m (11,500 ft).

A few small injection schemes in Western Canada have been described in the literature in some detail. These include West

Pembina, Alberta (Lock 1997), Wayne-Rosedale, Alberta (Ho et al. 1996), Puskwaskau, North Normandville, West Culp, and Rycroft, all in Alberta (Maddocks and Whiteside, 2004).

Most of these are merely for the disposal of the acid gas, but not all. For example, in 2002 Dominion Energy Canada Ltd commissioned an acid-gas flood for its West Stoddart field near Ft. St. John, BC, Canada. In this flood, 2.5 MMSCFD of acid gas that is a 75% H_2S and 25% CO_2 mixture is injected into a producing reservoir. The acid-gas mixture is delivered from a multistage compressor to an injection well via a 2.25-km long pipeline.

1.8.2 United States

In the USA there are fewer than 20 schemes, but these tend to be slightly larger than those in Canada.

An example of a scheme in the USA is the Anadarko Brady Plant in Wyoming (Miller et al. 1999). The raw gas to this plant contains approximately 40% CO_2 and 1.5% H_2S. The acid gas is removed in two stages. The first, which is an amine plant, removes all of the H_2S and about 1/3 of the CO_2. The second, a Benfield plant, removes the remainder of the CO_2. It is the gas from the first sweetening process that is injected. The injection rate is about 9 MMCFD and the composition of the gas is 85% CO_2 and 14% H_2S.

A few American schemes also have been discussed in the literature. These include: Dumas, Texas, USA (Whatley, 2000); Lisbon, Utah, USA, (Jones et al., 2004), and Artesia, New Mexico, USA, (Root et al., 2007). As the technology continues to prove itself, more and more producers in the USA are considering acid gas as an option for dealing with unwanted acid gas.

1.8.3 Other Locations

Another significant injection scheme is the offshore injection at Sleipner West, in the Norwegian North Sea, operated by Statoil. At this location, the produced gas contains no H_2S and approximately 10% CO_2. The CO_2 is injected at a rate of about 1 million tonne per year (approximately 55 MMCFD).

Norway is one of the few countries in the world that imposes a carbon tax. Tax rates vary from industry to industry, but for gas production in the North Sea the rate is around 308 Norwegian Kroner per tonne CO_2 equivalents (about $45 [US]).

1.8.4 CO_2 Flooding

Although strictly not an acid-gas disposal method, miscible flooding using carbon dioxide is, in some situations, an economic method of enhanced oil recovery. It shares many characteristics with its disposal cousin, particularly the surface equipment.

In Canada, the Encana (originally PanCanadian) project at Weyburn, Saskatchewan, is a significant EOR project. At the Weyburn plant approximately 90 MMSCFD of a CO_2 blend is injected. Currently, the majority of this gas comes from the Dakota Gasification Company (DGC) plant in Beulah, North Dakota, United States, and is transported to Weyburn via a 320-km (220-mile) long pipeline. The remainder of the gas injected is recycled gas (gas separated from the produced oil). The recycle gas is largely CO_2 but also contains a small amount of H_2S and light hydrocarbons. As the project continues, more of the injected gas will come from recycle and less from DGC. The recycled gas is at low pressure and must be compressed for injection. This project produces about 8,000 bpd.

In the United States, there are approximately 70 CO_2 miscible flood projects in Texas, Oklahoma, Wyoming, New Mexico, Kansas, and Michigan. Total production from these projects is about 200,000 bpd.

1.9 In Summary

Acid gas, a mixture of hydrogen sulfide and carbon dioxide, is a toxic by-product of the sweetening of natural gas. Acid-gas injection has become an environmentally friendly way to dispose of this by-product. In the remainder of this book, the detailed design considerations for acid-gas injection are presented.

References

Gas Processors Association, 1996. Table of physical constants of paraffin hydrocarbons and other components of natural gas. Standard 2145–96, Gas Processors Association, Tulsa, OK.

Ho, K.T., J. McMullen, P. Boyle, O. Rojek, M. Forgo, T. Beatty, and H.L. Longworth. 1996. Subsurface acid gas disposal scheme in Wayne-Rosedale, Alberta. *SPE Paper No. 35848.*

Jones, S.G., D.R. Rosa, and J.E. Johnson. 2004. Acid gas injection design requires numerous considerations. *Oil & Gas J.*: Mar. 8:45–51.

Kohl, A. and R. Nielsen. 1997 edition. *Gas purification*. Houston, TX: Gulf Publishing.

Lock, B.W., 1997. Acid gas disposal a field perspective. 76th Annual GPA Convention, San. Antonio, TX.

Maddocks, J. and D. Whiteside. 2004. Acid gas injection: An operator s perspective. *SOGAT*, Abu Dhabi, United Arab Emirates.

Miller, E.W., S.J. Soychak, A,E. Reed, R.K. Bartoo, and R. Ackman. 1999. Brady Plant Treating Project. Laurance Reid Gas Conditioning Conference, Norman, OK.

Root, C., H. Schadler, R. Bentley and Steve Tzap. 2007. Acid-gas injection in New Mexico relieves sulfur-recovery unit duty. *Oil & Gas J.* Sept. 17, pp. 72–82.

Whatley, L. 2000. Acid-gas injection proves economic for West Texas gas plant. *Oil & Gas J.* May 22, pp. 58–61.

Appendix 1A Oxides of Nitrogen

Nitrogen forms several oxides commonly referred to as NO_x. Nitrogen is capable of forming several oxidation states. Of these compounds only the following are significant:

NO: nitrogen (II) oxide

- nitrogen monoxide, nitrogen oxide, nitric oxide
- Molar mass: 30.006
- Color: colorless
- State at room conditions: gas
- Melting point: –164°C
- Boiling point: –152°C
- Density: 1.3 kg/m^3

NO_2: nitrogen (IV) oxide

- nitrogen dioxide, nitrogen oxide
- Molar mass: 46.006
- Color: brown
- State at room conditions: gas
- Melting point:
- Boiling point:
- Density: 2.0 kg/m^3

N_2O: nitrogen oxide

- dinitrogen oxide, nitrous oxide
- Molar mass: 44.013
- Color: colorless
- State at room conditions: gas
- Melting point: –91°C
- Boiling point: –88°C
- Density: 1.9 kg/m^3

N_2O_3: nitrogen (II, IV) oxide

- nitrogen oxide, nitrogen trioxide, dinitrogen trioxide
- Molar mass: 76.012

- Color: pale blue
- State at room conditions: unstable at room temperature
- Melting point: –102°C
- Boiling point: 3°C
- Density: 1400 kg/m^3 (liquid, 2°C)

N_2O_4: nitrogen (IV) oxide

- nitrogen oxide, nitrogen oxide dimer, dinitrogen tetraoxide, dinitrogen tetrooxide
- Molar mass: 92.011
- Color: colorless
- State at room conditions: gas
- Melting point: –10°C
- Boiling point: 22°C
- Density: 1450 kg/m^3 (liquid)

N_2O_5: nitrogen (V) oxide

- nitrogen oxide, nitrogen pentoxide, dinitrogen pentoxide
- Molar mass: 108.01
- Color: white
- State at room conditions: crystalline solid
- Melting point: 30°C
- Boiling point: 47°C
- Density: 2050 kg/m^3 (solid)

Appendix 1B Oxides of Sulfur

From the electron structure of the elements sulfur and oxygen, one would predict that an oxide of the form SO should arise. However, this compound is highly unstable. Sulfur forms two stable oxide: SO_2 and SO_3, commonly referred to as sulfur dioxide and sulfur trioxide.

SO_2: sulfur (IV) oxide

- sulfur dioxide, sulfur oxide
- Molar mass: 64.065
- Color: colorless
- State at room conditions: gas
- Melting point: –72°C
- Boiling point: –10°C
- Density: 2.8 kg/m^3 (gas)

SO_3: sulfur (VI) oxide

- sulfur oxide, sulfur trioxide
- Molar mass: 80.064
- Color: colorless
- State at room conditions: liquid
- Melting point: 17°C (gamma form)
- Boiling point: 45°C
- Density: 1920 kg/m^3

2

Hydrogen Sulfide and Carbon Dioxide

The foundation of a good process design is accurate physical property calculations. This is no less true for acid gas injection than for any design. The design of an acid gas injection scheme requires knowledge of the density, enthalpy, entropy, viscosity, thermal conductivity, and other properties of the acid gas mixtures.

In this chapter, techniques are presented for estimating the physical properties of fluids along with some recommended values for hydrogen sulfide, carbon dioxide, methane, and water – the last two being the major impurities in acid gas. However, we will concentrate on the physical properties of hydrogen sulfide and carbon dioxide and mixtures of these two components.

This discussion is not meant to be a thorough review of the science of physical property estimation. For a thorough review, the reader is referred to the book by Reid et al. (1987) and earlier editions of their text.

To begin, several properties for the four components mentioned above are summarized in table 2.1. These values come from various sources and are used throughout this text in the example problems.

Table 2.1 Some properties of hydrogen sulfide, carbon dioxide, methane, and water.

	H_2S	CO_2	CH_4	H_2O
Molar Mass, kg/kmol	34.082	44.010	16.043	18.015
Critical Temperature, K	373.5	304.2	190.6	647.1
Critical Temperature, °C	100.4	31.1	−82.6	374.0
Critical Pressure, MPa	8.963	7.382	4.604	22.055
Critical Volume, m^3/kmol	0.0985	0.0940	0.0993	0.0560
Critical Density, kg/m^3	346	468	162	322
Critical Compressibility, $(P_C v_C/RT_C)$	0.284	0.274	0.288	0.229
Triple Point Temperature, K	187.7	216.6	90.7	273.16
Triple Point Temperature, °C	−86.5	−56.6	−182.5	0.01
Triple Point Pressure, kPa	23.2	518	11.7	0.611
Normal Boiling Point, K	212.8	–†	111.7	373.2
Normal Boiling Point, °C	−60.4	–†	−161.5	100.0
Melting Point, K	187.7	–†	90.7	273.2
Melting Point, °C	−85.5	–†	−182.5	0.0
Enthalpy of Vaporization at T_b, kJ/mol	18.68	–†	8.20	40.65
Enthalpy of Vaporization at 25°C, kJ/mol	14.08	5.32	–	43.98
Gross Heating Value (Gas), MJ/m^3	23.8	–‡	37.7	–‡
Specific Gravity of Gas*, unitless	1.177	1.520	0.535	0.622

† carbon dioxide sublimes at 194.7 K and 101.325 kPa

‡ carbon dioxide and water are non-combustible

* relative to air

2.1 Properties of Carbon Dioxide

There are significantly more data available for carbon dioxide than for hydrogen sulfide, particularly for transport properties. One reason for this is that carbon dioxide is significantly easier to deal with than hydrogen sulfide. As noted in chapter 1, hydrogen sulfide is toxic and requires special precautions when used in the lab. In addition, carbon dioxide has a much lower critical point making the interesting critical region in the range of more experimenters. The vicinity of critical point is attractive to researchers because of the nature of the physical properties in that region – the properties change dramatically with small changes in either the temperature or the pressure.

Thermodynamic properties were reviewed by Angus et al. (1976) and tables of thermodynamic properties were constructed. Vukalovich and Altunin (1968) reviewed both the thermodynamic and transport properties. These are similar to the *Steam Tables* (Haar et al., 1984), which should be familiar to most engineers. The latest tables for the thermodynamic properties of CO_2 are those of Span and Wagner (1996).

The physical properties of saturated vapor carbon dioxide are listed in table 2.2 and those for the saturated liquid are in table 2.3. The

Table 2.2 Properties of saturated liquid carbon dioxide.

Temp. (°C)	Vapor Pressure (MPa)	Density (kg/m³)	Heat Capacity (kJ/kg·K)	Viscosity (cp)	Thermal Conduct. (W/m·K)
−10	2.649	983	2.29	0.1202	0.1218
−5	3.046	957	2.40	0.1113	0.1158
0	3.485	928	2.54	0.1028	0.1097
5	3.969	897	2.73	0.0904	0.1035
10	4.502	862	3.01	0.0794	0.0972
15	5.086	821	3.44	0.0702	0.0907
20	5.728	773	4.26	0.0612	0.0837
25	6.432	711	6.41	0.5016	0.756
30	7.211	595	33.21	0.0413	0.0628
31.1	7.382	468	∞	0.0322	0.0508

Table 2.3 Properties of saturated vapor carbon dioxide.

Temp. (°C)	Vapor Pressure (MPa)	Density (kg/m³)	Heat Capacity (kJ/kg·K)	Viscosity (μp)	Thermal Conduct. (W/m·K)
−10	2.649	71.3	1.55	149	0.0177
−5	3.046	83.5	1.71	152	0.0188
0	3.485	97.8	1.92	155	0.0200
5	3.969	114.8	2.21	162	0.0214
10	4.502	135.4	2.62	172	0.0231
15	5.086	161	3.29	183	0.0250
20	5.728	194	4.57	198	0.0279
25	6.432	243	7.97	218	0.0319
30	7.211	344	47.5	267	0.0402
31.1	7.382	468	∞	322	0.0508

Note: 1 cp = 0.01 poise = 10 000 μp = 0.001 kg/m•s = 0.001 Pa•s

properties are compiled from several sources including Vukalovich and Altunin (1968), Golubev (1970), and Angus et al. (1976). The values in these tables represent a compromise between the various sets of data.

Here are a few comments on the values in the tables. First, the density of liquid carbon dioxide is only slightly less than water. At the temperatures listed in the table, carbon dioxide is fairly compressible since it is near the critical temperature. Under pressure, carbon dioxide can become more dense than water.

The infinite heat capacity at the critical point looks unusual, but this is true of all pure substances. This has been observed experimentally and can be demonstrated using the principles of classical thermodynamics. However, even though the heat capacity is infinite, the enthalpy at the critical point is finite.

Example

2.1 The Prandtl number is an important parameter in convective heat transfer calculations. Calculate the Prandtl number for liquid carbon dioxide at 10°C. The Prandtl number is given by:

$$Pr = \frac{C_P \mu}{k}$$

Answer: The physical properties are taken from table 2.2:

$$Pr = \frac{C_P \mu}{k} = \frac{(3.01 \times 1000)(0.0794/1000)}{0.0972} = 2.46$$

The first 1000 in this calculation is to convert from kJ to J and the second is to convert from cp to kg/m·s (Pa·s). The Prandtl number of saturated liquid carbon dioxide at 10°C is 2.46. Readers should satisfy themselves that the units are correct, remembering that the Prandtl number has no units.

2.2 Properties of Hydrogen Sulfide

As was mentioned earlier, there is significantly less data available for hydrogen sulfide than for carbon dioxide, particularly for the transport properties. This is partially because of the high toxicity of H_2S, which makes it difficult to study in the laboratory. Therefore the data for carbon dioxide, combined with the principle of corresponding states, will be used to approximate the transport properties of H_2S.

Goodwin (1983) reviewed the thermodynamic properties of hydrogen sulfide. Using an advanced equation of state a table of properties was constructed over a wide range of pressures and temperatures.

The physical properties of saturated vapor hydrogen sulfide are listed in table 2.4 and those for the saturated liquid are in table 2.5. The vapor pressure, densities, and heat capacities are taken from Goodwin (1983). Transport properties were estimated using techniques given by Neuberg et al. (1977) and from a corresponding states interpretation of the CO_2 values. The transport properties given in these tables should be considered as preliminary and subject to change.

Examples

2.2 Calculate the Prandtl number for liquid hydrogen sulfide at 50°C.

Answer: The physical properties are taken from table 2.4:

$$Pr = \frac{C_P \mu}{k} = \frac{(2.64 \times 1000)(0.0934/1000)}{0.112} = 2.20$$

Table 2.4 Properties of saturated liquid hydrogen sulfide.

Temp. (°C)	Vapor Pressure (MPa)	Density (kg/m³)	Heat Capacity (kJ/kg·K)	Viscosity (cp)	Thermal Conduct. (W/m·K)
−10	0.754	856	2.02	0.167	0.198
0	1.024	835	2.05	0.152	0.181
10	1.358	813	2.10	0.139	0.165
20	1.767	790	2.18	0.127	0.150
30	2.58	465	2.29	0.116	0.137
40	2.841	738	2.44	0.104	0.124
50	3.525	710	2.64	0.0934	0.112
60	4.320	677	2.93	0.0819	0.100
70	5.234	640	3.37	0.0700	0.082
80	6.277	596	4.14	0.0575	0.067
90	7.459	539	5.81	0.0440	0.053
100.4	8.963	346	∞	0.0255	0.030

2.3 A gas stream containing pure H_2S flows at a rate of 1 MMSCFD. What is the mass flow rate of this stream in kg/h? What is the actual volumetric flow rate in m^3/day, L/min, ft^3/day, and USgpm (US gallons per minute)?

Answer: From the previous chapter, we have:

$$1 \text{ MMSCF} = 1.195 \times 10^6 \text{ mol}$$

therefore the flow rate of the gas is 1.195×10^6 mol/d or 1.195×10^3 kmol/d. From table 2.1, the molar mass of H_2S is 34.082 kg/kmol. So 1 MMSCFD of H_2S is:

$$1.195 \times 10^3 \text{ kmol/d} \times 34.082 \text{ kg/kmol} = 40\,730 \text{ kg/d}$$

$$40\,730 \text{ kg/d}/(24 \text{ h/d}) = 1697 \text{ kg/h}$$

Table 2.5 Properties of saturated vapor hydrogen sulfide.

Temp. (°C)	Vapor Pressure (MPa)	Density (kg/m³)	Heat Capacity (kJ/kg·K)	Viscosity (μp)	Thermal Conduct. (W/m·K)
−10	0.754	12.8	1.15	113	0.0124
0	1.024	17.1	1.19	121	0.0132
10	1.358	22.4	1.23	124	0.0140
20	1.767	28.9	1.29	127	0.0148
30	2.58	37.0	1.36	133	0.0156
40	2.841	46.7	1.45	141	0.0164
50	3.525	58.7	1.56	149	0.0173
60	4.320	73.6	1.73	155	0.0182
70	5.234	92.3	1.98	161	0.0192
80	6.277	116.6	2.42	169	0.021
90	7.459	150.5	3.43	189	0.022
100.4	8.963	346	∞	255	0.030

From table 2.4 the density of saturated liquid H_2S is 710 kg/m³.

$$1697 \text{ kg/h}/(710 \text{ kg/m}^3) = 2.39 \text{ m}^3/\text{h}$$

Converting to L/min:

$$2.39 \text{ m}^3/\text{h} \times 1000 \text{ L/m}^3/(60 \text{ min/h}) = 39.8 \text{ L/min}$$

Converting to ft³/h:

$$2.39 \text{ m}^3/\text{h} \times 35.3145 \text{ ft}^3/\text{m}^3 = 84.4 \text{ ft}^3/\text{h}$$

Converting to USgpm:

$$39.8 \text{ L/min} \times 0.264172 \text{ USgal/L} = 10.5 \text{ USgpm}$$

2.4 Acid gas from a small amine plant is produced at a rate of 2×10^3 m³[std]/d of hydrogen sulfide. Standard conditions are 15.56°C and 101.325 kPa.

a) Calculate the equivalent tonnes of sulfur for this stream.
b) If the gas is compressed to a saturated liquid at 10°C, calculate the flow rate in actual m³/d.

Answer: Convert the flow rate to a molar flow:

$$n = PV/RT = (101.325)(2 \times 10^3)/8.314/(15.55 + 273.15)$$
$$= 84.43 \text{ kmol/d}$$

a) One mole of hydrogen sulfide produces 1 mole of elemental sulfur, if it is assumed that the chemical formula for sulfur is S. Therefore, the sulfur production is also 84.43 kmol/d. The molar mass of S is 32.066 kg/kmol and converting to a mass flow rate:

$$m = (84.43)(32.066) = 2707 \text{ kg/d} = 2.7 \text{ tonne/d}$$

Sulfur occurs in several species. A common sulfur form is S_8. If we assume that the sulfur is in this form, then 10.55 kmol/d of sulfur are produced. The molar mass of S_8 is 256.53 kg/kmol. Converting to a mass flow:

$$m = (10.55)(256.53) = 2707 \text{ kg/d} = 2.7 \text{ tonne/d}$$

Therefore, this plant produces an equivalent of 2.7 tonne/d. And note, when expressed in terms of mass, the result is independent of the assumed form of the sulfur.

b) Convert the molar flow rate of H_2S to a mass flow rate:

$$m = (84.33)(34.082) = 2874 \text{ kg/d}$$

Use the density from table 2.4 to convert from mass flow rate to volumetric flow rate:

$$V = 2874/813 = 3.535 \text{ m}^3\text{[act]/d} = 2.45 \times 10^{-3} \text{ m}^3\text{[act]/min}$$

The 2000 m³[std] shrinks to about 3.5 m³[act] – a factor of 566.

2.3 Estimation Techniques for Physical Properties

There are many methods for estimating the physical properties of fluids. In this section we will discuss those which are appropriate for acid gases. These methods tend to be more general in nature.

In this discussion, the thermodynamic properties (P-v-T [density], enthalpy, entropy, and heat capacity) and transport properties (viscosity and thermal conductivity) will be treated separately.

2.3.1 Thermodynamic Properties

2.3.1.1 Ideal Gas

At low pressure, less than about 300 kPa, it is safe to assume that a gas behaves as an ideal gas. Or at least, its physical properties are predicted with acceptable accuracy using ideal gas principles. This is true of any gas, even acid gas and even acid gas saturated with water. The first consequence of assuming ideal gas behavior is that the density can be easily calculated from the ideal gas law:

$$\rho = \frac{MP}{RT} \tag{2.1}$$

where: ρ – density, kg/m^3
M – molar mass, kg/kmol
P – pressure, kPa
R – universal gas constant, 8 314 m^3·Pa/kmol·K
T – absolute temperature, K

Example
2.5 Estimate the density of pure hydrogen sulfide at 50°C and 190 kPa.

Answer: Since the pressure is low, the ideal gas law, equation (2.1) can be used:

$$\rho = \frac{MP}{RT} = \frac{(34.082)(190)}{(8.314)(50+273.15)}$$
$$= 2.41\,\text{kg/m}^3$$

The reader should take a moment to confirm that the units are correct.

The second consequence of the ideal gas assumption is that enthalpies are only a function of the temperature. Thus the enthalpy change for an ideal gas can be readily calculated from:

$$h_2^* - h_1^* = \int_{T_1}^{T_2} C_P^* \, dT \tag{2.2}$$

where: h – molar enthalpy, J/mol
T – temperature, K
C_P – isobaric heat capacity, J/kg·K

and the superscript * is used to indicate the ideal gas state and the subscripts 1 and 2 are the two states. Note changes in enthalpy of an ideal gas are independent of the pressure.

Ideal gas heat capacities are available for many components and are usually expressed in the form of a polynomial in temperature:

$$C_P^* = A + BT + CT^2 + DT^3 \tag{2.3}$$

Substituting the polynomial form for the heat capacity into equation (2.2) and integrating yields:

$$h_o^* - h_1^* = A\left(T_2 - T_1\right) + \frac{B}{2}\left(T_2^2 - T_1^2\right) + \frac{C}{3}\left(T_2^3 - T_1^3\right) + \frac{D^3}{4}\left(T_2^4 - T_1^4\right) \tag{2.4}$$

Table 2.6 summarizes the ideal gas coefficients for the four components of interest here. When using these coefficients the temperature in equation (2.3) must be in Kelvin and the resulting heat capacity has units of J/mol·K. These values come from Reid et al. (1987).

Finally, the entropy change of an ideal gas can be calculated from the following expression:

$$s_2^* - s_1^* = \int_{T_1}^{T_2} \frac{C_P^*}{T} dT - R\,ln\left(P_2/P_1\right) \tag{2.5}$$

where: s – entropy, J/mol·K

The subscripts 1 and 2 represent arbitrary states. Note that the entropy change for an ideal gas is a function of both the temperature and the pressure. This is different from the enthalpy of an ideal gas, which is only a function of the temperature.

Table 2.6 Ideal gas heat capacity correlation coefficients for use with equation (2.3).

	A	B	C	D
H_2S	3.194E+1	1.436E-3	2.432E-5	−1.176E-8
CO_2	1.980E+1	7.344E-2	−5.602E-5	1.715E-8
CH_4	1.925E+1	5.213E-2	1.197E-5	−1.132E-8
H_2O	3.224E+01	1.924E-3	1.055E-5	−3.596E-9

Substituting the polynomial form for the heat capacity into equation (2.5) yields:

$$s_2^* - s_1^* = A\, ln(T_2/T_1) + B\,(T_2 - T_1) + \frac{C}{2}(T_2^2 - T_1^2) + \frac{D}{3}(T_2^3 - T_1^3) - R\, ln(P_2/P_1) \tag{2.6}$$

Example

2.6 Calculate the change in enthalpy for a stream containing H_2S when it is heated from 300 to 350 K (26.9 to 76.9°C). Assume that at these conditions H_2S is an ideal gas.

Answer: Using equation (2.4) along with the constants in table 2.6 yields:

$$\begin{aligned} h_2^* - h_1^* &= 3.194\times10^1(350-300) + \frac{1.436\times10^{-3}}{2}(350^2 - 300^2) \\ &\quad + \frac{2.432\times10^{-5}}{3}(350^3 - 300^3) + \frac{-1.176\times10^{-8}}{4}(350^4 - 300^4) \\ &= 1597.00 + 23.33 + 193.04 - 40.61 \\ &= 1772.8\ \text{J/mol} \end{aligned}$$

2.3.1.2 *Real Gas*

To calculate the density of a real gas the following equation is used:

$$\rho = \frac{MP}{zRT} \tag{2.7}$$

where: z – compressibility factor, unitless

The reader should note the similarity between this equation and that for an ideal gas. Lost in the simplicity of equation (2.7) is the fact that the compressibility factor is a rather complex function of the temperature and the pressure.

The compressibility factor is usually calculated using either an equation of state or using the corresponding states principle. Both of these methods will be discussed in this section.

For the calculation of thermodynamic properties the cubic equations of state have become the workhorse of the process simulation business. In particular, the equations of state of Soave (1972) [SRK] and of Peng and Robinson (1976) [PR] and modifications of these original forms are the most commonly used.

Boyle and Carroll (2002) performed a detailed study investigating the accuracy of cubic equations of state for estimating the density of acid gas mixtures. Except in the region near a critical point, they showed that a volume-shifted SRK or PR equation is sufficiently accurate for engineering calculations in the gas, liquids, and supercritical regions.

Basically, there are three equations of state used in the study: 1. Soave-Redlich-Kwong (SRK), 2. Peng-Robinson (PR), and 3. Patel-Teja (PT). Also two forms of volume-shifting were examined: 1. Peneloux et al. (P) and 2. Mathias et al. (M) (so PR-P means the Peng-Robinson equation of state with Peneloux et al. volume-shifting).

The results of their study are summarized in table 2.7 for the density of CO_2, table 2.8 for hydrogen sulfide, and table 2.9 for mixtures of H_2S and CO_2. The following definitions are used in the construction of the tables. The average error, AE, expressed as a percentage, is defined as:

$$AE = \frac{1}{NP}\sum_{i=1}^{NP}\frac{\text{value(i)} - \text{estimate(i)}}{\text{value(i)}} \times 100\% \tag{2.8}$$

Where: NP is the number of points.

The average error can have either a positive or negative values. However, the better the fit, the closer this value is to zero.

The absolute average error, AAE, is defined as:

$$AAE = \frac{1}{NP}\sum_{i=1}^{NP}\frac{\left|\text{value(i)} - \text{estimate(i)}\right|}{\text{value(i)}} \times 100\% \tag{2.9}$$

Table 2.7 Errors in predicting the density of carbon dioxide using several equations of state.

	Average Error (%)	Average Absolute Error (%)	Maximum Error (%)
SRK	5.41	5.41	24.7
SRK-P	−0.90	2.41	17.3
PR	0.45	2.25	16.7
PR-P	−0.93	2.39	15.0
PR-M	−1.21	1.83	7.5
PT	0.75	2.30	17.3

Table 2.8 Errors in predicting the density of hydrogen sulfide using several equations of state.

	Average Error (%)	Average Absolute Error (%)	Maximum Error (%)
SRK	4.08	4.49	21.3
SRK-P	0.66	2.56	18.3
PR	−2.47	3.58	12.7
PR-P	0.03	2.41	15.1
PR-M	−1.24	1.94	7.7
PT	0.83	2.45	16.9

Table 2.9 Errors in predicting the mixture density from Kellerman et al. (1995) using several equations of state.

	Average Error (%)	Average Absolute Error (%)	Maximum Error (%)
SRK	3.54	3.55	18.87
SRK-P	−2.46	2.64	10.73
PR	−1.86	2.27	9.94
PR-P	−2.52	2.68	9.41
PR-M	−3.26	3.28	11.83
PT	−1.11	1.82	10.56

The difference between the AE and the AAE is that in the average error, positive and negative errors tend to cancel each other, which makes the prediction look better than it actually may be. The average absolute error can have only a positive value, because of the absolute value function. It is a better indication of the "goodness of fit" than is the average error. A small AE and a relatively large AAE usually indicates a systematic deviation between the function (values) and the predictions (estimates).

Finally the maximum error, MaxE, is:

$$\text{MaxE} = \textit{maximum}\left[\frac{|\text{value(i)} - \text{estimate(i)}|}{\text{value(i)}} \times 100\%, \text{i} = 1,2,...,\text{NP}\right] \quad (2.10)$$

The maximum error gives the largest deviation of the model from the data values.

2.3.2 Saturated Liquid and Vapor Densities

Figure 2.1 shows a comparison between the *IUPAC Tables* (Wagner et al., 1977) and the Peng-Robinson equation. The density of the saturated vapor is fairly accurately predicted by the equation of state, except for very close to the critical point. On the other hand, the predictions for the saturated liquid are not as good. At low temperatures, the equation of state overestimates the density, whereas at high temperature it underestimates it. It is only in the region near the critical point that the errors become large. At -50°C the error in the predicted liquid density is about 3.5%, whereas at 20°C the error is about 7.5%. Such errors may be tolerable in some design calculation, but the design engineer should be aware of this potential problem.

Figure 2.2 is a similar plot except for hydrogen sulfide. The predictions from the Peng-Robinson equation are compared with the *NBS Tables* (Goodwin, 1983). Note also the similar behavior in the prediction of the densities.

Although the equations of state have the form P = *f*(T,v), in combination with the ideal gas heat capacities they can be used to calculate all of the thermodynamic properties, including phase equilibrium, which will be discussed in the next chapter.

2.3.2.1 Liquids

As with gases under pressure, the usual approach is to use an equation of state. However, the commonly used equations of state are

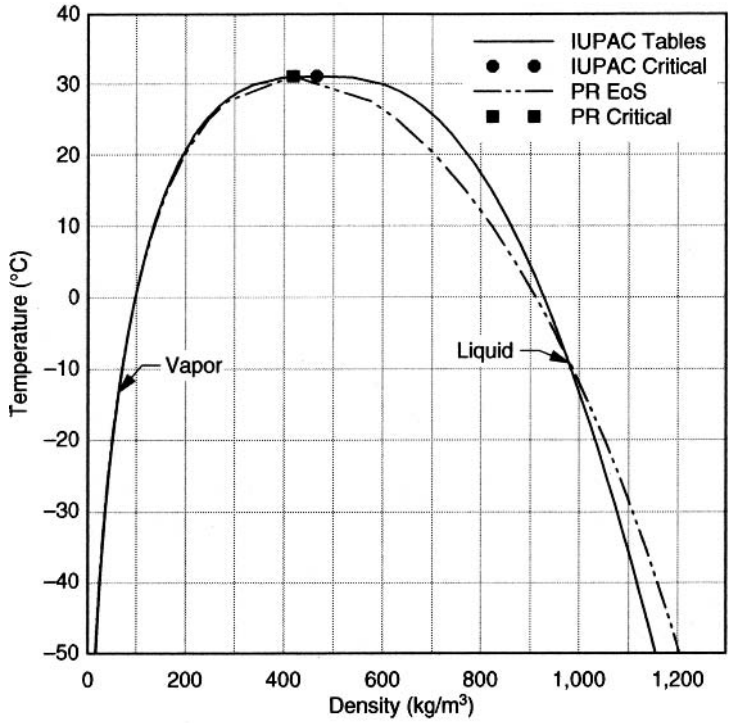

Figure 2.1 The density of saturated vapor and liquid carbon dioxide.

notoriously poor for estimating the densities of liquids. Equation (2.5) can also be used for liquids, provided the appropriate compressibility factor is used. However, it is more common to use a correlation for the liquid density.

2.3.2.2 *Corresponding States*

Essentially, the theorem states that if the properties are scaled properly, then the scaled properties of all substances should be the same. Most applications of the theory begin with the critical point. Thus, we define the reduced temperature as:

$$T_R = \frac{T}{T_C} \tag{2.11}$$

where: T_R – reduced temperature, unitless
T – temperature, K
T_C – critical temperature, K

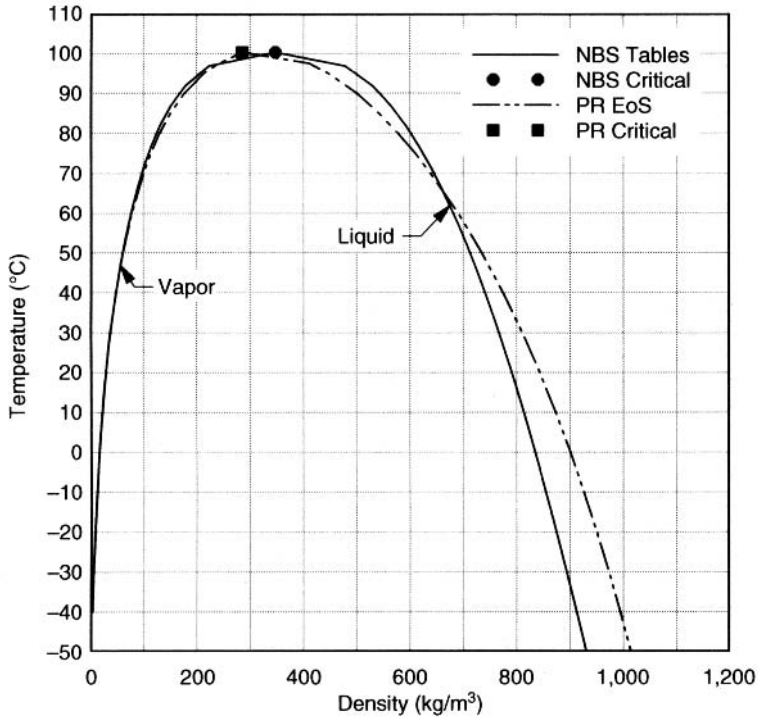

Figure 2.2 The density of saturated vapor and liquid hydrogen sulfide.

and reduced pressure as:

$$P_R = \frac{P}{P_C} \tag{2.12}$$

where: T_R – reduced pressure, unitless
T – pressure, kPa
T_C – critical pressure, kPa

In its simplest form, the theory of corresponding states says that if two substances are at the same reduced temperature and reduced pressure, then the other "reduced" properties should be equal.

According to the principle, the properties of any fluid were dependent on only the reduced temperature and pressure. Therefore, the properties of a fluid depend only on its temperature and pressure relative to its critical point:

$$z = \frac{Pv}{RT} = g(T_R, P_R) \tag{2.13}$$

The z-factor thus obtained is used in equation (2.7) in order to calculate the density of the gas.

The observation that the properties could be expressed in terms of the reduced quantities had many important ramifications. These including the possibility that if you plotted the reduced vapor pressure as a function of reduced temperature, all substances would fall onto a single curve. Furthermore, if you plotted the compressibility factor versus the reduced pressure with the reduced temperature as a parameter, all fluids would lie on the same plot.

The two-parameter corresponding-states principle is sufficiently accurate for approximations of the physical properties of simple fluids, and its simplicity makes it attractive for such calculations. It even can provide reasonably accurate predictions for other fluids.

A new chart was developed for use with acid gas mixtures. It is based on the well-known properties of carbon dioxide, but it should be reasonably accurate for mixtures of CO_2+H_2S. The new chart is shown in figure 2.3.

2.3.3 Thermodynamic Properties

The ideal gas law is used to calculate the enthalpy and entropy of fluids at low pressure. The principles of thermodynamics can be used to extend these to higher pressure. This is done through the so-called departure functions. For the enthalpy, the departure function is given as follows:

$$h - h^* = \int_0^P \left(v - T \left(\frac{\partial v}{\partial T} \right)_P \right) dP \qquad (2.14)$$

Where:
- h – enthalpy under pressure
- h^* – ideal gas enthalpy, which is calculated as shown above
- P – pressure
- v – molar volume
- T – absolute temperature

An equation of state can be used to calculate the molar volume and the derivative of the molar volume.

According to Reid et al. (1987) the simple cubic equations of state can be used to estimate the enthalpies of mixtures of light hydrocarbons, CO_2, H_2S, and nitrogen to within 4 kJ/kg (1.7 Btu/lb).

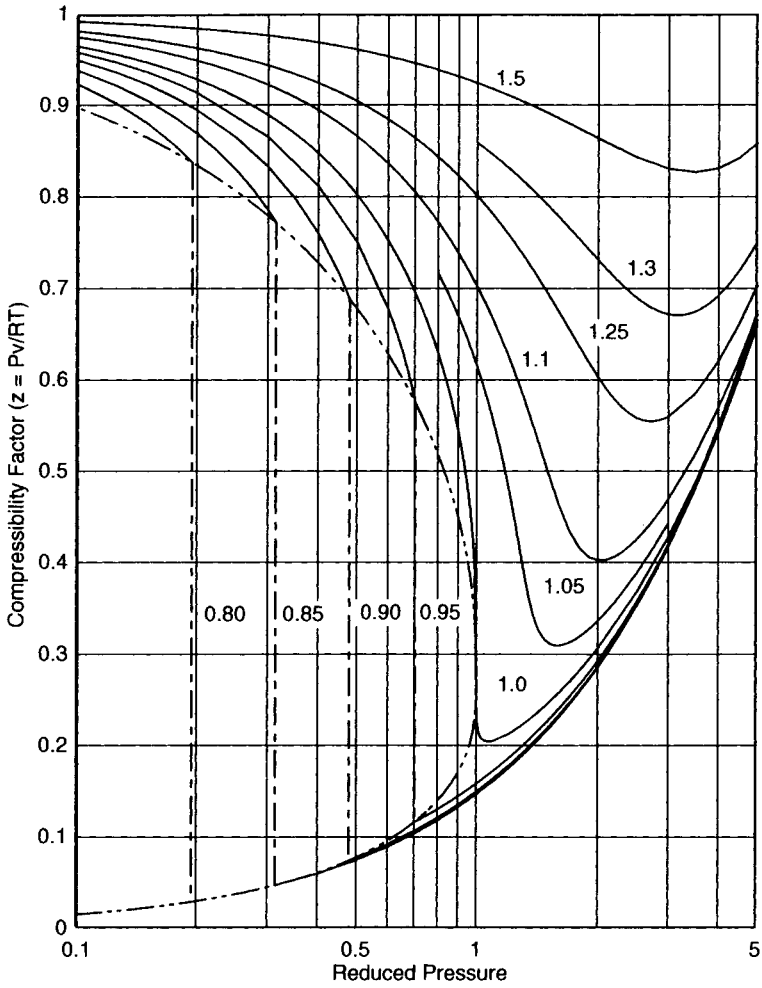

Figure 2.3 Generalized compressibility factor chart for acid gas mixtures (based on pure CO_2).

2.3.4 Transport Properties

2.3.4.1 Low Pressure Gas

The kinetic theory of gases provides some basis for these correlations. Without going into the details, the kinetic theory predicts that for an ideal gas, the viscosity and thermal conductivity are independent of the pressure and vary with the square root of the

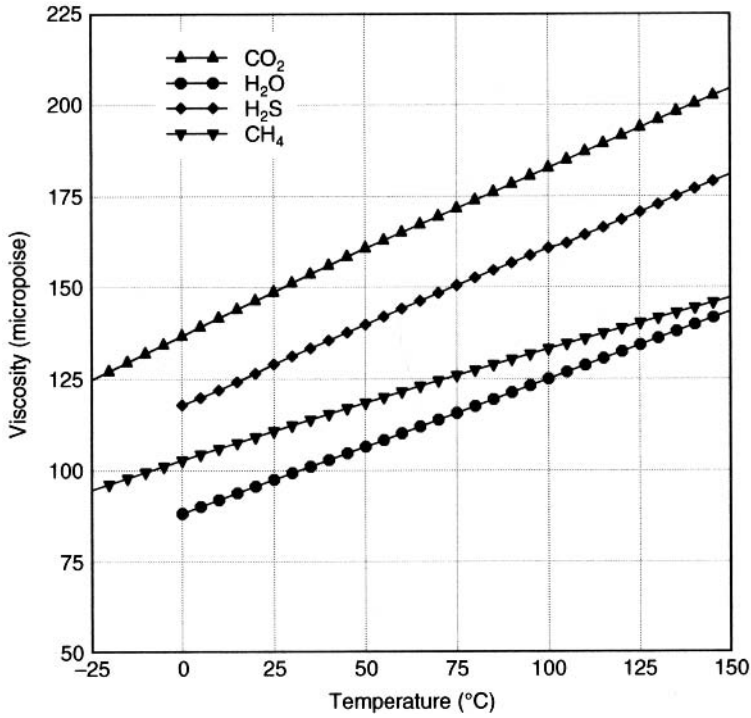

Figure 2.4 The low pressure ($P \approx 0$) viscosity for four gases.

temperature. This can be used to extrapolate data for gases over small ranges of pressure and temperature, even if the gas does not behave ideally.

At low pressure, the viscosity and thermal conductivity are independent of the pressure. This is observed experimentally, in confirmation of the kinetic theory. Therefore, these quantities can be expressed as a function of the temperature alone. Most of these correlations will also be based on the square root of the temperature, although the exact expressions tend to be more complicated.

Figure 2.4 shows the low pressure viscosity for the four gases of interest here.

2.3.4.2 Gases Under Pressure

Experience has shown that the viscosity of a gas under pressure is more highly correlated with the density than it is with either the temperature or the pressure or a combination of both. This was

clearly demonstrated by Herreman et al. (1970) for pure carbon dioxide. Thus, it is common to correlate the viscosity as a function of the density. However, this assumes that one is able to calculate the density with a high degree of accuracy, which is not always the case, particularly for mixtures.

Consider for example, the corresponding states method of Jossi et al. (1962), which is used to correct for the high density:

$$\left[(\mu-\mu_o)\xi+1\right]^{1/4} = 1.0230 + 0.23364\rho_R + 0.58533\rho_R^2 - 0.40758\rho_R^3 + 0.0923324\rho_R^4 \quad (2.15)$$

where: μ_o – low pressure viscosity (from above)
ρ_R – reduced density ($\rho_R = \rho/\rho_C$)

The ξ for the mixture is calculated using

$$\xi = \left[\frac{RT_C N_A^2}{M^3 P_C^4}\right]^{1/6} \quad (2.16)$$

where: N_A – Avogadro's number, 6.022×10^{23} mol^{-1}

It may not be clear by looking at equation (2.16), but the quantity ξ has units of reciprocal viscosity. Thus the product of ξ and the viscosity is dimensionless.

Note that this equation indicates that the high pressure viscosity is a function of the density alone. All other parameters in this equation are either scaling factors or constants.

The correction is reported to be valid for the range $0.1 \leq \rho_R \leq 3$. In addition, this correlation was derived for non-polar gases, but it is used for our mixtures nonetheless.

2.3.4.3 Liquids

Unfortunately, there is no good theory equivalent to the kinetic theory that is applicable to liquids. Thus liquid correlations tend to be more empirical than the equivalent ones for the gas phase.

A relatively simple procedure for estimating the viscosity of a liquid is to assume the equation presented earlier for gases under pressure. However, when applying the Jossi et al. equation

(equation 2.15), use the liquid density. This provides estimates that are in the range of 25%, which is often of sufficient accuracy for many applications.

2.3.5 Viscosity Charts

As was mentioned earlier, the properties of carbon dioxide have been studied thoroughly. Thus it is relatively easy to construct a diagram that shows the viscosity of pure CO_2 over a wide range of pressure and temperature. Figure 2.5 is such a diagram, which shows the range of temperature and pressure of interest to acid gas injection. The curve labeled 0 MPa is the same as the low pressure viscosity shown in figure 2.4.

Unfortunately, there are very few experimental measurements for the viscosity of hydrogen sulfide. A review of the available data is presented in the appendix of this chapter. However, from the few data available and by applying the principle of corresponding states to the viscosity, a chart for the viscosity of H_2S was constructed. The resulting plot is shown in figure 2.6. Details of this new correlation are also in the appendix to this chapter.

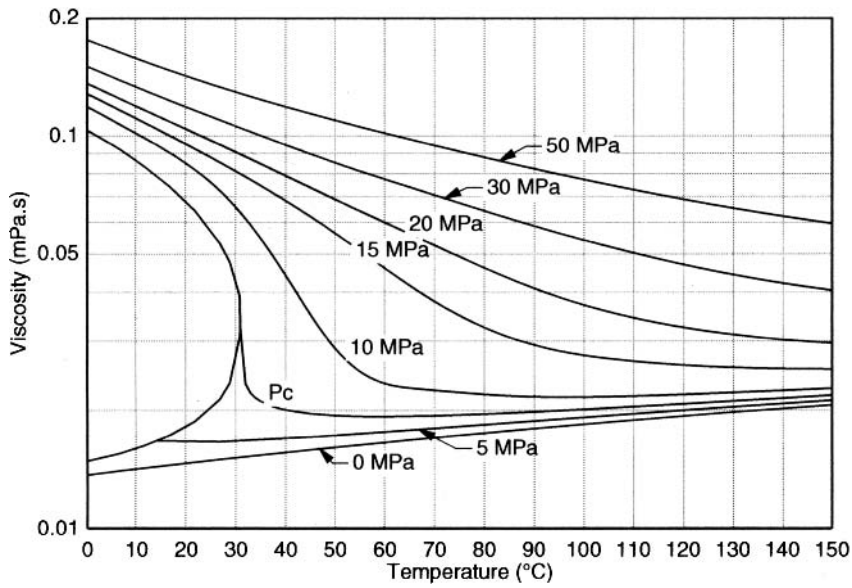

Figure 2.5 The viscosity of carbon dioxide as a function of the pressure and temperature.

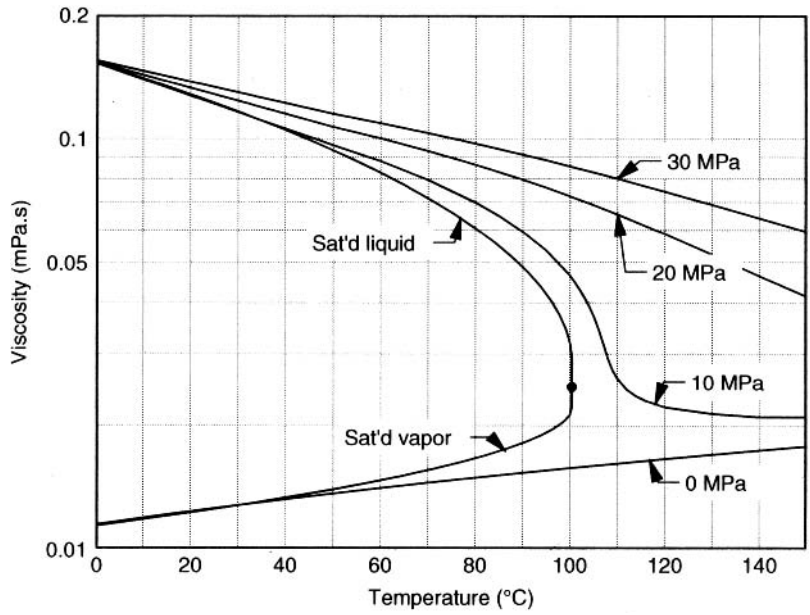

Figure 2.6 The estimated viscosity of hydrogen sulfide as a function of the pressure and temperature.

There are a couple of things of interest from these two charts. In the liquid phase the viscosity decreases with increasing temperature – which tends to be the common experience. On the other hand, in the gas phase the viscosity increases with increasing temperature. This was demonstrated earlier at low pressure and reaffirmed by the behavior shown in the new plots. Furthermore, these charts show the viscosity of the acid gas components over a rather wide range of pressure and temperature, and yet the viscosity only varies by about an order of magnitude (from about 0.02 to 0.2 mPa·s).

2.4 Properties of Acid Gas Mixtures

2.4.1 Thermodynamic Properties

The equations of state mentioned earlier are powerful tools for dealing with mixtures. All of the thermodynamic properties for mixtures are easily calculated with an equation of state and this method approach handles the phases intrinsically.

All of the thermodynamic properties of the gas phase should be calculated using an equation of state. This is typically true for the liquid as well, with the exception of the density. The commonly used equations of state do a poor job of estimating liquid density. Often the liquid density from the equation of state is rejected in favor of one from the more accurate empirical expression such as the COSTALD equation. In this case the following equation can be used:

$$v_{mix} = \sum_{i=1}^{NC} x_i v_i^{pure} \tag{2.17}$$

where: v_{mix} – molar volume of the mixture, $m^3/kmol$
v_i^{pure} – molar volume of pure i, $m^3/kmol$
x_i – mole fraction of component I
NC – number of components

The density is then calculated from:

$$\rho = \frac{M}{v} \tag{2.18}$$

The previous equation is an approximation of the thermodyna mically exact equation:

$$v_{mix} = \sum_{i=1} x_i \bar{v}_i \tag{2.19}$$

where: $\bar{v}_i$ – partial molar volume of component i, $m^3/kmol$

The reader should consult a textbook on chemical thermodynamics for a detailed discussion of this equation.

2.4.1.1 Corresponding States

To apply the principle of corresponding states to a mixture, one must employ a mixing rule. A mixing rule is a method to estimate the critical properties of the mixture for use with the correlation (i.e., not the true critical point). The simplest and most widely used

is Kay's rule (often referred to as the pseudocritical temperature and pseudocritical pressure):

$$pT_C = \sum_i x_i T_{Ci} \tag{2.20}$$

$$pP_C = \sum_i x_i P_{Ci} \tag{2.21}$$

Note, these values are not meant to be the actual critical properties of the fluid. They are used simply to estimate the properties of the fluid based on the corresponding states principle.

Reduced properties are then calculated for the mixture based on the pseudocritical properties.

Example

2.7 Use the generalized compressibility chart to estimate the density of a mixture containing 39% H_2S and 61% CO_2 at 90°C and 16 MPa.

Answer: Calculate the pseudo-critical pressure using the critical pressures from table 2.1:

$$pP_C = (0.39)\ (8.963) + (0.61)(7.382) = 7.999 \text{ MPa}$$

Next, calculate the reduced pressure:

$$P_R = P/pP_C = 16.0/7.999 = 2.00$$

Calculate the pseudo-critical temperature using the critical temperatures from table 2.1:

$$pT_C = (0.39)(373.5) + (0.61)(304.2) = 331.2 \text{ K}$$

Next, calculate the reduced temperature:

$$T_R = T/pT_C = (90 + 273.15)/331.2 = 1.10$$

Remember, the temperature must be absolute, so 90°C must be converted to Kelvin by adding 273.15.

From the generalized compressibility chart (figure 2.3) the z is about 0.40.

Next, calculate the molar mass of the mixture:

$$M = (0.39)(34.082) + (0.61)(44.010) = 40.138 \text{ g/mol}$$

And finally use equation (2.7) to calculate the density:

$$\rho = \frac{MP}{zRT} = \frac{(40.138)(16000)}{(0.40)(8.134)(90+273.15)}$$
$$= 531.8 \text{ kg/m}^3$$

Using this simplified approach the estimated density is 531.8 kg/m³.

This calculation is very close to the critical temperature of the mixture (T_R = 1.10). Simple methods (and some complex methods as well) are not very accurate for predicting densities in this region. From the generalized compressibility chart it can be seen that z changes rapidly with small changes in the reduced temperature.

2.4.2 Transport Properties

For the transport properties, we must resort to some other method. These methods are usually specific to the phase, but there are those that are applicable regardless of the phase.

For example, the viscosity of low pressure gases can be estimated by the following combining rule:

$$\mu = \sum_i \frac{y_i \mu_i}{\sum_j y_j \phi_{ij}} \tag{2.22}$$

where: μ_i – pure component viscosity
y_i – mole fraction of component i
ϕ_{ij} – represents the interaction between component i and component j.

Most correlations use this approach, and the problem becomes one of estimating the parameters ϕ_{ij}. For example, Wilke (Reid et al., 1987) gives the following expression:

$$\phi_{ij} = \frac{\left[1+\left(\mu_i/\mu_j\right)^{1/2}\left(M_i/M_j\right)^{1/4}\right]^2}{\left[8\left(1+M_j/M_i\right)\right]^{1/2}} \tag{2.23}$$

where: M – molar mass of the component, kg/kmol

On the other hand, for liquids, the mixing rule is logarithmic in the pure component viscosity:

$$\ln \mu = \sum_i x_i \ln \mu_i + \sum_i \sum_j x_i x_j \eta_{ij} \tag{2.24}$$

where: x_i – mole fraction of component i
η_{ij} – interaction parameter, which requires some experimental data for the mixture

Unfortunately, no such data exist for acid gas mixtures. And unlike gas mixtures, there is no good correlation available for the interaction parameters. Although not true for all systems, it is probably safe to set η_{ij} equal to zero in this case. The liquid mixture equation reduces to:

$$\ln \mu = \sum_i x_i \ln \mu_i \tag{2.25}$$

Similar expressions are available for the thermal conductivity of a liquid mixture.

2.4.3 Word of Caution

A significant problem has been overlooked in many of the mixture correlations presented above. Many of the mixture correlations require the pure component property at the temperature and pressure of interest. For example, the specific volume of a liquid mixture can be calculated using the following equation, which was presented earlier:

$$v_{mix} = \sum_{i=1} x_i v_i^{pure}$$

How do we apply this equation if all of the substances are not liquids? For example, consider a mixture containing 10% carbon dioxide and 90% hydrogen sulfide at 50°C and 7 MPa. At these conditions, the mixture is a liquid as is H_2S, but pure CO_2 is not. At this temperature, carbon dioxide is supercritical and behaves like a gas regardless of the pressure. What value should be used for the specific

volume of pure CO_2 in the above equation in order to obtain the specific volume of the mixture? To avoid this problem, we need some mixture information from which we could extract a mixture-specific pure pseudo-property. Such a problem should not arise when using either an equation of state or a corresponding states approach. With these methods, the mixture properties are calculated directly and not as a combination of the pure component properties.

A similar problem can arise in any of the correlations that relate the properties of a mixture to the pure component properties at the temperature and pressure of the mixture. In this module these included the viscosity and thermal conductivity of both liquids and gases.

Example

2.8 Estimate the density and viscosity of an equimolar mixture of H_2S and CO_2 at 10°C and 5000 kPa.

Answer: At these conditions, assume that the mixture is a liquid (the pressure is greater than the vapor pressure of either pure component). In the next chapter, methods will be presented for determining which phases are present for a given condition. Further assume that the properties of the liquid are independent of the pressure. The pure component properties are taken from the tables presented earlier in this chapter.

Density: In order to estimate the density, they must be converted to molar volumes, since they are more fundamental than densities.

$$v = M/\rho$$

H_2S: $v_{H_2S} = 34.082/813 = 0.04192 \text{ m}^3/\text{kmol}$

CO_2: $v_{CO_2} = 44.010/862 = 0.05106 \text{ m}^3/\text{kmol}$

From equation (2.11):

$$v_{mix} = \sum_{i=1} x_i v_i^{pure} = 0.5(0.04192) + 0.5(0.05106) = 0.04649 \text{ m}^3/\text{kmol}$$

Calculate the molar mass of the mixture

$$M_{mix} = 0.5(34.082) + 0.5(44.010) = 39.046 \text{ kg/kmol}$$

Convert the molar volume back to a density:

$$\rho = M/v = 39.046/0.04649 = 840 \text{ kg/m}^3$$

Viscosity: To calculate the viscosity of the mixture use equation (2.25):

$$\ln \mu = \sum_i x_i \ln \mu_i = 0.5\, ln(0.139) + 0.5\, ln(0.0794) = -2.2533$$

$$\mu = 0.105 \text{ cp}$$

2.5 Effect of Hydrocarbons

In this section we will examine the effect that hydrocarbons, specifically methane, have on the physical properties of acid gases. The effect on the vapor pressure (i.e., the vapor-liquid equilibrium) will be discussed in a subsequent chapter.

Methane is the most common hydrocarbon in acid gas mixtures. Large quantities of other hydrocarbons are probably indicative of problems with the amine plant and should be addressed. For example, foaming will cause carry-over of the hydrocarbons into the stripper. In the regeneration of the amine, the hydrocarbons will end up in the acid gas.

The flowing discussion presents some rules of thumb regarding the addition of hydrocarbons on the properties of acid gas mixtures. The exact effect can be only estimated using the models presented above. In each of the examples given it is assumed that only a small amount of hydrocarbon is added to the acid gas mixture.

2.5.1 Density

In the gas phase, methane and ethane reduce the density of an acid gas mixture. Propane has an approximately neutral effect – in H_2S rich mixtures it tends to reduce the density and in CO_2-rich mixtures it has little effect. Hydrocarbons butane and heavier increase the density of the acid gas mixture.

The situation is different in the liquid phase. All of the light hydrocarbons methane through pentane reduce the density of the acid gas mixture in the liquid phase.

2.5.2 Viscosity

The addition of light hydrocarbons to the acid gas mixture tends to reduce the viscosity.

It is common in natural-gas engineering to calculate the viscosity of a sour gas mixture using a two-step procedure. First, you estimate the viscosity of a sweet gas at the temperature and pressure of interest. This viscosity is corrected for the presence of hydrogen sulfide and carbon dioxide. Such correlations are usually limited to a small amount of acid gas and thus are not applicable to acid gas mixtures. Therefore, a different approach must be used for acid gas.

2.6 In Summary

Hydrogen sulfide and carbon dioxide are the key components in acid gas, and water and methane are important secondary components. The design engineer must be able to estimate the properties of these substances in order to design the injection scheme. In this chapter some properties were presented along with methods for estimating them.

References

Angus, S., B. Armstrong, and K.M. de Reuck. 1976. *International thermodynamic tables of the fluid state – carbon dioxide.* Oxford, UK: Pergamon Press.

Boyle, T. and J.J. Carroll. 2002. Study determines best methods for calculating acid-gas density. *Oil & Gas J.* Jan. 14:45–53.

Golubev, I.F. 1970. *Viscosity of gases and gas mixtures. A handbook.* U.S Dept. Interior, Washington, DC. Translated by R. Kondor.

Goodwin, R.D. 1983. *Hydrogen sulfide provisional thermophysical properties from 188 to 700 K at pressure to 75 MPa.* Report No. NBSIR 83-1694, National Bureau of Standards, Boulder, CO.

Kellerman, S.J., C.E. Stouffer, P.T. Eubank, J.C. Holste, K.R. Hall, B.E. Gammon, and K.N. Marsh. 1995. Thermodynamic properties of CO_2 + H_2S mixtures. GPA Research Report RR-141, Tulsa, OK.

Haar, L., J.S. Gallagher, and G.S. Kell. 1984. *NBS/NRC Steam tables.* Washington, DC: Hemisphere.

Herreman, W, W. Grevendonk, and A. De Bock. 1970. Shear viscosity measurements of liquid carbon dioxide. *J. Chem. Phys.* 53:185–189.

Neuberg, H.J., J.F. Atherley, and L.G. Walker. 1977. *Girdler-sulfide process physical properties*. Atomic Energy of Canada Ltd., Report No. AECL-5702.

Peng, D-Y. and D.B. Robinson. 1976. A new two-constant equation of state. *Ind. Eng. Chem. Fund.* 15:59–64.

Reid, R.C., Prausnitz, J.M. and Poling, B.E. 1987. *The properties of gases & liquids*, 4th edition. NewYork: McGraw-Hill.

Span, R. and W.Wagner. 1996. A new equation of state for carbon dioxide covering the fluid region from the triple-point temperature to 1100 K at pressures up to 800 MPa. *J. Phys. Chem. Ref. Data*. 25:1509–1596.

Soave, G. 1972. Equilibrium constants from a modified Redlich-Kwong equation of state. *Chem. Eng. Sci.* 27:1197–1203.

Vukalovich, M.P. and V.V. Altunin. 1968. *Thermophysical properties of carbon dioxide*. London: Collet's Publishers, Ltd. Translated by D.S. Gaunt.

Appendix 2A Transport Properties of Pure Hydrogen Sulfide

The purpose of this appendix is to review the experimental data available in the scientific literature for the transport properties (viscosity and thermal conductivity) of hydrogen sulfide or perhaps more accurately, the purpose is to demonstrate the paucity of data available for this important industrial compound.

2A.1 Viscosity

There is only a very small data set for the viscosity of hydrogen sulfide.

2A.1.1 Liquid

There have been three experimental investigations of the viscosity of liquid hydrogen sulfide. The three studies are summarized in table 2A.1. For the two low-temperature studies, Steele et al. (1906) and Runovskaya et al. (1970), the pressure was probably 1 atm (101.325 kPa), whereas the study of Hennel and Krynicki (1959) was at the vapor pressure of pure H_2S.

In spite of their age, the data of Steele et al. (1906) have been used in many reference books including Golubev (1957) and the DIPPR Data Book (Danner et al., 1999).

Runovskaya et al. (1970) reported some measurements for the viscosity of liquid H_2S for a similar temperature as Steele et al. (1906).

Table 2A.1 Summary of measurement of the viscosity of liquids hydrogen sulfide.

Reference	Temperature Range
Steele et al (1906)	−82.2 to −63.4°C 191.0 to 209.8 K
Hennel and Krynicki (1959)	−11.5 to 50.0°C 261.7 to 232.2 K
Runovskaya et al. (1970)	−83.1 to −61.4°C 190.1 to 211.8 K

Unfortunately, the English translation of the work of Runovskaya et al. (1970) does not give the original data, only a correlation of the values. The correlation provided is:

$$ln\,\mu = 36.598 - \frac{1.78504\times10^4}{T} + \frac{1.881420\times10^7}{T^2} \qquad (2A.1)$$

where: μ – viscosity, centipoise*
T – absolute temperature, K

It is important that this equation not be used to extrapolate to higher temperatures because it exhibits a minimum at –62.4°C (210.8 K). Such a minimum is physically impossible.

Unfortunately, there is significant disagreement between the two low-temperature sets of data. An attempt will be made to resolve this with the inclusion of the higher temperature data of Hennel and Krynicki (1959).

Figure 2A.1 shows a plot of the three data sets for the viscosity of liquid hydrogen sulfide. The plot reveals the discrepancy between the data of Steele et al. (1906) and Runovskaya et al. (1970). Also shown on this plot is a correlation of the data. This is based on all three sets of data and represents a reasonable agreement, especially for the low temperature data. The equation is:

$$ln\,\mu = 2.13461 + \frac{788.636}{T} \qquad (2A.2)$$

where: μ – viscosity, μPa·s

Unlike the correlation of Runovskaya et al. (1970), this equation does not have a minimum. Nonetheless, it should not be extrapolated beyond the given temperature range.

2.A.1.2 Vapor

The only experimental data for the low-pressure viscosity of vapor hydrogen sulfide are those of Rankine and Smith (1921). The values

*1 centipoise = 0.001 Pa·s = 1 mPa·s = 1000 μPa·s

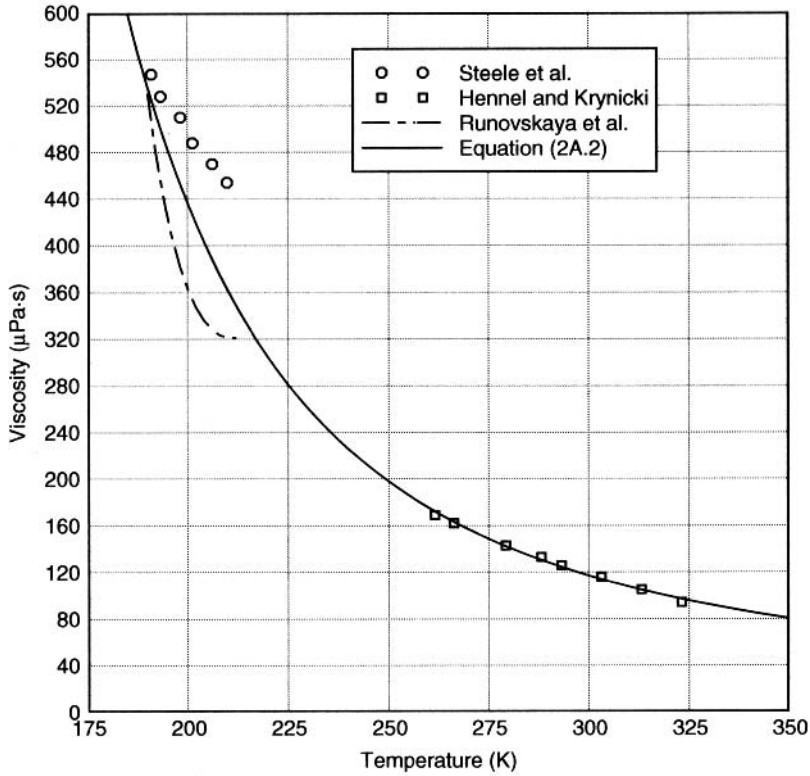

Figure 2A.1 Experimental data for the viscosity of liquid hydrogen sulfide.

given in Golubev (1957) are based on the measurements of Rankine and Smith (1921). However, most of the data in the literature are generated using generalized correlations. Furthermore, there are no data for the viscosity of H_2S under pressure.

Figure 2A.2 shows a comparison between the experimental data of Rankine and Smith (1921) and the correlation from the DIPPR Data Book (Daubert et al., 1999). Even though there is a slight disagreement between the experimental data and the DIPPR correlation, the correlation was deemed satisfactory for our purposes.

2A.2 Thermal Conductivity

There are even less data available for the thermal conductivity of hydrogen sulfide than there are for the viscosity. To the best of the author's knowledge, the only measured data for the thermal

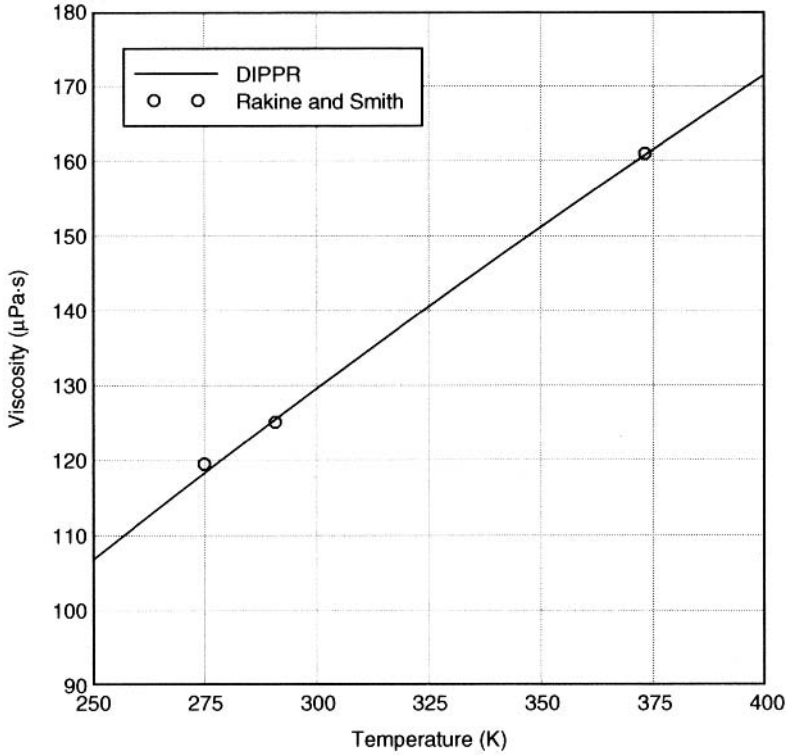

Figure 2A.2 Experimental data for the viscosity of gaseous hydrogen sulfide.

conductivity of H_2S are those of Barua et al. (1968). These data are for low-pressure gas in the temperature range –78.5° to 200°C. Any data in the literature for the liquid or high-pressure gas regions were undoubted based on generalized correlations.

The DIPPR Data Book (Daubert et al., 1999) gives the following correlation for the low-pressure thermal conductivity of H_2S:

$$\lambda^* = \frac{3.6900\,T^{-0.3838}}{1+964.00/T} \tag{2A.3}$$

where: λ^* – low pressure thermal conductivity, W/m·K
T – absolute temperature, K.

Figure 2A.3 shows a comparison between this correlation and the data of Barau et al. (1968). There is clearly a disagreement between the two.

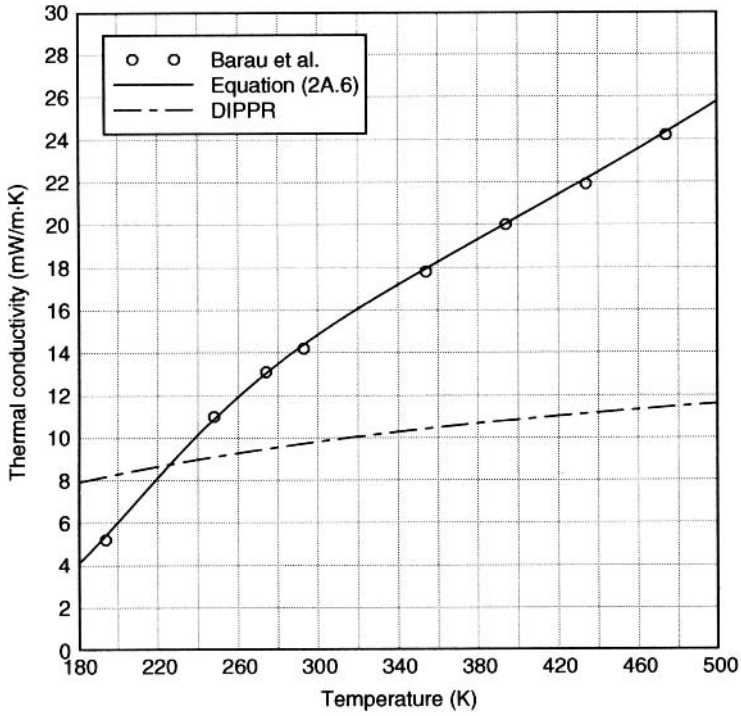

Figure 2A.3 Experimental data for the thermal conductivity of gaseous hydrogen sulfide.

The form of the DIPPR equation was retained, but new coefficients were fit to the data of Barua et al. (1968). The resulting equation is:

$$\lambda^* = \frac{7.6552 \times 10^{-5}\, T^{1.920}}{1 - 368.39/T + 46973/T^2} \qquad (2A.4)$$

This equation is also plotted on figure 2A.3 and demonstrates the improvement in the prediction of the thermal conductivity.

References

Barua, A.K., A. Manna, and P. Mukhopadhay. 1968. Thermal conductivity and rotational relaxation in some polar gases. *J. Chem. Phys.* 49:2422–2424.

Daubert, T.E., R.P. Danner, H.M. Sibul, C.C. Stebbins, R.L. Rowley, W.V. Wilding, J.L. Oscarson, M.E. Adams, and T.L. Marshall. 1999. *Physical*

and thermodynamic properties of pure chemicals. Evaluated Process Design Data. New York: AIChE.

Golubev, I.F. 1970. *Viscosity of gases and gas mixtures. A handbook.* U.S Dept. Interior, Washington, DC. Translated by R. Kondor.

Hennel, J.W. and K. Krynicki. 1959. Viscosity of liquid hydrogen sulfide *Acta Phys. Polonica.* XIX:523–526.

Jossi, J,A., L.I. Stiel, and D. Thodos. 1962. The viscosity of pure substances in the dense gaseous and liquid phases. *AIChE J.* 8:59–62.

Rankine, A.O. and C.J. Smith. 1921. On the viscosities and molecular dimensions of methane, sulphuretted hydrogen, and cyanogen. *Phil. Mag.* 62:615–620.

Reid, R.C., J.M. Prausnitz, and B.E. Poling. 1986 ed. *The properties of liquids and gases.* New York: McGraw-Hill.

Runovskaya, I.V., A.D. Zorin, and G.G. Devyatykh. 1970. Viscosity of liquefied volatile inorganic hydrides of elements of Mendeleev Periodic Groups III–VI. *Russ. J. Inorg. Chem.* 15:1338–1339.

Steele, B.D., D. McIntosh, and E.H. Archibald. 1906. The halogen hydrides as conducting solvents. Part I – The vapour pressures, densities, surface energies and viscosities of the pure solvents. *Phil. Trans. Roy. Soc.* A205:99–167.

Appendix 2B Viscosity of Acid Gas Mixtures

In this appendix a new correlation is presented for estimating the viscosity of acid gas mixtures in the gas, liquid and super critical phases. The basis for this correlation is the well-known viscosity of pure CO_2.

The correlation begins with the low pressure viscosity. The procedure for calculating the low pressure viscosity of both pure components and mixtures was outline in the main text of this chapter. That method is used here as well. The basis of the correlation is that the viscosity is a function of the density, rather than of the pressure and temperature directly.

Thus, the key to the new correlation for acid gas mixtures is the density. Boyle and Carroll (2001, 2002) studied some methods for estimating the density of such mixtures. They found that a volume-shifted Peng-Robinson (1976) equation of state was adequate for predicting the densities. This method will be used here, and the reader is referred to the original papers for details of the method and its accuracy.

2B.1.1 Correcting for High Pressure

Jossi et al. (1962) presented a generalized correlation for the viscosity of high density fluids as a function of the reduced density via a corresponding states method. This method was discussed earlier. Among the gases that Jossi et al. (1962) used to build their correlation were carbon dioxide, methane, ethane, and propane. This gives us some confidence that this approach should be satisfactory for our acid gas mixtures.

2B.1.2 Carbon Dioxide

Although the Jossi et al. (1962) correlation will not be used in this study, it will be used as a guide for building a new correlation. Therefore, we seek a function of the form:

$$\mu - \mu^* = f(\rho) \tag{2B.1}$$

Pure CO_2 will be used as the reference fluid and take the viscosity data from the tables of Vesovic et al. (1990). The densities will be

calculated using the volume-shifted PR equation of state. Although better density data are available for pure CO_2, the rest of the software will use the volume-shifted PR EoS for estimating the density. Thus for consistency, the volume-shifted PR equation will be used to develop the new correlation.

The first attempt at correlating the viscosity used a polynomial in density. The correlation that resulted was:

$$\mu - \mu^* = 5.40032 - 6.7550\times10^{-2}\rho + 3.5123\times10^{-4}\rho^2 - 3.9906\times10^{-7}\rho^3 + 2.0028\times10^{-10}\rho^4 \quad (2B.2)$$

where: $\mu - \mu^*$ is in μPa.s and ρ is in kg/m^3.

By most statistical measures, this was an excellent fit of the data (for example $r^2 = 0.9929$). However, this correlation was deemed unsatisfactory for two reasons. First, the equation had a curvature that was not indicated by the data set. This is a common problem when one attempts to fit a set of data with a polynomial. Second, it resulted in significant errors in the low-density region. Seeming small statistical errors translate into large errors in the estimate viscosity.

The next correlation examined was a logarithmic function. This function resulted in a much better fit of the high-density region, but problems with the low-density region were not resolved. To resolve this problem with the low-pressure region, the correlation was split into two pieces.

The second piece of the correlation was empirical in nature. First, it had to exhibit the following limit:

$$\lim_{\rho \to 0}(\mu - \mu^*) = 0 \quad (2B.3)$$

In other words, at low density, the viscosity must equal the ideal gas viscosity. The second property of the correlation is that it must have a smooth transition between the two pieces. In order to achieve this, both the value of the function and the first derivative of the two pieces of the correlation must be equal at the point of transition.

The high-density portion ($\rho \geq 80$ kg/m^3) of the correlation was obtained by a least-squares fit. The resulting equation is:

$$ln(\mu - \mu^*) = -3.15801 - 0.064652\, ln(\rho) + 0.17073[ln(\rho)]^2 \quad (2B.4)$$

The low-density ($\rho < 80$ kg/m^3) region is a simple correlation:

$$\mu - \mu^* = 6.5625 \times 10^{-3}\rho + 4.8825 \times 10^{-5}\rho^2 \qquad (2B.5)$$

For both pieces of the correlation, $\mu - \mu^*$ is in μPa·s and ρ is in kg/m^3. It may not be obvious by comparing the two equations, but they have the same value and first derivative at 80 kg/m^3. In the low pressure region the correction is quite small, less than 1 μPa·s, whereas the low pressure viscosities of these components are about 10 to 20 μPa·s.

Furthermore, this correlation is applicable to the liquid, vapor, and dense-phase regions. However, it is limited to densities less than 1250 kg/m^3, which is sufficient for most acid gas injection applications.

2B.1.3 Generalization

In order to use the correlation developed for CO_2 with our acid gas mixtures, it must be generalized. Again following the lead of Jossi et al. (1962), first change from the viscosity to the reduced viscosity by multiplying by a modified ξ-factor, called here Ξ. This results in:

$$\Xi = \left[\frac{T_C}{M^3 P_C^4}\right]^{1/6} = \frac{T_C^{1/6}}{M^{1/2} P_C^{2/3}} \qquad (2B.6)$$

where T_C is in K, M is in kg/kmol, and P_C is in kPa. For substituting in the appropriate values gives $\Xi = 1.0311 \times 10^{-3}$ for CO_2 and $\Xi = 1.0686 \times 10^{-3}$ for H_2S. Second, the density is replaced with the reduced density, which is defined as:

$$\rho_R = \frac{\rho}{\rho_c} \qquad (2B.7)$$

Again for consistency, the critical density will be estimated using the PR EoS and not the more accurate value from tabulated data. For CO_2, the critical density used for this purpose is 419.2 kg/m^3.

For the high-density region the correlation [equation (2B.4)] becomes:

$$ln\left[(\mu-\mu^*)\Xi\right] = -4.20064 + 1.99717\, ln(\rho_R) + 0.17073\left[ln(\rho_R)\right]^2 \qquad (2B.8)$$

which is applicable for $\rho_R \geq 0.191$. For the low-density region, the correlation is:

$$(\mu-\mu^*)\Xi = 2.609\times10^{-3}\rho_R + 1.0380\times10^{-2}\rho_R^2 \qquad (2B.9)$$

where: $\rho_R < 0.191$.

This fits the viscosity of pure CO_2 to within better than ±20%.

2B.1.4 Mixtures

Finally, we require mixing rules in order to calculate the Ξ and ρ_C for the mixture. For the temperature, the mixture critical is estimated assuming a mole fraction weighted average of the pure component critical temperatures.

$$T_{C,mix} = \sum_{i=1}^{NC} y_i T_{C,i} \qquad (2B.10)$$

The same approach is used for the critical pressure:

$$P_{C,mix} = \sum_{i=1}^{NC} y_i P_{C,i} \qquad (2B.11)$$

For the mixture molar mass we can use the following exact expression:

$$M_{mix} = \sum_{i=1}^{NC} y_i M_i \qquad (2B.12)$$

The mixture critical density is then estimated from the following equation:

$$v_{C,mix} = \frac{0.30\, R\, T_{C,mix}}{P_{C,mix}} + \sum_{i=1}^{NC} y_i c_i \qquad (2B.13)$$

And finally:

$$\rho_{c,mix} = \frac{M_{mix}}{v_{c,mix}} \tag{2B.14}$$

2B.1.5 Final Comments

This correlation was used to generate the viscosity chart for pure H_2S which is shown in figure 2.6. Furthermore it has been implemented in *AQUAlibrium* and used for many acid gas projects.

One should be careful because this utilizes the volume shifted PR equation. Substituting other density data will result in increased errors in the viscosity predictions.

References

Boyle, T. and J.J. Carroll. 2002. Study determines best methods for calculating acid-gas density. *Oil & Gas J.* Jan. 14:45–53.

Boyle, T.B. and J.J. Carroll. 2001. Calculation of acid gas density in the vapor, liquid, and dense-phase regions. 51st Canadian Chemical Engineering Conference, Halifax, Nova Scotia.

Jossi, J,A., L.I. Stiel, and D. Thodos. 1962. The viscosity of pure substances in the dense gaseous and liquid phases. *AIChE J.* 8:59–62.

Peng, D-Y. and D.B. Robinson. 1976. A new two-constant equation of state. *Ind. Eng. Chem. Fund.* 15:59–64.

Vesovic, V., W.A. Wakeham, G.A. Olchowy, J.V. Sengers, J.T.R. Watson, and J. Millat. 1990. The transport properties of carbon dioxide. *J. Phys. Chem. Ref. Data.* 19:763–808.

Appendix 2C Equations of State

The material that follows provides the details of the three equations of state used in this study. Only the equations are provided, no discussion or derivation. However, the interested reader should note subtle similarities amongst the various equations.

2C.1.1 Soave-Redlich-Kwong Equation of State

$$P = \frac{RT}{v-b} - \frac{a}{v(v+b)}$$

where:

$$a_{ci} = 0.42748\frac{(RT_{ci})^2}{P_{ci}}$$

$$a_i = a_{ci}\alpha_i$$

$$\alpha_i^{0.5} = 1 + m_i(1 - T_{Ri}^{0.5})$$

$$m_i = 0.48 + 1.574\omega_i - 0.176\omega_i^2$$

$$a = \sum_{i=1}^{N}\sum_{j=1}^{N} x_i x_j (a_i a_j)^{0.5}(1 - k_{ij})$$

$$b_i = 0.08664\frac{RT_{ci}}{P_{ci}}$$

$$b = \sum_{i=1}^{N} x_i b_i$$

2C.1.2 Peng-Robinson Equation of State

$$P = \frac{RT}{v-b} - \frac{a}{v(v+b)+b(v-b)}$$

where:

$$a_{ci} = 0.457235\frac{(RT_{ci})^2}{P_{ci}}$$

$$a_i = a_{ci}\alpha_i$$

$$\alpha_i^{0.5} = 1 + m_i(1 - T_{Ri}^{0.5})$$

$$m_i = 0.37646 + 1.54226\omega_i - 0.26992\omega_i^2$$

$$a = \sum_{i=1}^{N}\sum_{j=1}^{N} x_i x_j (a_i a_j)^{0.5}(1 - k_{ij})$$

$$b_i = 0.077796\frac{RT_{ci}}{P_{ci}}$$

$$b = \sum_{i=1}^{N} x_i b_i$$

2C.1.3 The Patel-Teja Equation of State

$$P = \frac{RT}{v - b} - \frac{a}{v(v + b) + c(v - b)}$$

where:

$$a_{ci} = \Omega_a \frac{(RT_{ci})^2}{P_{ci}}$$

$$a_i = a_{ci}\alpha_i$$

$$\alpha_i^{0.5} = 1 + F(1 - T_{Ri}^{0.5})$$

$$a = \sum_{i=1}^{N}\sum_{j=1}^{N} x_i x_j (a_i a_j)^{0.5}(1 - k_{ij})$$

$$b_i = \Omega_b \frac{RT_{ci}}{P_{ci}}$$

$$b = \sum_{i=1}^{N} x_i b_i$$

$$c_i = \Omega_c \frac{RT_{ci}}{P_{ci}}$$

$$c = \sum_{i=1}^{N} x_i c_i$$

$$\Omega_a = 3\zeta_c^2 + 3(1-2\zeta_c)\Omega_b + \Omega_b^2 - 3\zeta_c^3$$

and Ω_b is the smallest real root of the following equation:

$$\Omega_b^3 + (2-3\zeta_c)\Omega_b^2 + 3\zeta_c^2\Omega_b - \zeta_c^3 = 0$$

$$\Omega_c = 1 - 3\zeta_c$$

The parameters F and ξ_c can be optimized from a set of data or they can be obtained from the following generalized equations:

$$F = 0.452413 + 1.30982\omega - 0.295967\omega^2$$

$$\zeta_c = 0.329032 - 0.076799\omega - 0.0211947\omega^2$$

The following tables summarize the parameters used for the Peng-Robinson calculations presented in this paper. The pure component properties could also be used for Soave-Redlich-Kwong calculations. Binary interaction parameters are given for both equations.

From Knapp et al. (1982) except for H_2S + CH_4, which are from this work.

Table 2C.1 Pure component parameters for equation of state calculations.

	T_C (K)	P_C (kPa)	ω (-)	MW (g/mol)
Hydrogen Sulfide	373.2	8960	0.100	34.080
Carbon Dioxide	304.2	7376	0.225	44.010
Methane	190.6	4600	0.008	16.043
Ethane	305.4	4880	0.099	30.070
Propane	369.8	4250	0.153	44.094

Table 2C.2 Binary interaction parameters for acid gas components for the PR and SRK equations.

		H_2S	CO_2	CH_4	C_2H_6	C_3H_8
CO_2	PR	0.0974	0.0000			
	SRK	0.0989	0.0000			
CH_4	PR	0.0840	0.0919	0.0000		
	SRK	0.0849	0.0933	0.0000		
C_2H_6	PR	0.0833	0.1322	−0.0020	0.0000	
	SRK	0.0852	0.1363	−0.0078	0.0000	
C_3H_8	PR	0.0878	0.1241	0.0330	−0.0067	0.0000
	SRK	0.0855	0.1289	0.0289	−0.0100	0.0000

The lower reduced temperature corresponds to 0°C, the lowest temperature of interest in this study. For the SRK, the following Peneloux-type volume shift parameters were used:

$$c_{CO_2} = -8.6650\,cm^3/mol$$
$$c_{H_2S} = -3.3826\,cm^3/mol$$

And for the PR equation, the following parameters were used here:

$$c_{CO_2} = -1.7493\,cm^3/mol$$
$$c_{H_2S} = +2.2176\,cm^3/mol$$

For the Mathias-type correction to the PR equation, the s parameter was obtained by fitting the saturated liquid density at $T_r = 0.7$ (or nearly so). The v_c values were obtained by minimizing the AAE for the range of saturated liquid given above.

$S_{CO_2} = 1.585\,cm^3/mol$ (from matching the saturated liquid density at $T_r = 0.712$, CO_2 triple point)
$S_{H_2S} = 2.998\,cm^3/mol$ (from matching the saturated liquid density at $T_r = 0.7097$)
$v_{c,CO_2} = 96.001\,cm^3/mol$(2% larger than the experimental critical volume)
$v_{c,H_2S} = 100.490\,cm^3/mol$(2.5% larger than the experimental critical volume)

This Page Intentionally Left Blank

3

Non-Aqueous Phase Equilibrium

An important aspect of the design of an acid gas injection scheme is the non-aqueous phase equilibrium. Fluid phase equilibrium involving water, which is also very important, will be discussed in chapter 4 and hydrates in chapter 5.

It is important to identify the conditions for the liquefying of acid gas. Therefore, the construction of a phase envelope is the first step in analyzing an acid gas injection scheme. The state of the mixture has a dramatic effect on all aspects of the acid gas injection design. For example, the injection pressure, as discussed in chapter 8, is critically related to the phase of the fluid being injected.

3.1 Overview

Several experimental investigations of phase equilibrium that are relevant to acid gas injection were summarized by Carroll (1999, 2002).

The binary mixture hydrogen sulfide + carbon dioxide is the most important non-aqueous system involved in acid gas injection, since acid gas is composed almost exclusively of these components.

Two early studies of the phase equilibrium in the system hydrogen sulfide + carbon dioxide were Bierlein and Kay (1953) and Sobocinski and Kurata (1959). Bierlein and Kay (1953) measured vapor-liquid equilibrium (VLE) in the range of temperature from 0° to 100°C and pressures to 9 MPa, and they established the critical locus for the binary mixture. For this binary system, the critical locus is continuous between the two pure component critical points. Sobocinski and Kurata (1959) confirmed much of the work of Bierlein and Kay (1953) and extended it to temperatures as low as −95°C, the temperature at which solids are formed. Furthermore, liquid phase immiscibility was not observed in this system. Liquid H_2S and CO_2 are completely miscible.

Robinson and Bailey (1957) and Robinson et al. (1959) studied the VLE in the ternary mixtures of hydrogen sulfide + carbon dioxide + methane. These investigations also included a few points for the binary system H_2S + CO_2. The points for the binary mixtures were at temperatures between 4° and 71°C and at pressures from 4 to 8 MPa.

More recently Kellerman et al. (1995) reported data for the thermodynamic properties, including VLE, for the system H_2S + CO_2. Their measurements of the phase boundary were for temperatures between −25° and 60°C and pressures up to 9 MPa.

3.2 Pressure-Temperature Diagrams

3.2.1 Pure Components

Figure 3.1 shows the vapor pressure of pure hydrogen sulfide and carbon dioxide. These curves terminate at the critical point, which for these two components is given in table 2.1. Only if the conditions of interest fall exactly on the curve in the plot does the fluid exist in two phases. Otherwise, the fluid is single phase.

For a system containing only a single component, boundaries between the vapor and the liquid determine the state of the substance. For the substance to be in the liquid phase, the temperature must be less than the critical temperature and the pressure must be greater than the vapor pressure. To be in the gas phase, the pressure must be less than the critical pressure and the temperature must be less than the vapor pressure. If the pressure is less than the critical

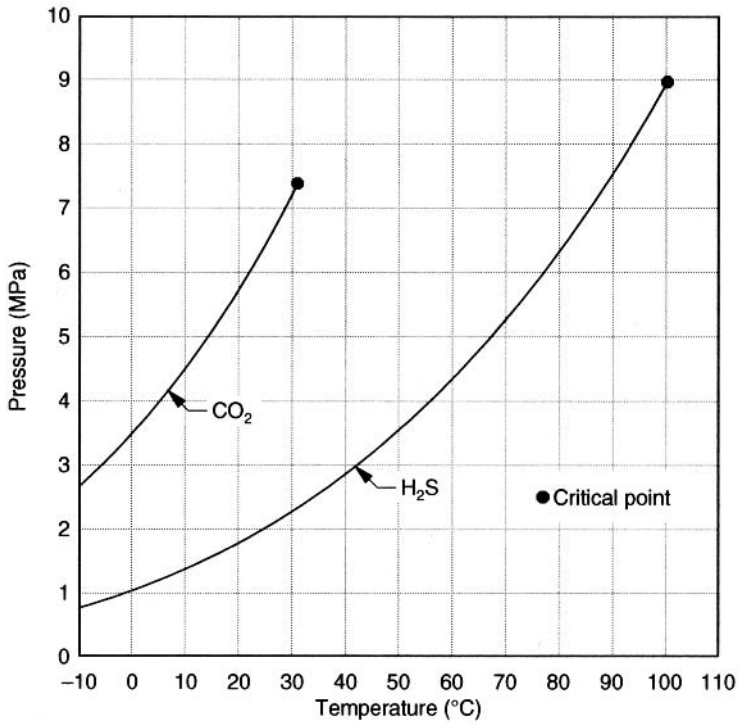

Figure 3.1 The vapor pressure of carbon dioxide and of hydrogen sulfide.

pressure but the temperature is greater than the critical temperature, the substance is in the gas region.

In engineering, we designate three fluid phases: vapor, liquid, and supercritical (sometimes called dense phase). A fluid can be any one of these three phases.

The gas phase is characterized by high compressibility. The application of pressure or a change in temperature has a significant effect on the density of the gas. As we have seen, for an ideal gas the density of the gas varies directly with the pressure (double the pressure and you double the density) and inversely with the absolute temperature.

However, the liquid phase is non-compressible. The density of an ideal liquid is not a function of either the pressure or the temperature. For a real liquid, the density is a weak function of the pressure (except near the critical point) and a weak function of the temperature. The table below demonstrates these points for H_2S well removed from the critical point.

A critical point is the point at which properties of the vapor and the liquid become the same. As one approaches a critical point, the density of the liquid decreases and the density of the vapor increases.

This leaves one other region. If the pressure is greater than the critical pressure and the temperature is greater than the critical temperature, then the fluid is said to be supercritical. The supercritical fluid shares characteristics with both gases and liquids. A supercritical fluid may have a high density (similar to a liquid) but it may also have a significant compressibility (like a gas).

For a pure component, there is a clear transition between gas and liquid phases: the vapor pressure. However, it is possible to find a path in the pressure-temperature plane where the fluid goes from the gaseous region to the liquid region without seeing a phase transition.

However, there are no clear transitions from the gas phase to the supercritical region or from the liquid to the supercritical. The fluid passes through these transitions without discontinuities in the physical properties of the fluid.

Example

3.1 Use figure 3.1 to determine the state of the fluid at the following conditions:

a) H_2S at 20°C and 3 MPa
b) CO_2 at 20°C and 3 MPa
c) H_2S at 80°C and 5 MPa
d) CO_2 at 80°C and 5 MPa
e) H_2S at 90°C and 10 MPa
f) CO_2 at 90°C and 10 MPa

Answer:

a) For hydrogen sulfide, 20°C is less than the critical temperature, and at 3MPa, this is above the vapor pressure curve. Therefore, at these conditions H_2S is a liquid.
b) For carbon dioxide, 20°C is also less than the critical temperature; however, 3 MPa is less than the vapor pressure. Therefore, at these conditions CO_2 is a gas.
c) Readers should verify the result given in the summary.
d) For CO_2, 80°C is greater than the critical temperature. However, 5 MPa is less than the critical pressure. This means that at this condition, CO_2 is a gas.

e) Readers should verify the result given in the summary.
f) For CO_2, 90°C is greater than the critical pressure and 10 MPa is greater than the critical pressure. Therefore, at these conditions CO_2 is a supercritical fluid.

Summary:
a) H_2S at 20°C and 3 MPa – **liquid**
b) CO_2 at 20°C and 3 MPa – **gas**
c) H_2S at 80°C and 5 MPa – **gas**
d) CO_2 at 80°C and 5 MPa – **gas**
e) H_2S at 90°C and 10 MPa – **liquid**
f) CO_2 at 90°C and 10 MPa – **supercritical fluid**

3.2.2 Mixtures

For mixtures, the phase envelopes expand from a curve to a region for the single component. Recall that in order for a single component to exist in two phase (vapor + liquid), the conditions had to fall exactly on the vapor pressure curve. For a mixture, there is a region over the pressure-temperature plane where two phases exist.

The condition at which the liquid just begins to form is called the dew point. The condition at which the vapor just begins to form is called the bubble point. A curve can be plotted showing the temperature and pressure at which a mixture just begins to liquefy. Such a curve is called a dew-point curve or dew-point locus. A similar curve can be constructed for the bubble point. The phase envelope is the combined loci of the bubble and dew points, which intersect at a critical point. The phase envelope maps out the regions where the various phases exist.

Figure 3.2 shows a phase envelope for an acid gas mixture. Note that the locus at lower pressure is the dew-point curve, whereas the one at higher pressure is the bubble-point curve. In fact, any point inside the phase envelope is a two-phase point.

The phase of a given mixture is determined by a method similar to the rules for a pure component. At pressures greater than the bubble point pressure, the mixture exists as a liquid. At pressures less than the dew point, the mixture exists as a gas. At a pressure between the bubble and dew points, the mixture is two phase.

For mixtures of carbon dioxide and hydrogen sulfide, a binary critical locus extends from the critical point of CO_2 and terminates at the critical point of H_2S. This is the case for H_2S and CO_2, but not for all binary mixtures.

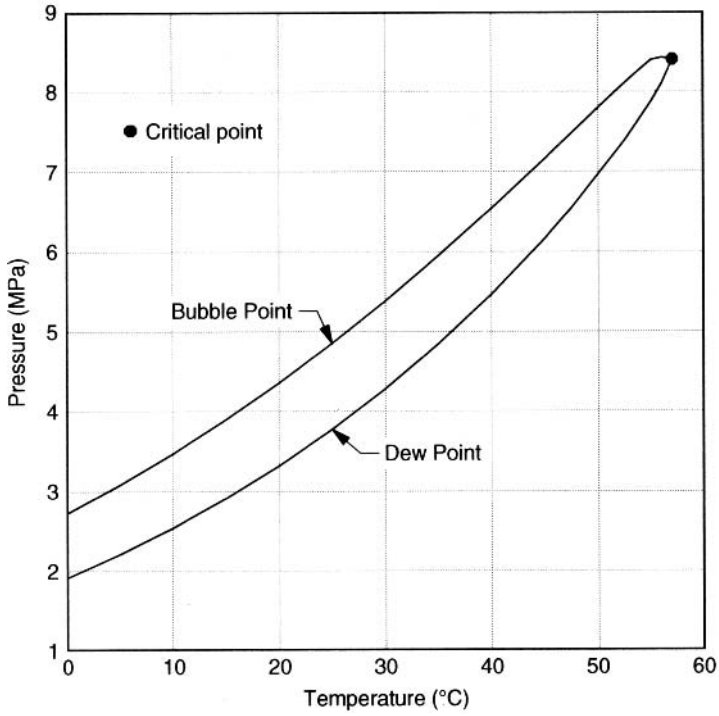

Figure 3.2 Phase envelope for an acid gas mixture containing 50 mol% CO_2 and 50 mol% H_2S.

Phase envelopes for typical natural gas tend to be fairly broad. That is, they cover a large range of temperature and pressure. On the other hand, the phase envelopes for acid gas mixtures tend to be quite narrow. Figure 3.2 shows the phase envelope for a mixture containing 50 mol% H_2S and 50 mol% CO_2. This phase envelope was calculated using the Peng-Robinson equation of state, and the bubble, dew, and critical points are labeled.

Figure 3.3 shows phase envelopes for four mixtures of hydrogen sulfide and carbon dioxide. These mixtures are based on experimental data from Bierlein and Kay (1953). The vapor pressures of the pure components are also given on this plot. For each mixture, the lower curve is the dew point and the upper curve is the bubble point.

For rapid approximations of the phase envelope, the process engineer is wise to keep this chart handy. With some insight, the design engineer can use this chart to obtain estimates of the phase equilibrium for mixtures other than those shown.

Examples

3.2 Use figure 3.2 to determine the state of an equimolar mixture of $H_2S + CO_2$ at the following conditions.

a) 20°C and 2 MPa
b) 20°C and 4 MPa
c) 20°C and 6 MPa

Answer:

a) The point at 20°C and 2 MPa is at a pressure less than the dew point, and thus the mixture is a gas.
b) The point at 20°C and 4MPa is within the phase envelope. Therefore, this is two phase.
c) The point at 20°C and 6MPa lies above the bubble point; therefore this is a liquid.

3.3 From figure 3.3, estimate the dew point at 40°C for a mixture containing 26.08% CO_2 and 73.92% H_2S. Estimate the bubble point for this mixture at 40°C.

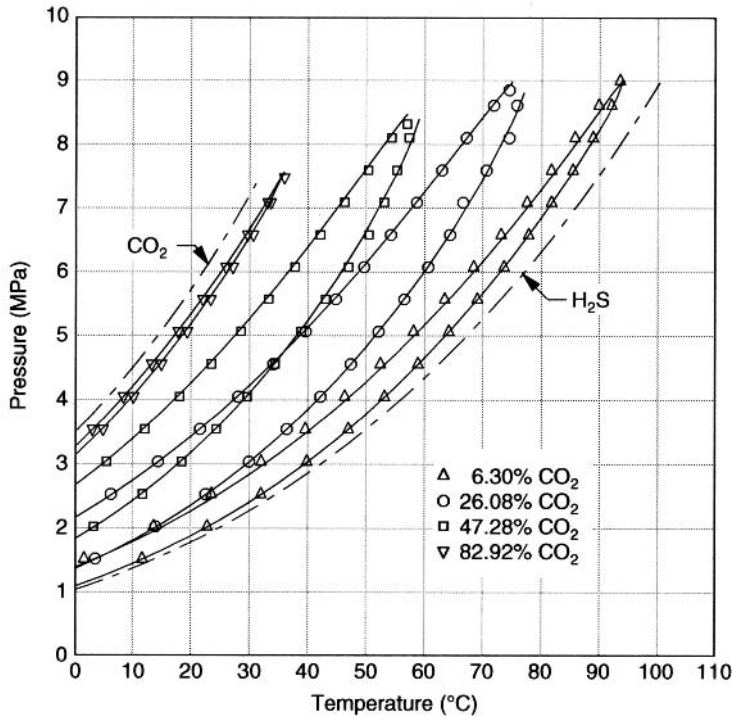

Figure 3.3 Phase envelopes for mixtures of $CO_2 + H_2S$ – data from Bierlein and Kay (1953) [curves from the Peng-Robinson equation of state].

Answer: From the plot, the dew point is about 3.8 MPa. The bubble point is almost exactly 5 MPa. For pressures less than 3.8 MPa, the mixture exists as a gas, and for pressures greater than 5 MPa the mixture is a liquid. If the pressure is between 3.8 and 5 MPa, the mixture is two-phase gas + liquid.

3.2.3 Binary Critical Points

For binary mixtures of hydrogen sulfide and carbon dioxide, the critical locus extends uninterrupted from the critical point of CO_2 to that of H_2S. The critical point of a binary mixture can be estimated from the next two figures. Figure 3.4 shows the critical temperature as a function of the composition, and figure 3.5 gives the critical pressure.

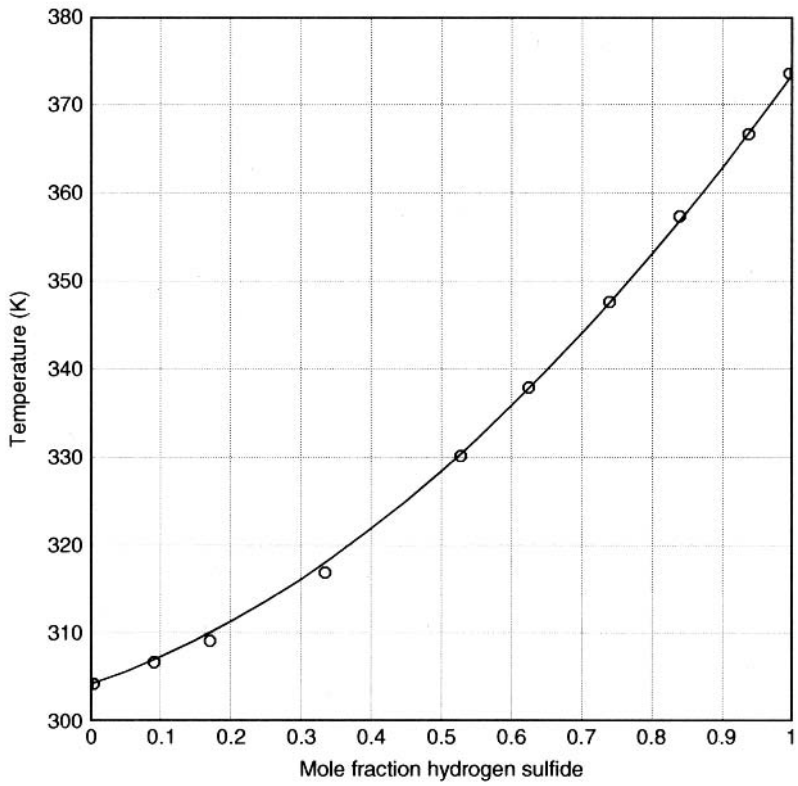

Figure 3.4 Critical temperatures for binary mixtures of H_2S and CO_2.

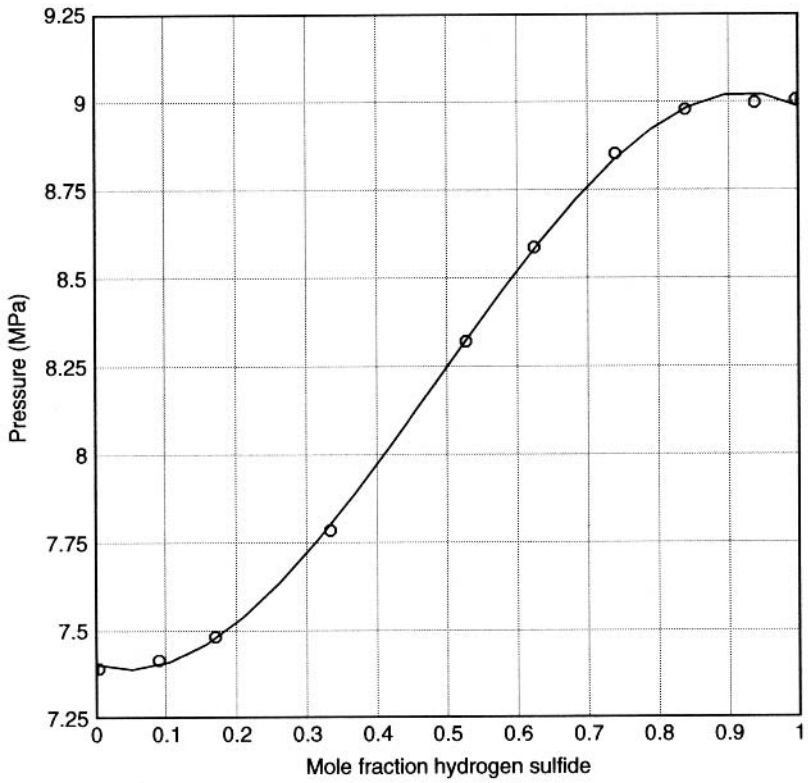

Figure 3.5 Critical pressures for binary mixtures of H_2S and CO_2.

Examples

3.4 Use figures 3.4 and 3.5 to estimate the critical point of a mixture containing 40% H_2S and 60% CO_2.

Answer: From figure 3.4 the critical temperature is:

$T_C = 322\ K = 49°C = 120°F$

and from figure 3.5:

$P_C = 7950\ kPa = 1150\ psia$

3.2.4 Effect of Hydrocarbons

Hydrocarbons are a significant impurity in an acid gas mixture. If an aqueous solution is used to sweeten the natural gas, then the hydrocarbon content of the acid gas can be 2 to 4 mol%. If a physical

solvent or a mixed solvent is used then the hydrocarbon content can be significantly higher – perhaps up to 10 mol%.

3.2.4.1 *Methane*

Methane is more volatile than H_2S and CO_2. Methane tends to vaporize more readily than acid gas and so is said to be *lighter* than acid gas.

Methane, a common impurity in acid gas, tends to broaden the phase envelope because it is lighter than the acid gas components. Figure 3.6 shows two phase envelopes. The first is the phase envelope for an equimolar mixture of hydrogen sulfide and carbon dioxide. This is the same phase envelope shown in figure 3.2. The other phase envelope is for a mixture with 2 mol% methane.

The phase envelope with the methane is broader than the one without. In essence, the dew point loci are the same for the two

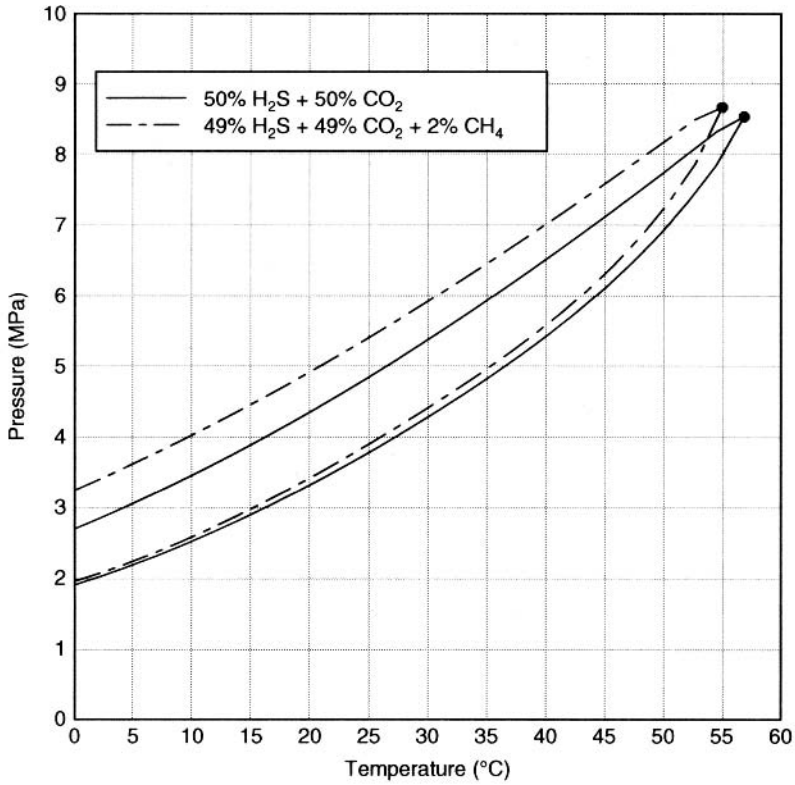

Figure 3.6 Phase envelope for an equimolar mixture of H_2S + CO_2 and showing the effect of a small amount of methane (2 mol%).

mixtures. This is because the dew point is more dependent on the less volatile components (the CO_2 and H_2S). However, the bubble point has increased significantly. The methane is harder to liquefy than the CO_2 or H_2S and this tends to increase the bubble point.

3.2.4.2 *Ethane and Propane*

When combined with acid gas mixtures, ethane and carbon dioxide exhibit azeotropy, as do propane and hydrogen sulfide. Although the azeotrope does not have a significant effect on the acid gas injection process, it tells a tale about the phase equilibrium in these mixtures.

To demonstrate the effect of ethane and propane on the phase envelopes of acid gas mixtures, consider figures 3.7 and 3.8, which

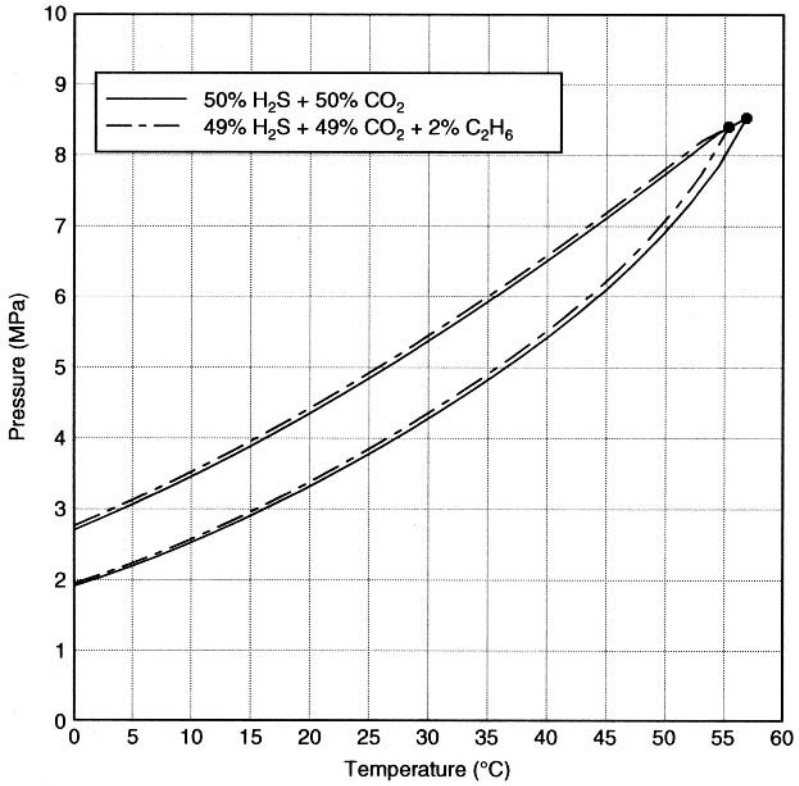

Figure 3.7 Phase envelope for an equimolar mixture of H_2S + CO_2 and showing the effect of a small amount of ethane (2 mol%).

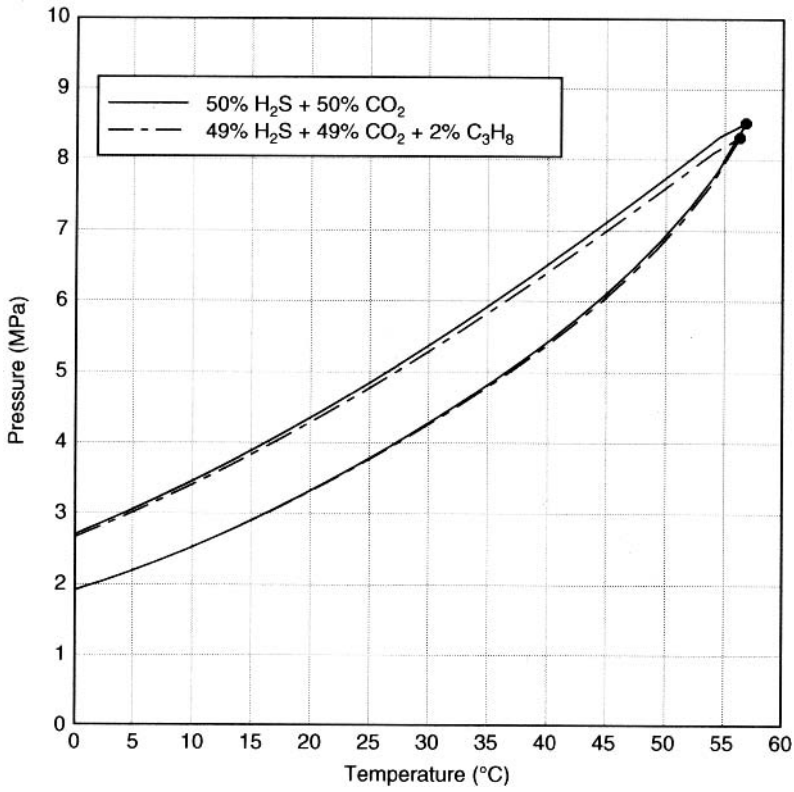

Figure 3.8 Phase envelope for an equimolar mixture of H_2S + CO_2 and showing the effect of a small amount of propane (2 mol%).

are similar to figure 3.6. Figure 3.7 shows the phase envelope for an equimolar mixture of H_2S and CO_2 and a mixture containing 2 mol% ethane, and figure 3.8 is similar except that the second phase envelope contains 2 mol% propane.

3.2.4.3 Butane and Heavier

The hydrocarbons butane and larger (and larger?) are less volatile than acid gas.

Figure 3.9 shows the effect of n-butane on the phase envelope of an equimolar mixture of H_2S and CO_2. Note how the butane decreases the dew point pressure but has only a small effect on the bubble point pressure.

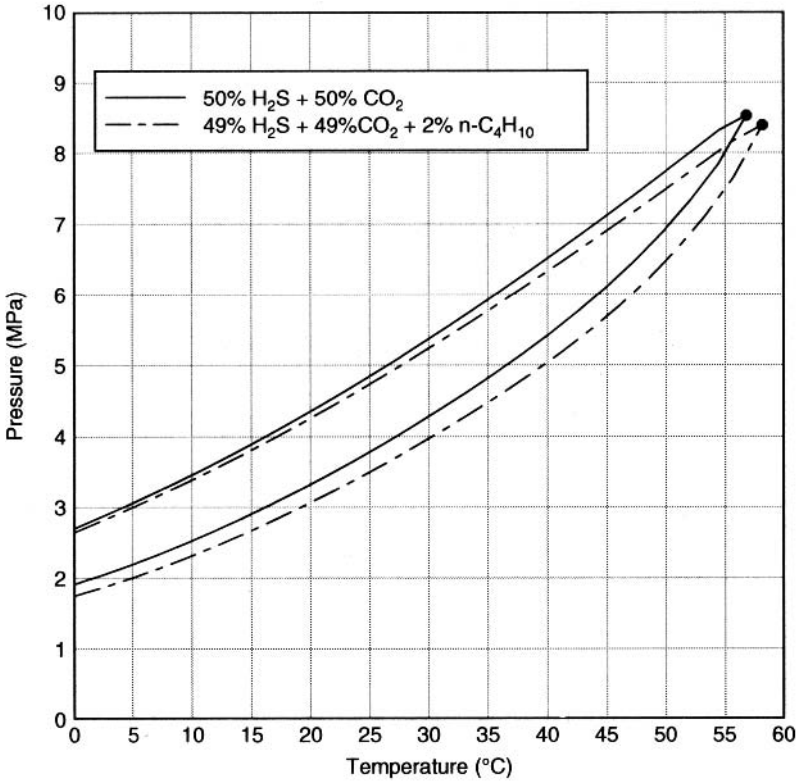

Figure 3.9 Phase envelope for an equimolar mixture of H_2S + CO_2 and showing the effect of a small amount of n-butane (2 mol%).

3.2.4.4 In Summary

The above observations can be summarized in the following points:

1. Methane is more volatile than acid gas. The presence of methane in an acid gas mixture tends to increase the bubble point pressure.
2. Ethane has approximately the same volatility as carbon dioxide.
3. Propane has approximately the same volatility as hydrogen sulfide.
4. Hydrocarbons larger than propane (butane, pentane, hexane, etc.) are less volatile than acid gas. The presence of these heavier hydrocarbons tend to decrease the bubble point pressure.

3.3 Calculation of Phase Equilibrium

Phase equilibrium calculations are usually based on the concept of the K-factor. The K-factor is defined as follows:

$$K_i = y_i/x_i \tag{3.1}$$

where: x_i – mole fraction component i in the liquid
y_i – mole fraction component i in the vapor

There are three basic phase equilibrium calculations: (1) a flash calculation – phase split at specified conditions, (2) bubble point calculation, and (3) dew point calculation. For bubble and dew points, there are two types of calculations. First, the temperature is specified and the pressure is calculated. The alternative occurs when the pressure is specified and the temperature is calculated.

3.3.1 Equations of State

The cubic equations of state have become the workhorse of the process industry, particularly in the case of natural gas. Most designs in the natural gas business are based on such equations. In chapter 2, the use of these equations for calculating thermodynamic properties was discussed. Here, their use for phase equilibrium calculations is presented.

The equations of state, commonly used for the calculation of phase equilibrium in natural gas systems, are applicable to acid gas mixtures as well. In a study of equilibrium in a single system, Clark et al. claimed that equations of state were not applicable to acid gas systems. Subsequently, Carroll (1999) demonstrated that Clark et al. (1998) were probably incorrect. Carroll (1999) performed a thorough review of the phase equilibria for these systems, which cover many systems, including acid gas and hydrocarbon systems.

The phase envelopes shown in figure 3.3, along with the experimental points from Bierlein and Kay (1953), were calculated using the original PR equation with a single interaction parameter. Figure 3.10 is a similar plot showing the predictions from the PR equation and the experimental data of Sobocinski and Kurata (1959). Finally, figure 3.11 shows the experimental data from Kellerman et al. (1995) and the predictions from the

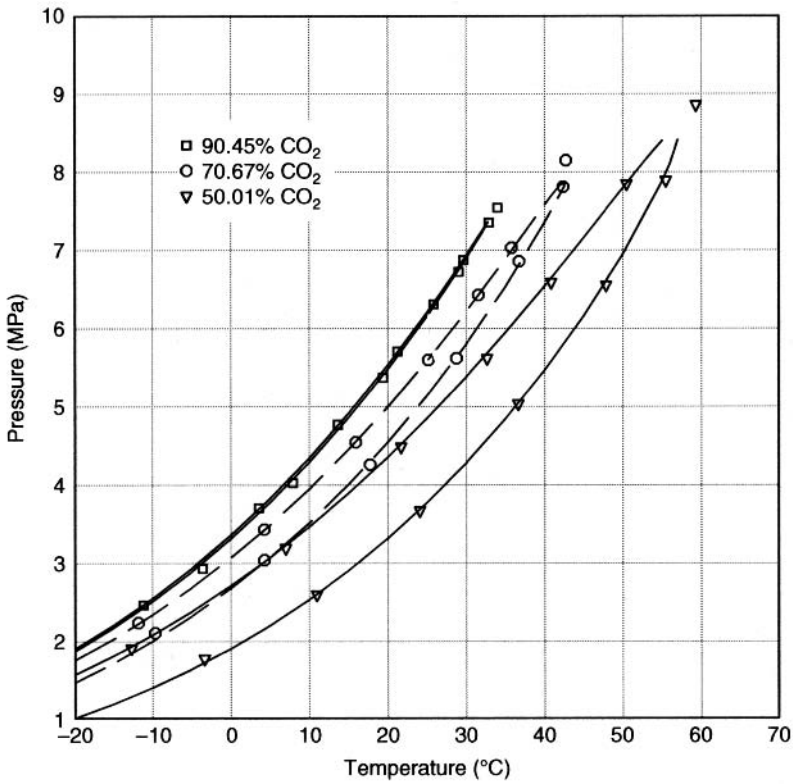

Figure 3.10 Phase envelopes for three mixtures of CO_2 + H_2S – data from Kellerman et al. (1995) and curves from the Peng-Robinson equation of state.

PR equation. These three figures demonstrate the accuracy of this equation of state for predicting the phase envelopes of acid gas mixtures.

The advantages of equations of state, and the cubic equations of state in particular, is their simplicity. However, the calculation of phase equilibrium with an equation of state is too difficult to be performed by hand. Such calculations require a computer. Fortunately, many software packages are available for such calculations.

3.3.2 K-Factor Charts

The K-factor method is designed for hand calculations. The *GPSA Engineering Data Book* contains a series of K-factor charts for estimating

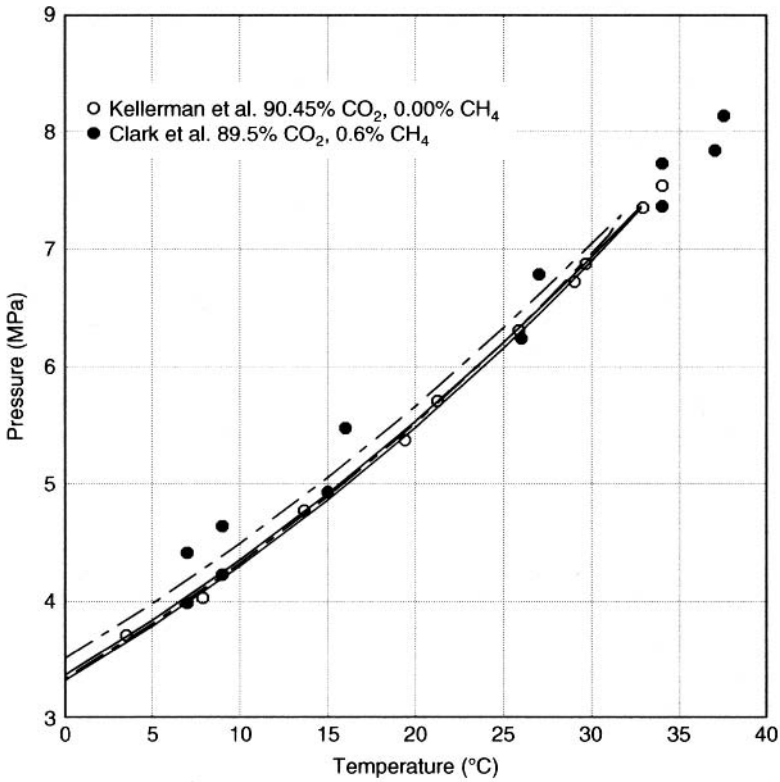

Figure 3.11 Comparison of the phase envelopes for two acid gas mixtures 1. Clarke et al. (1998) and 2. Kellerman et al. (1995) for mixtures containing approximately 90 mol% CO_2. Curves are from the Peng-Robinson equation of state.

phase equilibrium. These are fairly accurate for hydrocarbon mixtures, but their application to non-hydrocarbons is less accurate. The data book does not include a chart for carbon dioxide, but it recommends that the K-factor for carbon dioxide can be approximated as the geometric mean of the K-factors for methane and ethane.

$$K_{CO_2} = \sqrt{K_{CH_4} \times K_{C_2H_6}} \tag{3.2}$$

The charts provide estimates of the K-factors given the temperature and the pressure, but the engineer must do iterative calculations in order to obtain actual estimates of the equilibrium. A single calculation is quite time-consuming; thus repeated calculations are frustrating and take a considerable amount of time. The

construction of a phase envelope based on such methods is almost impossible.

3.4 In Summary

Phase equilibrium is also important in the design of an acid gas injection scheme. In fact, the first step in the design process is the construction of a phase envelope for the acid gas under consideration. This provides the engineer with a map indicating which phases will be encountered and under which conditions. These calculations are tedious; fortunately, software packages are available for the calculations.

Design engineers are responsible for verifying the models selected for their project – and this is true for the calculation of acid gas mixtures. Appendix A lists references to several experimental measures for systems related to acid gas. Design engineers should seek these data in order to verify their choice of models.

References

Bierlein, J.A. and W.B. Kay. 1953. Phase-equilibrium properties of system carbon dioxide-hydrogen sulfide. *Ind. Eng. Chem.* 45:618–24.

Carroll, J.J. 1999. Phase equilibria relevant to acid gas injection. Second Quarterly Meeting CGPA/CGPSA, Calgary, AB.

Carroll, J.J. 2002. Phase equilibria relevant to acid gas injection. Part 1 – Non-aqueous phase behavior. *Can. J. Petroleum Tech* 41(7):39–43.

Clark, M.A., W.Y. Svrcek, W.D. Monnery, A.K.M. Jamaluddin, D.B. Bennion, F.B. Thomas, E. Wichert, A.E. Reed, and D.J. Johnson. 1998. Designing an optimized injection strategy for acid gas disposal without dehydration. 77th Annual GPA Conv. Dallas, TX.

Robinson, D.B., and J.A. Bailey. 1957. The carbon dioxide-hydrogen sulfide-methane system. Part I. Phase behavior at 100°F. *Can. J. Chem. Eng.* 35:151–58.

Sobocinski, D.P. and F.Kurata. 1959. Heterogeneous phase equilibria of the hydrogen sulfide-carbon dioxide system. *AIChE J.* 5:545–551.

Stouffer, C.E., Kellerman, S.J., Hall, K.R., Holste, J.C., Gammon, B.E., Marsh, K.N. 2001. Densities of carbon dioxide + hydrogen sulfide mixtures from 220 K to 450 K at pressures up to 25 MPa. *J. of Chem. Eng. Data* 46:1309–18.

Appendix 3A Some Additional Phase Equilibrium Calculations

Although there are only a few studies of the VLE of acid gas mixtures, there are many studies of mixtures with CO_2 + hydrocarbons and H_2S + hydrocarbons. These data are useful for building and testing models.

3A.1.1 Hydrogen Sulfide + Hydrocarbons

Experimental investigations into binary systems containing hydrogen sulfide and light hydrocarbons are summarized in table 3A.1.

One of the interesting features of the system hydrogen sulfide + methane is liquid-phase immiscibility. The H_2S-rich and CH_4-rich liquids are immiscible. However, this occurs at temperatures well below those of interest in acid gas injection. Unusual looking phase diagrams are often obtained for mixtures rich in H_2S and CH_4 because the algorithms typically are not designed for multiple

Table 3A.1 Experimental investigations vapor-liquid equilibrium (non-aqueous) for mixtures containing hydrogen sulfide and light hydrocarbons.

Other Gas	Temp. (°C)	Pressure (MPa)	Reference
CH_4	4 to 171	1.4 to 70	Reamer et al. (1951a)
	−100 to 100	up to 13.8	Kohn and Kurata (1958)
C_2H_6	−6 to 100	up to 8.9	Kay and Rambosek (1953)
	10	1.6 to 3.1	Robinson and Kalra (1974)
	−73 to 10	0.06 to 3.1	Kalra et al. (1977)
C_3H_8	50 to 94	2.8 to 4.1	Gilliland and Scheeline (1940)
	−30 to 15	0.2 to 1.7	Steckel (1946)
	−1 to 100	1.4 to 8.3	Kay and Brice (1953)
	−56 to 71	0.1 to 2.8	Brewer et al. (1961)
	25 to 100	up to 7 MPa	Jou et al. (1995)– azeotropy

liquid phases and they get "confused" (as does the design engineer generating them).

3A.1.2 Carbon Dioxide + Hydrocarbons

Experimental investigations into binary systems containing carbon dioxide and light hydrocarbons are summarized in table 3A.2.

Among the interesting equilibria observed in these systems is that ethane and carbon dioxide exhibit azeotropy. This makes separation

Table 3A.2 Experimental investigations vapor-liquid equilibrium (non-aqueous) for mixtures containing carbon dioxide and light hydrocarbons.

Other Gas	Temp. (°C)	Pressure (MPa)	Reference
CH_4	−73 to 23	1.4 to 8.3	Donnelly and Katz(1954)
	−176 to −61	up to 4.8	Davis et al. (1962)
	−68 to −75	4 to 5.5	Sterner (1961)
	−40 to 10	3.7 to 8.2	Kaminishi et al. (1968)
	−87 to −53	2.7 to 6.9	Neumann and Walch (1968)
	−20 to 15	2.6 to 8.6	Arai et al. (1971)
	−120 to −54	1.2 to 6.4	Hwang et al. (1976)
	−43 to −23	0.9 to 8.5	Davalos et al. (1976)
	−3	3.2 to 8.4	Somait and Kidnay (1978)
	−120 to −54	0.6 to 4.7	Mraw et al. (1978)
	−54 to −3	0.6 to 8.5	Al-Sahhaf et al. (1983)
	15 and 20	5.1 to 8.15	Xu et al. (1992)
	28	6.9 to 7.7	Bian et al. (1993)
	−43 to −3	0.9 to 8.3	Wei et al. (1995)
C_2H_6	10 to 20	3.1 to 6.3	Khazanova and Lesnevshaya (1967)
	−31 to 10	up to 5	Gugnoni et al. (1973)

Table 3A.2 (Cont.) Experimental investigations vapor-liquid equilibrium (non-aqueous) for mixtures containing carbon dioxide and light hydrocarbons.

Other Gas	Temp. (°C)	Pressure (MPa)	Reference
	−31 to 10	up to 5	Gugnoni et al. (1974)
	−20	1.4 to 2.3	Nagahama et al. (1974)
	16	3.6 to 5.5	Robinson and Kalra (1974)
	−50 to 20	0.5 to 6.3	Fredenslund and Mollerup (1974)
	−23	1.3 to 2.1	Davalos et al. (1976)
	10 to 25	3 to 6.6	Ohgaki and Katayama (1977)
	−33 to −3	1.5 to 3.6	Brown et al. (1988)
	−33 to −3	0.3 to 3.3	Wei et al. (1995)
C_3H_8	17 to 93	up to 7	Poettmann and Katz (1945)
	4 to 71	up to 7	Reamer et al. (1951b)
	−40 to 0	0.1 to 3.5	Akers et al. (1954)
	32 to 88	5 to 7	Roof and Baron (1967)- critical
	−20 to 0	0.2 to 3.5	Nagahama et al. (1974)
	−29 and −7	0.5 to 2.6	Hamam and Lu (1976)

of these two components by binary distillation impossible. Another feature of systems containing CO_2 is that solids (dry ice) may form at temperatures encountered in cryogenic processing. Although these temperatures are not of interest in acid gas injection, the design engineer should be aware of them for other applications.

3A.1.3 Multicomponent Mixtures

Table 3A.3 summarizes the experimental investigations into multicomponent systems containing hydrogen sulfide and/or carbon dioxide with light hydrocarbons.

Table 3A.3 Experimental investigations vapor-liquid equilibrium (non-aqueous) for mixtures containing hydrogen sulfide and/or carbon dioxide and light hydrocarbons.

Gas	Temp. (°C)	Pressure (MPa)	Reference
$H_2S+CO_2+CH_4$	38	4.1 to 12.4	Robinson and Bailey (1957)
	4 and 71	6.9 to 12.4	Robinson et al. (1959)
	−34 to −51	2.1 to 4.8	Hensel and Massoth (1964)
	−83 to 29	1 to 13	Ng et al. (1985)†
$CO_2+CH_4+C_2H_6$	−23	2.1 to 3.0	Davalos et al. (1976)
	−43	1.1 to 6.6	Wei et al. (1995)
$H_2S+CO_2+CH_4+H_2O$	6 to 37	4.0 to 8.5	Clark et al. (1998)

†these measurements cont ained a small amount of water in a mixture of H_2S + CO_2 + CH_4 but are not water-content measurements

An interesting investigation of the ternary mixture $H_2S + CO_2 + CH_4$ was performed by Ng et al. (1985). Although much of this study was at temperatures below those of interest in acid gas injection, it provides data useful for testing phase-behavior prediction models. The multiphase equilibrium that Ng et al. observed for this mixture, including multiple critical points for a mixture of fixed composition, should be of interest to all engineers working with such mixtures. It demonstrates that the equilibria can be complex, even for relatively simple systems.

As another illustration, consider the ternary mixture H_2S + CO_2 + CH_4. Figure 3A.1 shows the triangular diagram for this ternary mixture at 37.8°C at two pressures, 4.137 and 8.274 MPa. The calculation from the PR equation is shown along with experimental data from Robinson and Bailey (1957).

Figure 3A.1 requires explanation. At 4.137 MPa, the two-phase region is a trapezoid. The trapezoid extends from binary VLE between CO_2 and H_2S to binary VLE between H_2S and CH_4. To the left of this trapezoid, the fluid is a vapor. These fluids would be rich in methane. To the right of the trapezoid the mixture is a liquid.

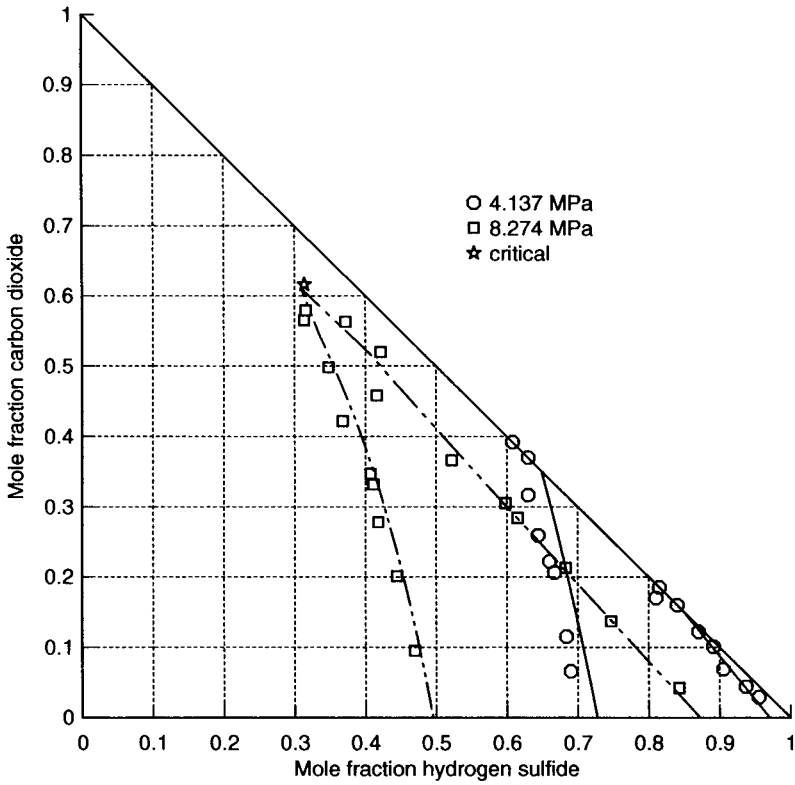

Figure 3A.1 Ternary phase diagram for two mixtures of hydrogen sulfide + carbon dioxide + methane [data from Robinson and Bailey (1957) and curves from the Peng-Robinson equation of state].

At the higher pressure, the two-phase region is the space bounded by the triangle (one apex of the triangle being a critical point). As before, to the left of this triangle, the fluid exists as a vapor and to the right the mixture is a liquid. For a given temperature and pressure, the overall composition dictates the nature of the phase equilibrium. For example, a mixture containing 30% H_2S, 30% CO_2, and 40% CH_4 would be a vapor at 37.8°C and 8.274 MPa. A mixture with an overall composition of 50% H_2S, 30% CO_2, and 20% CH_4 would be two-phase at 37.8°C and 8.274 MPa. The composition of the equilibrium phases is given by a tie-line, which is not shown. Therefore, the compositions of the phases are not obvious from the given figure. Finally, a mixture 75% H_2S, 20% CO_2, and 5% CH_4 would be a liquid at 37.8°C and 8.274 MPa. If the pressure of

this mixture was reduced to 4.137 MPa, then it would be in the two-phase region (inside the trapezoidal region).

Figure 3A.1 demonstrates that the PR equation is a good prediction of the ternary phase behavior. This is noteworthy because the model only includes binary parameters. No additional tuning was performed to do the ternary predictions.

As a final case, figure 3A.2 shows the pressure-temperature diagram (phase envelope) for the mixture containing 40.23% H_2S, 9.88% CO_2, and 49.89% CH_4, which is the mixture studied by Ng et al. (1985.) The data points on the plot are their data.

Again, this figure requires some explanation. Only the region greater than −15°C is shown. This limit was imposed for two reasons. First, this is the region of interest to acid gas injection. Second, at lower temperatures some of the unusual phase behavior mentioned earlier manifests. Although interesting, this phase behavior

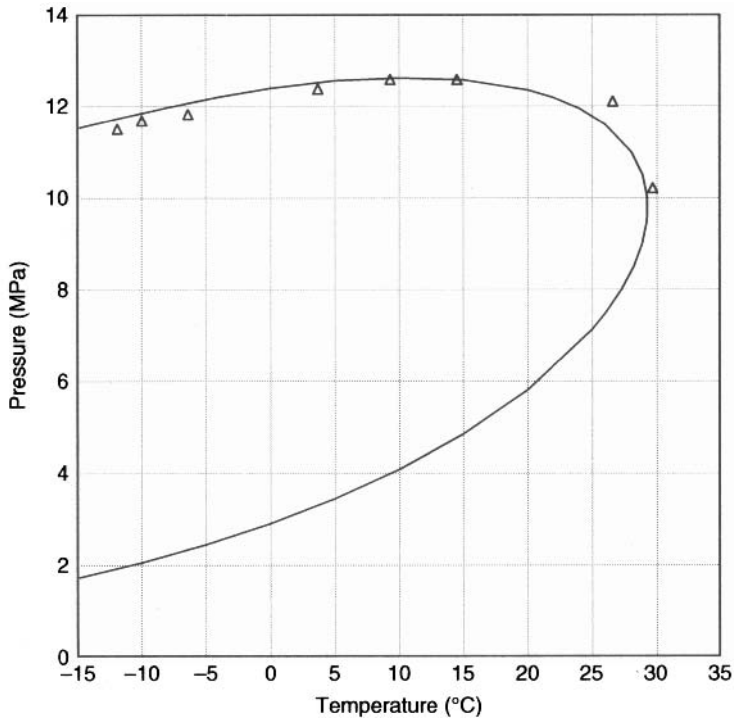

Figure 3A.2 Phase envelope for a ternary mixture of H_2S (40.23 mol%), CO_2 (9.88 mol%), and methane (49.89 mol%) [data from Ng et al. (1985) and curves from the Peng-Robinson equation of state].

is not important to this study or to the design of acid gas injection. The reader is referred to the original work for discussion of this phenomenon.

The curve and the data points shown in figure 3A.2 are all dew points, incipient liquid formation. The experimental critical temperature for this mixture is −16.9°C. Therefore, the plot presents the large retrograde region for this mixture. From the PR calculations, the cricondentherm is estimated to be 29°C. In this mixture, liquid can form at a temperature almost 45 Celsius degrees higher than the critical temperature. The cricondenbar is estimated to be 12.5 MPa. It is difficult to confirm the location of either the cricondenbar or the cricondentherm with the available experimental data. However, the PR fits the data, and thus it can be concluded that the estimation of these points is quite accurate as well.

References

Akers, W.W., R.E. Kelly, and T.G. Lipscomb. 1954. "Carbon Dioxide-Propane System", *Ind. Eng. Chem.*, 46:2535–2536.

Al-Sahhaf, T.A., A.J. Kidnay, and E.D. Sloan. 1983. "Liquid+Vapor Equilibria in the N_2+CO_2+CH_4 System", *Ind. Eng. Chem. Fundam.*, 22:372–380.

Arai, Y., G.-I. Kaminishi, and S. Saito. 1971. "The Experimental Determination of the P-V-T-X Relations for the Carbon Dioxide-Nitrogen and the Carbon Dioxide-Methane Systems"; *J. Chem. Eng. Japan*, 4:113–122.

Bian, B., Y. Wang, J. Shi, E. Zhao, and B.C.-Y. Lu. 1993. "Simultaneous Determination of Vapor-Liquid Equilibrium and Molar Volumes for Coexisting Phases up to the Critical Temperature with a Static Method", *Fluid Phase Equil.*, 90:177–187.

Bierlein, J.A. and Kay, W.B. 1953. "Phase-Equilibrium Properties of System Carbon Dioxide-Hydrogen Sulfide"; *Ind. Eng. Chem.*, 45:618–624.

Brewer, J., N. Rodewald, and F. Kurata. 1961. "Phase Equilibria of the Propane-Hydrogen Sulfide System from the Cricondentherm to Solid-Liquid-Vapor Region", *AIChE J.* 7:13–16.

Brown, T.S., A.J. Kidnay, and E.D. Sloan. 1988. "Vapor-Liquid Equilibria in the Carbon Dioxide-Ethane System" *Fluid Phase Equil.*, 40:169–184.

Clark, M.A., W.Y. Svrcek, W.D. Monnery, A.K.M. Jamaluddin, D.B. Bennion, F.B. Thomas, E. Wichert, A.E. Reed, and D.J. Johnson. 1998. "Designing an Optimized Injection Strategy for Acid Gas Disposal Without Dehydration"; *77th Annual GPA Convention*, Dallas, TX.

Davalos, J., W.R. Anderson, R.E. Phelps, and A.J. Kidnay. 1976. "Liquid-Vapor Equilibria at 250.00 K for Systems Containing Methane, Ethane, and Carbon Dioxide", *J. Chem. Eng. Data*, 21:81–84.

Davis, J.A., N. Rodewald, and F. Kurata. 1962. "Solid-Liquid-Vapor Phase Behavior of the Methane-Carbon Dioxide System", *AIChE J.*, 8:537–539.

Donnelly, H.G. and Katz, D.L. 1954. "Phase Equilibria in the Carbon Dioxide-Methane System", *Ind. Eng. Chem.*, 46:511–517.

Fredenslund, Aa. and Mollerup, J. 1974. "Measurement and Prediction of Equilibrium Ratios for the C_2H_6+CO_2 System", *J. Chem. Soc. Faraday Trans. I*, 70:1653–1660.

Gilliland, E.R. and Scheeline, H.W. 1940. "High-Pressure Vapor-Liquid Equilibrium for Systems Propylene-Isobutane and Propane-Hydrogen Sulfide", *Ind. Eng. Chem.*, 32:48–54.

Gugnoni, R.J., J.W. Eldrige, V.C. Okay, and T.J. Lee. 1973. "CO_2-Ethane System Predictions", *Hydro. Process.*, 52 (9):197–198.

Gugnoni, R.J., J.W. Eldrige, V.C. Okay, and T.J. Lee. 1974. "Carbon Dioxide-Ethane Phase Equilibrium and Densities from Experimental Measurements and the B-W-R Equation", *AIChE J.*, 20:357–362.

Hamam, S.E.M. and Lu, B.C.-Y. 1976. "Isothermal Vapor-Liquid Equilibria in Binary System Propane-Carbon Dioxide", *J. Chem. Eng. Data*, 21:200–204.

Hensel, W.E. and Massoth, F.E. 1964. "Phase Equilibria for the Ternary System: CH_4-CO_2-H_2S at Low Temperature", *J. Chem. Eng. Data*, 9:352–356.

Huang, S.S.-S., A.-D. Leu, H.-J. Ng, and D.B. Robinson. 1985. "The Phase Behavior of Two Mixtures of Methane, Carbon Dioxide, Hydrogen Sulfide, and Water"; *Fluid Phase Equil.*, 19:21–32.

Huron, M.-J., G.-N. Dufour, and J. Vidal. 1978. "Vapor-Liquid Equilibrium and Critical Locus Curve Calculations with the Soave Equation for Hydrocarbon Systems with Carbon Dioxide and Hydrogen Sulphide"; *Fluid Phase Equil.*, 1:247–265.

Hwang, S.-C., H.-M. Lin, P.S. Chappelear, and R. Kobayashi. 1976. "Dew Point Study in the Vapor-Liquid Region of the Methane-Carbon Dioxide System", *J. Chem. Eng. Data*, 21:493–497.

Jou, F.-Y, J.J. Carroll, and A.E. Mather. 1995. "Azeotropy and Critical Behavior in the System Propane-Hydrogen Sulfide", *Fluid Phase Equil.*, 109:235–244.

Kalra, H., D.B. Robinson, and T.R. Krishnan. 1977. The Equilibrium Phase Properties of Ethane-Hydrogen Sulfide System at Subambient Temperatures", *J. Chem. Eng. Data*, 22:85–88.

Kaminishi, G., Arai, S. Saito, and S. Maeda. 1968. "Vapor-Liquid Equilibria for Binary and Ternary Mixtures Containing Carbon Dioxide", *J. Chem. Eng. Japan*,1: 109–116.

Kay, W.B. and Brice, D.B. 1953. "Liquid-Vapor Equilibrium Relations in Binary Systems. Propane-Hydrogen Sulfide System", *Ind. Eng. Chem.*, 45:221–226.

Kay, W.B. and Rambosek, G.M. 1953. "Liquid-Vapor Equilibrium Relations in the Ethane-Hydrogen Sulfide System", *Ind. Eng. Chem.*, 45:615–618.

Kellerman, S.J., C.E. Stouffer, E.U. Eubank, J.C. Holste, K.R. Hall, B.E. Gammon, and K.N. Marsh. 1995. "Thermodynamic Properties of

CO_2+H_2S" Mixtures; *Research Report RR-141*, Gas Processors Association, Tulsa, OK.

Khazanova, N.E. and Lesnevskaya, L.S. 1967. "Phase and Volume Relations in the System Ethane-Carbon Dioxide", *Russ. J. Phys. Chem.*, 41:1279–1282.

Kohn, J.P. and Kurata, F. 1958. "Heterogeneous Phase Equilibria of the Methane-Hydrogen Sulfide System", *AIChE J.*, 4:211–216.

Mraw, S.C., S.-C. Hwang, and R. Kobayashi. 1978. "Vapor-Liquid Equilibrium of the CH_4-CO_2 System at Low Temperature", *J. Chem. Eng. Data*, 23:135–139.

Nagahama, K., H. Konishi, D. Hoshino, and M. Hirata. 1974. "Binary Vapor-Liquid Equilibria of Carbon Dioxide-Light Hydrocarbons at Low Temperature;",*J. Chem. Eng. Japan*, 7:323–328.

Ng, H.-J., D.B. Robinson, and A.-D. Leu. 1985. "Critical Phenomena in a Mixture of Methane, Carbon Dioxide and Hydrogen Sulfide"; *Fluid Phase Equil.*, 19:273–286.

Neumann, A. and Walch, W. 1968. "Dampf/Flüssigkeits-Gleichwicht CO_2/CH_4 im Bereich tiefer Temperaturen und kleiner CO_2-Molenbrüche", *Chem. Ing. Tech.*, 40:241–244.

Ohgaki, K. and Katayama, T. 1977. "Isothermal Vapor-Liquid Equilibrium Data for the Ethane-Carbon Dioxide System at High Pressure" *Fluid Phase Equil.*, 1:27–32.

Peng, D.-Y. and Robinson, D.B. 1976. "A New Two-Constant Equation of State"; *Ind. Eng. Chem. Fundam.*, 15:59–64.

Poettmann, F.H. and Katz, D.L. 1945. "Phase Behavior of Binary Carbon Dioxide-Paraffin Systems", *Ind. Eng. Chem.*, 37:847–853.

Reamer, H.H., B.H. Sage, and W.N. Lacey. 1951a. "Phase Equilibria in Hydrocarbon Systems. Volumetric and Phase Behavior of the Methane-Hydrogen Sulfide System", *Ind. Eng. Chem.*, 43:976–981.

Reamer, H.H., B.H. Sage, and W.N. Lacey. 1951b. "Phase Equilibria in Hydrocarbon Systems. Volumetric and Phase Behavior of the Propane-Carbon Dioxide System", *Ind. Eng. Chem.*, 43:2515–2520.

Robinson, D.B., and Bailey, J.A. 1957. "The Carbon Dioxide-Hydrogen Sulfide-Methane System. Part I. Phase Behavior at 100°F"; *Can. J. Chem. En.*, 35:151–158.

Robinson, D.B. and Kalra, H. 1974. "The Phase Behavior of Selected Hydrocarbon-Non Hydrocarbon Systems; *53rd Annual GPA Convention*, Denver, CO.

Robinson, D.B., A.P. Lorenzo, and C.A. Macrygeorgos. 1959. "The Carbon Dioxide-Hydrogen Sulfide-Methane System. Part II. Phase Behavior at 40°F and 160°F"; *Can. J. Chem. Eng.*, 37:212–217.

Roof, J.G. and Baron, J.D. 1967. "Critical Loci of Binary Mixtures of Propane with Methane, Carbon Dioxide, and Nitrogen", *J. Chem. Eng. Data*, 12:292–293.

Soave, G. 1972. "Equilibrium Constants from a Modified Redlich-Kwong Equation of State"; *Chem. Eng. Sci.*, 27:1197–1203.

Sobocinski, D.P. and Kurata, F. 1959. "Heterogeneous Phase Equilibria of Hydrogen Sulfide-Carbon Dioxide System"; *AIChE J.*, 5:545–551.

Somait, F.A. and Kidnay, A.J. 1978. "Liquid-Vapor Equilibria at 270.00 K for Systems Containing Nitrogen, Methane, and Carbon Dioxide", *J. Chem. Eng. Data*, 23:301–305.

Steckel, F. 1946. "Dampf-Flüssigkeit-Gleichwichte einiger binärer schwefel-wasserstoff-haltiger Systeme unter Druck", *Svensk. Kem. Tid.*, 57:209–216.

Sterner, C.J. 1961. "Phase Equilibria in CO_2-Methane Systems", *Advan. Cryo. Eng.*, 6:467–474.

Wei, M.S.-W., T.S. Brown, A.J. Kidnay, and E.D. Sloan. 1995. "Vapor+Liquid Equilibria for the Ternary System Methane+Ethane+ Carbon Dioxide at 230 K and Its Constituent Binaries at Temperatures from 207 to 270 K", *J. Chem. Eng. Data*, 40:726–731.

Xu, N., J. Dong, Y. Wang, and J. Shi. 1992. "High Pressure Vapor Liquid Equilibria at 293 K for Systems Containing Nitrogen, Methane and Carbon Dioxide", *Fluid Phase Equil.*, 81:175–186.

Appendix 3B Accuracy of Equations of State for VLE in Acid Gas Mixtures

In the late 1970's Knapp et al. (1982) performed a very thorough review of VLE for systems of interest in the natural gas processing industry. They summarized their results in terms of the estimate bubble point pressure ($\Delta P/P$) and the estimate vapor composition (Δy). They reported other errors associated with their predictions, but these are the most significant to this discussion.

For the purposes of this appendix, only three equations will be discussed and they are the Peng-Robinson (PR), the Soave-Redlich-Kwong (SRK), and the starling modification of the BWR equation (BWRS). The first two are cubic equations of state and were discussed in some detail in the appendix to Chapter 2. The BWRS is a multi-constant equation of state (Starling, 1966). Each of

Table 3B.1 The performance of three equations of state for predicting the phase behavior of binary mixtures of hydrogen sulfide and other components in the acid gas mixture.

Binary Pair	Equation of State	$\Delta P/P$ (%)	Δy (mole %)	Rejected Points
$H_2S + CO_2$	PR	1.30	0.93	2
	SRK	1.13	0.96	2
	BWRS	3.53	2.70	47
$H_2S + C_2H_6$	PR	1.47	1.06	0
	SRK	1.29	0.92	0
	BWRS	3.52	2.70	0
$H_2S + C_3H_8$	PR	2.32	1.90	5
	SRK	2.46	1.98	0
	BWRS	3.26	4.04	5
$H_2S + i\text{-}C_4H_{10}$	PR	1.36	2.35	3
	SRK	1.62	1.95	1
	BWRS	2.93	4.68	3
$H_2S + N_2$	PR	16.22	2.27	0
	SRK	16.82	2.36	0
	BWRS	81.34	19.19	2

Table 3B.2 The performance of three equations of state for predicting the phase behavior of binary mixtures of carbon dioxide and other components in the acid gas mixture.

Binary Pair	Equation of State	ΔP/P (%)	Δy (mole %)	Rejected Points
$CO_2 + H_2S$	PR	1.30	0.93	2
	SRK	1.13	0.96	2
	BWRS	3.53	2.70	47
$CO_2 + CH_4$	PR	2.19	0.70	21
	SRK	2.21	0.69	17
	BWRS	6.29	2.68	13
$CO_2 + C_2H_6$	PR	0.70	0.87	0
	SRK	0.73	0.86	0
	BWRS	1.67	2.31	75
$CO_2 + C_3H_8$	PR	2.98	1.61	0
	SRK	3.05	1.68	0
	BWRS	5.40	5.77	37
$CO_2 + i\text{-}C_4H_{10}$	PR	3.61	1.99	3
	SRK	3.77	2.06	2
	BWRS	7.05	8.23	6
$CO_2 + n\text{-}C_4H_{10}$	PR	2.79	0.79	1
	SRK	3.08	0.75	4
	BWRS	5.74	6.21	11
$CO_2 + N_2$	PR	2.88	1.04	14
	SRK	2.66	1.13	15
	BWRS	9.68	2.25	20

these equations of state has only one binary parameter and it was obtained by fitting the vapor liquid equilibrium. In this case the interaction parameters were obtained by minimizing the error in the predicted bubble point pressure.

The study of is summarized in table 3B.1 for binaries containing H_2S and table 3B.2 for those contain CO_2. For some reason, the binary pairs $H_2S + CH_4$ and $H_2S + n\text{-}C_4H_{10}$ were not included in their study. Also included in this table is the number of points for which

the calculation routine did not converge – the "Rejected Points". Although this could be an indication of the skill of the programmer, it is most likely a reflection of the robustness of the model.

In general the PR and SRK equation perform equally well for these mixtures with errors in the bubble point pressure typically less than 3% and errors in the vapor composition typically less than 2 mol%. A notable exception to this is the binary H_2S + N_2, which has significantly larger errors. The authors of the original study do not provide an explanation for this result and none is present here.

Perhaps the key binary from an acid gas injection point of view is H_2S + CO_2. From the study of Knapp et al. (1982) it can be seen that the PR and SRK equations result in excellent predictions for this binary with errors in the estimated bubble point pressure less than 1.5% and errors in the vapor phase composition less than 1 mol%.

The more complex BWRS equation performs worse than the two cubic equations (the errors are consistently higher for both the bubble point and the vapor composition) and consistently had more rejected points (i.e is less robust).

This demonstrates in a quantitative way that the commonly used cubic equations of state are sufficiently accurate for predicting the phase equilibria in acid gas mixtures.

References

Knapp, H., Döring, R., Oellrich, L., Plöcker, U. and Prausnitz, J.M. 1982. *Vapor-Liquid Equilibria for Mixtures of Low Boiling Point Substances. DECHEMA Chemistry Data Series, Vol. VI*, DECHEMA, Frankfurt, Germany.

Starling, K.E. 1966. "A New Approach for Determining Equation-of-State Parameters Using Phase Equilibria Data", *Soc. Petrol. Eng. J*, 363–371.

4

Fluid Phase Equilibria Involving Water

Water is almost always associated with the acid gas resulting from the sweetening of natural gas. This is not produced water, which contains dissolved salts, which causes additional problems – this is condensed water and contains no dissolved solids. Since the water in the acid gas is present originally in the gas phase, there is no concern regarding brine.

The presence of water in the acid gas poses several problems. These include corrosion and hydrate formation. Hydrates are discussed in detail in the next chapter and corrosion is mentioned throughout this textbook, where appropriate. However, at this point it is important to state that "dry" acid gas, that is acid gas with no free water present, is not corrosive to common steels, even carbon steel. Thus it is important to: 1. Predict where liquid water may form in the system and 2. Design to prevent water formation form occurring.

The water content of a fluid is the amount of water that it can hold at the given temperature and pressure. If the overall mixture contains less than this amount, then it is said to be undersaturated and a water-rich phase will not form. If the stream contains more than this amount, then it is over saturated and a water-rich phase

will form. Depending upon the conditions, this water-rich phase may be liquid water, ice, or a hydrate.

Many of the results regarding the phase equilibria presented in this chapter are from Carroll (1999b, 2002). The reader is referred to that paper for a detailed review of the experimental investigations and for additional calculations. A recent study by Marriott et al. (2009) also provides an interesting review of the water content of acid gas mixtures. Valtz et al. (2004) provide a thorough review of the phase equilibra in mixture of CO_2 + water, including water content. Chapoy et al. (2005) Provide a similar study for the equilibria in H_2S + water.

In this chapter, the solubility of acid gas in water and brine is also discussed. Although brine is not a problem in the injection system, the reservoir may contain brine and thus the solubility in brine is important in reservoir modeling.

4.1 Water Content of Hydrocarbon Gas

The water content of hydrocarbon gas[1] has been studied thoroughly and there are several shortcut methods that are accurate for the prediction of this behavior. It is not our intention to present a complete review of the water content of hydrocarbon gas, but to present an introduction and to contrast its behavior with that of acid gases.

One observation can be made about the water content of sweet gas: As the pressure increases, the water content decreases. This is the case for all pressures of concern to the natural gas production and processing industries – that is, for pressures up to about 100 MPa (15,000 psi).

Figure 4.1 shows the water content of methane as a function of pressure for three isotherms. The data are from Olds et al. (1942), and the calculations (solid lines) are from *AQUAlibrium*.[2] *AQUAlibrium* will be discussed in more detail later in this chapter.

---

1. Normally this would be referred to as "sweet" gas but sweet gas includes gas that is rich in CO_2. Thus one must be cautious with this terminology because a gas rich in CO_2 behaves more like sour gas than hydrocarbon gas even though by the strict definition it is considered sweet.

2. *AQUAlibrium* is a software package available from FlowPhase. See www.flowphase.com

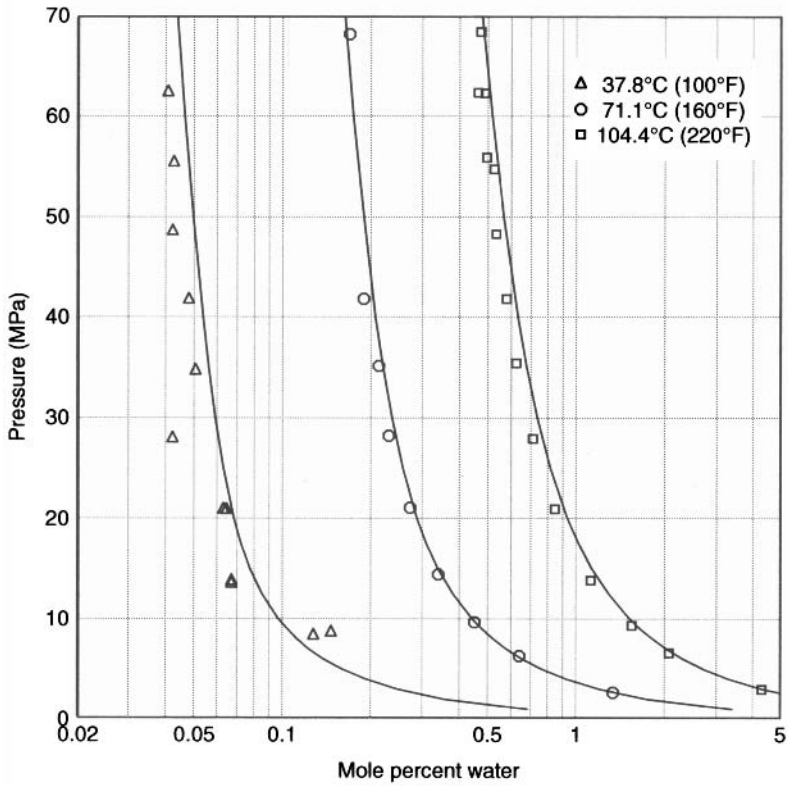

Figure 4.1 Water content of methane [data from Olds et al. (1942), curves from *AQUAlibrium*].

4.2 Water Content of Acid Gas

The water content of acid gases is significantly different from that of sweet gas. Water is significantly more soluble in acid gas than it is in hydrocarbon gas. In addition, as will be demonstrated, the water content of acid gas mixtures exhibit a minimum.

Another important aspect of the water content is that acid gases tend to liquefy much more readily than light hydrocarbon gas. Furthermore, the water content of the liquefied acid gas increases dramatically. That is, the water content of liquid acid gas is significantly greater than the vapor acid gas at the same conditions.

4.2.1 Carbon Dioxide

Figure 4.2 shows the water content of carbon dioxide for four isotherms. The experimental data come from several sources; hence the number of different points. The calculations are from *AQUAlibrium*. The minimum in the water content of the gas can be seen clearly in this plot. For example, at 50°C the minimum water content occurs at about 8.5 MPa, which is a water content of about 0.33 mol%.

At the temperatures plotted in figure 4.2, carbon dioxide does not liquefy. Only at temperatures below about 32°C will a CO_2-rich liquid form. This is in contrast to the isotherms that will be shown for hydrogen sulfide, which show a distinct break at the liquefaction point.

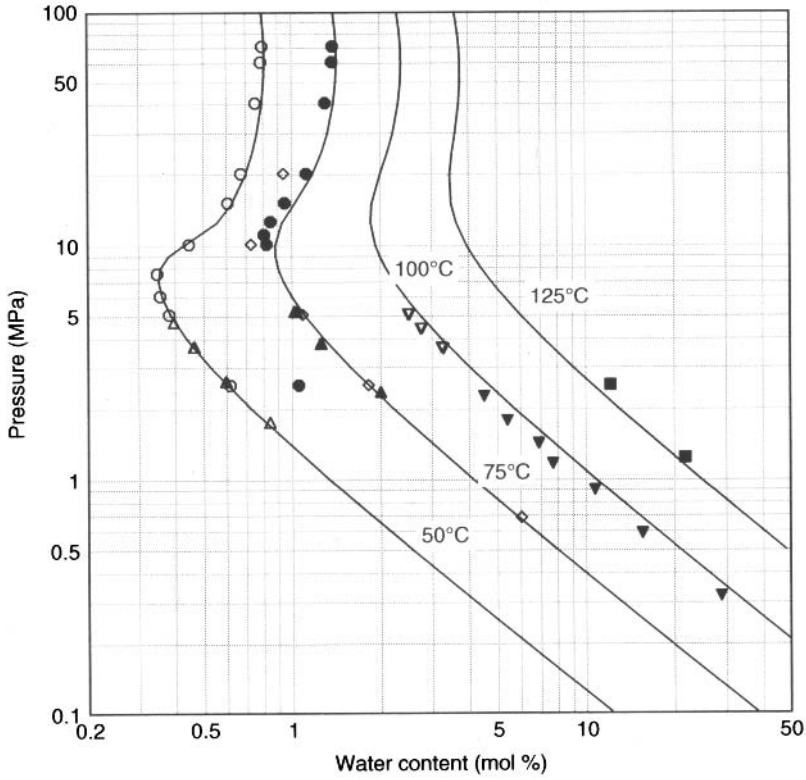

Figure 4.2 Water content of carbon dioxide [data from several sources, curves from *AQUAlibrium*].

4.2.2 Hydrogen Sulfide

Figures 4.3 and 4.4 show the water content of hydrogen sulfide. The data are from Selleck et al. (1952) and from Gillespie et al. (1984). The reader is referred to the appendix at the end of this chapter for a brief comment on the work of Selleck et al. (1952). As with the earlier plots, the calculation shown on these two plots are from *AQUAlibrium*.

Figure 4.3 shows three isotherms where the hydrogen sulfide can condense. The dashed plateaus on this figure are three-phase points. The leftmost point on the plateau is the water content of the gas and the rightmost is that of the H_2S-rich liquid. The water content of the H_2S-rich liquid is greater than the water content of the vapor. For example,

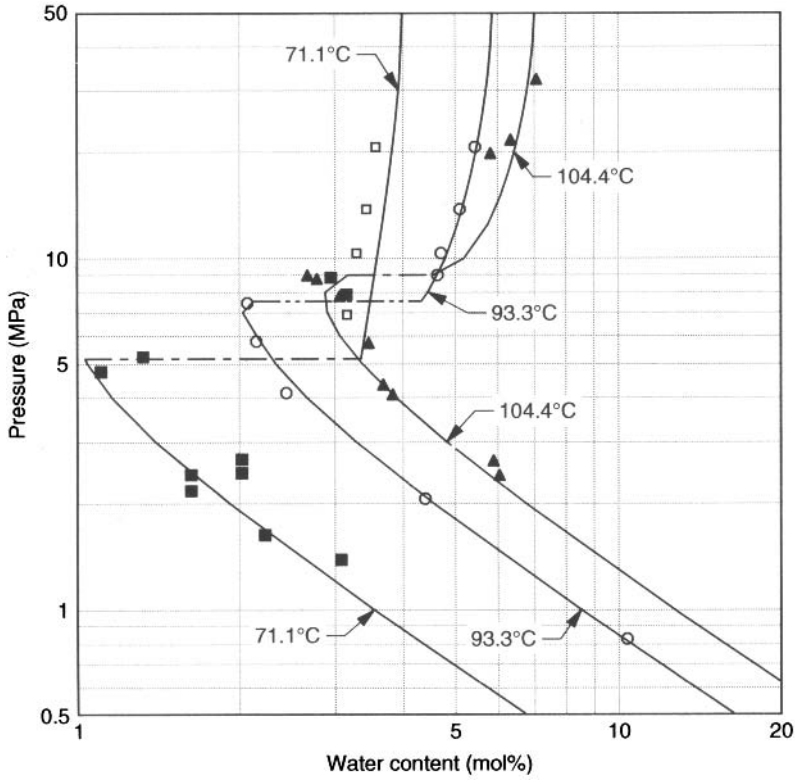

Figure 4.3 Water content of hydrogen sulfide at low temperature [data from Selleck et al. (1952) and Gillespie et al. (1984), curves from *AQUAlibrium*].

at 71.1°C the water content of the gas is about 1 mol%, whereas that for the H_2S-rich liquid is about 3.2 mol%. This phenomenon is important in optimizing the design of an acid gas injection scheme.

Furthermore, note that as the temperature increases the water content of the gas increases. This is as expected. For the H_2S-rich liquid, as the temperature increases the water content also increases. This is a little difficult to interpret from this figure because the plot is "busy." At 71.1°C and 20 MPa, where the second phase is a liquid, the water content is about 3.5 mol%, whereas at 104.4°C and 20 MPa the water content is about 6.3 mol%.

Figure 4.4 is for temperatures where hydrogen sulfide does not liquefy. The isotherms in figure 4.4 are similar to those for carbon dioxide shown in figure 4.2. Again, note the minima in the water content.

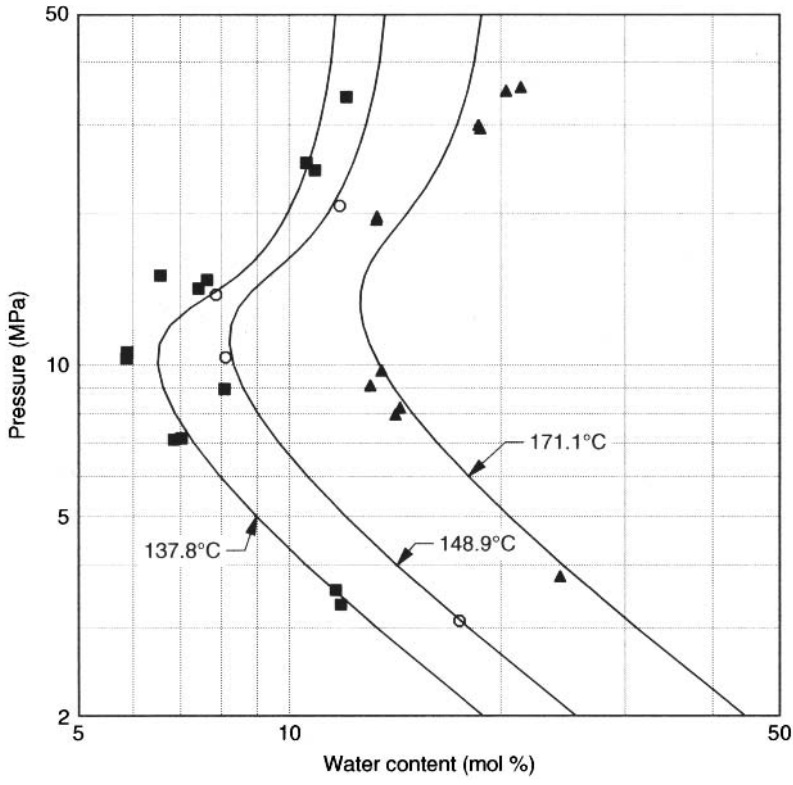

Figure 4.4 Water content of hydrogen sulfide at high temperature [data from Selleck et al. (1952) and Gillespie et al. (1984), curves from *AQUAlibrium*].

Example

4.1 What is the water content of carbon dioxide at 50°C and 1 MPa? Express the result in grams of water per m^3[std] of gas.

Answer: From figure 4.2 the gas contains 1.3 mol% water. Convert 1.3 mol of water to mass:

$$(1.3)(18.015) = 23.42 \text{ g water}$$

Convert 100 moles of gas to m^3 at standard conditions (15.56°C and 101.325 kPa). From the ideal gas law:

$$V = \frac{nRT}{P} = \frac{(100)(8.314)(273.15+15.56)}{(101.325)(1000)} = 2.369 \text{ m}^3\text{[std]}$$

Note the 1000 in the denominator is to convert the pressure from kPa to Pa. Therefore 1.3 mol water per 100 moles of gas gives:

$$23.42/2.369 = 9.9 \text{ g } H_2O/m^3\text{[std]}$$

4.2 What is the water content of carbon dioxide at 50°C and 10 MPa? Express the result in grams of water per m^3[std] of gas.

Answer: The procedure is the same as the previous example, so it will be presented in less detail. The reader should verify the results. From figure 4.2 the water content is 0.42 mol%. Converting this gives 3.2 g/m^3[std].

If we assume a Raoult's law viewpoint, then one would assume that increasing the pressure by a factor of ten should decrease the water content by a factor of ten. Clearly, for carbon dioxide, this rule of thumb does not apply.

4.3 What is the water dew point of a CO_2-water mixture containing 1 mol% water at 50°C?

Answer: From figure 4.2 the dew point is about 1.4 MPa.

4.4 What is the water dew point of a CO_2-water mixture containing 0.5 mol% water at 50°C?

Answer: From figure 4.2 the dew point is approximately 3.2 MPa. But there is a second dew point at higher pressure which occurs at about 11 MPa.

4.5 A mixture of CO_2 (99.5%) and water is place in a long piston to be compressed. What phases are encountered as the mixture is compressed from low pressure to high pressure?

Answer: At low pressure the mixture is a single phase gas. Compressing the mixture we reach a point where the first drop of aqueous phase forms – the dew point pressure and this pressure is 3.2 MPa.

As we compress, more aqueous phase is produced. But we reach a point where the amount of aqueous phase starts to decrease at about 7 MPa. As we continue to compress, the aqueous phase completely disappears – a second dew point at about 11 MPa.

This mixture has two dew points – a normal dew point and a retrograde dew point. The figure below shows the amount of aqueous phase present as a function of the pressure. At pressure below the first dew point, there is no aqueous phase present. At 3.4 MPa, the water dew point, the first infinitesimal amount of water appears. At first as the pressure increases so does the amount of water. From the figure we can see that the amount of water present reaches a maximum at about 7 MPa. At higher pressures the amount of water starts to decrease.

4.2.3 Practical Representation

The figures presented earlier are interesting for showing the phase equilibria encounter in acid gas + water mixtures, but they are less useful for applications. A more useful representation is given in figure 4.5.

It is important that the reader have an understanding of the behavior described in the followings paragraphs. They are key to the optimum design of an injection scheme.

Figure 4.5 shows the water content of five acid gas mixtures: (1) pure H_2S, (2) pure CO_2, (3) an equimolar mixture of H_2S and CO_2 (labeled 50-50), (4) a 75 mol% H_2S + 25 mol% CO_2 (75-25), and (5) a 25 mol% H_2S + 75 mol% CO_2 (25-75). All of these compositions are on a water-free basis. The curves presented in this plot were calculated with *AQUAlibrium*. The comments in the rest of this section are observations based on this figure, and thus many of them apply only for the 48.9°C (120°F) isotherms.

At pressures less than about 3 MPa (450 psia), the water content of the acid gas is essentially independent of the composition (the

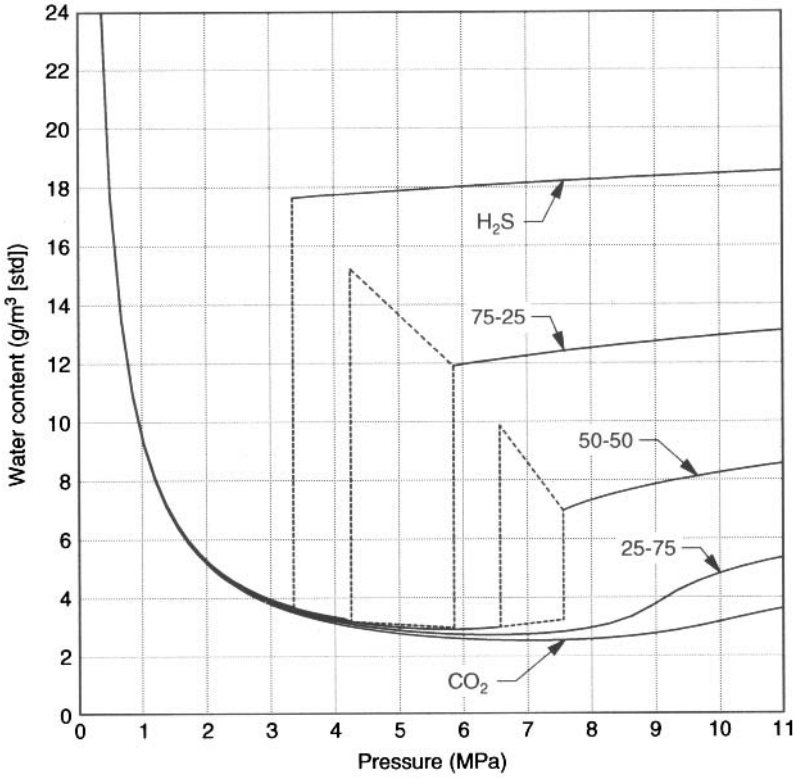

Figure 4.5 Water content of four acid gas mixtures 1. 100% H_2S, 2. 75% H_2S + 25% CO_2, 3. 50% H_2S + 50% CO_2, 4. 25% H_2S + 75% CO_2, 5. 100% CO_2, at 48.8°C (120°F).

curves are essentially coincident). In addition, up to this pressure the water content is a decreasing function of the pressure.

For CO_2, which does not liquefy at this temperature, the water content follows a single curve. The curve has a minimum at approximately 7 MPa (1025 psia). As the pressure increases from that point, the CO_2 will hold more water.

The 25% H_2S + 75% CO_2 mixture behaves similarly to pure CO_2 in as much as it does not liquefy. It does show a minimum in the water carrying capacity, which is at about 6.4 MPa (930 psia). And at higher pressure it holds more water than the pure CO_2.

The other three mixtures will liquefy if subjected to sufficient pressure. The pressure at which they liquefy (a three-phase dew point) depends on the composition of the mixture. As the pressure

is increased, eventually all of the mixture will be liquefied (three-phase bubble point). Note that for the pure H_2S the bubble point and dew point are equal. In figure 4.5, the three-phase regions for the 50-50 and 75-25 mixtures are the trapezoids with dotted boundaries.

For pure H_2S, the water content increases by a factor of approximately 5 when the phase changes from the gas to the liquid. The liquid H_2S can hold significantly more water than the gas phase. For the other two mixtures there is a significant increase in the water-holding capacity upon liquefaction as well. For the 75-25 mixture the liquid holds about 4 times more water than the gas and for the 50-50 mixture the factor is about 3.

With the 50-50 and 75-25 binary mixtures, there is a range of pressure over which the three phases exist. The initial drop of the non-aqueous liquid is richer in H_2S than the overall composition. Therefore, this mixture can hold more water than once the entire mixture is liquefied. For this reason, there is a large change in the water content of the liquid as the three-phase region is traversed.

4.2.3.1 In Summary

Figure 4.5 shows the two characteristic shapes for the water content of acid gas:

1. A continuous curve with a minimum in the water content
2. A discontinuous curve showing a transition from acid gas in the vapor phase to liquefied acid gas. The liquefied acid gas can hold more water than the vapor at similar pressures.

It bears repeating that hydrocarbon gas shows a third shape. For hydrocarbon gas the water content continually decreases as the pressure increases.

The minimum in the water content depends upon the composition, but is approximately 3 to 4 g/m^3[std].

4.3 Estimation Techniques

There are many shortcut techniques available for estimating the water content of sweet gas.

4.3.1 Simple Methods

There are several models available for calculating the water content of natural gas. Only a few of them will be examined here.

4.3.1.1 Ideal Model

In the Ideal Model, the water content of a gas is assumed to be equal to the vapor pressure of pure water divided by the total pressure of the system. This yields the mole fraction of water in the gas and this is value converted to g water per m^3[std] by multiplying by 760.4. Mathematically this is:

$$w = 760.4 \frac{P^{sat}_{water}}{P_{total}} \tag{4.1}$$

where: w – water content, g/m^3[std]
P^{sat}_{water} – vapor pressure of pure water
P_{total} – total, absolute pressure

This equation yields w in g/m^3[std] and the units on the two pressure terms must be the same. A slight modification results in:

$$w = 47484 \frac{P^{sat}_{water}}{P_{total}} \tag{4.1a}$$

where: w – water content, lb/MMSCF

Clearly, this model is very simple and should not be expected to be highly accurate except at very low pressures.

4.3.1.2 McKetta-Wehe Chart

In 1958, McKetta and Wehe published a chart for estimating the water content of sweet natural gas. This chart has been modified slightly over the years and has been reproduced in many publications, most notably the *GPSA Engineering Data Book*. A version of this chart is appended to this chapter.

The McKetta-Wehe chart is quite accurate for all gases (sweet, sour, and acid) for pressure up to about 1400 kPa (200 psia). However, it is not applicable to sour gas at high pressure. Fortunately, most

engineers who work in the natural gas industry are aware of this limitation. There have been corrections proposed to make the chart applicable to these systems. Two will be discussed in the next section of this chapter.

4.3.1.3 Maddox Correction

Maddox (1974) developed a method for estimating the water content of sour natural gas. His method assumes that the water content of sour gas is the sum of three terms: 1. a sweet gas contribution, 2. a contribution from CO_2 and, 3. a contribution from H_2S.

The water content of the gas is calculated as a mole fraction weighted average of the three contributions.

$$w = y_{HC} w_{HC} + y_{CO_2} w_{CO_2} + y_{H_2S} w_{H_2S} \tag{4.2}$$

where: w – water content, lb/MMCF or g/Sm^3
y – mole fraction
the subscript HC refers to hydrocarbon, CO_2 is carbon dioxide and H_2S is hydrogen sufide

Charts are provided to estimate the contributions for CO_2 and H_2S. The chart for CO_2 is for temperatures between 27° and 71°C (80° and 160°F) and the chart for H_2S is for 27° and 138°C (80° and 280°F). Both charts are for pressures from 700 to 20 000 kPa (100 to 3000 psia).

To use this method, one finds the water content of sweet gas, typically from the McKetta-Wehe chart. Then the corrections for the acid gases are obtained from their respective charts.

Although these charts have the appearance of being useful for calculating the water content of pure H_2S and pure CO_2, they should not be used for this purpose.

4.3.1.4 Wichert Correction

Wichert and Wichert (1993) proposed a relatively simple correction based on the equivalent H_2S content, of the gas. The equivalent H_2S content, $y_{H_2S,equiv}$, used in this correlation is that defined by:

$$y_{H_2S,equiv} = 0.7 y_{CO_2} + y_{H_2S} \tag{4.3}$$

This method was recently revised to account for new observations (Wichert and Wichert, 2003).

They presented a single chart where given the temperature pressure and equivalent H_2S one could obtain a correction factor, F_{corr}. Correction factors range from 0.95 to 5.0. The correction factors tend to increase with increasing H_2S equivalent and increasing pressure, and decrease with increasing temperature.

The water content of the sour gas is calculated as follows:

$$w = F_{corr} w_{M-W} \tag{4.4}$$

where: w – water content of the sour gas, mg/Sm³ or lb/MMCF
F_{corr} – correction factor, unitless
w_{M-W} – water content of sweet gas from the McKetta-Wehe chart, g/Sm³ or lb/MMCF

F_{corr} is dimensionless so the two water content terms simply have the same units, typically mg/m³[std] or lb/MMCF, in order to be dimensionally consistent.

This method is limited to an H_2S equivalent of 55 mol% and is applicable for temperatures from 10° and 175°C (50° to 350°F) and pressure from 1400 to 70 000 kPa (200 to 10,000 psia). Therefore it is not applicable to acid gas mixtures.

4.3.1.5 Alami et al.

Alami et al. (2005) developed a relatively simple method for estimating the water content of acid gas mixtures. It is too complex to repeat here and probably too complex for multiple hand calculations. However, it is suitable for a spreadsheet calculation.

This method has proved to be sufficiently accurate and robust for design calculations.

4.3.2 Advanced Methods

4.3.2.1 AQUAlibrium

AQUAlibrium is a software package specifically designed for calculating fluid phase behavior in mixtures of natural gas and water. It is designed for use with sweet and sour gas and more particularly, acid gas. It can also handle liquefied gases. This makes *AQUAlibrium*

an excellent tool for analyzing the phase equilibria encountered in acid gas injection schemes.

For more information about *AQUAlibrium* contact FlowPhase at www.flowphase.com.

4.3.2.2 *Other Software*

There are other software packages available for doing such calculations, including those available in general-purpose process simulators. The design engineer is wise to verify that the models selected are applicable to acid gas-water mixtures. Failure to do so could lead to significant errors.

Example

4.6 Use the McKetta chart to estimate the water content of carbon dioxide at 50°C and 10 MPa. Compare this with the value obtained in the earlier example.

Answer: First, convert 10 MPa to psia (even though this is the SI Chart, the pressure is still given in psia).

$$10\ (14.696/0.101325) = 1450\ \text{psia}$$

Reading from the chart at 50°C and 1450 psia gives about 1200 mg/m^3[std] or 1.2 g/m^3[std]. This is significantly less than the 3.2 g/m^3[std] obtained from the experimental data and shown in a previous example.

4.7 Repeat the previous example using *AQUAlibrium*.

Answer: The output from the *AQUAlibrium* calculation is given in the box below. Not surprisingly, the *AQUAlibrium* is in excellent agreement with the value obtained earlier (remember, the curves on figure 4.2 are from *AQUAlibrium*).

Example 4.7

Water Content Calculation

Conditions

Temperature:	50.00	C
Pressure:	10.00	MPa

Component Fractions

Components	Feed	Vapor	Aqueous	K-factor 1
Water	0	0.00427295	0.980727	0.00435692
CO_2	1	0.995727	0.0192726	51.6655
Total	1	1	1	

Phase Properties

Properties	Units	Vapor	Aqueous
Mole Percent		100	0
Molecular Weight	kg/kmol	43.8989	18.516
Z-factor		0.419226	0.0687417
Density	kg/m³	389.755	1002.57
Enthalpy	kJ/kmol	-4513.17	-40719.3
Heat Capacity	kJ/kmol.K	227.368	77.8449
Viscosity	Pa.s	2.78346e-05	0.000553655
Thermal Conductivity	W/m.K	0.0413475	0.657862
Specific Volume	m³/kg	0.00256571	0.000997442

Water Content

Water Content of Gas	3.24915	g/m³ (60°F and 1 atm)

Solubility

Solubility	1.09083	mol/kg water

4.4 Acid Gas Solubility

Another important aspect in the design of an acid gas injection scheme is the solubility of the acid gas in water and brine. In the design of the surface equipment it is useful to know the amount of acid dissolved in the water removed in the interstage scrubbers. From a reservoir engineering point of view, it is important to know the solubility of the acid gas in the formation water. The water removed in the interstage scrubbers does not contain any dissolved solids because it is water of condensation.

4.4.1 Henry's Law

At low pressure, the solubility of the acid gas components in the vapor phase can be calculated using the simple Henry's law.

$$x_i H_{ij} = y_i P \tag{4.5}$$

where: x_i – mole fraction of component i in the liquid
H_{ij} – Henry's constant for solute i in solvent j, kPa/mol frac
y_i – mole fraction of component i in the gas
P – the total pressure, kPa

As the pressure is increased, a form of Henry's law can still be applied, but it must account for some of the non-idealities. A complete form of Henry's law is:

$$\gamma_i x_i H_{ij} \exp\left[\int_P^{P^\circ} \left(\bar{v}_i^\infty / RT\right) dP\right] = y_i P \hat{\phi}_i^V \tag{4.6}$$

where: γ_i – the activity coefficient
$\bar{v}_i^{\infty}$ – the partial molar volume of I in solvent j at infinite dilution, $m^3/kmol$
R – universal gas constant, 8.314 kJ/kmol·K
T – absolute temperature, K
$\hat{\phi}_i^V$ – fugacity coefficient for component i in the vapor, unitless (must be calculated with an equation of state)

The exponential term is the Poynting correction, which is the effect of pressure on the reference fugacity, and is only important at high pressure.

Figure 4.6 shows the Henry's constants for H_2S, CO_2, and three light hydrocarbons in water. The larger the Henry's constant the lower the solubility. For the five components shown in figure 4.6 hydrogen sulfide is the most soluble, whereas the three hydrocarbons are the least soluble.

The interested reader can learn more about Henry's law from the series of papers by Carroll (1991, 1992, 1999a).

Example
4.8 At 50°C the Henry's constant for H_2S in water is approximately 100 MPa/mol frac (see figure 4.6). If the partial pressure of H_2S is 100 kPa, estimate the solubility.

Answer: The solubility can be calculated from Equation (4.5).

$$x_i H_{ij} = y_i P$$

The partial pressure is defined as the total pressure times the mole fraction of the component in the vapor phase. Therefore:

$$x\ (100\ MPa) = 100\ kPa$$

Ensure that the units are the same on both sides of the equation

$$x\ (100\ MPa) = 0.100\ MPa$$

Solve for x

$$x = 0.1/100 = 0.001$$
$$x = 0.1\ mol\%$$

So the estimated solubility is 0.1 mol%.

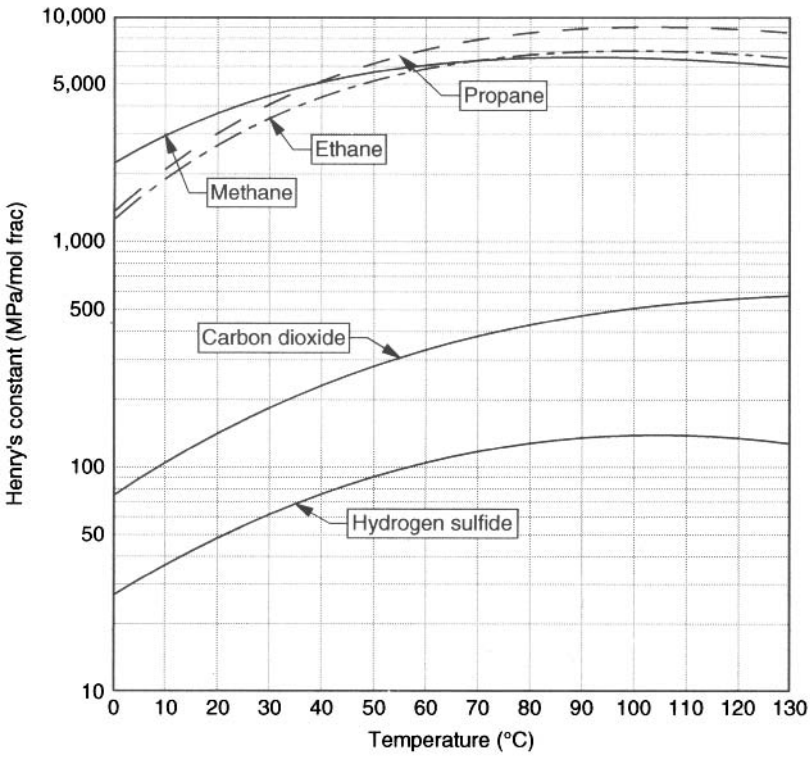

Figure 4.6 Henry's constants for hydrogen sulfide, carbon dioxide, methane, ethane, and propane in water.

4.4.2 Solubility in Brine

For most gases the solubility in a brine solution is less than the solubility in pure water. This is called "the salting-out effect." The following equation, proposed by Sechenov more than a century ago, can be used to approximate the salting-out effect:

$$\log(S_{water}/S_{electrolyte}) = k\,I \tag{4.7}$$

where: S_{water} – solubility in pure water
$S_{electrolyte}$ – solubility in the electrolyte solution
I – concentration of the electrolyte
k – salting-out coefficient.

Various units could be used for the solubilities, but the values given in the next section, the solubilities of both the acid gas components and the NaCl must be in molality (moles of salt per kilogram of solute).

Rearranging Equation (4.7) to a form that is applicable for calculating the solubility in the electrolyte solution given the solubility on pure water.

$$\log(S_{water}) - \log(S_{electrolyte}) = k\,I$$
$$\log(S_{electrolyte}) = \log(S_{water}) - k\,I \qquad (4.7a)$$

The salting-out coefficient is a function of the temperature, but it is approximately independent of the pressure and assumed to be independent of the nature of the phase of the solute.

4.4.2.1 *Carbon Dioxide in NaCl*

There is a relatively large database of experimental data for the solubility of carbon dioxide in water, much of which is at low pressure. Clever (1996) critically reviewed the data and generated salting-out coefficients. He separated the data into low pressure and high pressure regions.

The values he obtained are shown graphically in figure 4.7. No attempt is made to distinguish the original source of the data, but a distinction is made between the low pressure and high pressure data.

Both sets of data were used to generate the following correlation.

$$k_{CO_2-NaCl} = 0.09897 - 0.2805 \times 10^{-3} t \qquad (4.8)$$

where: t – temperature, °C

In addition to the correlation shown by the figure, this plot also demonstrates the large scatter in the results obtained from the experimental data.

4.4.2.2 *Hydrogen Sulfide in NaCl*

There are significantly less data for the solubility of hydrogen sulfide in sodium chloride solutions (and even less for the solubility in other electrolyte solutions). Sulemeimenov and Krupp (1994) measured some solubilities at high temperature and reviewed the existing data for the solubility of H_2S in NaCl solutions. Although they give a

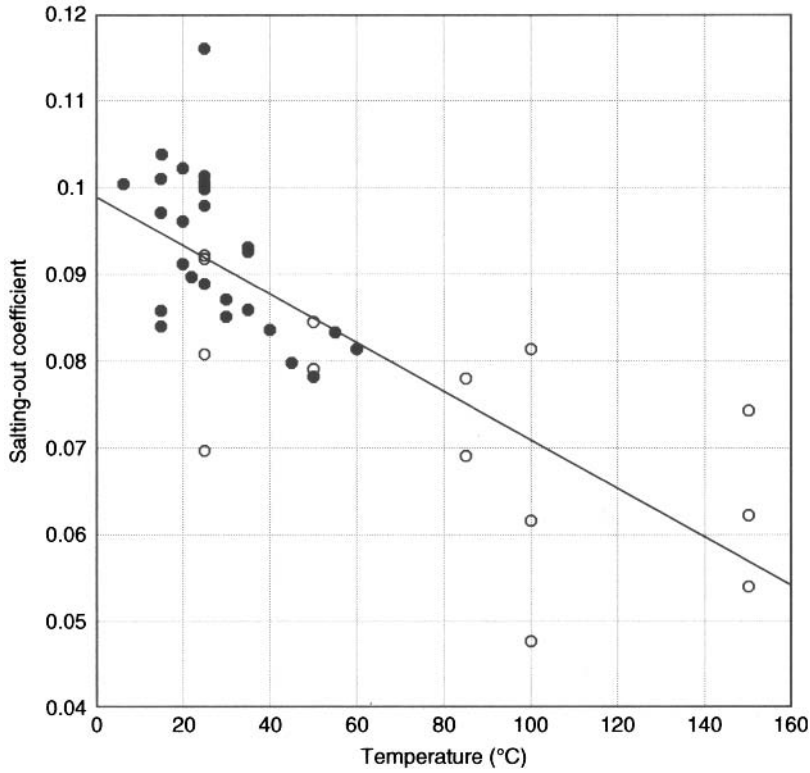

Figure 4.7 Salting-out coefficient for carbon dioxide in solution of sodium chloride (open circles – low pressure data and filled circles – high pressure data).

fairly complex correlation for the salting out coefficient for the temperature range from 0° to 200°C, a constant value is probably all that is justified. Therefore, to a very good approximation:

$$k_{H_2S-NaCl} = 0.0721 \tag{4.9}$$

In addition, the polynomial correlation from Sulemeimenov and Krupp (1994) shows curvature (including maxima and minima) which is probably not justified based on the limited set of experimental data used to generate the correlation.

Example

4.9 Estimate the solubility of H_2S in a 10 wt% brine at 50°C and an H_2S partial pressure of 100 kPa. Start with the solubility of H_2S in water from Ex. 4.8.

Answer: As noted earlier, all solubilities must be expressed in molality in order to use the equations given. First convert the brine weight per cent to molality.

$$10 \text{ g NaCl}/90 \text{ g water} \qquad M_{NaCl} = 58.44 \text{ g/mol}$$
$$0.1712 \text{ mol NaCl}/90 \text{ g water} = 0.1712 \text{ mol NaCl}/0.090 \text{ kg water}$$
$$= 1.903 \text{ molal}$$

Next convert the H_2S solubility calculated previous to molality:

$$0.1 \text{ mol \%} = 0.001 \text{ mol } H_2S/0.999 \text{ mol water}$$
$$M_{H2O} = 18.015 \text{ g/mol}$$
$$0.001 \text{ mol } H_2S/17.997 \text{ g water} = 0.001 \text{ mol } H_2S/0.017\,997 \text{ kg water}$$
$$= 0.055\,65 \text{ molal}$$

From Equation (4.9), k = 0.0721. Now apply Equation (4.7):

$$\log(S_{electrolyte}) = \log(S_{water}) - kI$$
$$= \log(0.05565) - (0.0721)(1.903)$$
$$= -1.3917$$
$$S_{electrolyte} = 0.0406 \text{ molal}$$

So the solubility in the brine solution is 0.0406 molal compared to 0.05565 molal in pure water.

Expressing this concentration in terms of mole fraction, we must account for both the water and the salt in the brine solution. A solution that is 0.0406 molal is 0.0406 moles of H_2S per kilogram of solute. In this case, 1 kg of solvent is composed of 900 g of water and 100 g of NaCl. Thus the moles in the solution are:

H_2S	0.0406
water	900/18.015 = 49.958
NaCl	100/58.44 = 1.711

So the mole fraction is:

$$x = \frac{0.0406}{0.0406 + 49.958 + 1.711} = 0.000785$$
$$x = 0.0785 \text{ mol\%}$$

In the pure water, the H_2S concentration is 0.1 mol%, whereas in the brine solution the concentration is 0.0785 mol%.

4.4.2.3 *Mixtures of Gases*

There is no good theory for applying this approach to mixtures of solutes. In addition, there is very little data for the solubility of gas mixtures in electrolytes (and none for acid gas mixtures) upon which to base a new model or to test a model. Fortunately, at the temperature of interest here, the k for both H_2S and CO_2 are approximately the same. So a simple average value will be used.

Furthermore, this salting-in coefficient will be applied to all components in the mixture, including the hydrocarbons, so a single correlation will be applied to the mixture solubility.

4.4.2.4 *Effect of pH*

There is an interesting effect of pH on the solubility of acid gas in water. In a solution with a high pH (a basic solution), the solubility of the acid gas components is dramatically increased. This is due to the acid-base reactions that occur between the dissolved acid gas and the base in the original solution.

On the other hand, the effect of a low pH (acidic) solution is less dramatic. In low pH solutions, the effect is more like the salting-out seen with neutral electrolyte solutions. In fact, at low pH the type of acid present is more significant than the pH. Kendall and Andrews (1921) showed that solubility of H_2S in hydrochloric acid increases slightly as the pH decreases. However, at a pH of about 0.7 (a very acidic solution) the solubility only increased by 6% over the solubility in pure water. Doubal and Riley (1979) showed essentially no difference in the solubility of H_2S in pure water versus a 5 molal solution of H_2SO_4.

4.5 In Summary

The formation of an aqueous phase is critical in acid gas injection scheme. The presence of the aqueous phase greatly increases the possibility of corrosion. In this chapter, methods are presented for estimating water content of acid gas, both in the gas and liquid phases.

As always, the design engineer should verify the accuracy of the models used. This is particularly true for the water content of acid gases where simple models give erroneous results and may lead to poor design decision. The appendix to this chapter presents a review of the available experimental data for these systems.

References

Alami, I., W. Monnery, and W. Svrcek. 2005. Model predicts equilibrium water content of high-pressure acid gases. *Oil & Gas J.* (July 11).

Carroll, J.J. 1991. What is Henry's law? *Chem. Eng. Prog.* 87(9):48–52.

_____. 1992. Use Henry's law for multicomponent mixtures. *Chem. Eng. Prog.* 88(8):53–58.

_____. 1999a. Henry's law revisited. *Chem. Eng. Prog.* 94(1):49–56.

_____. 1999b. Phase equilibrium relevant to acid gas injection. *CGPA/CGPSA 2nd Quarterly Meeting*, Calgary, AB, May.

_____. 2002. Phase equilibria relevant to acid gas injection. Part 2 – Aqueous phase behavior. *Canadian Journal of Petroleum Technology*. 41(6):25–31.

Carroll, J.J. and A.E. Mather. 1989. Phase equilibrium in the system water-hydrogen sulphide: Modelling the phase behaviour with an equation of state. *Can. J. Chem. Eng.* 67:999–1003.

Chapoy, A., A.H. Mohammadi, B. Tohidi, A. Valtz, and D. Richon. 2005. Experimental measurement and phase behavior modeling of hydrogen sulfide – Water binary system. *Ind. Eng. Chem. Res.* 44:7567–7574.

Clever, H.L. 1996. An evaluation of the solubility of carbon dioxide in aqueous electrolyte solutions. In *Solubility Data Series Vol.62 Carbon Dioxide in Water and Aqueous Electrolyte Solutions*, ed. P. Sharlin, Oxford: Oxford University Press, pp. 85–133.

Doubal, A.A. and J.P. Riley. 1979. *Deep-Sea Res.*, 26A:259–268. Quoted in Fogg, P.G.T. and C.L. Young, eds., *Solubility Data Series Vol. 32. Hydrogen Sulfide, Deutereium Sulfide and Hydrogen Selenide* (Oxford, UK: Pergamon Press, 1988.

Fogg, P.G.T. and C.L. Young, eds. 1988. *Solubility Data Series Vol. 32. Hydrogen Sulfide, Deutereium Sulfide and Hydrogen Selenide*, Oxford: Pergamon Press.

Gillespie, P.C., J.L. Owens, and G.M. Wilson. 1984. Sour water equilibria extended to high temperatures and with inerts present. AIChE winter meeting, Paper 34–b, Atlanta, GA.

_____, *GPSA Engineering Data Book*, 11th edition. 1999. Gas Processors Suppliers Association and Gas Processors Association, Tulsa, OK.

Kendall, J. and J.C. Andrews. 1988. *J. Amer. Chem. Soc.* 43:1545–1560, (1921). Quoted in Fogg and Young, eds. 1988, p. 29.

Maddox, R.N. 1974 edition. *Gas and liquid sweetening*. John M. Campbell Ltd.:39–42, and Maddox, R.N., L.L. Lilly, M. Moshfeghian, and E. Elizondo. 1988. Estimating water content of sour natural gas mixtures. Laurance Reid Gas Conditioning Conference, Norman, OK, March.

Marriott, R.A., E. Fitzpatrick, F. Bernard, H.H. Wan, K.L. Lesage, P.M. Davis, and P.D. Clark. 2009. Equilibrium water content measurements for acid gas mixtures. First International Acid Gas Injection Symposium, Calgary, AB.

Olds, R.H., B.H. Sage, and W.N. Lacey. 1942. Phase equilibria in hydrocarbon systems. Composition of dew-point gas in methane-water system. *Ind. Eng. Chem.* 34:1223–1227.

Selleck, F.T., L.T. Carmichael, and B.H. Sage. 1952. Phase behavior in the hydrogen sulfide-water system. *Ind. Eng. Chem.* 44:2219–2226.

Sulemeimenov, O.M. and Krupp, R.E. 1994. Solubility of hydrogen sulfide in pure water and in NaCl solutions from 20 to 320°C and at saturation pressures. *Geochimica et Cosmochimica Acta* 58:2433–2444.

Valtz, A., A. Chapoy, C. Coquelet, P. Paricaud, and D. Richon. 2004. Vapor-liquid equilibria in the carbon dioxide-water system. *Fluid Phase Equil.* 226:333–344.

Wichert, G.C. and E. Wichert. 1993. Chart estimates water content of sour natural gas. *Oil & Gas J.* Mar. 29:61–64.

Wichert, G.C. and E. Wichert. 2003. New charts provide accurate estimations for water content of sour natural gas. *Oil & Gas J.* Oct 27:64–66.

Appendix 4A Compilation of the Experimental Data for the Water Content of Acid Gas

As with other aspects of acid gas injection, the selection of the correct models is important in the proper design. And this is especially true for the water content of acid gas mixtures. This purpose of this appendix is to provide the reader with the source of the data upon which they can test their models. Table 4A.1 lists experimental investigations into the water content of mixtures containing hydrogen sulfide and/or carbon dioxide.

The study of Selleck et al. (1952) is considered the benchmark investigation of the system hydrogen sulfide + water. They published tables of smoothed data, which are commonly quoted in the literature. However, these tables are based on relatively few and scattered experimental data points. A discussion of their data was presented in the next appendix.

The data of Lee and Mather (1972) for the water content of the gas are not readily available. Therefore they are reproduced in table 4A.2.

Table 4A.1 Experimental investigations of the water content of mixtures containing hydrogen sulfide and carbon dioxide.

Gas	Temp. (°C)	Pressure (MPa)	Reference
H_2S	5 to 60	up to 0.50	Wright and Maass (1932)
	37 to 171	2.7 to 35	Selleck et al. (1952)
	90 to 150	1.5 to 3.5	Lee and Mather (1977)
	37 to 315	up to 10	Gillespie et al. (1984)
	40 to 105	2.4 to 9.8	Carroll and Mather (1989)†
	25 to 45	0.5 to 2.8	Chapoy et al. (2005)
CO_2	25 to 75	0.1 to 71.0	Wiebe and Gaddy (1941)
	25 to 100	1.7 to 5.1	Coan and King (1971)
	100 to 200	0.2 to 5.0	Zawisza and Malesinska (1981)
	16 to 260	0.7 to 13.8	Gillespie et al. (1984)
	−28 to 25	0.7 to 13.8	Song and Kobayashi (1987)
	50	6.8 to 17.7	Briones et al. (1987)
	50 and 75	10.1 and 15.2	D'Souza et al. (1988)
	100 to 200	0.3 to 8.1	Müller et al. (1988)

Table 4A.1 (cont.) Experimental investigations of the water content of mixtures containing hydrogen sulfide and carbon dioxide.

Gas	Temp. (°C)	Pressure (MPa)	Reference
	15 to 40	5.2 to 20.3	King et al. (1992)
	50	10.1, 20.1, 30.1	Dohrn et al. (1993)
	50 to 80	4 to 14	Bamberger et al. (2000)
	40 and 50	8 to 21	Sabirzyanov et al. (2002)
	5 to 45	0.5 to 8	Valtz et al. (2004)
$H_2S + CO_2$	20 to 60	up to 14	Clark (1999)
	40 and 60	up to 20	Marriott et al. (2009)
$H_2S + CH_4$	70	1.3 to 10.3	Lukacs and Robinson (1963)
	54 and 71	6.9 to 10.3	Maddox et al. (1988)
$CO_2 + CH_4$	37 and 71	6.9 and 13.8	Maddox et al. (1988)
	15 to 50	5.7 to 13.8	Song and Kobayashi (1989)
$H_2S + CO_2 + CH_4$	37 to 177	4.8 to 18.2	Huang et al. (1985)
	37	7.6 and 13.1	Maddox et al. (1988)
$H_2S + CO_2 + CH_4 + C_3H_8$	49 and 93	1.4 to 69	Ng et al. (1999)
	49 and 93	1.4 to 69	Ng et al. (2001)

† – water content of gas and H_2S-rich liquid along the LLV locus

Table 4A.2 Raw data from Lee and Mather (1977) for the water content of hydrogen sulfide.

Pressure (kPa)	Mole Frac H_2S	Pressure (kPa)	Mole Frac H_2S	Pressure (kPa)	Mole Frac H_2S
90°C		120°C		150°C	
1924	0.9614	1486	0.8865	1942	0.7409
2011	0.9606	2500	0.9298	2196	0.7812
2389	0.9709	3161	0.9415	2624	0.8199
		3174	0.9529	2699	0.8373
		3230	0.9314	3003	0.8292
		3401	0.9526	3079	8.8356

There have been many investigations of the water content of CO_2-rich fluids. In general, there is reasonable agreement among the various sets of data in the low and moderate pressure regions. The benchmark investigation of the phase behavior in the system carbon dioxide + water was that of Wiebe and Gaddy (1941).

References

Bamberger, A.G. Sieder, and G. Maurer. 2000. High-pressure (vapor + liquid) equilibrium in binary mixtures of (carbon dioxide + water or acetic acid) at temperatures from 313 to 353 K. *J. Supercrit. Fluids* 17:97–110.

Briones, J.A., J.C. Mullins, M.C. Thies, B.-U. 1987. Ternary phase equilibria for acetic acid-water mixtures with supercritical carbon dioxide. *Fluid Phase Equiil.* 36:235–246.

Carroll, J.J. and A.E. Mather. 1989. Phase equilibrium in the system water-hydrogen sulphide: Experimental determination of the LLV locus. *Can. J. Chem. Eng.* 67:468–470.

Chapoy, A., A.H. Mohammadi, B. Tohidi, A. Valtz, and D. Richon. 2005. Experimental measurement and phase behavior modeling of hydrogen sulfide – water binary system. *Ind. Eng. Chem. Res.* 44:7567–7574.

Clark, M.A. 1999. "Experimentally obtained saturated water content, phase behavior and density of acid gas mixtures", MS thesis, University of Calgary, Calgary, AB.

Coan, C.R. and A.D. King. 1971. Solubility of water in compressed carbon dioxide, nitrous oxide, and ethane. Evidence for hydration of carbon dioxide and nitrous oxide in the gas phase. *J. Am. Chem. Soc.* 98:1857–1862.

Dohrn, R., A.P. Bünz, F. Devlieghere and D. Thelen. 1993. Experimental measurements of phase equilibria for ternary and quaternary systems of glucose, water, CO_2, and ethanol with a novel apparatus. *Fluid Phase Equil.* 83:149–158.

D'Souza, R., J.R. Patrick, and A.S. Teja. 1988. High pressure phase equilibria in the carbon dioxide – n-hexadecane and carbon dioxide – water systems. *Can. J. Chem. Eng.* 66:319–323.

Gillespie, P.C., J.L. Owens, and G.M. Wilson. 1984. Sour water equilibria extended to high temperatures and with inerts present. *AIChE Winter Meeting*, Paper 34-b, Atlanta, GA.

Huang, S.S.-S., A.-D. Leu, H.-J. Ng, and D.B. Robinson. 1985. The phase behavior of two mixtures of methane, carbon dioxide, hydrogen sulfide, and water. *Fluid Phase Equil.* 19:21–32.

King, M.B., A. Mubarak, J.D. Kim, and T.R. Bott. 1992. The mutual solubilities of water with supercritical and liquid carbon dioxide. *J. Supercritical Fluids* 5:296–302.

Lee J.I. and A.E. Mather. 1977. Solubility of hydrogen sulfide in water. *Ber. Bunsen-Ges. Phys. Chem.* 81:1021–1022.

Lukacs, J. and D.B. Robinson. 1963. Water content of sour hydrocarbon systems. *Soc. Petrol. Eng. J.* 3:293–297.

Maddox, R.N., L.L. Lilly, M. Moshfeghian, and E. Elizondo. 1988. Estimating water content of sour natural gas mixtures. 38th Laurance Reid Gas Cond. Conf., Norman, OK.

Marriott, R.A., E. Fitzpatrick, F. Bernard, H.H. Wan, K.L. Lesage, P.M. Davis, and P.D. Clark. 2009. Equilibrium water content measurements for acid gas mixtures. First International Acid Gas Injection Symposium, Calgary, AB.

Müller, G., E. Bender, and G. Maurer. 1988. Das Dampf-Flüssigkeitsgleichgewicht des ternären Systems Ammoniak-Kohlendioxid-Wasser bei hohen Wassergehalten im Bereich zwischen 373 und 473 Kelvin. *Ber. Bunsenges. Phys. Chem.* 92:148–160.

Ng, H.-J., J.J. Carroll, and J. Maddocks. 1999. Impact of thermophysical properties research on acid gas injection process design. 78th Annual GPA Conv., Nashville, TN.

Ng, H.-J., C.-J. Chen, and H. Schroeder. 2001. *Water Content of Natural Gas Systems Containing Acid Gas*, Research Report RR-174, Gas Processors Association, Tulsa, OK.

Sabirzyanov, A.N., A.P. Il'in, A.R. Akhunov, and F.M. Gumerov. 2002. Solubility of water in supercritical carbon dioxide. *High Temperature* 40:203–206.

Selleck, F.T., L.T. Carmichael, and B.H. Sage. 1952. Phase behavior in the hydrogen sulfide-water system. *Ind. Eng. Chem.* 44:2219–2226.

Song, K.Y. and R. Kobayashi. 1987. Water content of CO_2 in equilibrium with liquid water and/or hydrates. *SPE Form. Eval.* 500–508.

Song, K.Y. and R. Kobayashi. 1989. Water content values of a CO_2 – 5.31 mol percent methane mixture. *Research Report RR-120*, Gas Processors Association, Tulsa, OK.

Valtz, A., A. Chapoy, C. Coquelet, P. Paricaud, and D. Richon. 2004. Vapor-liquid equilibria in the carbon dioxide-water system. *Fluid Phase Equil.* 226:333–344.

Wiebe, R. and V.L. Gaddy. 1941. Vapor phase composition of carbon dioxide-water mixtures at various temperatures and at pressures to 700 atmospheres. *J. Am. Chem. Soc.* 63:475–477.

Wright, R.H. and O. Maass. 1932. The solubility of hydrogen sulphide in water from the vapor pressures of the solutions. *Can. J. Research* 6:94–101.

Zawisza, A. and B. Malesinska. 1981. Solubility of carbon dioxide in liquid water and of water in gaseous carbon dioxide in the range 0.2 to 5 MPa at temperatures up to 473 K. *J. Chem. Eng. Data* 26:388–391.

Appendix 4B Comments on the Work of Selleck et al.

The work of Selleck et al. (1952) is often quoted for the phase equilibria in the system water + hydrogen sulfide. Their study consisted of two pieces: (1) the collection of raw data, which are on deposit and difficult to obtain, and (2) the smooth tables that they published.

By and large, the raw data are accurate and should be the only values used for testing models, etc. The smoothing employed by Selleck et al. (1952) exhibits some bias, as do all models. As was demonstrated by Carroll and Mather (1989), the smoothed data of Selleck et al. (1952) are erroneous. Unfortunately, the smoothed data of Selleck et al. (1952) continue to be quoted, even in such important reference books as the *GPSA Engineering Data Book.*

Actually, this is a good rule for all data and not just those of Selleck et al. (1952). In the past, it was commonplace to publish smoothed data. The logic was that the smoothed data would be more useful in a practical sense. However, when building and testing models, the raw, experimental data should be used as much as possible, otherwise you end up comparing your model with theirs.

Therefore, table 4B.1 gives the raw data from Selleck et al. (1952) only for the water content of the H_2S-rich phase. The data presented are exactly those from the original document. Thus the pressure is in psia, and both weight fraction and mole fraction of H_2S are given. To obtain the mole fraction and weight fraction of water in the sample, merely subtract the value in the table from one.

Table 4B.1 Raw data from Selleck et al. for the water content of the H_2S-rich phases.

Pressure (psia)	Wt Frac H_2S	Mol Frac H_2S	Pressure (psia)	Wt Frac H_2S	Mol Frac H_2S
100°F			280°F		
390.67	0.9978	0.9958	484.5	0.9337	0.8816
604.9[a]	0.9915	0.9840	518.3	0.9349	0.8836
791.9[a]	0.9906	0.9824	1030.0	0.9626	0.9315
160°F			1036.5	0.9616	0.9298
201.4	0.9835	0.9692	1297.2	0.9556	0.9191

Table 4B.1 (cont.) Raw data from Selleck et al. for the water content of the H_2S-rich phases.

Pressure (psia)	Wt Frac H_2S	Mol Frac H_2S	Pressure (psia)	Wt Frac H_2S	Mol Frac H_2S
160°F			280°F		
236.7	0.9881	0.9777	1491.5	0.9681	0.9413
316.1	0.9913	0.9837	1535.4	0.9680	0.9412
351.3	0.9913	0.9837	2056.1	0.9593	0.9257
355.4	0.9892	0.9798	2139.5	0.9581	0.9236
388.4	0.9892	0.9798	2182.9	0.9642	0.9344
688.4	0.9941	0.9889	3532.6	0.9394	0.8913
759.1	0.9929	0.9867	3657.1	0.9412	0.8943
1142.1[a]	0.9831	0.9685	4937.1	0.9324	0.8794
1279.1[a]	0.9842	0.9705	340°F		
220°F			547.6	0.8551	0.7573
346.4	0.9672	0.9397	1145.5	0.9198	0.8584
380.8	0.9680	0.9412	1181.3	0.9185	0.8563
586.5	0.9794	0.9617	1307.5	0.9266	0.8696
626.2	0.9802	0.9632	1399.9	0.9236	0.8647
822.5	0.9814	0.9654	2795.7	0.9249	0.8669
1117.6	0.9836	09694	2833.7	0.9248	0.8667
1254.3	0.9851	0.9722	4246.5	0.8916	0.8130
1285.4	0.9857	0.9733	4310.3	0.8922	0.8140
2848.5	0.9684	0.9419	5037.6	0.8810	0.7965
3108.6	0.9655	0.9367	5121.6	0.8745	0.7865
4625.9	0.9614	0.9294			

[a] – hydrogen sulfide-rich liquid

Appendix 4C Density of Brine (NaCl) Solutions

In order to convert between the various concentrations to molality (moles of solute per mole of solution) requires the density of the solution. Table 4C.1 list the densities of brine as a function of the brine concentration at 20°C.

Correlating these values as a function of the weight per cent resulting in the following simple correlation:

$$\rho = 998.516 + 6.941\,073\,X + 0.026\,470\,406\,X^2 \qquad (4C.1)$$

where: ρ – density, kg/m^3
X – concentration of NaCl, wt%

As an approximation, these effect of pressure and temperature on the brine solution can be obtained using the following equation:

$$\frac{\rho_{brine}(T,P)}{\rho_{water}(T,P)} = \frac{\rho_{brine}(20°C)}{\rho_{water}(20°C)} \qquad (4C.2)$$

Table 4C.1 The density of brine (NaCl) solutions as a function of salt concentration at 20°C.

NaCl Conc. (wt%)	Density (kg/m^3)	NaCl Conc. (wt%)	Density (kg/m^3)	NaCl Conc. (wt%)	Density (kg/m^3)
0	998.2	9	1063.3	18	1131.9
1	1005.3	10	1070.7	19	1139.8
2	1012.5	11	1078.1	20	1147.8
3	1019.6	12	1085.7	21	1155.8
4	1026.8	13	1093.2	22	1164.0
5	1034.0	14	1100.8	23	1172.1
6	1041.3	15	1108.5	24	1180.4
7	1048.6	16	1116.2	25	1188.7
8	1055.9	17	1124.0	26	1197.2

where: $\rho_{brine}(T,P)$ – density of brine at the temperature and pressure of interest, kg/m³
$\rho_{water}(T,P)$ – density of water at the temperature and pressure of interest, kg/m³
$\rho_{brine}(20°C)$ – density of brine from table 4C.1, kg/m³
$\rho_{water}(20°C)$ – density of water from table 4C.1, kg/m³

The density of pure water, as a function of temperature and pressure can be obtained from the *Steam Tables*.

Example
4C.1 A formation water analysis reports that the brine concentration in a sample is equivalent to 1.5 moles of NaCl per liter of solution (1.5 M). What is the brine concentration in weight percent and molality?

Answer: To begin, note that 1.5 moles of NaCl are equal to 87.66 g of NaCl (molar mass equals 58.44 g/mol)

In order to estimate the mass of water in the solution, we must assume a density for the solution. As an initial estimate try 1000 kg/m³. Therefore 1 L of solution has a mass of 1000 g. Our first estimate of the weight percent is:

$$\frac{87.66}{1000} \times 100 = 8.77 \text{ wt\%}$$

Update the density estimate using Equation (4C.1):

$$\rho = 998.516 + 6.941\,073(8.77) + 0.026\,470\,406(8.77)^2$$
$$= 1061.4 \text{ kg/m}^3$$

Therefore, 1 L of solution has a mass of 1061.4 g, and update the estimate of the weight percent:

$$\frac{87.66}{1061.4} \times 100 = 8.26 \text{ wt\%}$$

Trial 3:

$$\rho = 998.516 + 6.941\,073(8.26) + 0.026\,470\,406(8.26)^2$$
$$= 1057.6 \text{ kg/m}^3$$

$$\frac{87.66}{1057.6} \times 100 = 8.29 \text{ wt\%}$$

Trial 4:

$$\rho = 998.516 + 6.941\,073(8.29) + 0.026\,470\,406(8.29)^2$$
$$= 1057.8 \text{ kg/m}^3$$

$$\frac{87.66}{1057.8} \times 100 = 8.29 \text{ wt\%}$$

The procedure has converged and the salt concentration is 8.29 wt%.

Now converting to molality (moles of solute per kilogram of solvent). The solution 87.66 g of NaCl (or from earlier 1.5 mol) and therefore the solution contains 1057.8 – 87.66 = 970.1 g, 0.9701 kg of water. The concentration is:

$$\frac{1.5}{0.9701} = 1.546 \text{ molal}$$

5

Hydrates

Another consequence of the presence of water in natural gas and acid gas is the formation of solid compounds called hydrates. Hydrates are important because they form at conditions where a solid phase would not otherwise be expected. In addition, hydrates are notorious for plugging production and processing facilities. In this chapter, we will examine hydrates as they relate to acid gas injection.

The topic of gas hydrates is a rather large one that deserves a book all of its own (see Carroll, 2003). An overview of hydrates, specifically tailored to acid gas injection, is presented in this chapter (i.e., hydrates in acid gas mixtures). In addition, Hendrick et al. (2009) present an interesting study of hydrates in acid gas systems.

5.1 Introduction to Hydrates

Gas hydrates are solid ice-like materials that form at relatively high temperature. That is, they form at temperatures above the freezing point of water (0°C).

In a gas hydrate, water forms a hydrogen-bonded cage and different molecules reside inside the cage. Water is called the "host,"

and the other molecule is called a "guest," or a "hydrate former". The guest must of sufficient size to fit inside the lattice formed by water molecules. Hydrate formers include: methane, ethane, propane, hydrogen sulfide, carbon dioxide, and nitrogen.

In order for a hydrate to form, three conditions must be met:

1. The right combination of temperature and pressure
2. A sufficient amount of water
3. A hydrate former must be present

Hydrate formation is favored by low temperature and high pressure, but the actual hydrate formation condition is a function of the gas under consideration. Different gases form hydrates at different conditions.

It may seem obvious that some water must be present; however, just having "some" water present is not enough. There must be enough water to form the hydrate phase. Ironically, if there is too much water present, a hydrate will not form either. If the hydrate former is present in too low a concentration, then it will merely dissolve in the water. Some acid gas disposal schemes take advantage of this property.

5.2 Hydrates of Acid Gases

The hydrate formation conditions for pure H_2S (Carroll, and Mather, 1991; and Glew, 2000) and pure CO_2 (Yang et al., 2000) are well established. However, a review of the literature revealed that there are no data for acid gas mixtures. Thus we must proceed with some caution.

Of the components commonly found in natural gas, none forms a hydrate as easily as hydrogen sulfide.

Figure 5.1 shows the pressure and temperature at which a hydrate will form for hydrogen sulfide, carbon dioxide, and methane. From this figure it can be seen that the hydrate for hydrogen sulfide forms at temperatures greater than 30°C (85°F). It is difficult to imagine, *a priori*, that a solid water phase could form at 30°C!

Because of the lack of experimental data for mixtures of $H_2S + CO_2$, we must rely on predictions to see the effect of varying the composition on the hydrate forming conditions. Figure 5.2 shows the hydrate formation for binary mixtures of H_2S and CO_2 as predicted by the

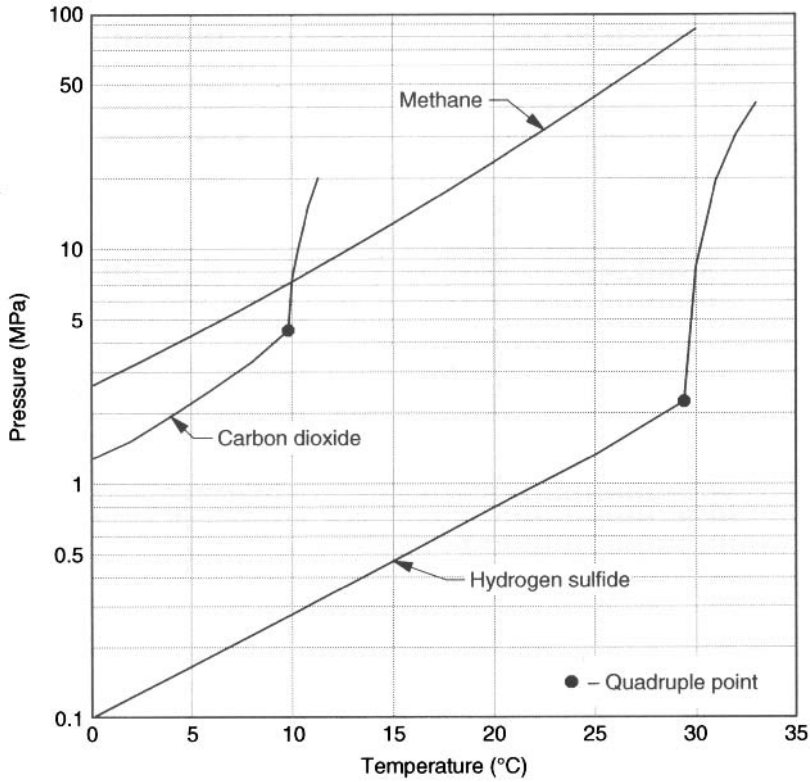

Figure 5.1 The hydrate loci for hydrogen sulfide, carbon dioxide, and methane.

CSMGem software (Sloan and Koh, 2007). The broken portion of these curves is where the acid gas liquefies and crosses the phase envelope. The steep portion is for the hydrate for the liquefied acid gas.

Example

5.1 From figure 5.1 determine whether or not a hydrate will form under the following circumstances. Assume that sufficient water is present.

a) hydrogen sulfide at 30°C and 1 MPa
b) carbon dioxide at 15°C and 5 MPa
c) methane at 15°C and 20 MPa
d) hydrogen sulfide at 15°C and 20 MPa
e) carbon dioxide at 15°C and 20 MPa

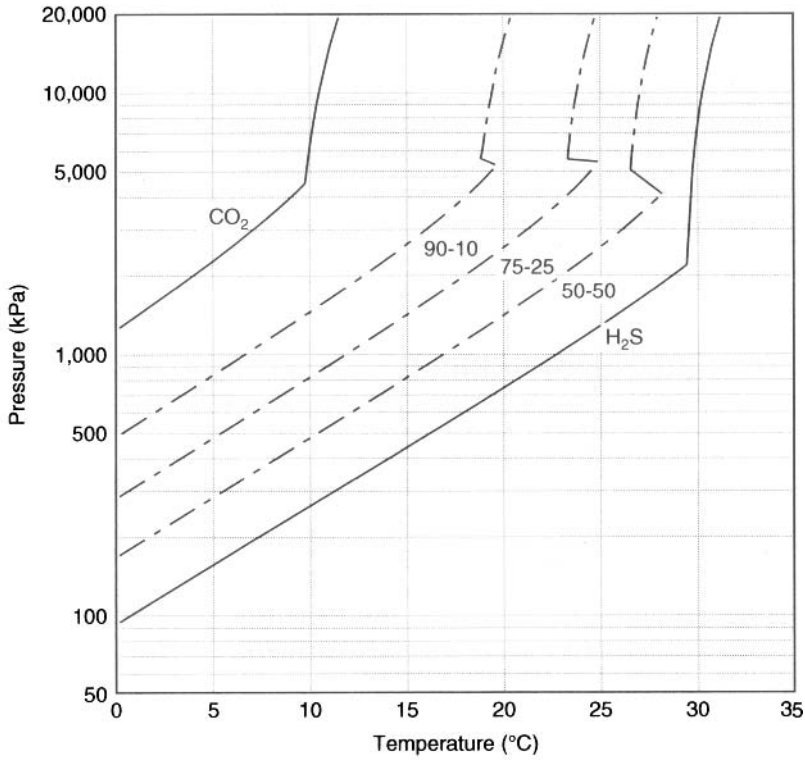

Figure 5.2 The hydrate loci for five mixtures for hydrogen sulfide + carbon dioxide.

Answer: For a hydrate to form, the pressure and temperature must be such that the point is above and to the left of the curves in figure 5.1. For case (a) the point is below the hydrate curve and thus a hydrate does not form. For carbon dioxide at 15°C a hydrate will never form regardless of the pressure, so for case (b) a hydrate does not form. For methane at 15°C and 20 MPa, case (c), the point is above the hydrate curve, so a hydrate does form. For H_2S at 15°C and 20 MPa, this point is above the hydrate curve and thus a hydrate forms. Finally, for CO_2 at 15°C and 20 MPa, the point is to the right of the hydrate curve and thus a hydrate does not form.

In summary:

a) hydrogen sulfide at 30°C and 1 MPa – **no hydrate**
b) carbon dioxide at 15°C and 5 MPa – **no hydrate**

c) methane at 15°C and 20 MPa – **hydrate forms**
d) hydrogen sulfide at 15°C and 20 MPa – **hydrate forms**
e) carbon dioxide at 15°C and 20 MPa –**no hydrate**

5.3 Estimation of Hydrate Forming Conditions

The chart presented in figure 5.1 is useful for pure components, but is less useful for mixtures. It is important to be able to predict at what conditions a hydrate will form in the mixtures encountered in acid gas injection.

5.3.1 Shortcut Methods

The *GPSA Engineering Data Book* provides two methods for performing hand calculations of the hydrate formation. Although these methods are not recommended for acid gas mixture, they will be reviewed here briefly.

The first of these is based on the gas gravity. A simple chart is provided that plots the temperature-pressure locus with the gas gravity as the third parameter.

The first reason the chart method is not recommended for acid gases is that the chart is limited to gases with gravities less than 1.0. Typical acid gas mixtures have gravities greater than 1.1 (see table 2.1). The second reason is the chart was developed for sweet gas. *It should be used with caution for sour gases and never used for acid gas.*

The second is a K-factor approach. This method is slightly more rigorous but also requires more time to perform the calculations. Using the K-factor charts requires an iterative procedure. This method should not be used for acid gas. Carroll (2004) showed that this method is not very accurate for sour gas mixtures. It predicts the real hydrate temperature to within 1.7 Celsius degrees (3 Fahrenheit degrees) only 40% of the time. It is anticipated that this method would be significantly worse for acid gas.

In fact, none of the methods designed for rapid estimation of the hydrate formation conditions should be used for acid gas mixtures. If one must do such calculations, without a computer and a rigorous model, then it is probably wise to assume the hydrate formation conditions for the acid gas mixture are the same as

those for pure H_2S. The first step should be to construct the phase envelope for the acid gas mixture. Then plot the hydrate locus for pure H_2S up to the point where it intersects the dew point locus. From that point, assume that the hydrate curve extends vertically upward.

5.3.2 Rigorous Methods

For accurate prediction of the hydrate formation conditions for acid gases, the advanced methods are preferred. The more advanced methods for predicting hydrate formation are based on the work of van der Waals and Platteeuuw (1959). This is a statistical thermodynamic model.

Parrish and Prausnitz (1972) and Ng and Robinson (1979) proposed extensions to the model of van der Waals and Platteeuuw (1959). These models extended the principles of van der Waals and Platteeuuw (1959) to: (1) mixtures, (2) gases under pressure, and (3) liquids.

Several software packages are available commercially for predicting hydrate formation. In addition, the multipurpose process simulators can also be used for this purpose.

5.4 Mitigation of Hydrate Formation

Once we have concluded that hydrates are a potential problem, we must address the question of what can be done to alleviate the problem.

Earlier, the three criteria for hydrate formation were presented. These give us some insight into methods for battling their formation. Of the three criteria, the one that we can do nothing about is the presence of a hydrate former. Obviously, in an acid gas injection scheme a hydrate former will be present. This is unavoidable.

5.4.1 Inhibition with Methanol

Perhaps the most common method to combat hydrate formation is the use of methanol, although other inhibitors could be used as well (such as glycols). Methanol is inexpensive and very effective.

Figure 5.3 shows the inhibiting effect of methanol on the hydrate of hydrogen sulfide. The experimental data shown in this figure are

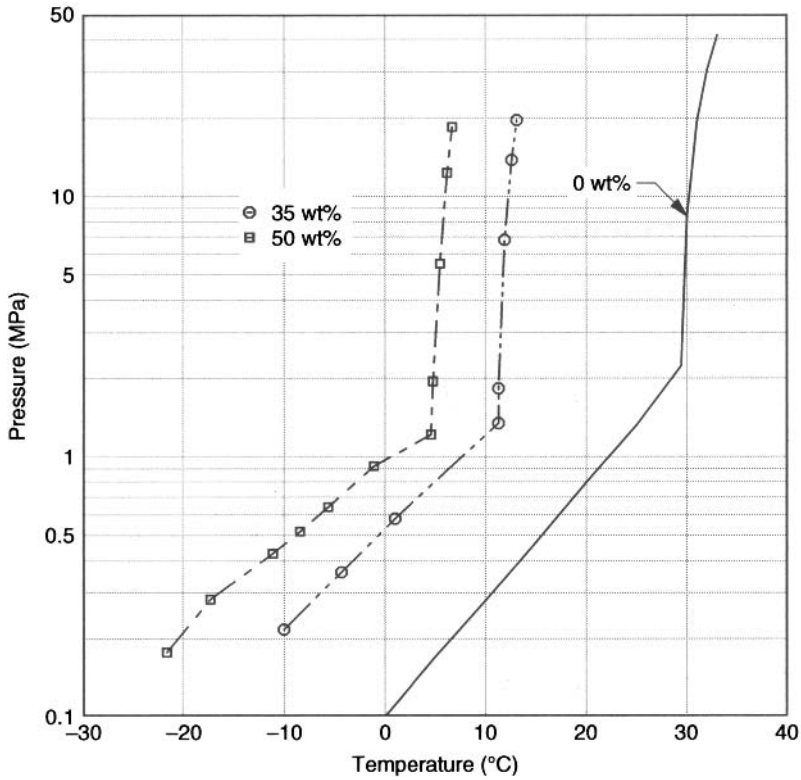

Figure 5.3 The inhibiting effect of methanol on the hydrate of hydrogen sulfide.

from Ng et al. (1985). The solid curve on this plot is the same as that on figure 5.1 but appears slightly different because of the different axes on the two plots.

The simplest method of estimating the inhibiting effect is from the Hammerschmidt equation:

$$\Delta T = \frac{1297\,W}{M(100 - W)} \tag{5.1}$$

where: ΔT – temperature depression, °C
M – molar mass of the inhibitor, g/mol
W – concentration of the inhibitor, weight per cent

This concentration is on an inhibitor plus water basis (that is, it does not include the other components in the stream).

Equation (5.1) can be rearranged in order to calculate the concentration of inhibitor required to yield an expression for the temperature depression:

$$W = \frac{100\ M\ \Delta T}{1297 + M\ \Delta T} \tag{5.2}$$

As noted earlier, typically methanol is used as the inhibitor. The molar mass of methanol is 32.042 g/mol, which is required in the Hammerschmidt equation.

Again, it is also important to note that these methanol concentrations are based on the aqueous phase. The 35 and 50 wt% noted in figure 5.3 are not the concentrations in the total mixture, but only in the aqueous phase.

To use the Hammerschmidt equation you must first estimate the hydrate conditions without an inhibitor present. The Hammerschmidt equation predicts only the deviation from the temperature without an inhibitor present, not the hydrate forming conditions themselves.

The advanced models based on van der Waals and Platteeuuw (1959) mentioned earlier have been adapted for use with inhibitors.

Example

5.2 From figure 5.3 H_2S forms a hydrate at 30°C and 8 MPa. From the Hammerschmidt equation, what weight per cent methanol is required to depress the hydrate temperature by 18°C?

Answer: From equation (5.2):

$$W = \frac{100\ M\ \Delta T}{1297 + M\ \Delta T} = \frac{(100)(32.042)(18)}{1297 + (32.042)(18)} = 30.8\ \text{wt\%}$$

For comparison, from figure 5.2 the depression in a 35 wt% methanol is about 12°C. This is very good agreement and should not otherwise be expected. The Hammerschmidt equation is a crude approximation.

5.4.2 Water-Reduced Cases

Another method of combating hydrate formation is to remove the water from the stream. No water, no hydrate – it is that simple.

The mixture requires a certain water content in order to fall on the curves shown in figures 5.1 and 5.2. If the water content is reduced below this level, then the hydrate temperature, at a given pressure, is reduced. Reducing the water content is a common method for combating hydrate formation in acid gas injection systems.

5.4.2.1 Carbon Dioxide

Figure 5.4 shows the effect of reduced water on the hydrate of CO_2 at 2068 and 3447 kPa. The plot shows the raw experimental data from Song and Kobayashi (1987). Unfortunately, a similar set of data do not exist for H_2S. The curves merely represent "best fits" through the data points. At higher temperatures the equilibrium is between hydrate and vapor, whereas at lower temperatures the equilibrium is between a CO_2-rich liquid and a hydrate. The broken vertical

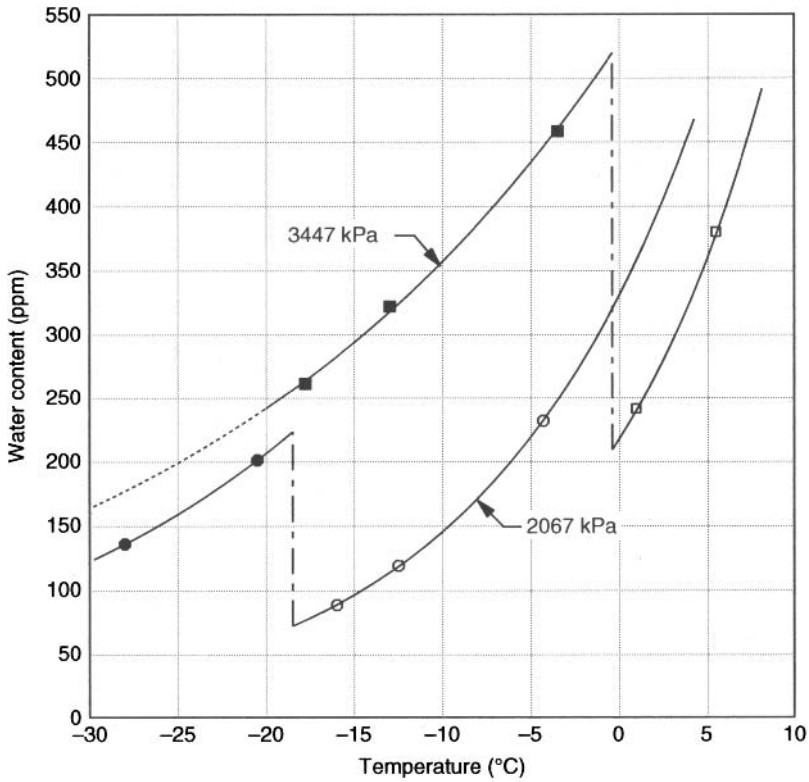

Figure 5.4 Hydrate formation in carbon dioxide at 2068 and 3447 kPa (300 and 500 psia) at reduced water conditions (data from Song and Kobayashi, 1987).

lines on the plot is the transition from one phase regime to the other. Because water is more soluble in liquid CO_2, than it is in gaseous CO_2, there is a significant inhibition in the hydrate formation.

If the stream has a sufficient amount of water (greater than about 500 ppm), then at 3447 kPa a hydrate will form at about 8°C (see figure 5.1). However, if the water content is reduced to 250 ppm (190 mg/Sm^3), the hydrate does not form until about 2.5°C if the fluid is a gas and about –19°C if the fluid is a liquid.

The data of Song and Kobayashi (1987) indicate that in the CO_2-rich liquid + hydrate region there is a strong pressure effect. Hendrick et al. (2009) modeled the hydrate forming conditions using a rigorous thermodynamic model. Their model does not show this strong pressure dependence. Predictions from the *CSMGem* software (Sloan and Koh, 2007) show similar behavior. This is not evidence that the experimental data are in error, but they show once again that the design engineer must proceed with caution.

5.4.2.2 Dehydration

There are other reasons for dehydrating a stream. In the natural gas business, the gas should be "dry," relatively free of water, in order to prevent hydrates and to prevent the formation of an aqueous phase, especially during transportation. In acid gas injection, this becomes more important since aqueous solutions of acid gases are highly corrosive.

Figure 5.5 shows the phase envelope and two hydrate loci for this acid gas mixture. The first curve labeled "Saturated" assumes that there is plenty of water present. The other hydrate locus is labeled "3.2 g/m^3[std]," and this is the hydrate curve for the acid gas containing the specified amount of water.

From the discussion in chapter 4 which will be further demonstrated in Chapter 6, 3.2 g/m^3[std] is a water content level that can be achieved simply by proper design of the compressor.

For both cases the hydrate curve for the vapor is essentially the same. Typical of an acid gas, the hydrate can form at fairly high temperatures; in this case up to about 26°C.

On the other hand, for the liquefied acid gas reducing the water content to 3.2 g/m^3[std] has a dramatic effect on the hydrate temperature. For the case where there is plenty of water, the hydrate forms at between 24° and 26°C. On the other hand, the reduced water case, the hydrate forms at less than –16°C.

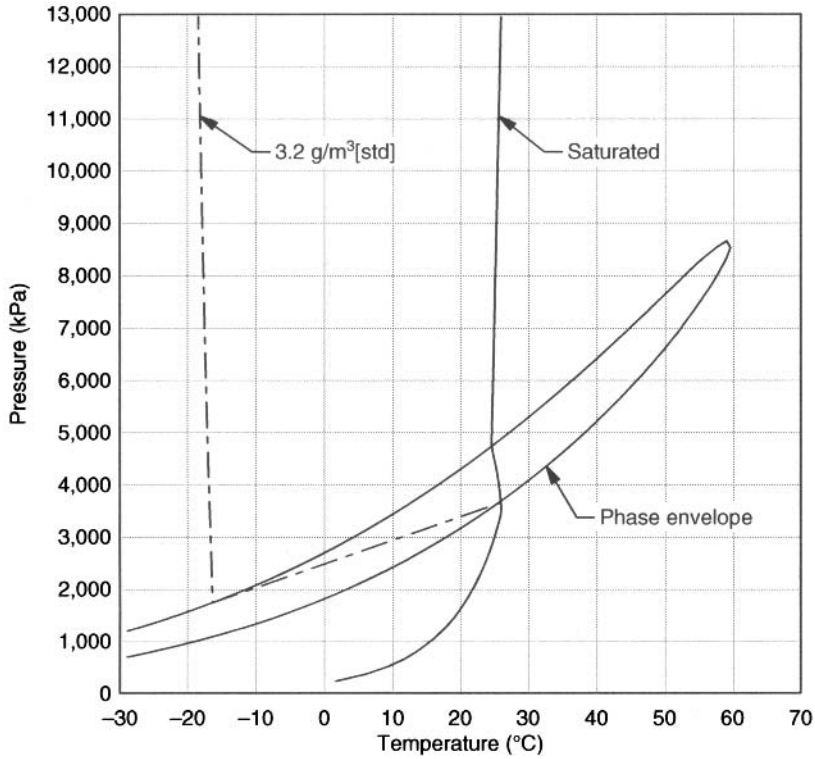

Figure 5.5 Phase envelope and hydrate curves for an acid gas mixture.

It is important to note that this effect is largest for mixtures rich in H_2S and less for mixture rich in CO_2. The design engineers must examine this effect for their specific case and draw conclusion based only on their own design.

5.4.2.3 *To Dehydrate or Not To Dehydrate? – That is the Question!*

In the annals of acid gas injection there is much debate about the necessity of dehydration. The dehydration of acid gas is a messy and corrosive problem. Some who originally installed a dehydration unit no longer use it (Lock, 1999).

In chapters 4 and 6, it is demonstrated how compression, combined with thermodynamics, can be utilized as a means of water knockout, making dehydration unnecessary.

5.4.3 Application of Heat

Another method used to combat hydrates is the use of heat. In this scheme we alter the temperature such that a hydrate will not form. From an earlier example, this means that the temperature must be such that it moves the conditions to the right of the hydrate formation curve.

5.4.3.1 Line Heaters

In pipelines, heat is usually supplied with a line heater. In the design of a line heater, sufficient heat must be supplied to the fluid such that it is never at a temperature where a hydrate will form. That means the fluid must be heated well above the hydrate formation temperature. As it flows through the line it will cool, losing energy to the environment. Once it arrives at its destination, usually the plant site, it must be warmer than the hydrate temperature. It may be necessary to use more than one line heater.

5.4.3.2 Heat Tracing

Heat tracing can also be used; however, it is usually best used if the problem is localized, for example around a valve. Points notorious for freezing in the acid gas injection scheme are the dump valves from the interstage knockout drums.

5.4.3.3 Final Comment

There may be other reasons why the temperature at the well head should be kept low. Often it is desirable to inject the acid gas in the liquid phase (more on injection pressure is presented in chapter 8).

5.5 Excess Water

As was mentioned earlier, if there is a large excess of water, then a hydrate will not form. In some disposal schemes there is a large amount of produced water that must also be disposed (Kopperson et al., 1998).

In general, the disposal of acid gas with produced water is not recommended. First, the injection pressure must be sufficiently high to keep the acid gas in solution. Typical water disposal wells are operated on vacuum. Without some pressure to keep the acid gas in

solution, problems can arise. Second, the potential to form hydrates remains high. A small change in the ratio of water to acid gas can upset the balance, and a major freezing problem may result.

5.6 Hydrates and AGI

In a well designed acid gas injection scheme, hydrates should not be a problem in normal operation. However, during start up, hydrates often occur in both pipelines and wells. This is because there is residual water left over from hydrotesting of the pipeline. Wells may have water in them from injection testing. When the high pressure acid gas comes in contact with the residual water, it will quickly freeze.

Another place where hydrates occasional occur is in the coolers of the compressor. It is important not to over-cool and thus freeze the coolers.

5.7 In Summary

Hydrates are solid ice-like compounds that are notorious for plugging process equipment and pipelines. Acid gases readily form hydrates, and thus the design engineer must be able to predict when the hydrates will form and what can be done to prevent them.

References

Carroll, J.J. 2003. *Natural gas hydrates: A guide for engineers*. Amsterdam: Gulf Professional Publishers.

Carroll, J.J. 2004. An examination of the prediction of hydrate formation conditions in sour natural gas. GPA Europe Spring Meeting, Dublin, Ireland.

Carroll, J.J. and Mather, A.E. 1991. Phase equilibrium in the system water-hydrogen sulphide: hydrate-forming conditions. *Can. J. Chem. Eng.* 69:1206–1212.

Glew, D.N. 2000. Aqueous nonelectrolyte solutions. Part XVII. Formula of hydrogen sulfide hydrate and its dissociation thermodynamic functions. *Can. J. Chem.* 78:1204–1213.

Hendrick, C., V. Hernandez, M. Hlavinka, and G. McIntyre. 2009. An analysis of hydrate conditions in acid gas injection systems. *First International Acid Gas Injection Symposium*, Calgary, AB.

Kopperson, D., S. Horne, G. Kohn, D. Romansky, C. Chan, and G.L. Duckworth. 1998. Injecting acid gas with water creates new disposal option. *Oil Gas J.* 96(31):33–37.

Lock, B.W. 1997. Acid gas disposal a field perspective. 76th Annual GPA Convention, San Antonio, TX.

Ng, H.-J. and D.B. Robinson. 1977. The Prediction of hydrate formation in condensed systems. *AIChE J.* 23:477–482.

Ng, H.-J., C.-J. Chen, and D.B. Robinson. 1985. Hydrate formation and equilibrium phase compositions in the presence of methanol: Selected systems containing hydrogen sulfide, carbon dioxide, ethane, or methane. *GPA Research Report RR–87*, Tulsa, OK.

Sloan, E.D. and Koh, C. 2007. *Clathrate hydrates of natural gases*, 3rd ed. Boca Raton, FL: CRC Press.

Song, K.Y. and R. Kobayashi. 1987. Water content of CO_2 in equilibrium with liquid water and/or hydrates. *SPE Format. Eval.* 2:500–508.

Parrish, W.R. and J.H. Prausnitz. 1972. Dissociation pressures of gas hydrates formed by gas mixtures. *Ind. Eng. Chem. Process Des. Devel.* 11:26–35.

van der Waals, J.H. and J.C. Platteeuw. 1959. Clathrate solutions. *Adv. Chem. Phys.* 2:1–57.

Yang, S.O., Yang, I.M., Kim, Y.S., and Lee, C.S. 2000. Measurement and prediction of phase equilibria for water + CO_2 in hydrate forming conditions. *Fluid Phase Equil.* 175:75–89.

6

Compression

The most significant piece of equipment in an acid gas injection scheme is the compressor. It is clearly the most complex piece of equipment in an injection scheme and it is the most expensive.

The compressor is designed using some standard techniques, but it also requires an understanding of all of the phase equilibrium presented earlier.

6.1 Overview

The purpose of a compressor is to increase the pressure of a gas. In this case we must raise the pressure of the fluid to a level such that injection of the gas into a subsurface formation can be achieved. Schematically, a four-stage compressor is shown in figure 6.1. The feed gas first enters a scrubber to remove any residual liquids – liquids can do severe damage to a compressor and must be removed.

Compression increases the temperature of the gas and thus the fluid must be cooled after each stage of compression. The cooling is usually achieved using an aerial cooler.

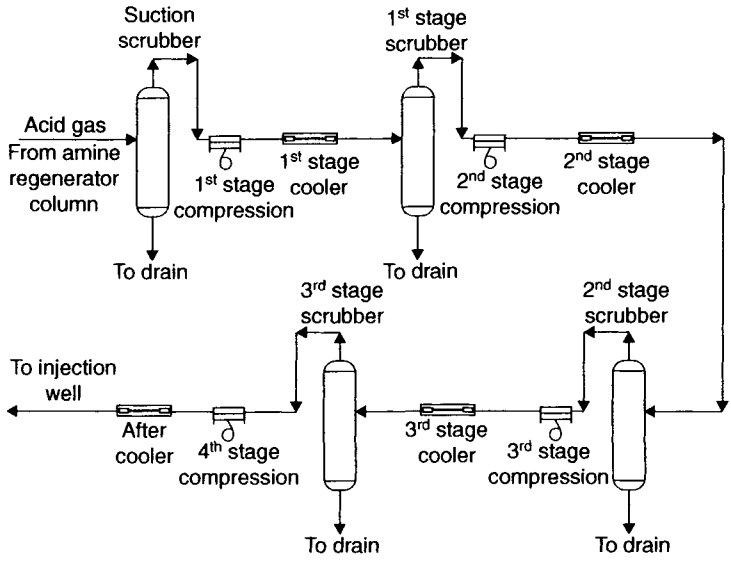

Figure 6.1 Schematic diagram of a four-stage compressor with interstage cooling and scrubbers.

After the cooling a liquids may form. In the case of acid gas injection this liquid is an aqueous phase. These liquids are removed in interstage scrubbers or knockout drums.

Figure 6.2 provides a rule of thumb criteria for selecting a reciprocating compressor versus a centrifugal compressor. Most acid gas injection schemes are low flow rate, high discharge pressure applications. From figure 6.2 it can be seen that usually a reciprocating compressor is the compressor of choice for this application. And indeed most acid gas injection schemes use a multistage reciprocating compressor.

Typically acid gas injection schemes are low flow rate (under 1 MMSCFD) and low pressure (under 200 kPa) at suction conditions. table 6.1 lists some typical flow rates both at standard conditions and actual conditions. Note, when applying figure 6.2, the abscissa is the actual flow rate. For all of the flows listed in table 6.1, the actual flow rate is less than 100 m^3[act]/min which means that reciprocating compressors are applicable.

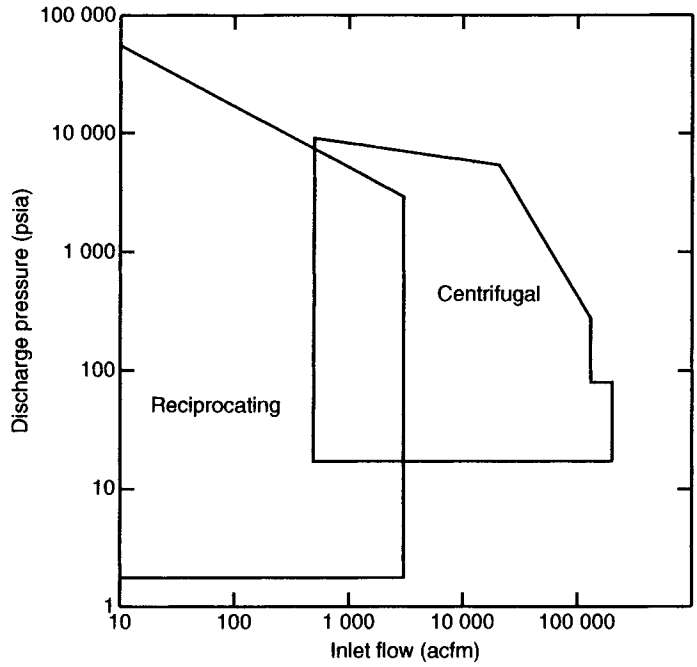

Figure 6.2 Approximate application ranges for reciprocating and centrifugal gas compressors.

Table 6.1 Typical flow rates at suction conditions for acid gas injection.

Standard Flow Rate		Actual Flow at 50°C (m^3/min)			
(MMCFD)	(10^3 m^3/d)	130 kPa	160 kPa	190 kPa	220 kPa
0.1	2.83	1.71	1.40	1.17	1.01
0.25	7.08	4.29	3.49	2.93	2.53
0.5	14.16	8.58	6.98	5.87	5.07
1.0	28.32	17.16	13.97	11.74	10.14
5.0	141.6	85.8	69.8	58.7	50.7

6.2 Theoretical Considerations

The required compression scheme is dictated by two concerns. The first, and perhaps most obvious, is the wellhead pressure

at the injection well. The pressure of the acid gas must be increased to a level sufficient for injection into the selected formation. The calculation of the injection pressure was discussed in Chapter 8.

The second criterion is an attempt to take advantage of the water holding capacity of the acid gas. A discussion of the calculation of the injection pressure for these schemes is given in a subsequent section.

For acid gas injection, the compressor is typically a small four-stage, four-throw reciprocating designed to increase the pressure of the acid gas from approximately 35 to 70 kPa(g) (5 to 10 psig) to a pressure dictated by the remainder of the injection scheme, which may be several thousand kilopascals (up to 15 MPa [2200 psi] or more).

Before the acid gas enters the compressor, a suction scrubber is used to remove any residual liquids in the acid gas stream. Additional water will drop out in the interstage scrubbers. Since there is only a pre-set amount of water present in the gas, the gas will likely be undersaturated after the fourth stage. In order to minimize the amount of water present in the gas, it is advantageous to set the final stage suction pressure at roughly the pressure of minimum water content. The water content of acid gas mixtures is discussed in a subsequent section and a previous chapter, including the maximum water content effect. By taking advantage of the thermodynamics of the acid gas mixture, one can avoid the need for dehydration of the acid gas Compression alone can be used to effectively dehydrate the gas.

6.3 Compressor Design and Operation

Acid gas behaves differently from sweet gas inside the compressor. Simulation of the actual compression horsepower and temperature rise inside the compressor must be given careful consideration. Of course, the cooling is also an important consideration. Not properly accounting for water condensation and non-aqueous phase changes (especially in final stage) can result in undersized coolers.

Compressor speed is automatically controlled to ensure that the system can respond rapidly and accurately to changes in acid

gas volumes. As well, the compressor is equipped with fuel gas make-up, fuel gas purge, auto-bypass, auto-recirculation of warm air, and a number of other safety and operations performance features.

The low suction pressure is not a major concern in the design of the compressor other than the need to be very conservative in sizing of piping, valves, and vessels.

"What-if" planning is very important. The compressor performance should be examined for a range of pressures around the intended suction pressure. Turndown is extremely important since predicting the acid gas volumes can at times be very difficult. In this respect, one needs to consider speed changes (minimum and maximum), compressor internal temperatures with volume pockets in operation, and possible gas recycle.

Discharge temperatures should be limited to about 150°C (300°F) and should never exceed 180°C (350°F). By maintaining relatively low discharge temperatures damage to the compressor, notably the packing, is reduced. In addition, high temperature can cause degradation of the compressor fluids, such as the lube oil.

Fuel gas make-up should not be used to boost suction pressure. The effect on wellhead injection is too volatile and unpredictable. As will be demonstrated, the light hydrocarbons can significantly affect the required injection pressures.

The drains after the dump valve should be heat traced. The water content is high, and with a high acid gas content, these lines freeze easily. As we have seen, hydrates readily form in acid gas mixtures.

6.4 Design Calculations

The design of a compressor begins with the First Law of Thermodynamics, the conservation of energy. The work required to compressed the gas is calculated as follows:

$$W_S = m(h_o - h_i) + Q \tag{6.1}$$

where: W_S – shaft work, W
h – enthalpy, kJ/kg
m – mass flow rate, kg/s
Q – heat transfer rate, kW

The subscript i refers to the inlet conditions and the o refers to the outlet.

It is typical to assume in the design stage that the compressor is adiabatic (Q = 0). In reality what is assumed is that the heat transfer rate is small in comparison to the other terms in the equation. Therefore equation (6.1) reduces to:

$$W_S = m(h_o - h_i) \tag{6.1a}$$

As with many equations in thermodynamics, what at first glance appears to be a simple equation is in practice quite difficult. How does one calculate the enthalpies? And what are the conditions at the exit stage in order to calculate the enthalpy once a model has been selected to do so?

The best that a compressor can operate at is isentropically. That is the entropy of the stream remains unchanged upon compression. The entropy of the stream entering is equal to the stream exiting.

$$s_i = s_o \tag{6.2}$$

where: s – entropy, J/mol·K

If we have a means to calculate the entropies, this gives us a method to calculate the outlet conditions.

6.4.1 Compression Ratio

The compression ratio for a compressor is defined as the outlet pressure divided by the inlet pressure. Mathematically:

$$C_R = \frac{P_{out}}{P_{in}} \tag{6.3}$$

where: C_R – compression ratio, unitless

By definition, the compression ratio is always greater than one. If there are n stages of compression and the compression ratio is equal on each stage, then the compression ratio per stage is given by:

$$C_{R,stage} = \left(\frac{P_{out}}{P_{in}}\right)^{1/n} \tag{6.4}$$

If the compression ratio is not equal on each stage, then Equation (6.3) should be applied to each stage.

In the early stage of the design of an acid gas injection compressor it is typical to assume equal compression ratios for each stage. This is not a hard rule and adjustments can be made taking into account other considerations.

Typically compression ratios should be less than four-to-one per stage. For cases with compression ratios larger than four, it is recommended that additional stages be added.

Example

6.1 An acid gas stream is to be compressed from 200 kPa to 10 000 kPa. What is the over all compression ratio for this process? If a four-stage compressor is used estimate the compression ratio per stage if equal compression ratio per stage are used.

$$C_{R,overall} = \frac{P_{out}}{P_{in}} = \frac{10\,000}{200} = 50$$

$$C_{R,stage} = \left(\frac{P_{out}}{P_{in}}\right)^{1/n} = \left(\frac{10\,000}{200}\right)^{1/4} = 2.659$$

Therefore ideally, the outlet pressures for each stage are:

$P_{1,out} = 2.659\ P_{1,in} = 2.659(200) = 532\ kPa$

$P_{2,out} = 2.659\ P_{2,in} = 2.659(532) = 1\,415\ kPa$

$P_{3,out} = 2.659\ P_{3,in} = 2.659(1415) = 3\,762\ kPa$

$P_{4,out} = 2.659\ P_{4,in} = 2.659(3762) = 10\,003\ kPa$

The result is not exactly 10 000 kPa because of round-off error. However, it is very close.

6.4.2 Ideal Gas

Then enthalpy of an ideal gas is a function only of the temperature and can be calculated as follows:

$$h_o^* - h_i^* = \int_{T_i}^{T_o} C_P^*\, dT \qquad (6.5)$$

where: C_P^* – isobaric heat capacity, J/kg·K

and the superscript * is used to indicate the ideal gas state.

It is typical to further assume that the heat capacity is a constant. This makes the integration easy:

$$h_o^* - h_i^* = C_P^* (T_o - T_i) \tag{6.5a}$$

This equation now gives us a means to calculate the work [from equation (7.1)], but we still require the outlet temperature. Again we resort to the isentropic approximation.

The isentropic expansion of an ideal gas is

$$Pv^k = \text{constant} \tag{6.6}$$

or

$$P_i v_i^k = P_o v_o^k \tag{6.6a}$$

where: v – molar volume, $m^3/kmol$
k – ratio of the heat capacities (C_P/C_V), dimensionless

Finally in terms of temperature:

$$\frac{T_o}{T_i} = \left(\frac{P_o}{P_i}\right)^{(k-1)/k} = \left(\frac{v_i}{v_o}\right)^{k-1} \tag{6.7}$$

It was noted earlier that the exit temperature is an important design parameter. As can be seen from equation (6.7) one way to reduce the exit temperature from a compression stage is to reduce the final pressure. Alternatively, the outlet temperature can be reduced by reducing the inlet temperature.

Combining the equation for the work of compression with the isentropic expansion yields:

$$W_S^* = \frac{k n R T_i}{k-1}\left[\left(\frac{P_o}{P_i}\right)^{(k-1)/k} - 1\right] \tag{6.8}$$

where: n – molar flow rate, mol/s
R – universal gas constant, 8.314 J/mol·K

The interested reader can find the derivation of these equations in most books on classical thermodynamics.

Real gas behavior can be partially accounted for by including the compressibility factor:

$$W_S^* = \frac{\langle z \rangle k n R T_i}{k-1}\left[\left(\frac{P_o}{P_i}\right)^{(k-1)/k} - 1\right] \tag{6.8a}$$

where the angle brackets indicate the average compressibility factor, the average between inlet and outlet conditions.

Examples

6.2 Hydrogen sulfide is to be compressed from 200 kPa to 400 kPa in the single stage compressor. At the suction the gas is at 310 K (37°C). Estimate the work per kilogram of hydrogen sulfide compressed and the exit temperature. Assume the compressor is 100% efficient and that H_2S is an ideal gas. At these conditions assume that $C_P = 35$ J/mol K and $k = 1.31$.

Answer: Calculate the work using equation (6.8)

$$\frac{W_S^*}{n} = \frac{kRT_i}{k-1}\left[\left(\frac{P_o}{P_i}\right)^{(k-1)/k} - 1\right] = \frac{(1.31)(8.314)(310)}{1.31-1}\left[\left(\frac{400}{200}\right)^{(1.31-1)/1.31} - 1\right]$$

$$= 1941 \text{ J/mol} = 1941/34.082 = 57.0 \text{ J/g}$$

$$= 57.0 \text{ kJ/kg}$$

The exit temperature can be estimated from equation (6.6):

$$\frac{T_o}{T_i} = \left(\frac{P_o}{P_i}\right)^{(k-1)/k} \quad \text{or} \quad T_o = T_i\left(\frac{P_o}{P_i}\right)^{(k-1)/k}$$

$$T_o = 310\left(\frac{400}{200}\right)^{(1.31-1)/1.31} = 365.26 \text{ K} = 92.1°\text{C}$$

For comparison, the work can be calculated from the change in enthalpy:

$$\frac{W_s^*}{n} = h_o^* - h_i^* = C_P^*(T_o - T_i)$$

$$= 35(365.26 - 310) = 1934 \text{ J/mol}$$

$$= 1934/34.084 = 56.7 \text{ J/g}$$

which is very good agreement.

The estimated work required to compress the gas is 57 kJ per kilogram of hydrogen sulfide compressed.

6.3 Repeat the above example assuming that H_2S is an ideal gas.

Answer: Guess the exit temperature and calculate the change in entropy using Equation (2.6):

$$T_2 = 350K \qquad \Delta s = -1.559\ J/mol{\cdot}K$$
$$T_2 = 400K \qquad \Delta s = +3.151\ J/mol{\cdot}K$$

Performing a linear interpolation to update the exit temperature:

$$T_2 = 366.55\ K$$

Using this temperature to update the entropies gives:

$$\Delta s = +0.059\ J/mol{\cdot}K$$

Adjusting the temperature slightly in order to span the root.

$$T_2 = 365\ K \qquad \Delta s = -0.090\ J/mol{\cdot}K$$

And one last interpolation:

$$T_2 = 365.93\ K \qquad \Delta s = 0.000\ J/mol{\cdot}K$$

The calculated change in enthalpy, and hence the work, is:

$$\Delta h = w = 1943.7\ J/mol$$

The reader should verify these calculations.

6.4 Repeat the above example using the *H_2S Tables* (Goodwin, 1983) for the properties.

Answer: At 310 K and 200 kPa the entropy of H_2S is 212.664 J/mol·K and the enthalpy is 23667.9 J/mol. At 400 kPa, this puts the outlet temperature at between 360 and 370 K. Linear interpolation is used to calculate the exit temperature.

360 K s = 212.014 J/mol·K
370 K s = 212.995 J/mol·K
s = 212.664 J/mol·K at 366.63 K (93.5°C)

Next use the pressure and the temperature to obtain the enthalpy at the outlet conditions. This again requires linear interpolation

360 K h = 25346.9 J/mol
370 K h = 25705.3 J/mol
366.63 K h = 25584.5 J/mol

$$\frac{W_S}{m} = h_o - h_i$$
$$= (25584.5 - 23667.9)/34.082$$
$$= 56.23\,J/g = 56.23\,kJ/kg$$

Note, the 34.082 in the above equation is the molar mass of hydrogen sulfide and is used to convert the enthalpies from the tables from molar values (per mole) to specific values (per gram).

Therefore it requires about 56 kJ of energy to compress each kilogram of hydrogen sulfide.

In this case the gas is at low pressure and the ideal gas is an excellent approximation.

6.5 Use the ideal gas to repeat Example 6.2 for the following mixtures:

1. 75% H_2S, 25% CO_2
2. 50% H_2S, 50% CO_2
3. 25% H_2S, 75% CO_2
4. 100% CO_2
5. 98% H_2S, 2% CH_4
6. 74% H_2S, 24% CO_2, 2% CH_4
7. 49% H_2S, 49% CO_2, 2% CH_4
8. 24% H_2S, 74% CO_2, 2% CH_4
9. 98% CO_2, 2% CH_4

Answer: The table below summarizes the calculations which were performed with the spreadsheet provided. Also included in the

table is the case for pure hydrogen sulfide which was taken from the earlier example.

On a molar basis the compression work does not change very much for the various mixtures ranging from a low of 1927.7 J/mol to 1945.2 J/mol – the difference being less than 1%. Expressing the work on a molar basis is significant because the molar flow rate is proportional to the standard volumetric flow rate. Thus to compress 1 Sm^3 of each of these mixtures requires approximately the same amount of work. This is true even though the exit temperatures is different for the various mixtures.

However, there is a trend where mixtures rich in hydrogen sulfide require slightly more work than do mixtures rich in carbon dioxide.

Mixture	Work (J/mol)	Work (kJ/g)	Exit Temp (K)	Exit Temp (°C)
100% H_2S	1943.7	57.03	365.93	92.78
75% H_2S, 25% CO_2	1939.2	53.04	364.22	91.07
50% H_2S, 50% CO_2	1935.1	49.56	362.63	89.48
25% H_2S, 75% CO_2	1931.1	46.50	361.14	87.99
100% CO_2	1927.7	43.28	359.75	86.60
98% H_2S, 2% CH_4	1945.2	57.68	366.43	93.28
74% H_2S, 24% CO_2, 2% CH_4	1940.9	53.76	364.76	91.61
49% H_2S, 49% CO_2, 2% CH_4	1936.4	50.19	363.13	89.98
24% H_2S, 74% CO_2, 2% CH_4	1932.7	46.67	361.62	88.47
98% CO_2, 2% CH_4	1929.0	44.40	360.25	87.10

On the other hand, when the work is expressed on a per unit mass basis it requires significantly more work to compress H_2S than

CO_2. The reason for this is that CO_2 has a much larger molar mass than does H_2S (see Chapter 2).

The addition of a small amount of methane to the mixture tends to increase the work per unit mole required to compress the gas.

Additional similar calculations are provided in the appendix. The reader can peruse these to investigate the subtleties of these calculations.

6.4.3 Efficiency

As was mention, the isentropic compression is the best that we can expect from a compressor. That is, it represents the minimum work of compression. The actual work of compression is usually described by an efficiency:

$$\eta = \frac{W_{isentropic}}{W_{actual}} \tag{6.9}$$

where: η – isentropic efficiency, dimensionless (often expressed as a percent)

The efficiency is between zero and one and thus the actual work is always greater than the isentropic work.

Adiabatic efficiencies typically are in the range from 70% to 90%. They tend to increase with increasing flow rate and compression ratio. That means that larger compressors tend to be more efficient than smaller ones.

Including the isentropic efficiency ion the equation for the temperature yields:

$$\frac{T_o}{T_i} = \left(\frac{P_o}{P_i}\right)^{(k-1)/\eta k} \tag{6.10}$$

When the exponent on the ratio of the pressures is other than the ratio of the heat capacities, this is a general expression for a polytropic expansion.

There is a third efficiency that is often used and that is the polytropic efficiency. It is directly related to the isentropic efficiency and cannot be specified in addition to the isentropic efficiency.

$$\frac{T_o}{T_i} = \left(\frac{P_o}{P_i}\right)^{(k/\chi-1)/k/\chi} \tag{6.11}$$

where: χ – is the polytropic efficiency, dimensionless, usually expressed as a percent

The mechanical efficiency is the ratio of the indicated horsepower in the compressing cylinders to the brake horsepower delivered to the shaft. It is usually expressed as a percent.

Including both the isentropic and mechanical efficiencies into the equation for the work, yields:

$$W^* = \frac{k\,n\eta R T_i}{E\,(k-1)}\left[\left(\frac{P_o}{P_i}\right)^{(k-1)/\eta k} - 1\right] \tag{6.12}$$

where: E is the mechanical efficiency.

Including the compressibility factor yields:

$$W = \frac{\langle z\rangle\, k\,n\eta R T_i}{E\,(k-1)}\left[\left(\frac{P_o}{P_i}\right)^{(k-1)/\eta k} - 1\right] \tag{6.13}$$

6.6 For Example 6.2, calculate the work require for compression if the compressor has an efficiency of 81%.

Answer: From equation (7.3):

$$\eta = \frac{W_{isentropic}}{W_{actual}} \quad \text{or} \quad W_{actual} = \frac{W_{isentropic}}{\eta}$$

$$W_{actual} = 56.23/0.81 = 69.4 \text{ kJ/kg}$$

Note, the actual work is larger than the isentropic work. The isentropic work being the minimum required for the specified compression.

6.4.4 Ratio of the Heat Capacities

As can be seen from the relatively simple design equations, the ratio of the heat capacities, k, is an important physical property

for compressor design. Figure 6.3 shows the ratio of the ideal gas heat capacities for H_2S, CO_2, and for three mixtures of the two components.

The heat capacities of real gases are a function of the pressure and thus may differ from the ideal gas case shown in the plot. However, the author's experience is that using the ideal gas k is sufficient for most engineering applications.

6.5 Interstage Coolers

As has been demonstrated, the acid gas warms significantly upon compression. In the design of a compressor the temperature should not exceed 180°C (350°F). In a multistage compressor the gas must be cooled on the interstage.

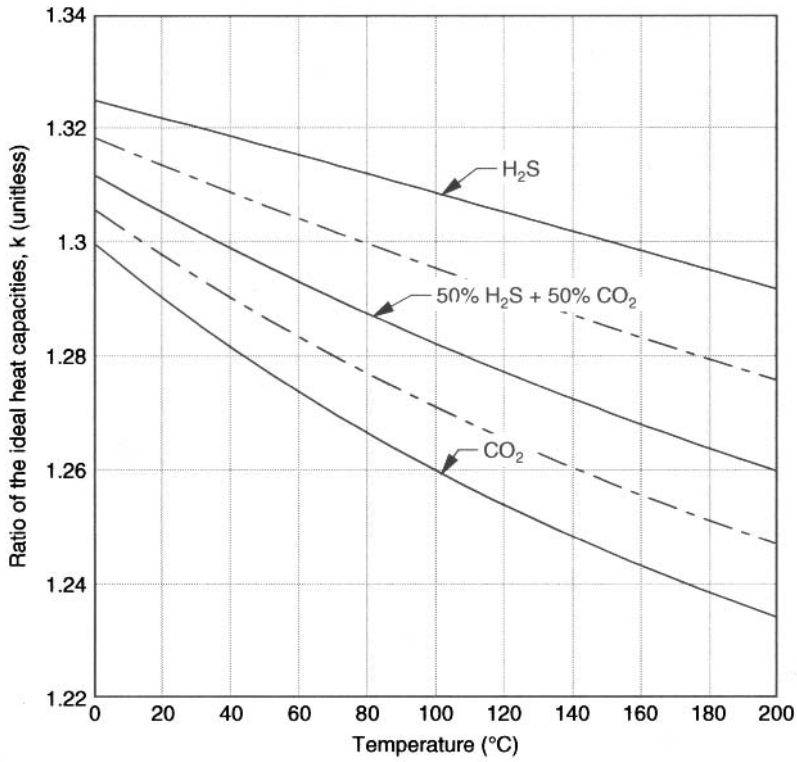

Figure 6.3 Ratio of the heat capacities for acid gas mixtures (100% CO_2, 75% CO_2 + 25% H_2S, 50% CO_2 + 50% H_2S, 25% CO_2 + 75% H_2S, and 100% H_2S).

Interstage cooling is usually achieved using aerial coolers. The design of these cooler is such that the exit temperature of the gas is about 40°C (120°F). In warmer climates this design temperature maybe as high as 50° or 55°C.

In acid gas compression the cooling will also result in a phase change. In the early stages of compression the phase change is the condensation of an aqueous phase. At higher pressure there may also be a liquefaction of the acid gas.

6.5.1 Design

The design on an aerial cooler is the same as for any heat exchanger. As with the compressor, our design begins with the First Law of Thermodynamics, Equation (6.1). However, in the case of the cooler, there is no shaft work and it is the heat transfer that we wish to calculate. Thus equation (6.1) becomes:

$$Q = m(h_o - h_i) \tag{6.14}$$

From conservation of energy considerations, and assuming that there is negligible heat loss to the surroundings, the cold fluid gains all of the energy lost by the hot fluid. In terms of enthalpy, this is

$$Q = m_C (h_{C,o} - h_{C,i}) \tag{6.15}$$

$$Q = m_H (h_{H,i} - h_{H,o}) \tag{6.16}$$

If there is no phase change, then the enthalpies can be replaced with the product of the temperature and the heat capacity. Equations (6.15) and (6.16) become:

$$Q = m_C C_C (T_{C,o} - T_{C,i}) \tag{6.17}$$

$$Q = m_H C_H (T_{H,i} - T_{H,o}) \tag{6.18}$$

Once again, the subscripts C and H refer to the cold and hot fluid respectively. Because equations (6.17) and (6.18) are explicit in temperature there is a temptation to use them in all situations.

However, again they cannot be used if there is a change of phase. As was already noted, a change in phase is common in acid gas compression.

In addition, there is an implied assumption that the heat capacities are constants. This is a satisfactory assumption if the is not a large change in temperature.

The design equations for a heat exchanger can be derived from theoretical considerations. Those interested in the derivations should consult a textbook on heat transfer such as Incropera and De Witt (1990). For brevity, the derivations will be omitted and only the final result is presented here:

$$Q = F\,U\,A\,\Delta T_{lm} \tag{6.19}$$

where: Q – heat transfer rate, kJ/s (kW)
F – geometric factor, unitless
U – overall heat transfer coefficient, kW/m^2·°C
A – area available for heat transfer, m^2
T_{lm} – logarithmic mean temperature difference, °C

Typical for aerial coolers, the U is between 50 and 175 W/m^2·°C (30 to 100 Btu/hr·ft^2·°F) but may be even larger if condensation is occurring.

Charts are available for the F for various flow configurations in the heat exchangers. These charts give the F as a function of the various temperatures. A chart for the typical configuration of an aerial cooler is given in Incropera and De Witt (1990) (and other textbooks on heat transfer).

The logarithmic mean temperature difference is defined as:

$$\Delta T_{lm} = \frac{\left(T_{H,in} - T_{C,out}\right) - \left(T_{H,out} - T_{C,in}\right)}{ln\left[\dfrac{T_{H,in} - T_{C,out}}{T_{H,out} - T_{C,in}}\right]} \tag{6.20}$$

where the subscripts H and C refer to the hot and cold fluids respectively and in and out refer to the inlet and outlet conditions.

The overall heat transfer coefficient is calculated from a combination of thermal resistances: (1) the resistances due to the fluids, (2) the resistance due to the material from which the heat exchanger is

constructed, and (3) fouling. More on fouling later. The overall heat transfer coefficient is calculated from the following equation:

$$\frac{1}{UA} = \frac{1}{h_C A_C} + \frac{ln(r_o/r_i)}{2\pi k L} + \frac{1}{h_H A_H} + \frac{R_{foul}}{A} \tag{6.21}$$

where: h – connective heat transfer coefficient, kW/m^2•°C
k – thermal conductivity of exchanger material, kW/m•°C
r_o – outside diameter of tubes, m
r_i – inside diameter of tubes, m
L – length of the tubes, m
R_{foul} – fouling factor, m^2•°C/kW

And as before the subscripts H and C refer to the hot and cold fluids.

One of the problems with engineering writing is the use of redundant symbols. Note the h in the above equation is a heat transfer coefficient and not an enthalpy as it was in previous equations.

It is convenient to use typical values for preliminary design of heat exchangers. However, for detailed design, the rigorous methods should be employed. Fortunately there are several software packages available for this purpose.

There are many correlations for estimating heat transfer coefficients. These are based on the properties of the fluid and flow considerations. However almost all of them can be expressed in the dimensionless form:

$$Nu = f(\text{Re or Gr,Pr}) \tag{6.22}$$

where: Nu – Nussult number, dimensionless heat transfer coefficient
Re – Reynolds number, flow conditions and fluid properties, dimensionless used for forced convection
Gr – Grashof number, flow conditions and fluid properties, dimensionless, used for free convection
Pr – Prandtl number, fluid properties, dimensionless

Examples

6.7 Estimate the energy required to cool 5000 m³[std]/d of hydrogen sulfide from 150°C to 50°C at 3000 kPa. Use the *H_2S Tables* (Goodwin, 1983) for the fluid properties.

Answer: First, convert 500 m³[std][1] to moles using the ideal gas law:

$$n = PV/RT = (101.325)(5000)/(8.314)(15.56 + 273.15)$$
$$= 211.07 \text{ kmol/d} = 8.794 \text{ kmol/h}$$

From the *H_2S Tables*:w

420 K h = 26708.1 J/mol
430 K h = 27112.3 J/mol

Linearly interpolating at 150°C (423.15 K) gives: h = 26835.4 J/mol
From the *H_2S Tables*:

320 K h = 22200.2 J/mol
330 K h = 22746.2 J/mol

Linearly interpolating at 50°C (323.15 K) gives: h = 22372.2 J/mol

$$Q = (8.794)(26835.4 - 22372.2) = 39249 \text{ kJ/h} = 10.9 \text{ kJ/s} = 10.9 \text{ kW}$$

6.8. Repeat the above example, but assume that 1.25 kg/h of water condense along with the cooling.

Answer: From the *Steam Tables* (Haar et al, 1983) the latent enthalpy of vaporization of water at 50°C is 2591.2 kJ/kg.

$$Q = (1.25)(2591.2) = 3239 \text{ kJ/h} = 0.9 \text{ kJ/s} = 0.9 \text{ kW}$$

and the total heat load is:

$$Q_{tot} = 10.9 + 0.9 = 11.8 \text{ kW}$$

1. Standard conditions being 1 atm (101.325 kPa) and 15.56°C (60°F).

So, in this case the condensation of water on the interstage adds about 7.6% to the total.

6.5.2 Pressure Drop

As the fluid flows through the cooler, there is a pressure drop. Typically this pressure drop is about 35 kPa (5 psi), but clearly it is a function of the cooler design. In preliminary design a value of 35 kPa can be used. Note this has a significant effect on the suction pressure to the low pressure stages.

6.5.3 Phase Equilibrium

During the compression-cooling cycle it is important that the acid gas is not liquefied. Therefore in the design of the compressor it is important to consider the phase envelope. The compression-cooling curve should be plotted on the phase envelope. This allows for rapid interpretation.

As a safe design the interstage cooling should not be within 5°C of the acid gas dew point. This concept is perhaps best explained by using an example.

Figure 6.4 shows the phase envelope for a mixture containing 6.3% CO_2 and 93.7% H_2S. the goal is to compre ss this mixture from 200 kPa to 11 000 kPa, with interstage cooling to 50°C. As a first approximation, it is assumed that the compression ratio is equal on each stage and that the polytropic and mechanical efficiencies are 85%. For simplicity it is assumed that the compressibility factor throughout the compression is one. The reader is encouraged to investigate the effect of changing the z-factor on this calculation.
Performing the calculation using equal compression ratio on each stage and using the simplified compressor equation, the results are summarized in table 6.2.

These values meet our first criteria that the discharge temperatures must be less than 180°C.
Plotting these values on the phase envelope reveals a problem. After cooling on the third stage, the fluid crosses the phase envelope and thus the acid gas is liquefied. This can be seen on figure 6.4a. The saw toothed curve on the figure represents the compression cooling cycle. The suction is at the lowest pressure and temperature (200 kPa and 50°C). In the first stage the gas is compressed to 545 kPa

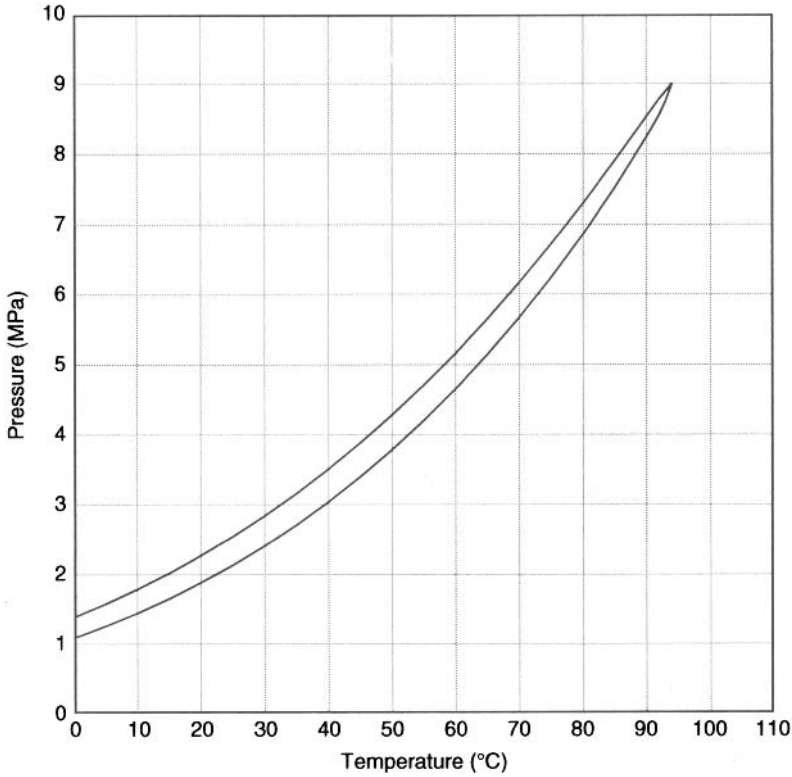

Figure 6.4 Phase envelope for an acid gas mixture (6.3% CO_2 and 93.7% H_2S).

Table 6.2 Summary of compression calculations for an acid gas mixture – first design.

	Suction Press (kPa)	Suction Temp (°C)	Discharge Press (kPa)	Discharge Temp (°C)
1st Stage	200	50	545	155
2nd Satge	545	50	1 483	155
3rd Stage	1 483	50	4 039	155
4th Stage	4 039	50	11 000	155

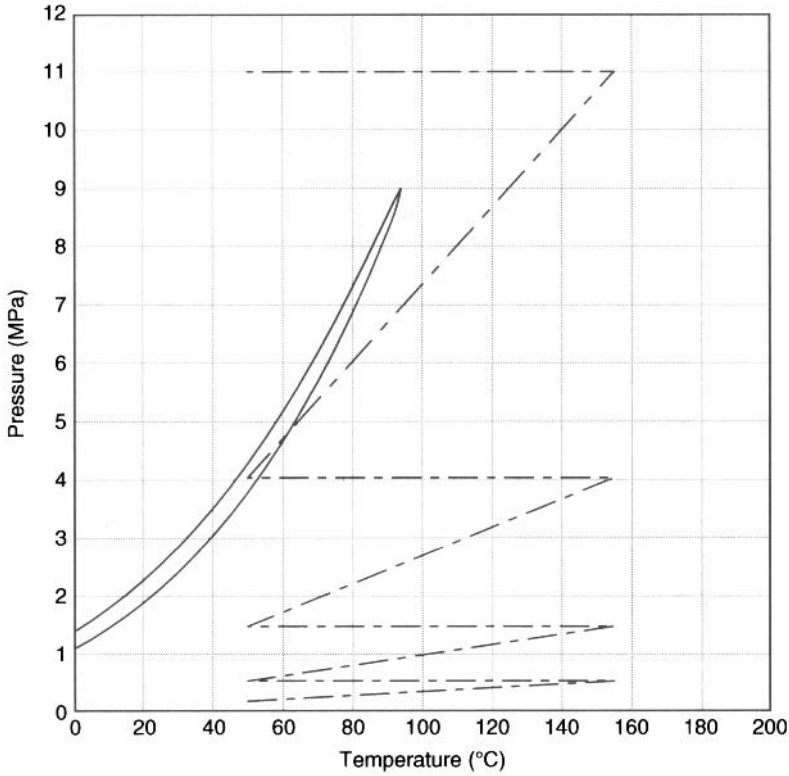

Figure 6.4a Phase envelope for an acid gas mixture (6.3% CO_2 and 93.7% H_2S) showing compression curve for first design.

and as a result of this compression is heated to 155°C. The gas is cooled, isobarically in this case, to 50°C. The remainder of the compression stages are plotted in a similar fashion.

As a second design attempt, the suction temperature to the third stage will be increased to 70°F, which will allow us to avoid acid gas condensation. The results of this design are summarized in table 6.2a.

In this case, the second design, we have violate our first criteria – the temperature rises above 180°C. Therefore this design is also unacceptable. In addition, as we shall see later, there are other reasons why we should avoid high interstage temperatures.

Next consider using 5 stages instead of four. The results of this simulation are summarized in table 6.2b.

Table 6.2b Summary of compression calculations for an acid gas mixture – third design (five stages).

	Suction Press (kPa)	Suction Temp (°C)	Discharge Press (kPa)	Discharge Temp (°C)
1st Stage	200	50	446	132
2nd Satge	446	50	994	132
3rd Stage	994	50	2 214	132
4th Stage	2 244	50	4 935	132
5th Stage	4 935	50	11 000	132

Using five stages did not solve the problem. As can be seen from figure 6.4b, the compression crosses the phase envelope on the second last stage.

By inspecting figure 6.4a, we can see that if the third stage discharge pressure is reduced to about 3500 kPa, then the liquefaction can be avoided. The results of this simulation are presented in table 6.2c and plotted on figure 6.4c.

This represents a preliminary design of the compressor. The ultimate design will be the responsibility of the compressor manufacturer. However, when checking their design all of the criteria outlined above should be considered. On occasion we have seen compressor designs that do not account for acid gas liquefaction on the interstage.

6.6 Compression and Water Knockout

The water content of both gaseous and liquefied acid gas was discussed in an earlier chapter.

In the compression of the acid gas we try to take advantage of one of two observations: (1) the minimum in the water content of acid gas or (2) liquefied acid gas can dissolve more water than the gas under pressure.

In the design of a compressor for optimal water knock out, a water content diagram is constructed.

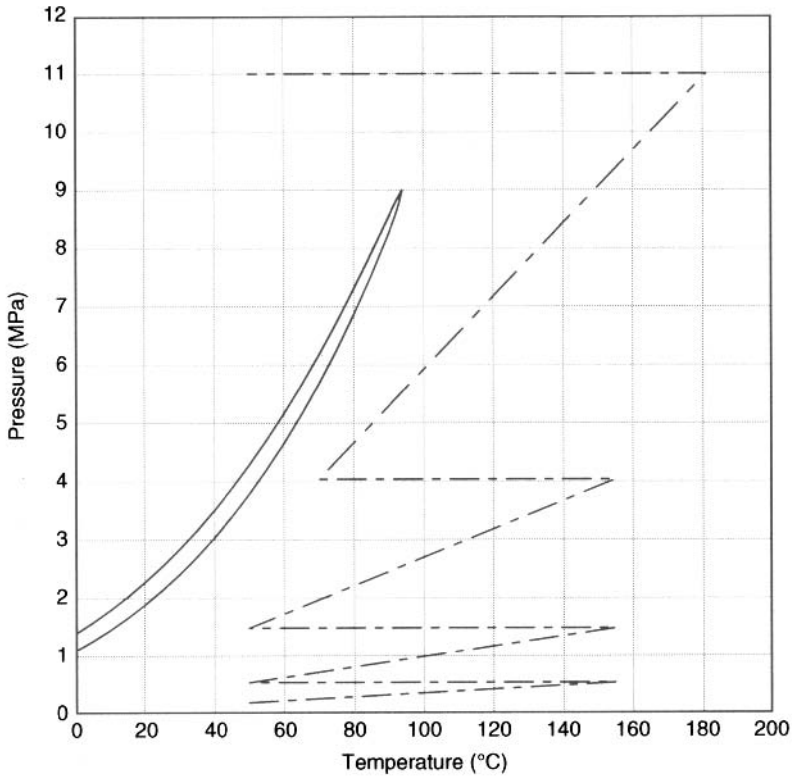

Figure 6.4b Phase envelope for an acid gas mixture (6.3% CO_2 and 93.7% H_2S) showing compression curve for second design.

Table 6.2c Summary of compression calculations for an acid gas mixture – fourth design.

	Suction Press (kPa)	Suction Temp (°C)	Discharge Press (kPa)	Discharge Temp (°C)
1st Stage	200	50	519	149
2nd Satge	519	50	1 348	149
3rd Stage	1 348	50	3 500	149
4th Stage	3 500	50	11 000	173

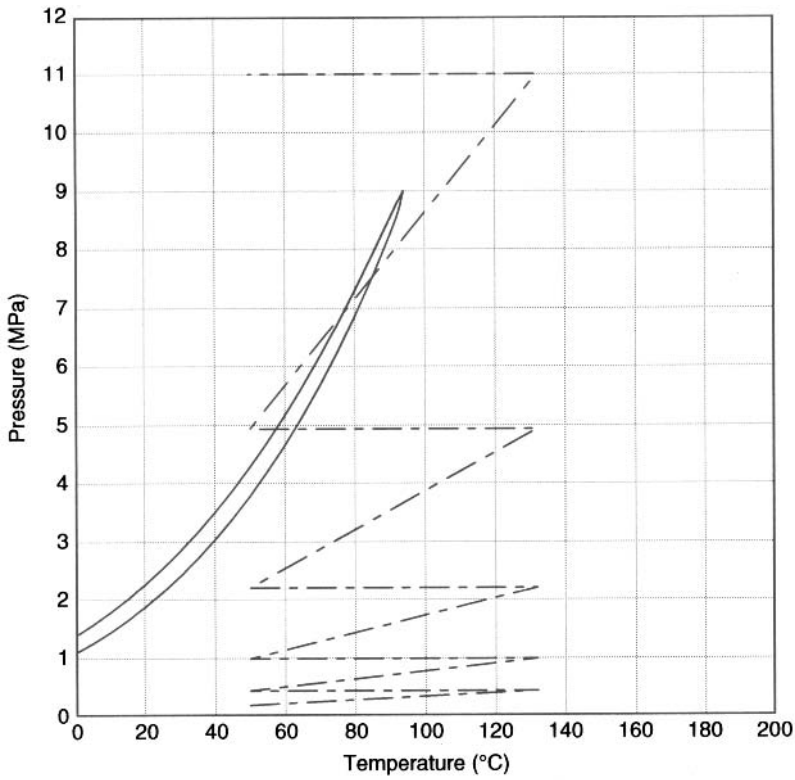

Figure 6.4c Phase envelope for an acid gas mixture (6.3% CO_2 and 93.7% H_2S) showing compression curve for third design.

In order to achieve optimal water knock out the discharge pressure from the next to last stage should be in the range of 3 to 7 MPa (435 to 1000 psia), again being careful to avoid liquefaction of the acid gas on the interstage.

To demonstrate this point, consider an example. Figure 6.5 shows the saturated water content for an acid gas mixture (the solid line representing the water content). Note the similarity between this curve and the curves shown in figure 4.5. The trapezoidal region represents the acid gas phase transition. For this acid gas mixture the dew point is at 7.56 MPa and the bubble point is 8.60 MPa.

Also shown in figure 6.5 is the compression curve. The compressor suction is 0.150 MPa and 48.9°C (21.8 psia and 120°F) and at these conditions the water content is off scale for this plot, but it is

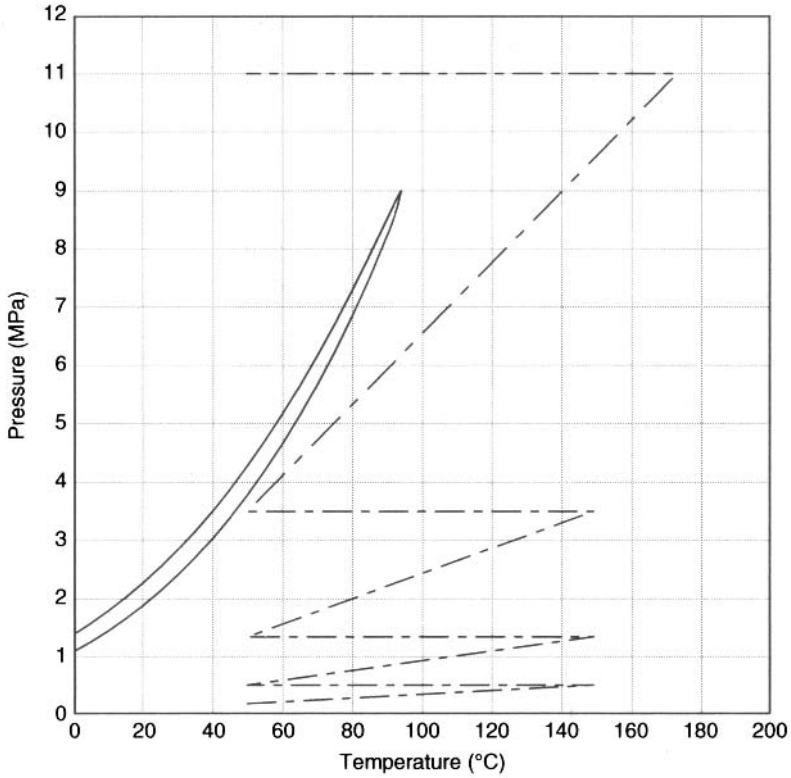

Figure 6.4d Phase envelope for an acid gas mixture (6.3% CO_2 and 93.7% H_2S) showing compression curve for fourth design.

estimated to be 60 g/Sm³. After the first stage of compression the gas is at 0.406 MPa ansd once cooled to 48.9°C the water content of the gas is about 22.3 g/Sm³. Similarly, after the second stage of compression and cooling the gas is at 1.17 MPa and has a water content of 8.30 g/Sm³. And after the third stage of compression the gas is at 3.36 MPa and has a water content of 3.58 g/Sm³. Examining figure 6.5 shows that this is not at exactly in the minimal water content region, but it is quite close.

Finally, the gas is compressed in the fourth stage to 9.65 MPa and cooled to 48.9°C. At these conditions the acid gas is completely liquefied. This seems like a contradiction to comments earlier about avoiding condensation of the acid gas. Liquefaction after compression is not problematic. Next, note from figure 6.5 that at the condition after the final stage of compression and after cooling that

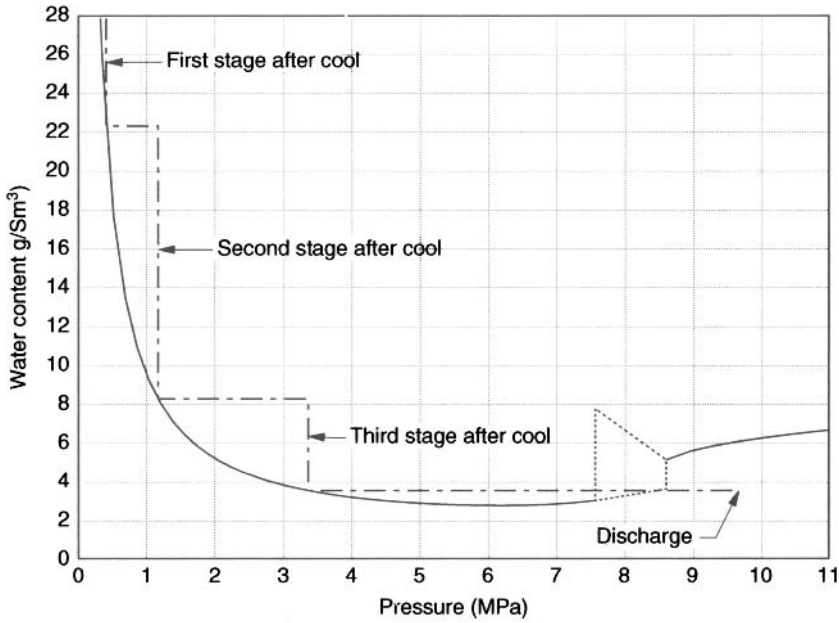

Figure 6.5 Water content curve for an acid gas mixture showing the water knockout due to compression and cooling.

the point lies below the saturated water content curve. That means that at these conditions the fluid is under saturated with respect to water. The saturated water content at 48.9°C and 9.65 MPa is 6.1 g/Sm³ whereas this fluid contains only 3.58 g/Sm³.

This chart can be used to estimate how much water is removed on each of the interstages. For example, compression from 0.150 kPa to 0.406 MPa the water content of the stream is reduced from 60 to 22.3 g/Sm³. If the flow rate of the acid gas is 30×10^3 Sm³/d (1.060 MMCFD) then $(60 - 22.3)(30 \times 10^3) = 1\ 131\ 000$ g/d = 1 131 kg/d of water condense on the first stage. Similar calculations can be used to estimate the water removal on the other stages.

6.6.1 Additional Cooling

In some acid gas injection schemes additional cooling is used on the interstage to knockout more water. If there is excess refrigeration capacity a slipstream could be use to cool the acid gas. In general this is probably not necessary.

One word of caution, the cooling must not be to too low of a temperature. The design engineer must be careful to avoid hydrate formation. Remember, hydrates in acid gas can form at temperatures as high as 30°C.

6.7 Materials of Construction

First stage suction piping and vessels can be constructed from carbon steel since it is the same design pressure and conditions as amine regeneration reflux vessel. All other downstream piping, vessels, coolers, and equipment should be constructed from stainless steel.

The materials used in the compressor are as follows: carbon steel cylinders with Teflon[2] piston rings, Teflon rod packing, stainless piston rod (tungsten coated), and NACE sour bolting. Of course, crankcase and packing ventilation and gas control are critical. Sometimes it can very difficult to achieve a good packing/seal on the piston rod, particularly on first stage where pressure differentials are low and a rod seal may not conform to the rod for the initial wear-in period.

Ring joint flanges seem to provide better seals than raised face flanges but getting valves and flanges apart can be difficult.

In addition, the use of stainless steel for valves, thermowells, instrument lines, manifolds, etc. is recommended. The cooler headers, bundles, tubes, connections etc., should also be constructed from stainless steel.

6.8 Advanced Design

6.8.1 Cascade

The water removed in the interstage scrubbers still contains some acid gas dissolved in it. If this gas is sent to flare (actually to the flare knockout drum), as was the case in most of the earlier designs, then some acid gas is being flared. In order to reduce this acid gas, the water from an interstage scrubber is sent back to the scrubber for the previous stage.

Figure 6.6 shows a schematic of a four stage compressor with the water from the interstage knockouts cascaded back to the previous stage, Theoretically the water from all subsequent stages

2. Teflon is a registered trade mark of Du Pont, Wilmington, Delaware and Teflon is a fluoropolymer.

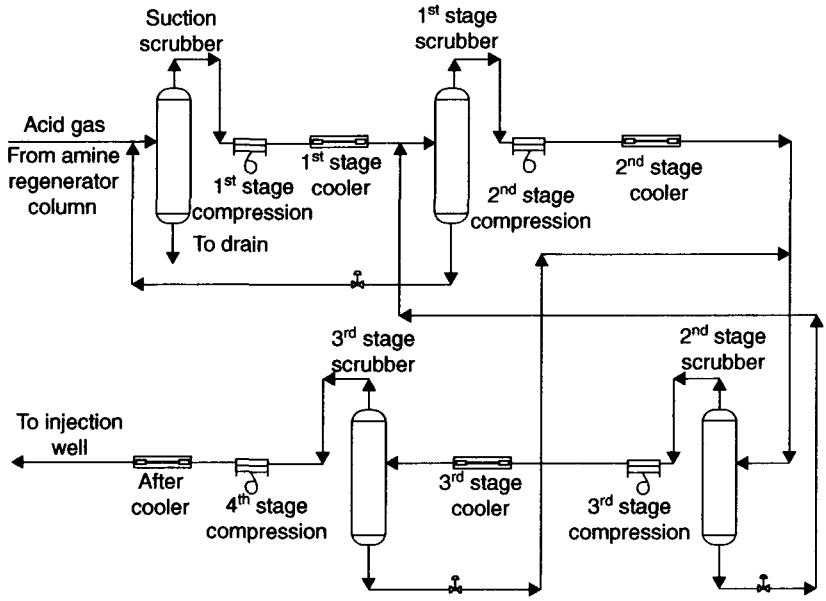

Figure 6.6 Schematic diagram of a four-stage compressor with interstage cooling and scrubbers and cascading the liquid produced to the previous stage.

could be sent to the suction scrubber, but many of the stages would take a large pressure drop resulting in a large cooling due to the Joule-Thomson effect. Even cascading back a single stage may result in freezing of the lines so heat tracing may be required.

6.8.2 CO_2 Slip

This is less a comment about compressor design and more a comment about the design of the sweetening unit. However, we have seen that the power required to compress a gas steam is directly proportional to the flow rate. Thus anything that can be done to reduce the flow of acid gas will have a direct impact on the compressor power. One amine design that has become quite popular is CO_2 slip – allowing some of the CO_2 to remain in the sweet gas stream. The MDEA-based solvents are design to permit some CO_2 slip. Typical gas contracts allow for approximately 2% CO_2 in the sweet gas.

For example a feed stream of 100 MMCFD containing 3% CO_2 and 1% H_2S will produce a 5 MMCFD acid gas stream, if all of the acid gas is removed from the feed. However, if CO_2 is allowed to

slip into the sales gas, such that the sales gas contains 2% CO_2, then the acid gas stream is reduced to 3 MMCFD.

6.9 Case Studies

This section present the design and operating conditions for three acid gas injection schemes as presented in the literature. The three examples are 1. Wayne-Rosedale (Ho et al. 1996), 2. Acheson (Lock, 1997), and 3. West Pembina (Lock, 1997).

These are all from the first generation and thus the science of AGI was not completely developed at that time. For example in each case the design discharge pressure was significantly greater than the actual. This is because of errors in the prediction of the required injection pressure. This is not an over design to reduce the water content.

For these compressors the average pressure drop through the coolers is about 20 kPa, which is significantly less than the design value of 35 kPa given in Chapter 6. In spite of this the value of 35 is still recommended for design. Note the 300 kPa drop from stage 3 to stage 4 at Wayne-Rosedale is due in part to the dehydration unit.

6.9.1 Wayne-Rosedale

Compressor: Knox Western TAP-445
Drive: electric motor
Power: 300 hp
Material: largely 316L Stainless

	Suction				Discharge			
	Pressure (kPa[g])		Temperature (°C)		Pressure (kPa[g])		Temperature (°C)	
	Design	Actual	Design	Actual	Design	Actual	Design	Actual
First	37	45	43	40	310	295	141	139
Second	302	285	49	44	1096	1015	143	145
Third	1073	1000	49	47	3103	3200	136	144
Forth	2863	3000	49	30	7377	5650	131	85
Fifth	7227	5600	49	40	22 715	6000	145	45

6.9.2 Acheson

Compressor: Ariel JG/4
Drive: electric motor
Power: 200 hp
Material: largely 316L Stainless

	Suction				Discharge			
	Pressure (kPa[g])		Temperature (°C)		Pressure (kPa[g])		Temperature (°C)	
	Design	Actual	Design	Actual	Design	Actual	Design	Actual
First	57.3	60	47.8	30	268.9	220	111.1	95
Second	234.4	200	48.9	25	823.5	690	125.7	90
Third	789.1	680	48.9	25	2091.2	1520	116.6	90
Forth	2022.3	1500	48.9	25	6538.8	3800	129.5	100

6.9.3 West Pembina

Compressor: Ariel JG/4
Drive: electric motor
Power: 200 hp
Material: largely 316L Stainless
fourth stage carbon steel due to dehydration on interstage

	Suction				Discharge			
	Pressure (kPa[g])		Temperature (°C)		Pressure (kPa[g])		Temperature (°C)	
	Design	Actual	Design	Actual	Design	Actual	Design	Actual
First	53	46	44	28	340	292	157	123
Second	283	276	43	40	1125	1025	153	145
Third	1050	1011	43	37	3575	3019	155	138
Forth	3422	2996	43	39	12 360	7954	169	130

6.10 In Summary

The compressor is the most expensive component of the acid gas injection process. The design of the compressor follows standard design procedures, but the design engineer should pay attention to the potential of using compression for water knockout. Also, acid gas tends to liquefy more readily than natural gas. Liquefaction of acid gas on the interstage posses a significant problem. Ergo the design should avoid this situation.

References

Goodwin, R.D., *Hydrogen Sulfide Provisional Thermophysical Properties From 188 to 700 K at Pressures to 75 MPa*, NBS Report No. NBSIR 83–1694, National Bureau of Standards (now the National Institute of Standards and Technology), Boulder, CO, (1983).

Haar, L., J.S. Gallagher, and G.S. Kell, *NBS/NRC Steam Tables*, Hemisphere, Washington, DC (1984).

Ho, K.T., J. McMullen, P. Boyle, O. Rojek, M. Forgo, T. Beatty, and H.L. Longworth, "Subsurface Acid Gas Disposal Scheme in Wayne-Rosedale, Alberta", *SPE Paper No. 35848.* (1996).

Incropera, F.P. and D.P. De Witt, *Introduction to Heat Transfer*, 2nd ed., John Wiley & Sons, New York, NY, (1990).

Lock, B.W., "Acid Gas Disposal a Field Perspective", *76th Annual GPA Convention*, San. Antonio, TX, (1997).

Span, R. and W. Wagner, "A New Equation of State for Carbon Dioxide Covering the Fluid Region from the Triple-Point Temperature to 1100 K at Pressures up to 800 MPa", *J. Phys. Chem. Ref. Data*, **25**, 1509–1596, (1996).

Van Wylen, G.J. and R.E. Sonntag, *Fundamentals of Classical Thermodynamics. SI Version*, 3rd ed., John Wiley & Sons, New York, NY, (1985).

Appendix 6A Additional Calculations

6A.1 An acid gas mixture is compressed from 200 kPa to 12 500 kPa in a four stage compressor. The composition of the gas is 50% H_2S, 49% CO_2, 1% CH_4. Calculate the required compression horsepower and the interstage cooling assuming the mixture is an ideal gas.

Answer: Using the ideal gas thermodynamic properties the compression details were calculated and are summarized in the two tables below.

Part a. Compression

	Suction Pressure (kPa)	Discharge Pressure (kPa)	Discharge Temp. (K)	Work (J/mol)
1st Stage	200	550	401.2	3 023
2nd Stage	550	1 550	403.3	3 105
3rd Stage	1 550	4 400	403.9	3 129
4th Stage	4 400	12 500	404.0	3 132
Overall	200	12 500	–	12 389

Part b. Interstage Cooling

	Inlet Temp. (K)	Outlet Temp. (K)	Heat Transfer (J/mol)
1st Stage	401.2	320.0	3 023
2nd Stage	403.3	320.0	3 105
3rd Stage	403.9	320.0	3 129
4th Stage	404.0	320.0	3 132
Overall	–	320.0	12 389

At first it may seem unusual that the work of compression equals the work of cooling. However, this is true for an ideal gas only. Remember the enthalpy of an ideal gas is independent of the pressure. Therefore, for an ideal gas, the work must equal the heat transfer.

6A.2 This is designed to be a severe test of our simple correlations for estimating compression power. Carbon dioxide at 305 K and 7000 kPa is to be compressed to 15 000 kPa.

a) Estimate the work using the tables of Span and Wagner (1996).
b) Repeat the calculation and using the simplified compressor equation with the compressibility factor and heat capacities from Span and Wagner (1996).
c) Repeat the calculation and using the simplified compressor equation with the k from the ideal gas heat capacities and the compressibility factor from Span and Wagner (1996).

Answer: a) First, with the tables: At 305 K and 7 000 kPa, we have the following properties:

$\rho = 243.08$ kg/m^3
$s = -1.0644$ kJ/kg·K
$h = -102.55$ kJ/kg
$C_v = 1.0602$ kJ/kg·K
$C_p = 5.0681$ kJ/kg·K

From the density, we can calculate the compressibility factor using Equation (2.5):

$$z = \frac{MP}{\rho RT} = \frac{(44.010)(7000)}{(243.08)(8.314)(305)} = 0.4917$$

And from the heat capacities given above, we can calculate the k:

$$k = 5.0681/1.6020 = 4.780$$

which will be used in Part (b) of this example.
At 15 000 kPa the entropy is spanned by the temperature range 350 to 360 K. Interpolating the T-s to get the exit temperature yields 359.24 K (86.1°C). Then this values for the temperature was used to interpolate the other properties. The results of the interpolations are provided in the table below:

	350 K	360 K	359.24 K
ρ (kg/m^3)	449.20	387.08	391.80
s (kJ/kg·K)	−1.1376	−1.0584	*−1.0644*
h (kJ/kg)	−103.39	−75.292	−77.43
C_v (kJ/kg·K)	0.93439	0.91214	0.91383
C_p (kJ/kg·K)	3.0688	2.5672	2.6053

Calculating the work from the enthalpy difference:

$$W/m = h_o - h_i = -75.292 - (-102.55) = 25.12 \text{ kJ/kg}$$

Converting to a molar basis:

$$W/n = 25.12 \times 44.01 = 1106 \text{ kJ/kmol}$$

We can calculate the compressibility factor at the exit conditions:

$$z = \frac{MP}{\rho RT} = \frac{(44.010)(15000)}{(391.80)(8.314)(359.24)} = 0.5641$$

and k:

$$k = 2.6053/0.91385 = 2.851$$

And averaging over the inlet and outlet conditions gives:

$$\langle z \rangle = 0.5279$$
$$\langle k \rangle = 3.816$$

These values will be used in Part (b) of this example.

b) Calculate the work by substituting into equation (6.8a):

$$\frac{W}{n} = \frac{\langle z \rangle k R T_i}{k-1}\left[\left(\frac{P_o}{P_i}\right)^{(k-1)/k} - 1\right]$$

$$= \frac{(0.5279)(3.816)(8.314)(305)}{3.816-1}\left[\left(\frac{15000}{7000}\right)^{(3.816-1)/3.816} - 1\right]$$

$$= (1814.0)(0.75491)$$

$$= 1369 \text{ kJ/kmol}$$

Calculate the exit temperature by substituting into Equation (6.7)

$$T_o = T_i\left(\frac{P_o}{P_i}\right)^{(k-1)/k}$$
$$= (305)\left(\frac{15000}{7000}\right)^{(3.816-1)/3.816}$$
$$= 535.2\ \text{K} = 262.1°\text{C}$$

Although the work calculated using the shortcut method and the actual k gives a reasonably good prediction of the required work, however it is about 25% too large. On the other hand, the estimate of the exit temperature is very poor – more than 175°C greater than the values obtain from the rigorous calculation.

The large errors cannot be explained in terms of efficiencies. In both the rigorous and simplified calculations the efficiencies are assumed to be one.

c) For carbon dioxide in the ideal gas state k = 1.293, substituting into Equation (6.8a):

$$\frac{W}{n} = \frac{\langle z\rangle k\, R\, T_i}{k-1}\left[\left(\frac{P_o}{P_i}\right)^{(k-1)/k} - 1\right]$$
$$= \frac{(0.5279)(1.293)(8.314)(305)}{1.293-1}\left[\left(\frac{15000}{7000}\right)^{(1.293-1)/1.293} - 1\right]$$
$$= 1114\,\text{kJ/kmol}$$

And for the exit temperature:

$$T_o = (305)\left(\frac{15000}{7000}\right)^{(1.293-1)/1.293}$$
$$= 362.5\,\text{K} = 89.3°\text{C}$$

The use of the ideal gas heat capacities has dramatically improved the results. The calculated work is within 1% of the value obtained from the rigorous calculation and the exit temperature is within 3.2°C of the rigorously calculated value.

6A.3 Hydrogen sulfide at 350 K and 5 000 kPa is to be compressed to 10 000 kPa.

a) Estimate the work using the tables of Goodwin (1983).
b) Repeat the calculation and using the simplified compressor equation with the compressibility factor and heat capacities from Goodwin (1983).
c) Repeat the calculation and using the simplified compressor equation with the k from the ideal gas heat capacities (1.315) and the compressibility factor from Godwin (1983).

Answer: a) First, with the tables: At 350 K and 5 000 kPa, we have the following properties:

$s = 184.404$ J/mol·K
$h = 22.330$ kJ/mol
$C_v = 34.56$ J/mol·K
$C_p = 71.82$ J/mol·K
$z = 0.71057$

From these values we can calculate the actual k

$$k = 71.82/34.56 = 2.078$$

At 10 MPa the desired entropy is spanned by 410 to 420 K. The properties from the tables are summarized below, as are the linear interpolations.

	410 K	**420 K**	**419.70 K**
s (J/mol·K)	182.611	184.459	*184.404*
z (–)	0.65878	0.70049	0.69924
h (kJ/mol)	23.145	23.912	23.889
C_v (J/mol·K)	34.89	33.72	33.76
C_p (J/mol·K)	82.84	71.52	71.86

Calculate the work from the enthalpy difference:

$$W = 23.889 - 22.330 = 1.559 \text{ kJ/mol} = 1559 \text{ J/mol}$$

The ratio of the heat capacities at the exit conditions is:

$$k = 71.86/33.76 = 2.129$$

For the calculations in the next two parts of this example, we need the average k and z:

$$\langle z \rangle = (0.71057 + 0.69924)/2 = 0.70491$$
$$\langle k \rangle = (2.078 + 2.129)/2 = 2.103$$

b)

$$\frac{W_S^*}{n} = \frac{\langle z \rangle k R T_i}{k-1}\left[\left(\frac{P_o}{P_i}\right)^{(k-1)/k} - 1\right]$$
$$= \frac{(0.7049)(2.103)(8.314)(350)}{2.103-1}\left[\left(\frac{10000}{5000}\right)^{(2.103-1)/2.103} - 1\right]$$
$$= 1715\ \text{kJ/kmol}$$

c)

$$\frac{W_S^*}{n} = \frac{\langle z \rangle k R T_i}{k-1}\left[\left(\frac{P_o}{P_i}\right)^{(k-1)/k} - 1\right]$$
$$= \frac{(0.7049)(1.315)(8.314)(350)}{1.315-1}\left[\left(\frac{10000}{5000}\right)^{(1.315-1)/1.315} - 1\right]$$
$$= 1547\ \text{kJ/kmol}$$

The table below summarizes the calculations from the three approaches. Again, the use of the ideal gas heat capacities results in a better estimate of the result obtained by the rigorous calculation. Furthermore, this has nothing to do with efficiencies because in each case all of the efficiencies are assumed to be 100%.

	Tables of Goodwin	**Simple with Goodwin Properties**	**Simple with Ideal Gas k**
Work (J/mol)	1559	1715	1547
Exit Temp (°C)	146.6	230.3	140.1

7

Dehydration of Acid Gas

When compression and cooling alone is inefficient to achieve the desired level of dehydration, then some additional dehydration is required in order to reduce the water content to the desired level. The commonly employed dehydration methods are applicable to acid gas dehydration, but there are several important considerations that apply when dehydrating a stream like this.

It was demonstrated in chapter 4 that it may be possible to dehydrate the acid gas to a sufficient level using compression and cooling alone. However, in some cases this level of dehydration is not sufficient, and additional dehydration is required.

1. High CO_2 stream – from figure 4.5 it can be seen that the minimum in the water content for pure CO_2 is not a deep as those for acid gas mixtures rich in H_2S.
2. High hydrocarbon stream – the presence of light hydrocarbons in the acid gas stream reduces its ability to hold water. Thus, acid gas stream with a high hydrocarbon content needs additional dehydration.
3. Low pressure injection – If the required pressure to inject the stream is low, it is not possible to minimize

the water content using compression, because the pressure does not reach the optimum water content range.

4. Company specification – some companies specify that the acid gas stream must be dehydrated to a company specification.

The focus of this chapter will not be dehydration in general, but rather the specific problems with dehydrating acid gas streams. However, some brief introduction to the common dehydration methods will be presented.

Even if some additionally dehydration is required, the water content does not have to meet the usual 65 to 110 mg/Sm^3 (roughly 4 to 7 lb/MMSCF) water specification. The design engineer must determine the point in the system where water will condense or hydrates will form. This is usually the coldest point in the system, but not necessarily. This is the key to determining the required water content.

7.1 Glycol Dehydration

The process is continuous and regenerative in nature, with the circulating glycol being continuously re-concentrated for reuse.

A typical triethylene glycol (TEG) dehydration unit is made up of two main components. The absorber, often known in the industry as the glycol "contactor" and the regenerator, is normally based on direct fired reboiling. The feed gas enters the bottom of the contactor and travels upward. The glycol enters the top of the tower and travels down. Thus dry gas leaves the top of the contactor and rich glycol (containing more water) leaves the bottom.

The pressure of the rich glycol stream is dropped to near atmospheric and is sent to the regenerator system. Heat is added to the bottom of the column, and the water is driven out of solution to produce the lean glycol stream, which is returned to the contactor. The water exits as the offgas from the top of the regenerator still. In the case of an acid gas dehydration unit, this offgas steam contains H_2S and CO_2 for reasons that will be discussed later, and cannot be vented to the atmosphere. In an acid gas dehydration

unit, this stream is often put through a condenser and the water stream removed is added to other sour water from the plant. The gas stream produced is recycled to the compressor.

There are three sources of glycol losses: 1. Exiting with the dry gas. 2. Exiting with the offgas. 3. Leaks from the systems. In a dehydration unit with H_2S, every precaution should be taken to avoid leaks. Release of even small amounts of H_2S should be avoided. Occasional make-up is required to combat losses and maintain a constant glycol inventory in the system. The lower the glycol losses, the less is the make-up rate.

A simplified flow sheet for the process is given in figure 7.1. This flow diagram does not include a flash tank, which is typically not recommended for acid gas, because it produces a sour (or CO_2-rich) stream that should not be vented to the atmosphere. Sending the entire glycol stream to the regenerator tower produces only a single offgas.

7.1.1 Acid Gas Solubility

One of the biggest problems with TEG dehydration of acid gas is the high solubility of H_2S and CO_2 in TEG. The solubility of CO_2 in

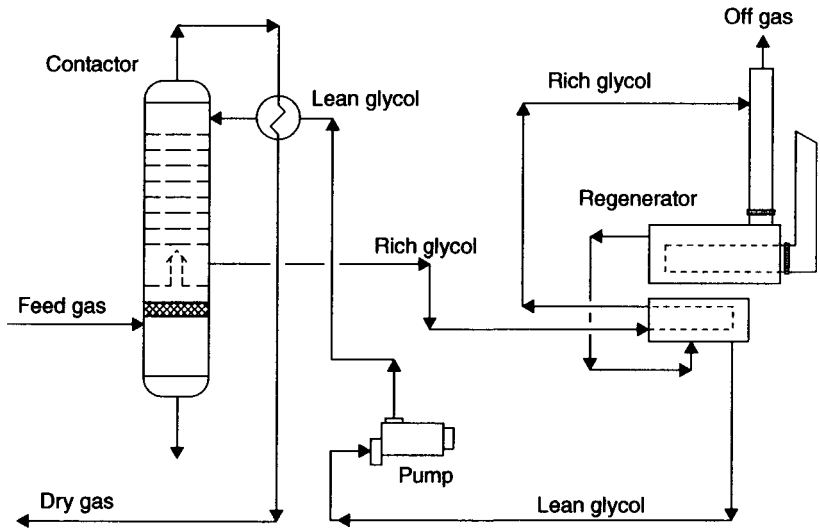

Figure 7.1 Simplified process flow diagram for a TEG dehydration unit.

TEG is shown in figure 7.2 and that for H_2S in figure 7.3. These data are from Jou et al. (1987). The data points are directly from Jou et al. (1987) and the curves are merely fit through the data points and do not represent a rigorous model.

At temperatures below the critical point of CO_2 (31°C), CO_2 and TEG exhibit liquid phase immiscibility. This can be seen for the 25°C isotherm shown on figure 7.2. At temperatures greater than 31°C, CO_2 + TEG mixtures have a miscibility gap. Thus, it is possible to dehydrate CO_2 at high pressures.

Hydrogen sulfide and TEG are completely miscible. Thus, at high pressure TEG cannot be used to dehydrate H_2S because they completely mix. Dehydration of an H_2S stream using TEG must be done at low pressure when the H_2S is still in the vapor phase. These

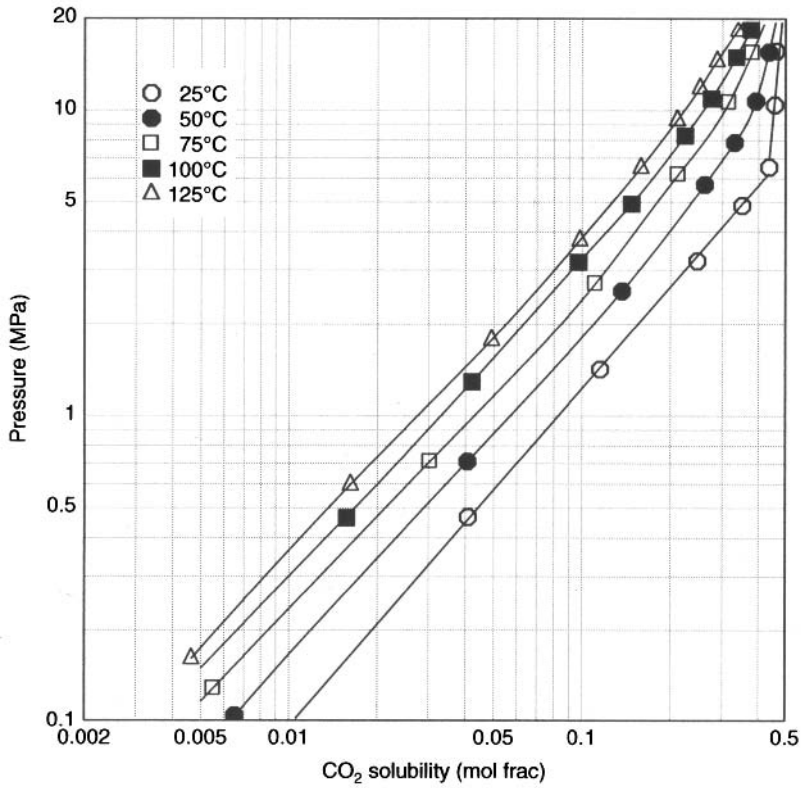

Figure 7.2 Solubility of carbon dioxide in TEG as a function of temperature and pressure (data points from Jou et al. 1987).

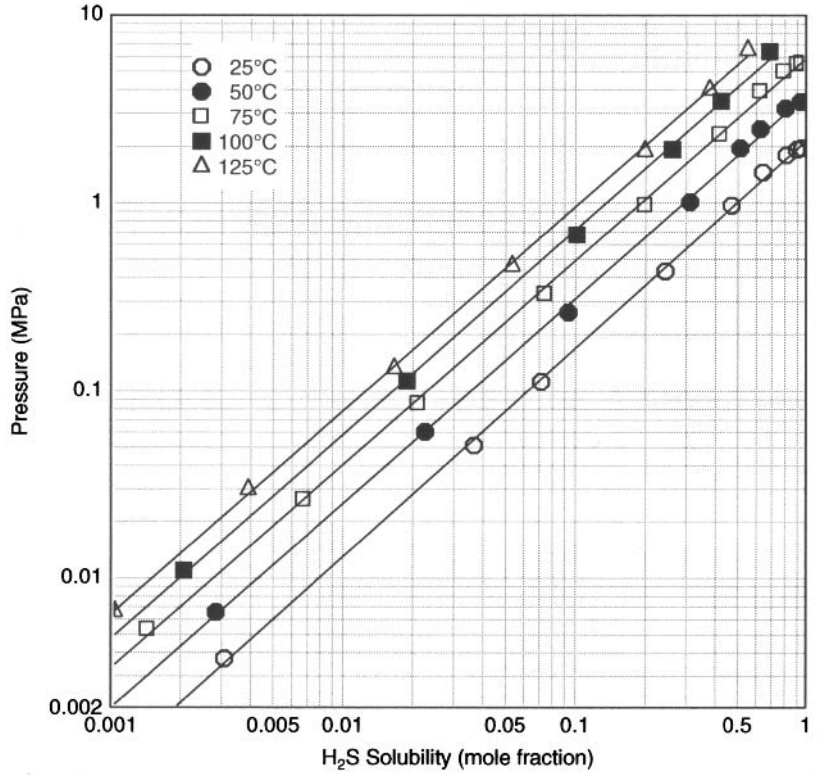

Figure 7.3 Solubility of hydrogen sulfide in TEG as a function of temperature and pressure (data points from Jou et al. 1987).

comments also apply to H_2S-rich streams, but the exact composition at which the switch occurs is not well known (i.e., it has not been measured experimentally).

7.1.2 Desiccant

Several of the limitations of using TEG as a desiccant were outlined above. This has led some to seek a new desiccant for this application. Some have suggested using glycerin as a desiccant for acid gas systems. Glycerin is highly hygroscopic but the acid gas components have a much lower solubility in glycerin.

Glycerin, also spelled glycerine, which is also called glycerol, has the empirical formula $C_3H_8O_3$ or $C_3H_5(OH)_3$ and the following structural formula:

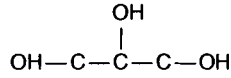

Some of the physical properties of glycerin and other desiccants are listed in table 7.1.

The advantages of using glycerin are two-fold: 1. The solubility of CO_2 in glycerin is lower than in the glycols. This means less CO_2 pick up by the desiccant solution. 2. Glycerin is less soluble in the CO_2 than are the glycols. This translates into lower solvent losses. The solubility of CO_2 in various desiccants is given in table 7.2 at 8.3 MPa.

Table 7.1 Physical properties of some gas treating chemicals used for dehydration.

	EG	TEG	methanol	glycerin
Empirical Formula	$C_2H_6O_2$	$C_6H_{14}O_4$	CH_4O	$C_3H_8O_3$
Molar Mass (g/mol)	62.07	150.17	32.04	92.09
Boiling Point (°C)	197	288	65	290
Freezing Point (°C)	−13	−4	−97	18
Density @ 20°C (kg/m³)	1115	1125	792	1261
Viscosity @ 20°C (mPa.s)	21	49	0.5	1005

Table 7.2 The solubility of CO_2 in various desiccants at 32.2°C and 8.3 MPa (90°F and 1200 psia) from Diaz and Miller (1984).

	SCF CO_2/lb solvent	Sm³ CO_2/kg solvent
Glycerin	0.1	0.0062
EG	0.1	0.0062
DEG	0.4	0.025
TEG	0.8	0.050

The solubility of the various desiccants in CO_2 at 8.3 MPa is given in table 7.3. Both of these tables are extracted from the patent of Diaz and Miller (1984).

Clearly, one of the drawbacks of glycerin as a process fluid is its high viscosity – more than twenty times that of TEG. This translates into higher pressure drop in the process piping, which in turn means more pumping power is required. It also means reduced tray and packing efficiencies.

Also note the high freezing point of glycerin. The temperature of the process must be greater than 18°C or else there is the potential for forming solid glycerin. In addition, the high freezing point makes it difficult to store and add to the dehydration system when make-up is required.

7.2 Molecular Sieves

The mole sieve dehydration is a semi-batch process using a solid adsorbent to remove water from a fluid stream. The water adsorbs onto the solid.

The simplest solid desiccant fixed bed system consists of a minimum of two dryer vessels or towers. One vessel is drying the process

Table 7.3 The solubility of various desiccants in CO_2 at 8.3 MPa (1200 psia) from Diaz and Miller (1984).

		22.8°C (73°F)	**35.0°C (95°F)**	**46.1°C (115°F)**
Glycerin	lb/MMSCF CO_2	0.3	0.2	0.09
	kg/Sm³	5	3	1.4
EG	lb/MMSCF CO_2	5	3	1
	kg/Sm³	80	48	16
DEG	lb/MMSCF CO_2	15	6	0.6
	kg/Sm³	240	96	10
TEG	lb/MMSCF CO_2	40	9	0.7
	kg/Sm³	640	140	11

stream while at the same time the second tower is undergoing regeneration. During regeneration all adsorbed material are desorbed by heat to prepare the tower for its next online cycle.

The flow of the process gas stream through the dryer bed is normally top to bottom. The wet gas stream entering the dryer could either be saturated or slightly unsaturated. As the process stream travels down the dryer bed, moisture is picked up by the desiccant and the gas stream becomes increasingly drier. The process gas stream exits the dryer bottom eventually moisture free.

All fixed bed dryer designs are based on a time cycle. The time cycle is distributed between the on-line and the on-regeneration. A 48 hour cycle will allocate 24 hours to on-line, when the dryer is drying the process stream, and 24 hours on regeneration, when the dryer bed is being reactivated.

A simplified process flow diagram for a two-bed absorber is shown in figure 7.4.

The main advantage of molecular sieve dehydration is that it is capable of producing a very dry stream, less than 1 ppm water. However, this is not necessary for acid gas injection applications.

Another advantage of the mole sieve process is that it requires minimal operator intervention: the process can be completely automated. This may be a significant advantage in a remote location.

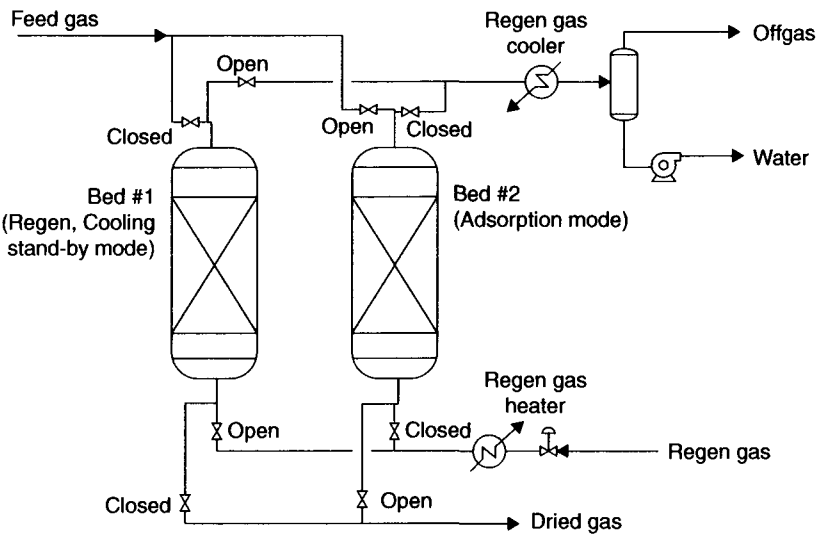

Figure 7.4 Simplified process flow diagram for a molecular sieve dehydration unit.

The biggest disadvantage of the standard mole sieve dehydration unit is the cost. As a rule of thumb, a mole sieve unit costs 1.5 times that of a similar TEG unit (Kohl and Nielsen, 1997).

7.2.1 Acid Gas Adsorption

Unfortunately, the acid gas components are also readily adsorbed onto most mole sieve materials. Figure 7.5 shows the adsorption isotherms for H_2S on three common mole sieve materials at 25°C. Similarly, figure 7.6 show the isotherms for CO_2 on two mole sieve materials. These plots are based on information provide in Kohl and Nielsen (1997).

The equilibrium adsorption in terms of mass of adsorbed material to mass of adsorbent is similar to that of water.

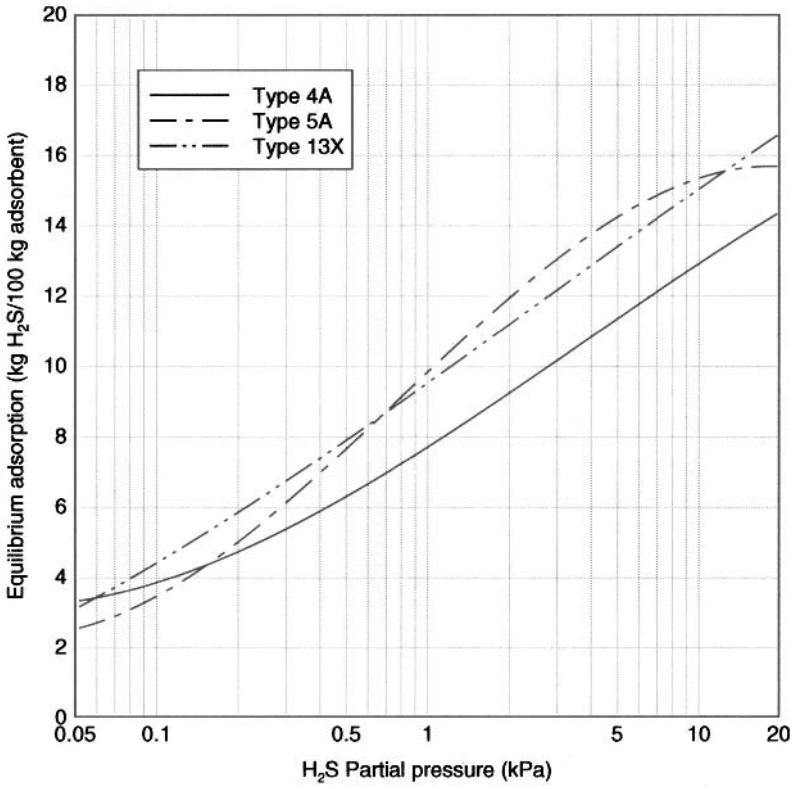

Figure 7.5 Adsorption of hydrogen sulfide on typical molecular sieve material.

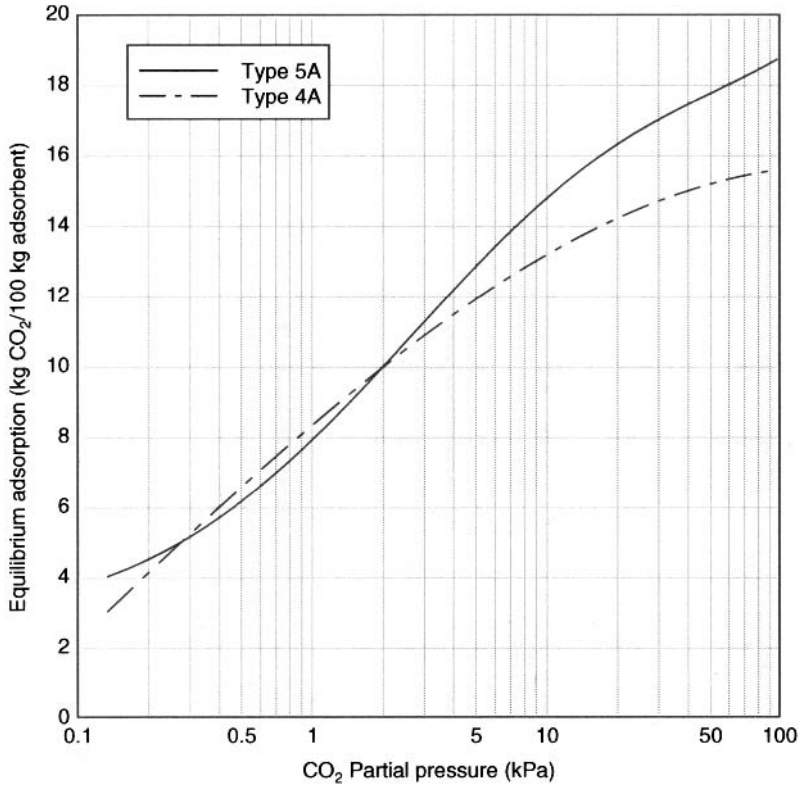

Figure 7.6 Adsorption of carbon dioxide on typical molecular sieve material.

7.3 Refrigeration

In the refrigeration process, the gas enters a gas/gas exchanger where it is pre-cooled. It then enters a chiller, which is usually a kettle reboiler. A refrigerant boils on the shell side, and the process fluid (in this case the acid gas) flows through the tubes. The temperature of the refrigerant is set by the pressure in the shell side of the exchanger. The process fluid can reach within 5 Celsius degrees of the refrigerant temperature. In the natural gas business, it is common to use propane as a refrigerant.

The cooled gas comes off the chiller and goes to the other side of the gas/gas exchanger to pre-cool the feed gas. The dehydrated gas is returned to the compressor.

A inhibitor (usually ethylene glycol) is sprayed into the process side of the gas/gas exchange and the process side of the chiller.

This is used in order to prevent solids from forming and plugging the equipment. The inhibitor-water stream off the separator is sent to a regenerator, which is similar to that for the EG dehydration unit discussed above.

It may not be necessary to inject a inhibitor/absorbent provided there is no danger of hydrate formation. For pure CO_2 this means that the process is at a temperature greater than 10°C and for pure H_2S greater than about 30°C (plus a small safety margin). Plus, at lower pressure, this temperature is reduced (see figure 5.1).

A simplified flow diagram for the refrigeration process is shown in figure 7.7. The inhibitor regeneration still is not shown.

7.3.1 Selection of Inhibitor

In a typical refrigeration unit, ethylene glycol is injected into the system to prevent hydrate formation and to absorb the liquid water that forms. For acid gas applications, some have chosen to inject methanol. The acid gas components are slightly less soluble in methanol than in glycol.

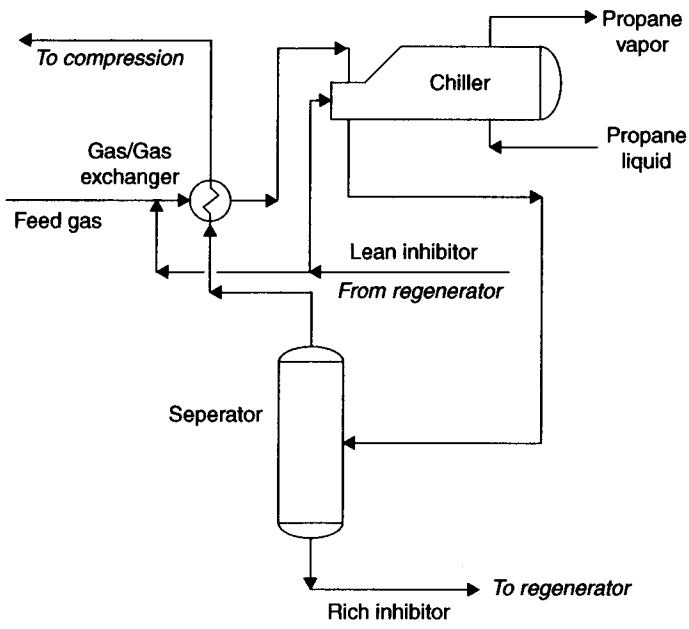

Figure 7.7 Simplified process flow diagram for a refrigeration unit (inhibitor regenerator system not shown.

7.4 Case Studies

7.4.1 CO_2 Dehydration

Zabcik and Frazier (1984) describe in some detail two CO_2 dehydration units. The details of these two dehydration units are given in table 7.4.

Table 7.4 Case study for CO_2 dehydration from Zabcik and Frazier (1984).

	Case 1		Case 2	
Inlet Gas				
Flow	14.7 MMSCFD	416 × 10^3 Sm^3/d	16.5 MMSCFD	467 × 10^3 Sm^3/d
Temperature	100°F	38°C	102°F	39°C
Pressure	590 psig	4068 kPa[g]	1080 psig	7446 kPa [g]
Water Content	110 lb/MSCF	1.6 g/Sm^3	105 lb/MSCF	1.7 g/Sm^3
Outlet Gas				
Water Content	10 lb/MSCF	0.16 g/Sm^3	16 lb/MSCF	0.26 g/Sm^3
TEG				
Flow	9.7 USgpm	37 L/min	6.0 USgpm	23 L/min
Rich	99.0 wt%	99.0 wt%	98.6 wt%	98.6 wt%
Lean	97.9 wt%	97.9 wt%	96.4 wt%	96.4 wt%
Absorber	10 trays	10 trays	8 trays	8 trays
Flash Tank				
Temperature	148°F	64°C	106°F	41°C
Pressure	57 psig	393 kPa[g]	50 psig	448 kPa[g]
Stripping Gas				
Flow	53 SCF/min	1.5 Sm^3/min	none	none
Reboiler				
Temperature	388°F	198°C	375°F	191°C
Heat Duty	0.42 MMBtu/hr	123 kW	0.25 MMBtu/hr	73 kW

The glycol circulation rate for Case 1 is equivalent to 9.7 gal of TEG per lb of water removed and in Case 2 it is 5.9 USgal/lb. These are well in excess of the typical 2 to 4 USgal/lb typically recommended for a natural gas dehydration unit. Zabcik and Frazier (1984) do not offer an explanation as to why the glycol circulation rate is so high.

The water contents given in table 7.4 come from the analysis from the literature data by Zabcik and Frazier (1984). The values predicted by *AQUAlibrium* are 113 lb/MMSCF for Case 1 and 111 for Case 2, which agree well with the data in table 7.4; differences of only 2.7% and 5.7%.

In Case 1, the TEG is preheated before the flash tank, and that is why the temperature seems a little high. In Case 2, the temperature increase is due merely to the absorption of the gaseous components into the glycol.

7.4.2 Acid Gas Dehydration

As has been stated earlier, dehydration is not commonly used for acid gas. However, a couple of processes have been discussed in the literature. They are also discussed here.

7.4.2.1 Wayne-Rosedale

Ho et al. (1996) describe briefly the dehydration unit at the Wayne-Rosedale injection project. The operating conditions for this dehydration unit are given in table 7.5. Note the values given are the operating conditions and not the design conditions. Unfortunately, no details about the TEG side of the process are reported.

The gas off the glycol regenerator is cooled to condense some of the water. The remaining vapor are returned to the suction of the compressor using a vapor recovery unit (VRU).

The entire dehydration units is constructed from 316L stainless steel. All parts of the dehydration unit are in contact with wet acid gas.

7.4.2.2 Acheson

The dehydration unit at Acheson is described briefly by Lock (1997). At Acheson they dehydrate about 13×10^3 Sm^3/d of acid gas (90% CO_2 and 10% H_2S) in a glycol dehydration unit. This dehydration unit operates at about 1500 kPa.

The regenerator offgas and flash tank gas are sent to a flare, and this represents an emission from their AGI process. This is estimated

Table 7.5 Operating data for an acid gas dehydration unit from HO et al. (1996).

Inlet Gas		
Composition	17% H_2S, 82% CO_2	17% H_2S, 82% CO_2
Rate	21 x 10^3 Sm^3/d	0.74 MMSCFD
Temperature	30°C	86°F
Pressure	3000 kPa	435 psia
Water Content†		
@30°C	1.5 g/Sm^3	92 lb/MMSCF
@50°C	4.0 g/Sm^3	254 lb/MMSCF
Absorber	8 trays	8 trays

† – water content calculated using *AQUAlibrium*

to be about 220 Sm^3/d (about 1.7% of the feed), although it is not clear how they obtained this number.

All of the equipment in contact with the glycol (including the absorber tower, flash tank, regenerator shell and firetube, and the preheat coils) are made from 316L stainless steel. All other components are made from carbon steel.

7.5 In Summary

In many case dehydration of acid gas beyond what can be achieved by compression and cooling alone is not necessary. However, there are potential problems with dehydrating acid gas, and the design engineer should be aware of these limitations.

References

Diaz, Z. and Miller, J.H. 1984. Drying substantially supercritical CO_2 with glycerol. US Patent No. 4,478,612. Filed: July 27, 1983. Date of Patent: Oct. 23, 1984.

Jou, F.-Y, Deshmukh, R.D., Otto, F.D., and Mather, A.E. 1987. Vapor-liquid equilibria for acid gases and lower alkanes in triethylene glycol. *Fluid Phase Equil.* 36:121–140.

Ho, K.T., J. McMullen, P. Boyle, O. Rojek, M. Forgo, T. Beatty, and H.L. Longworth. 1996. Subsurface acid gas disposal scheme in Wayne-Rosedale, Alberta. SPE Paper No. 35848.

Kohl, A. and Nielsen, R., edition. 1997. *Gas Purification*. Houston, TX: Gulf Professional Publishing.

Lock, B.W. 1997. Acid gas disposal a field perspective. 1997. 76th Annual GPA Convention, San Antonio, TX.

Zabcik, D.J. and C.W. Frazier. 1984. Dehydration of CO_2 with TEG: Plant operating data. Laurance Reid Gas Conditioning Conference, Norman, OK.

This Page Intentionally Left Blank

8

Pipeline

The acid gas is transported from the compressor to the injection well via a pipeline. The design of the pressure drop and temperature loss in the line are calculated using conventional methods.

8.1 Pressure Drop

In terms of calculating the pressure drop, the design of an acid gas pipeline is no different from other lines. One of the interesting aspects of the line is that it could be for gas, liquid, or two-phase.

8.1.1 Single Phase Flow

The calculation of the pressure drop in a single-phase pipeline begins with the Bernoulli equation:

$$\frac{v_o^2}{2} + g z_o = \frac{v_i^2}{2} + g z_i - \int_{P_i}^{P_o} dP/\rho - \frac{2\langle v \rangle^2 L f}{D} \qquad (8.1)$$

where: v – fluid velocity, m/s (the angle brackets indicate the average velocity)

g – acceleration due to gravity, 9.81 m/s^2
z – elevation, m
P – pressure, Pa
ρ – fluid density, kg/m^3
L – length of pipe, m
f – friction factor, dimensionless[1]
D – pipe diameter, m

and the subscript i is the inlet conditions and o is the outlet.

The integral term is evaluated differently depending upon the nature of the fluid. If it is a liquid, and hence incompressible (constant density), then:

$$\int_{P_i}^{P_o} dP/\rho = \frac{P_o - P_i}{\rho} \tag{8.2}$$

So for a horizontal pipeline, where the fluid is of constant density and the change in kinetic energy is small (a good assumption for most pipelines), equation (8.2) can be integrated to obtain:

$$\frac{P_o - P_i}{\rho} = \frac{2\langle v\rangle^2 L f}{D} \tag{8.3}$$

or

$$\frac{\Delta P}{\rho} = \frac{2\langle v\rangle^2 L f}{D} \tag{8.3a}$$

If the pressure drop is small, then even the flow of a gas can be consider incompressible and the above equations can be applied to estimate the pressure drop. However, if there is a significant pressure drop then a different approach is required.

---

1. In the engineering community there are two types of friction factors – Fanning and Darcy. Although basically the same, they differ by a factor of four: $f_{Darcy} = 4\, f_{Fanning}$. The Darcy factor is used here.

For an ideal gas:

$$\rho = \frac{MP}{RT} \tag{8.4}$$

where: M – molar mass, kg/kmol
R – universal gas constant, 8 314 m^3·Pa/kmol·K
T – absolute temperature, K

Substituting the ideal gas law into the pressure integral yields:

$$\int_{P_i}^{P_o} dP/\rho = \int_{P_i}^{P_o} \frac{RT}{MP} dP \tag{8.5}$$

In a typical long pipeline the temperature and the pressure change along the length of the line. However, if we assume that the line is isothermal, then the equation can be integrated to obtain:

$$\int_{P_i}^{P_o} \frac{RT}{MP} dP = \frac{RT}{M} ln \frac{P_o}{P_i} \tag{8.6}$$

Substituting into the energy equation and assuming horizontal flow and negligible kinetic energy effects yields:

$$\frac{RT}{M} ln\left[\frac{P_o}{P_i}\right] = \frac{2\langle v\rangle^2 L f}{D} \tag{8.6a}$$

In a detailed design of a pipeline, the integration should be done numerically by dividing the pipeline into segments where the fluid properties are approximately equal. Many software packages are available to perform such a calculation.

The reader is cautioned to pay careful attention to units. Even when using SI units, it is very easy to make a mistake.

It is common to express the flow rate in volumetric terms. To convert from volumetric flow rate to velocity:

$$Q = vA \tag{8.7}$$

where: Q – volumetric flow rate, m^3/s
A – cross sectional area, m^2

For circular pipes this becomes:

$$Q = \frac{\pi D^2 v}{4} \tag{8.8}$$

where: π is 3.14159...

Rearranging gives:

$$v = \frac{4Q}{\pi D^2} \tag{8.8a}$$

The reader is cautioned to note carefully that the volumetric flow rate at standard conditions is, in general, different from those at actual conditions. In the above equations the flow must be at actual conditions.

8.1.1.1 Friction Factor

The friction factor is a function of the Reynolds number and the diameter and roughness of the pipe. The Reynolds number is defined as:

$$Re = \frac{\langle v \rangle \rho D}{\mu} \tag{8.9}$$

where: Re – Reynolds number, dimensionless
μ – viscosity, Pa•s

The friction factor is a function of the flow regime, which is determined from the Reynolds number. In the laminar region, Re < 2000, then the friction factor:

$$f = \frac{16}{Re} \tag{8.10}$$

In the transition region (2000 < Re < 4000), the friction factor is more difficult to determine.

In the turbulent region, the friction factor is often given graphically. Figure 8.1 shows a plot of the friction factor as a function of the

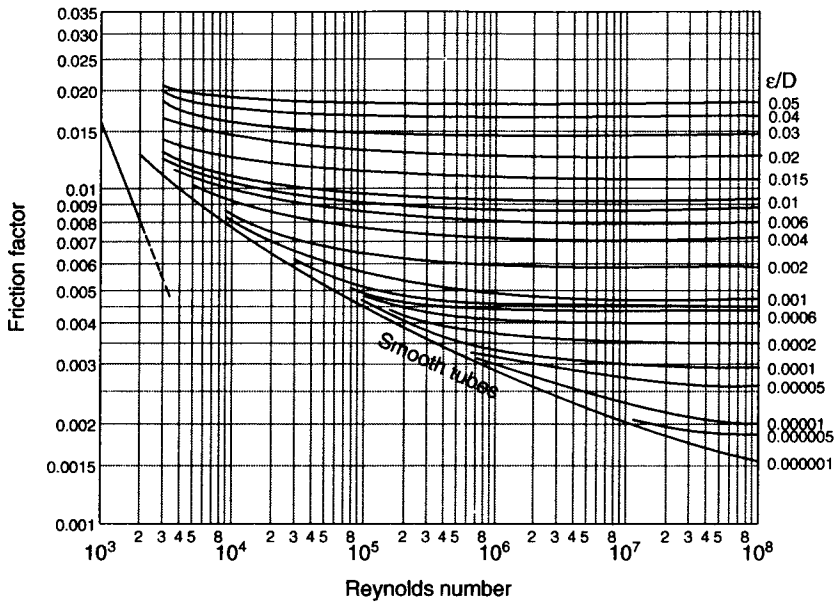

Figure 8.1 Friction factor as a function of the Reynolds number ($\rho vD/\mu$) and the relative roughness (ε/D) – adapted from various sources.

Reynolds number and the pipe roughness. The roughness of typical commercial pipe is 0.045 mm (0.000 15 ft).

In addition, there are several correlations for the friction factor. For smooth pipes, one of the simplest correlations is the Blasius equation:

$$f = 0.079\ \mathrm{Re}^{-1/4} \tag{8.11}$$

$$4000 < \mathrm{Re} < 100{,}000$$

Another form, which is applicable at higher Reynolds numbers, but also for smooth pipes, is the Kármán-Nikuradse equation:

$$\frac{1}{\sqrt{f}} = 4.0 \log\left(\mathrm{Re}\sqrt{f}\right) - 0.4 \tag{8.12}$$

$$\mathrm{Re} > 4000$$

For rough pipes, there is the Colebrook equation:

$$\frac{1}{\sqrt{f}} = -4.0 \log\left(\frac{\varepsilon}{D} + \frac{4.67}{\mathrm{Re}\sqrt{f}}\right) + 2.28 \tag{8.13}$$

where: ε – roughness, m

The reader will note that both the Kármán-Nikuradse and the Colebrook equations are implicit in the friction factor and require a trial and error solution. For hand calculations, it is often simpler to use the friction factor chart.

8.1.1.2 Additional Comments

Presented in this section is a very brief overview of the calculation of single-phase fluid flow in pipelines. The reader is referred to one of the many textbooks available on the subject, for example, De Nevers (1970) or Denn (1980).

The required fluid properties, notably the density and the viscosity, for the acid gas mixtures can be estimated using the techniques presented in Chapter 2.

Example

8.1 In the design of an acid gas injection scheme, 3.0×10^3 m³[std]/d of H_2S at 20°C and 2500 kPa are transported in a 50.8-mm (2-in) schedule 80 pipeline. Estimate the pressure drop. Assume the pipe is hydraulically smooth.

Answer: Convert from standard cubic meters to molar flow rate:

$$n = PV/RT = (101.325)(3.0 \times 10^3)/8.314/(15.55 + 273.15)$$
$$= 126.64 \text{ kmol/d} = 5.277 \text{ kmol/h}$$

Convert to mass flow rate:

$$m = nM = (5.277)(32.084) = 179.9 \text{ kg/h} = 0.050 \text{ kg/s}$$

Convert to actual volumetric flow. The actual inner diameter of 2-in schedule 80 pipe is 1.939 in or 49.25 mm. Further assume that the properties of liquid H_2S are independent of the pressure and can be taken from table 2.4.

$$Q_{act} = m/\rho = 0.050/790 = 6.33 \times 10^{-5} \text{ m}^3\text{[act]/s}$$

Calculate the fluid velocity:

$$v = 4Q/\pi D^2 = 4(6.33 \times 10^{-5})/\pi/(49.25 \times 10^{-3})^2 = 3.32 \times 10^{-2} \text{ m/s}$$

Calculate the Reynolds number. The viscosity of H_2S is 0.127 cp which is 0.127×10^{-3} Pa•s.

$$Re = v\rho D/\mu = (6.33 \times 10^{-5})(790)(49.325 \times 10^{-3})/0.127 \times 10^{-3} = 10{,}200$$

This is in the turbulent regime. Estimate the friction factor using the Blasius equation:

$$f = 0.079\,\mathrm{Re}^{-1/4} = 0.079(10\,200)^{-1/4} = 0.0079$$

The pressure drop is estimated using one of the versions of the Bernoulli equation derived earlier.

$$\frac{\Delta P}{\rho} = \frac{2\langle v\rangle^2 L f}{D}$$

$$\frac{\Delta P}{L} = \frac{2\left(3.32\times10^{-2}\right)^2 (790)(0.0079)}{49.25\times10^{-3}} = 0.279\ \mathrm{Pa/m}$$

$$= 0.279\ \mathrm{kPa/km}$$

This fairly small pressure drop is typical of small acid gas injection schemes.

8.1.2 Two-Phase Flow

Two-phase flow is significantly more complicated than single-phase flow. To begin with, depending on the relative amounts of gas and liquid, the flow falls into one of several regimes. Based on the flow rates of the vapor and liquid, a flow map is developed, which can be used to determine the flow regime. In a typical acid gas injection scheme, the flow rates of both the gas and the liquid are low. This would place it in the stratified regime. In the stratified regime, the liquid flows along the bottom of the line with the gas flowing on top. Design engineers are wise to verify this for their specific case.

Typically, the calculations for two-phase pressure drop are too complicated for hand calculations. It is recommended that the design engineer use one of the available programs specifically designed for such calculations. In addition, an excellent review of two-phase flow is presented in Govier and Aziz (1972).

8.1.3 Transitional Flow

Another possible scenario in the pipeline transport of acid gas is a transition from single-phase to two-phase flow or vice versa. For such a situation, it is very difficult to perform a calculation. These calculations, which involve a combination of fluid flow and phase equilibrium, should be performed using available software.

8.2 Temperature Loss

Another important consideration in the design of the pipeline is the temperature drop. The acid gas comes off the after cooling relatively warm and is transported in a buried pipeline, where it cools before reaching the injection well.

8.2.1 Carroll's Method

Carroll (2003) provided a method for estimating the heat loss from a buried pipeline. This method begins with the basic heat transfer equation:

$$Q = U\,A\,\Delta T_{lm} \tag{8.14}$$

where: Q – heat transfer rate, W
U – overall heat transfer coefficient, $W/m^2 \cdot °C$
A – heat transfer area, m^2
ΔT_{lm} – logarithmic mean temperature difference (LMTD), °C

The heat transfer is calculated from the enthalpy change for the fluid in the pipeline:

$$Q = m(h_o - h_i) \tag{8.15}$$

where: m – mass flow rate of fluid, kg/s
h_o and h_i – enthalpy of the stream, J/kg

For the case of a buried pipeline, there are four resistances that contribute to the overall heat transfer coefficient: (1) the convective heat transfer from the fluid to the pipe wall, (2) the conduction through the pipe wall, (3) the resistance due to the insulation, and (4) the conduction from the pipe to the soil. The overall heat transfer coefficient, U, is obtained from the following equation:

$$\frac{1}{UA} = \frac{1}{h_i A_i} + \frac{ln(d_o/d_i)}{2\pi k_p L} + \frac{ln[(d_o+2t)/d_o]}{2\pi k_{ins} L} + \frac{1}{k_s S} \tag{8.16}$$

where: h_i – convective heat transfer coefficient for the fluid in the pipe, $W/m^2 \cdot °C$

A_i – inner surface area of the pipe, m^2
d_o and d_i – outside and inside diameters of the pipe, m
t – thickness of the insulation, m
k_p – thermal conductivity of pipe (usually steel), W/m·°C
k_{ins} – thermal conductivity of the insulation, W/m·°C
L – length of a pipe segment, m
k_S – thermal conductivity of the soil, W/m·°C
S – shape factor for the buried pipe, dimensionless

The heat transfer coefficient for the fluid in the pipe is estimated using the Dittus-Boelter correlation:

$$Nu = 0.023\,Re^{0.8}\,Pr^{0.3} \tag{8.17}$$

where: Nu – Nusselt number, dimensionless
Re – Reynolds number, dimensionless
Pr – Prandtl, number, dimensionless

The exponent of 0.3 on the Prandtl number is because the fluid is cooling.

Finally, the shape factor for a buried pipe can be calculated from the following formula (Holman, 1982):

$$S = \frac{2\pi L}{ln(4D/d_o)} \tag{8.18}$$

where: D – depth of pipeline, m
and the other symbols are as defined previously.

Typical values for the overall heat transfer coefficient are approximately 2 to 5 W/m²·°C (0.5 to 1.0 Btu/ft²·hr·°F).

8.3 Guidelines

Good engineering practices should target pressure drop less than 500 kPa/km (2 psi/100 ft). For the small injection scheme, pressure drop is usually not a significant factor. For larger acid gas systems it may be necessary to exceed this amount in order to achieve safety goals (i.e., less fluid contained, and potentially released, in the pipeline).

In addition, according to the API (2007), in order to minimize erosion in the pipeline the velocity should be less than:

$$v_{max} = \frac{1220}{\sqrt{\rho}} \tag{8.19}$$

where: v_{max} – maximum velocity in m/s
ρ – fluid density in kg/m^3

Or in the original units:

$$v_{max} = \frac{100}{\sqrt{\rho}} \tag{8.20}$$

where: v_{max} – maximum velocity in ft/sec
ρ – fluid density in lb/ft^3

This velocity should never be exceeded for acid gas service because of the increased potential for a line failure due to erosion.

8.4 Metering

It is important to know the volumes of acid gas injected. This is significant from a process point of view, for process design or to de-bottleneck existing schemes. In addition, the amount of acid gas injected is also required by any regulatory board, such as the Energy and Utilities Board (EUB) in Alberta.

The best point to meter the acid gas is at the low-pressure suction. At this point, the gas is single phase and relatively easy to measure using an orifice meter. Furthermore, because the pressure is low, the gas behaves nearly ideally (i.e., $z \approx 1$).

Placing the meter elsewhere along the line may cause problems, particularly if the fluid enters the two-phase region, or worse, if it switches between the three regimes.

An orifice meter is merely a constriction in a flow line. The pressure drop across the constriction is directly related to the flow rate in the line. They are commonly used because they are simple to employ, and if used properly, can be quite accurate.

The theory behind the orifice meter is relatively simple and it begins with the Bernoulli equation. It can be summarized as follows:

$$Q = C_o\sqrt{\Delta P} \tag{8.21}$$

where: Q – flow rate
ΔP – pressure drop across the orifice
C_o – flow coefficient

The units in this equation vary and are often embedded in the flow coefficient. For gases, the traditional units are standard cubic feet per day for the flow rate and barrels per day for liquids. The pressure drop is traditionally in inches of water column. However, conversion to other units is relatively straightforward.

The flow coefficient is a function of many parameters including the ratio of the diameter of the orifice to the diameter of the pipe, flow rate, the temperature, and the nature of the fluid.

Although the orifice meter is simple to use, it is not infallible. First, it requires proper installation of the plate itself. If the plate is put in backwards, erroneous readings can result. In addition, the location of the pressure taps is critical. The locations must adhere to the strict guidelines.

The ratio of the diameter of the orifice to the pipe should fall in the range: 0.5 to 0.7. It should not be too small or the pressure drop will be too large. On the other hand, if it is too large then the pressure drop will be too small and difficult to measure accurately.

Another common problem with orifice meters is having the wrong plate in the meter. That is, the calibration of the meter was done assuming a certain size orifice; however, a different size plate was installed. This may seem silly, but it is a frequent occurrence and is usually difficult to detect.

8.5 Other Considerations

Since hydrogen sulfide is highly toxic and a leak from the pipeline could be catastrophic, it is recommended that the line be kept as short as possible. The disposal well should be near the plant, but off-site. The pipeline should therefore be from several hundred meters to two

or five kilometers in length. Safety risks increase as the length of the pipeline increases. The line may be filled with liquefied acid gas and a break in the line would result in a large release of hydrogen sulfide.

Theoretically, carbon steel could be used for pipeline construction because of the low water content. However, public safety is of paramount importance. Usually 304/316L stainless steel is employed for best corrosion resistance. The pipeline is coated with an external coating to prevent soil moisture from damaging the steel. ASME code is used for the maximum design pressure to limits of pipe or flanges. The design engineer should attempt to minimize the number of connections while still giving consideration for future expansion, for tie-ins, and extra instrumentation, just in case.

The pipeline is usually buried to a depth of 2 m (6 ft) to minimize freezing concerns. The line should be equipped with extensive redundant instrumentation to ensure complete safety and integrity of the system.

Additional safety considerations for the entire injection scheme are discussed in other chapters. But again, safety is paramount.

8.6 In Summary

The acid gas is transported from the compressor to the injection well in a pipeline. The design of such a pipeline follows that standard practice for all lines.

In addition, the line is filled with a highly toxic mixture. Therefore, safety must be paramount in the mind of the design engineer and in that of the operators.

References

American Petroleum Institute . 2007. API RP 14E. Recommended practice for design and installation of offshore production platform piping systems. Washington, DC: American Petroleum Institute.

Carroll, J.J. 2003. *Natural Gas Hydrates: A Guide for Engineers*. Amsterdam: Gulf Professional Publishing.

De Nevers, N. 1970. *Fluid Mechanics*. Menlo Park, CA: Addison-Wesley.

Denn, M.M. 1980. *Process Fluid Mechanics*. Englewood Cliffs, NJ: Prentice-Hall.

Govier, G.W. and K. Aziz. 1972. *The Flow of Complex Mixtures in Pipes*. Malabar, FL: Krieger Publishing Co.

Holman. J.P. 1981 edition. *Heat Transfer*. New York: McGraw-Hill.

Appendix 8A Sample Pipeline Temperature Loss Calculation

8A.1 An acid gas mixture (composed of 20% H_2S and 80% CO_2) with a flow rate of 0.5 MMCFD is transported in a 200-m long pipeline from the plant site to the injection well. The acid gas enters the pipeline at 50°C and 10 000 kPa. The pipe is a 2-in Schedule 160 steel line. Assuming the soil temperature is 5°C, use the method of Carroll (via the software supplied) to estimate the temperature loss in the line. Calculate the required physical properties of the fluid using *AQUAlibrium 3.0*.

Answer: First convert the volumetric flow rate to a molar flow rate:

$$\begin{aligned} n &= (0.5)(1.195 \times 106) \quad \text{this conversion is from Chapter 1} \\ &= 597\,500 \text{ mol/d} \\ &= 6.91551 \text{ mol/s} \end{aligned}$$

The molar mass of the mixture is:

$$\begin{aligned} M &= 0.20(34.082) + 0.80(44.101) \quad \text{Molar masses from} \\ &= 42.024 \text{ g/mol} \qquad\qquad\qquad\qquad \text{Chapter 2} \end{aligned}$$

Using the mixture molar mass, convert to a mass flow rate:

$$\begin{aligned} m = (6.91551)(42.024) &= 290.62 \text{ g/s} \\ &= 0.29062 \text{ kg/s} \\ &= 1046.2 \text{ kg/h} \end{aligned}$$

From standard tables of pipe data we get the following information about 2-in Sch. 160 pipe and converting to cm:

$$\begin{aligned} ID &= 1.689 \text{ in} = 4.290 \text{ cm} \\ t &= 0.343 \text{ in} = 0.871 \text{ cm} \end{aligned}$$

Therefore the OD of the pipe is 6.032 cm.

Next use AQUAlibrium to calculate the fluid properties.

8A.1 AQUAlibrium 3.0

8A.1.1 Acid Gas Properties

Pressure-Temperature Flash

8A.1.1.1 Conditions

Temperature:	50.00	C
Pressure:	11000.00	kPa

8A.1.1.2 Component fractions

Components	Feed	Condensate
H_2S	0.2	0.2
CO_2	0.8	0.8
Total	1	1

8A.1.1.3 Phase properties

Properties	Units	Condensate
Mole Percent		100
Molecular Weight	kg/kmol	42.024
Z-factor		0.320121
Density	kg/m^3	537.479
Enthalpy	kJ/kmol	−6553.6
Heat Capacity	kJ/kg.k	5.17618
Viscosity	cp	0.0407229
Thermal Conductivity	W/m.K	0.0593879

8A.1.1.4 Warnings

There are no errors or warnings for this Case.

Finally, use the pipeline temperature loss program provided to estimate the temperature loss:

```
    ************************************************
    **    Buried Pipeline Heat Loss Calculation   **
    **    Vers. 1.1                 Sept. 2000    **
    **    ----------- BETA RELEASE -----------    **
    ************************************************

Project: Acid Gas Injection Course Notes
Job Number:      Date: 10-29-2002     Time: 11:08:50

INPUT PARAMETERS:
-----------------

Fluid Properties:
-----------------
Heat Capacity (kJ/kg-K).....  5.176
Viscosity (cp)..............  .0407
Density (kg/m3).............  537.5
Thermal Conductivity (W/m-K).....  .0594
Mass Flow Rate (kg/hr)......  1046.2
Fluid Temperature (deg C)...  50

Pipe Properties:
----------------
Inside Diameter (cm)........  4.29
Outside Diameter (cm).......  6.032
Thermal Conductivity (W/m-K).....  45
Buried Depth (m)............  1.5
Length (km).................  .2

Insulation Properties:
----------------------
*** Pipe Uninsulated ***

Yellow Jacket:
--------------
Pipe coated with Yellow Jacket

Soil Properties:
----------------
Thermal Conductivity (W/m-K).....  1
Temperature (deg C).........  5

CALCULATED RESULTS:
-------------------

Fluid Exit Temperature......  42.89 deg C
Temperature Change..........   7.11 deg C
Log Mean Temperature Change.....  41.34 deg C

Reynolds Number.........  2.119E+05
Prandtl Number..........  3.547E+00
Nusselt Number..........  6.132E+02

Fluid Velocity..........  0.374 m/s
Pressure Drop...........  2.267E+01 Pa/m
        *** Approximate ***
Total Pressure Drop.....  4.533E+00 kPa
```

```
          *** Approximate ***

Inside Heat Transfer Coeff.............  8.491E+02 W/m2-K
Inside Overall Heat Transfer Coeff.....  9.599E+00 W/m2-K
Inside Surface Area....................  2.695E+01 m2
Outside Overall Heat Transfer Coeff.....  6.551E+00 W/m2-K
Outside Surface Area...................  3.950E+01 m2
Total Heat Transfer....................  1.070E+01 kW

Pipeline Profile
----------------

Distance     Fluid Temperature     Heat Loss
  (km)            (deg C)            (kW)
--------     -----------------     ---------
  0.000            50.00               -
  0.010            49.61              0.58
  0.020            49.23              0.57
  0.030            48.85              0.57
  0.040            48.48              0.56
  0.050            48.11              0.56
  0.060            47.74              0.56
  0.070            47.37              0.55
  0.080            47.01              0.55
  0.090            46.65              0.54
  0.100            46.29              0.54
  0.110            45.94              0.53
  0.120            45.59              0.53
  0.130            45.24              0.52
  0.140            44.90              0.52
  0.150            44.55              0.51
  0.160            44.21              0.51
  0.170            43.88              0.51
  0.180            43.55              0.50
  0.190            43.22              0.50
  0.200            42.89              0.49

Contributions to Overalll Heat Transfer Coefficient:
----------------------------------------------------

Resistance Due to Fluid.............   1.13%
Resistance Due to Pipe..............   0.16%
Resistance Due to Insulation........   0.00%
Resistance Due to Yellow Jacket.....   4.85%
Resistance Due to Soil..............  93.86%
```

From the output it can be seen that it is estimated that the fluid arrives at the well at about 43°C, which is a temperature drop of about 7°C. Even though this is a very short line, there is a significant temperature drop.

The program also uses a simple method to estimate the pressure drop, although this is not used in the calculations. From the output it can be seen that there is a fairly small pressure drop due to fluid friction, less than 5 kPa. The reader can use the methods presented earlier in this chapter to verify this result.

9

Injection Profiles

Another important aspect of acid gas injection is the calculation of the injection profile and ultimately the injection pressure. Regardless of other criteria in the design of the compressor, the ultimate factor is that the acid gas must arrive at the wellhead with sufficient pressure that it can be injected into the formation for disposal.

9.1 Calculation of Injection Profiles

The wellhead pressure at an injection well can be calculated as the sum of several contributions (Carroll and Lui, 1997):

$$\begin{aligned}\text{Wellhead pressure} = {} & \text{reservoir pressure} \\ & + \text{pressure drop due to formation porosity and permeability} \\ & + \text{pressure drop due to skin damage} \\ & + \text{pressure drop through the perforations} \\ & - \text{static head of tubing fluid} \\ & + \text{frictional pressure drop}\end{aligned} \tag{9.1}$$

For small acid gas injection schemes, the reservoir pressure and static head terms are the only ones of significance. In particular, it is assumed that the pressure drop due to friction is not important, although the design engineer is advised to review these factors in each case. Thus equation (9.1) reduces to:

$$\text{Wellhead pressure} = \text{reservoir pressure} - \text{static head of tubing fluid} \tag{9.1a}$$

In order to calculate the injection pressure, one integrates the differential hydrostatic equation from the reservoir conditions to the surface. The hydrostatic equation is:

$$\frac{dP}{dh} = -\rho g \tag{9.2}$$

where: dP/dh – pressure gradient, kPa/m
g – acceleration due to gravity, 9.81 m/s

9.1.1 Gases

Gases are compressible, that is, their density is a function of the temperature and the pressure. Thus when calculating the injection profile for a gas this fact must be accounted for.

9.1.1.1 Ideal Gas

The simplest model of gas behavior is the ideal gas. The density of an ideal gas is calculated as follows:

$$\rho = \frac{MP}{RT} \tag{9.3}$$

where: ρ – density, kg/m^3
M – molar mass, kg/kmol
P – pressure, kPa
R – universal gas constant, 8 314 m^3·Pa/kmol·K
T – absolute temperature, K

Substituting equation (9.3) into equation (9.2) yields the following expression:

$$\frac{dP}{dh} = -\frac{MP}{RT}g \tag{9.4}$$

Integrating this equation, assuming there is no temperature gradient, yields:

$$ln\,P = -\frac{Mgh}{RT} + C \tag{9.5}$$

where: C – integration constant
h – vertical depth

The integration constant is evaluated using the observation that the pressure is the reservoir pressure at the depth of the well. After some manipulation, this yields:

$$ln\,P - ln\,P_{res} = -\frac{Mg}{RT}(h_{res} - h) \tag{9.6}$$

where the subscript "res" indicates reservoir pressure and depth. This equation allows one to calculate the pressure at any point in the injection well.

To estimate the injection pressure (i.e., the wellhead pressure), substitute h = 0 (i.e., the surface) into the equation to obtain:

$$ln\,P_{inj} = ln\,P_{res} - \frac{Mg}{RT}h_{res} \tag{9.7}$$

where the subscript "inj" is the injection pressure.

Even when using SI units as outlined here, the reader is advised to be careful with the units. It is easy to make a mistake that can result in an error of several orders of magnitude.

9.1.1.2 Real Gas

A simple modification of the ideal gas law allows it to be used for real gases. This is the inclusion of the compressibility factor, z. equation (9.3) becomes:

$$\rho = \frac{MP}{zRT} \tag{9.8}$$

And substituting this into equation (9.2) yields:

$$\frac{dP}{dh} = -\frac{MP}{zRT}g \tag{9.9}$$

Although this equation looks relatively simple, it is complicated by the fact that the compressibility factor is a function of the temperature and the pressure.

If we assume the compressibility is constant and equal to some average value and again assuming the injection is isothermal, after some manipulation the injection pressure can be calculated as follows:

$$ln\,P_{inj} = ln\,P_{res} - \frac{Mg}{\langle z\rangle RT}h_{res} \tag{9.10}$$

where the angular brackets indicate the average compressibility.

In the derivation of these equations, some simplifying assumptions are made. First, it was assumed that the injection was isothermal. This is unlikely. Due to the geothermal gradient, the fluid heats up as it goes down the well. Second, it was assumed the compressibility was a constant. An advanced method should account for both of these effects.

Example

9.1 Calculate the injection pressure for a 50-50 mixture of hydrogen sulfide and carbon dioxide. The reservoir is at a pressure of 2000 kPa, is at a depth of 750 m, and is isothermal at 20°C. Assume the acid gas will remain gaseous throughout the injection. Further assume: (a) the gas is an ideal gas and (b) the gas is a real gas with properties described by the generalized compressibility chart. Take the properties of hydrogen sulfide and carbon dioxide from table 2.1.

Answer: The molar mass of the mixture is calculated as follows:

$$M = 0.5(34.082) + 0.5\,(44.010) = 39.046\ kg/kmol$$

a) From equation (9.7):

$$\begin{aligned} ln\,P_{inj} &= ln\,P_{res} - \frac{Mg}{RT}h_{res} \\ &= ln(2000) - \frac{(39.082)(9.81)}{(8314)(273.15+20)}(750) \\ &= 7.600\,902 - 0.117\,980 \\ &= 7.482\,922 \end{aligned}$$

$$P_{inj} = 1777\ kPa$$

Therefore the estimated injection pressure for the ideal gas case is 1777 kPa.

b) The pseudocritical properties for the mixture are:

$$pT_C = 0.5(373.5) + 0.5(304.2) = 338.9 \text{ K}$$
$$pP_C = 0.5(8963) + 0.5(7382) = 8173 \text{ kPa}$$

Calculate the reduced temperature:

$$T_R = \frac{20 + 273.15}{338.9} = 0.865$$

As a first approximation, assume the pressure is 2000 kPa. Calculate the reduced pressure:

$$P_R = \frac{2000}{8173} = 0.245$$

From the generalized compressibility chart this gives $z \approx 0.84$. From equation (9.10):

$$\begin{aligned} ln\, P_{inj} &= ln\, P_{res} - \frac{Mg}{\langle z \rangle RT} h_{res} \\ &= ln(2000) - \frac{(39.082)(9.81)}{(0.84)(8314)(273.15+20)}(750) \\ &= 7.600902 - 0.140463 \\ &= 7.460439 \end{aligned}$$
$$P_{inj} = 1738 \text{ kPa}$$

Now estimate the compressibility at the estimated bottom hole conditions:

$$P_R = \frac{1738}{8173} = 0.213$$

At these conditions $z \approx 0.88$. Therefore, the average values is 0.86. Repeating the calculation

$$
\begin{aligned}
ln\,P_{inj} &= ln\,P_{res} - \frac{Mg}{\langle z\rangle RT} h_{res} \\
&= ln(2000) - \frac{(39.082)(9.81)}{(0.86)(8314)(273.15+20)}(750) \\
&= 7.600902 - 0.137186 \\
&= 7.463716 \\
P_{inj} &= 1744 \text{ kPa}
\end{aligned}
$$

The estimated injection pressure is 1744 kPa. This is smaller than for the ideal gas because the density of the real gas is slightly larger than the ideal gas.

9.1.2 Liquids

Unlike gases, liquids are typically quite incompressible. That is, their densities can be assumed to be constant. The integration of the hydrostatic equation is simple. The result is:

$$P_{inj} - P_{res} = -\rho g h \tag{9.11}$$

Or rearranging slightly

$$P_{inj} = P_{res} - \rho g h_{res} \tag{9.12}$$

One caution when using this equation: It is possible that inserting the values for the parameters in this equation results in a negative injection pressure. Obviously, this cannot occur. Physically, this means that at some point in the injection well, the fluid begins to vaporize and there is a gas cap on the column of fluid.

Example

9.2 Estimate the injection pressure for a scheme where the acid gas is injected as a liquid. Assume the density is constant and equal to 775 kg/m^3. The reservoir pressure is 30 000 kPa and is at a depth of 2500 m.

Answer: Use equation (9.12):

$$
\begin{aligned}
P_{inj} &= 30\,000 - (750)(9.81)(2500)/1000 \\
&= 11\,600 \text{ kPa}
\end{aligned}
$$

Note the 1000 in the second term is to convert from Pa to kPa. The reader should verify that the units in this example are indeed correct.

9.1.3 Supercritical Fluids

Supercritical fluids are somewhat different – they have characteristics of both gases and liquids. The densities tend to be liquid-like, on the order of 200 to 300 kg/m^3; however, they can be less than or greater than this range. On the other hand, the densities are strong functions of the pressure and the temperature.

In order to estimate the injection pressure for a supercritical fluid, the hydrostatic equation must be carefully integrated – there are no short cuts.

However, the methods for calculating the density of a supercritical fluid are rather conventional. An equation of state or a corresponding state method can be used. They must be used with caution because the critical region is notorious as a region where the accuracy of density predictions is poor.

9.1.4 Friction

For most of the low-volume, liquid- or dense-phase injection schemes, it is sufficiently accurate to neglect the effect of fluid friction on the injection pressure. However, as we move to higher injection volumes, and thus higher velocities, this is no longer a good assumption. We must now import some of the methods from chap. 6 for estimating the effect of friction on the pressure.

9.1.5 AGIProfile

AGIProfile[1] is a software package for estimating acid gas injection profiles. This software is applicable to gases, liquids, or supercritical fluids. The density of the acid gas is calculated using the Peng-Robinson (1976) equation of state, with the option for using volume-shifting. The user can input a frictional pressure drop, but this is assumed to be constant throughout the injection well.

1. *AGIProfile* is copyright Gas Liquids Engineering, Ltd., Calgary, Alberta, CANADA.

Because of the rather complicated nature of the resulting equations, the injection equation is integrated numerically.

The temperature profile along the well is estimated via one of two methods: 1. Assumed to be linear and the fluid is assumed to be instantaneously at the temperature of the surroundings. 2. Obtained from a measured profile.

One of the major drawbacks to the current version of *AGIProfile* is that it does not independently determine the nature (i.e., the phase) of the acid gas. The user must tell the program what phase the user expects and then it is up to the user to verify this assumption. This is done by plotting the calculated profile on the phase envelope. This is also done to determine whether or not the injection profile intersects the phase envelope.

The software prints the integration diagnostics and typically the integration is completed without problem. Usually, difficulties in the integration can be interpreted as the injection profile intersecting the phase envelope or as an erroneous phase selection by the user. However, integration problems also occur near a critical point. Using the user input temperature profile also causes some difficulties in the integration, especially if the profile is unusual. Thus, employing the linear temperature profile is usually recommended, especially for preliminary designs.

Examples

9.3 Repeat Example 9.1 using *AGIProfile*. Furthermore, use the Peng-Robinson equation of state to calculate the density of the gas.

Answer: The following is the output from the *AGIProfile* run:

```
*****************************************
*               AGI Profile             *
* ACID GAS INJECTION PRESSURE CALCULATION *
*               Version 1.4             *
*             Copyright 1997            *
*      Gas Liquids Engineering Ltd.       *
*       #300, 2749 - 39 Avenue NE         *
*   Calgary, Alberta  CANADA   T1Y 4T8    *
* J.J. Carroll                 May  1999 *
*****************************************

RUN DATE: Oct. 20, 1999
---------

PROJECT: Example 9.3
```

WELL PROFILE:

Depth (m)	Pressure (kPa)	Temperature (deg C)	Density (kg/m**3)
750.0	2.0000E+03	2.0000E+01	3.7407E+01
712.5	1.9863E+03	2.0000E+01	3.7254E+01
675.0	1.9727E+03	2.0000E+01	3.6952E+01
637.5	1.9592E+03	2.0000E+01	3.6653E+01
600.0	1.9458E+03	2.0000E+01	3.6358E+01
562.5	1.9326E+03	2.0000E+01	3.6066E+01
525.0	1.9194E+03	2.0000E+01	3.5776E+01
487.5	1.9064E+03	2.0000E+01	3.5490E+01
450.0	1.8934E+03	2.0000E+01	3.5207E+01
412.5	1.8806E+03	2.0000E+01	3.4927E+01
375.0	1.8678E+03	2.0000E+01	3.4650E+01
337.5	1.8552E+03	2.0000E+01	3.4375E+01
300.0	1.8426E+03	2.0000E+01	3.4104E+01
262.5	1.8302E+03	2.0000E+01	3.3835E+01
225.0	1.8178E+03	2.0000E+01	3.3570E+01
187.5	1.8056E+03	2.0000E+01	3.3306E+01
150.0	1.7934E+03	2.0000E+01	3.3046E+01
112.5	1.7813E+03	2.0000E+01	3.2788E+01
75.0	1.7694E+03	2.0000E+01	3.2533E+01
37.5	1.7575E+03	2.0000E+01	3.2280E+01
.0	1.7457E+03	2.0000E+01	3.2030E+01

Estimated injection pressure = 1.7457E+03 kPa

Frictional pressure drop = 0.000E+00 kPa/m - input by user

STREAM DIAGNOSTICS:

DENSITY CORRELATION: Peng-Robinson equation of state
(SiPPS Version 2.0 – (C) J.J. Carroll, 1993)

SPECIFIED PHASE: gas - ** User should verify **

MIXTURE MOLAR MASS: 39.045 kg/kmol

ESTIMATED VISCOSITY:

Bottom hole conditions:	1.423E-05	Pa.s
	1.423E-02	centipoise
Surface conditions:	1.414E-05	Pa.s
	1.414E-02	centipoise
Approximate average:	1.419E-05	Pa.s
	1.419E-02	centipoise

DENSITY RANGE:

Maximum Density: 3.741E+01 kg/m**3
Minimum Density: 3.203E+01 kg/m**3
Approx. Average: 3.472E+01 kg/m**3

```
STREAM COMPOSITION          (mole %)    (wt %)

     CARBON DIOXIDE          50.000     56.358
     HYDROGEN SULFIDE        50.000     43.642

NTEGRATION DIAGNOSTICS:
-----------------------

  Maximum integration error: 9.814E-08 kPa/m
  Number of integration steps:  20
  Initial step size: 3.750E+01 m
  Maximum step size: 3.750E+01 m
  Minimum step size: 3.750E+01 m
  Step size halved    0 times
  Step size doubled   0 times

  Integration completed without step-size modification
```

The estimated injection pressure is 1746 kPa, which is comparable to those obtained in Example 9.1.

9.2 Effect of Hydrocarbons

The typical hydrocarbon impurity in acid gas is methane. Methane is lighter than the acid gas components, and thus the density of an acid gas mixture is reduced by the presence of methane. Even in a liquid mixture, the density is reduced by the presence of methane.

There is a second effect of the presence of methane in the injection gas. Methane, being more volatile than acid gas, tends to broaden the phase envelope. That is, the dew point pressures are significantly increased. The consequence of this is that it is now easier for the injection profile to intercept the phase envelope. In practical terms this means that presence of methane in the gas will tend to increase the likelihood that the acid gas will vaporize in the injection well.

Example

9.4 To demonstrate the effect of light hydrocarbons on the injection pressure, estimate the injection pressure for two acid mixtures:

	Mix 1	Mix 2
H_2S	20%	18%
CO_2	80%	78%
CH_4	0%	4%

The reservoir conditions are as follows: depth: 1525 m, pressure 15 000 kPa, and temperature 88°C. Assume the surface

(injection) temperature is 50°C. Calculate the injection profiles using *AGIProfile*.

Answer: The output from the two *AGIProfile* runs are given below. In summary, the estimated injection pressure for the mixture without methane is 9 439 kPa and this increases to 9 893 kPa for the mixture with methane – an increase of about 4.5%. The average density for the first mixture is 372 kg/m³ and it is only 343 kg/m³ for the second mixture.

```
*****************************************
*                                       *
*              AGI Profile              *
* ACID GAS INJECTION PRESSURE CALCULATION *
*                Version 1.4            *
*             Copyright 1997            *
*      Gas Liquids Engineering Ltd.     *
*       #300, 2749 - 39 Avenue NE       *
*   Calgary, Alberta  CANADA   T1Y 4T8  *
* J.J. Carroll                 May  1999 *
*****************************************

RUN DATE: Oct. 28, 2001
---------


PROJECT: Example 9.4 Mix 1
--------

WELL PROFILE:
-------------

        Depth       Pressure    Temperature      Density
         (m)         (kPa)        (deg C)       (kg/m**3)
        ------      ----------   -----------    -----------
        1525.0    1.5000E+04    8.8000E+01    3.7417E+02
        1448.8    1.4720E+04    8.6100E+01    3.7404E+02
        1372.5    1.4441E+04    8.4200E+01    3.7379E+02
        1296.3    1.4161E+04    8.2300E+01    3.7353E+02
        1220.0    1.3882E+04    8.0400E+01    3.7328E+02
        1143.8    1.3603E+04    7.8500E+01    3.7302E+02
        1067.5    1.3324E+04    7.6600E+01    3.7277E+02
         991.3    1.3045E+04    7.4700E+01    3.7252E+02
         915.0    1.2767E+04    7.2800E+01    3.7227E+02
         838.8    1.2489E+04    7.0900E+01    3.7203E+02
         762.5    1.2211E+04    6.9000E+01    3.7179E+02
         686.3    1.1933E+04    6.7100E+01    3.7155E+02
         610.0    1.1655E+04    6.5200E+01    3.7131E+02
         533.8    1.1377E+04    6.3300E+01    3.7108E+02
         457.5    1.1100E+04    6.1400E+01    3.7086E+02
         381.3    1.0823E+04    5.9500E+01    3.7064E+02
         305.0    1.0546E+04    5.7600E+01    3.7043E+02
```

```
          228.8    1.0269E+04    5.5700E+01    3.7023E+02
          152.5    9.9919E+03    5.3800E+01    3.7005E+02
           76.3    9.7152E+03    5.1900E+01    3.6988E+02
             .0    9.4387E+03    5.0000E+01    3.6973E+02

Estimated injection pressure =  9.4387E+03 kPa

Frictional pressure drop =  0.000E+00 kPa/m - input by user



 STREAM DIAGNOSTICS:
 -------------------

    DENSITY CORRELATION: Peng-Robinson equation of state -
                         volume shifted
                        (SiPPS Version 2.0 - (C)
                        J.J. Carroll, 1993)

    SPECIFIED PHASE: gas - ** User should verify **

    MIXTURE MOLAR MASS:  42.024 kg/kmol

    ESTIMATED VISCOSITY:
         Bottom hole conditions: 3.168E-05 Pa.s
                                 3.168E-02 centipoise
         Surface conditions:     2.966E-05 Pa.s
                                 2.966E-02 centipoise
         Approximate average:    3.067E-05 Pa.s
                                 3.067E-02 centipoise

    DENSITY RANGE:
         Maximum Density: 3.742E+02 kg/m**3
         Minimum Density: 3.697E+02 kg/m**3
         Approx. Average: 3.720E+02 kg/m**3

    STREAM COMPOSITION        (mole %)    (wt %)
         CARBON DIOXIDE        80.000     83.781
         HYDROGEN SULFIDE      20.000     16.219

 INTEGRATION DIAGNOSTICS:
 ------------------------

    Maximum integration error: 2.158E-05 kPa/m
    Number of integration steps:  20
    Initial step size: 7.625E+01 m
    Maximum step size: 7.625E+01 m
    Minimum step size: 7.625E+01 m
    Step size halved    0 times
    Step size doubled   0 times

    Integration completed without step-size modification
```

```
*****************************************
*                AGI Profile            *
* ACID GAS INJECTION PRESSURE CALCULATION *
*                Version 1.4            *
*             Copyright 1997            *
*      Gas Liquids Engineering Ltd.     *
*       #300, 2749 - 39 Avenue NE       *
*   Calgary, Alberta  CANADA   T1Y 4T8  *
* J.J. Carroll                May  1999 *
*****************************************
```

RUN DATE: Oct. 28, 2001

PROJECT: Example 9.4 Mix 2

WELL PROFILE:

Depth (m)	Pressure (kPa)	Temperature (deg C)	Density (kg/m**3)
1525.0	1.5000E+04	8.8000E+01	3.4662E+02
1448.8	1.4741E+04	8.6100E+01	3.4647E+02
1372.5	1.4482E+04	8.4200E+01	3.4616E+02
1296.3	1.4223E+04	8.2300E+01	3.4586E+02
1220.0	1.3965E+04	8.0400E+01	3.4554E+02
1143.8	1.3706E+04	7.8500E+01	3.4523E+02
1067.5	1.3448E+04	7.6600E+01	3.4491E+02
991.3	1.3191E+04	7.4700E+01	3.4459E+02
915.0	1.2933E+04	7.2800E+01	3.4427E+02
838.8	1.2676E+04	7.0900E+01	3.4394E+02
762.5	1.2419E+04	6.9000E+01	3.4361E+02
686.3	1.2162E+04	6.7100E+01	3.4327E+02
610.0	1.1906E+04	6.5200E+01	3.4293E+02
533.8	1.1649E+04	6.3300E+01	3.4259E+02
457.5	1.1393E+04	6.1400E+01	3.4224E+02
381.3	1.1138E+04	5.9500E+01	3.4188E+02
305.0	1.0882E+04	5.7600E+01	3.4151E+02
228.8	1.0627E+04	5.5700E+01	3.4114E+02
152.5	1.0372E+04	5.3800E+01	3.4076E+02
76.3	1.0118E+04	5.1900E+01	3.4037E+02
.0	9.8632E+03	5.0000E+01	3.3996E+02

Estimated injection pressure = 9.8632E+03 kPa

Frictional pressure drop = 0.000E+00 kPa/m - input by user

STREAM DIAGNOSTICS:

DENSITY CORRELATION: Peng-Robinson equation of state - volume shifted (SiPPS Version 2.0 – (C) J.J. Carroll, 1993)

```
   SPECIFIED PHASE: liquid - ** User should verify **

   MIXTURE MOLAR MASS:  41.104 kg/kmol

   ESTIMATED VISCOSITY:
        Bottom hole conditions: 3.012E-05 Pa.s
                                3.012E-02 centipoise
        Surface conditions:     2.798E-05 Pa.s
                                2.798E-02 centipoise
        Approximate average:    2.905E-05 Pa.s
                                2.905E-02 centipoise

   DENSITY RANGE:
        Maximum Density: 3.466E+02 kg/m**3
        Minimum Density: 3.400E+02 kg/m**3
        Approx. Average: 3.433E+02 kg/m**3

   STREAM COMPOSITION        (mole %)    (wt %)
        CARBON DIOXIDE        78.000     83.515
        HYDROGEN SULFIDE      18.000     14.924
        METHANE                4.000      1.561

INTEGRATION DIAGNOSTICS:
------------------------

   Maximum integration error: 1.506E-05 kPa/m
   Number of integration steps:  20
   Initial step size: 7.625E+01 m
   Maximum step size: 7.625E+01 m
   Minimum step size: 7.625E+01 m
   Step size halved    0 times
   Step size doubled   0 times

   Integration completed without step-size modification
```

9.3 Case Studies

In this section, a few existing injection wells will be examined. The calculated injection profiles are from *AGIProfile*.

9.3.1 Chevron Injection Wells

Complete details of acid gas injection schemes in the literature are rare. Lock (1997) gives details of two injection schemes operated by Chevron Canada Ltd. These are the most completely described schemes available in the open literature. Other schemes are described, but too much important information is omitted to do a reasonable job of calculating the profile.

9.3.1.1 *West Pembina*

From Lock (1997) the disposal well at the Chevron West Pembina site has a depth of 2800 m (9186 ft), and the composition of the acid gas injected is approximately 21.93% carbon dioxide, 77.17% hydrogen sulfide, and 0.90% methane (dry basis). Keushnig (1995) gives the reservoir pressure of 28.8 MPa (4177 psia). Lock (1997) gives this as "about 30 000 kPa" so the value from Keushnig (1995) will be used here. It was further estimated that the reservoir temperature was 110°C (230°F) and the injection temperature was 0°C (32°F).

Figure 9.1 shows the injection profile and the phase envelope for this case. This is a relatively simple case since the fluid does not change phase in the wellbore. The calculated injection pressure is 8770 kPa (1272 psia), which is about 17% larger than the value of 7446 kPa (1080 psia) given by Lock (1997).

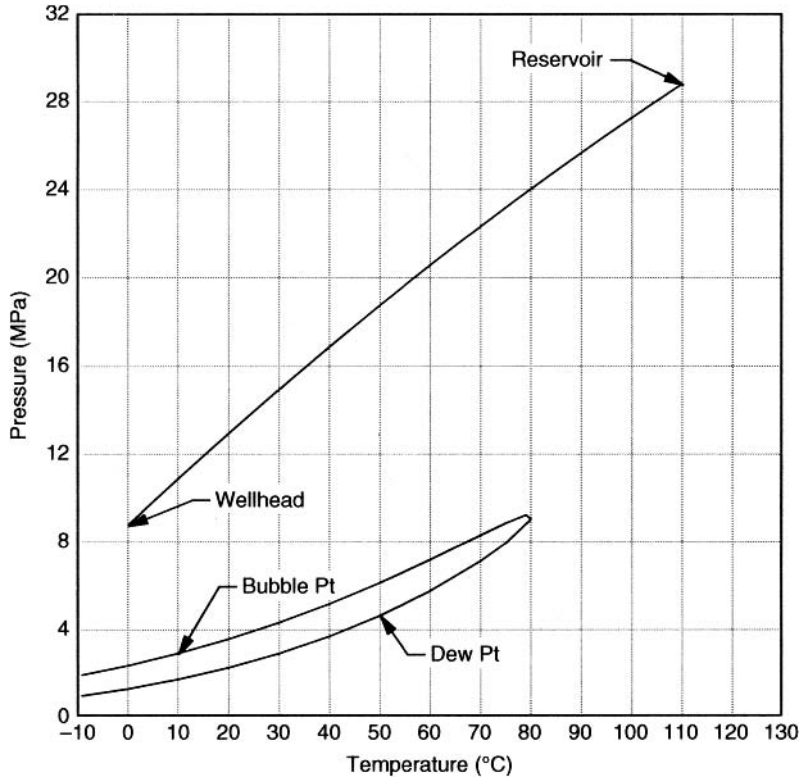

Figure 9.1 The calculated injection profile for the Chevron West Pembina Well.

Part of the reason for the higher than expected estimation of the injection pressure is because of the assumed reservoir temperature. If the reservoir is assumed to be 100°C (212°F), then the estimated injection pressure is 1211 psia (10% error) and at 90°C (194°F) it is 1150 psia (6% error). This demonstrates the strong effect of the temperature on these calculations.

Of course, another source of the error is that the volume-shifted Peng-Robinson equation of state may be in error by as much as 10 or 15%. Neglecting the additional terms in equation (5.1) also contributes to this error.

9.3.1.2 Acheson

From Lock (1997), the disposal well at the Chevron Acheson site has a depth of 1100 m (3610 ft) and the acid gas injected is 89.8% carbon dioxide and 10.2% hydrogen sulfide (dry basis). Keushnig (1995) gives the reservoir pressure of 9300 kPa (1349 psia) and this will be used here, although some of the other data in this paper are in conflict with those given by Lock (1997). It was further estimated that the reservoir temperature was 48°C (118°F) and the injection temperature was 0°C (32°F).

Using *AGIProfile*, the injection profile is calculated. The integration scheme has problems with this well indicating a potential problem – probably a phase change.

At reservoir conditions, the fluid is supercritical (density approximately 385 kg/m^3 or 24.0 lb/ft^3) and as we move up the injection well the fluid becomes a liquid (the pressure is greater than the bubble point pressure).

At a temperature of about 11°C (52°F) the injection profile intersects the phase envelope. From this point to the surface, the fluid remains in two phases. In this self-regulating system, any heat transfer from the surroundings to the fluid will condense or evaporate the liquid and thus the pressure will return to the equilibrium value.

Based on this calculation, for the first 250 m (820 ft), or so, in the well the mixture is two-phase. At greater depths the mixture has completely liquefied and remains liquid down to the reservoir.

According to this theory the injection pressure is estimated to be about 3 303 kPa (479 psia), which is in excellent agreement with the observation from the field that "the actual injection pressure upon start-up was only 3 500 kPa (508 psia) and remains at that level today" (Lock, 1997). Also according to this theory, the pressure will

remain steady at about 3 500 kPa, even though the reservoir pressure is increasing. According to the calculation, once the reservoir pressure reaches about 11 197 kPa (1624 psia), then the surface pressure should begin to rise. At that point the fluid will be liquid for the entire length of the well. This should also serve as a warning. Just because the wellhead pressure does not change over time (even over a fairly long period of time), one should not interpret this as "no problems" injecting into the reservoir.

The injection profile for this well is shown in figure 9.2. Notice how the injection profile intersects the phase envelope.

This well demonstrates two things clearly. First, phase equilibrium can play a significant role in calculating the injection pressure. Second, it shows that just because the wellhead pressure remains unchanged over a period of time does not mean that the operator can assume that there is no pressure build-up in the reservoir.

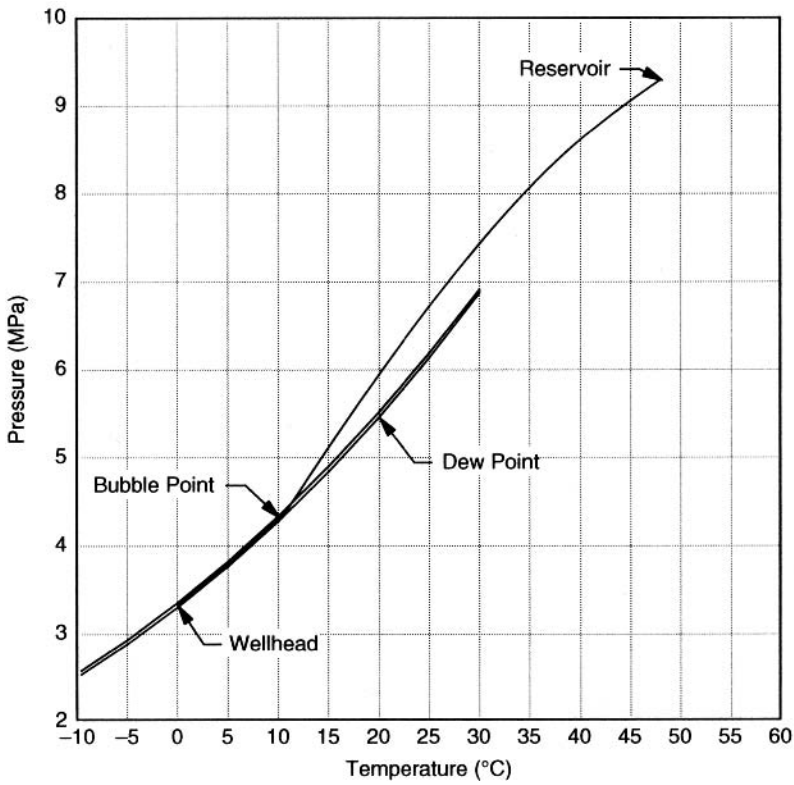

Figure 9.2 The calculated injection profile for the Chevron Acheson Well.

9.3.2 Anderson Puskwaskau

This well has a depth of 2682 m (8800 ft) and a reservoir pressure of 28 500 kPa (4134 psia) and temperature of 82°C (180°F). The composition of the acid gas injected has varied over time, but it is approximately 45% H_2S, 51% CO_2, and 4% CH_4. It was assumed that the wellhead temperature was 4.5°C (40°F). From *AGIProfile*, the injection pressure is estimated to 9240 kPa (1340 psia), which is in excellent agreement with the actual pressure of about 8480 to 8825 kPa (1230 to 1280 psia). This is an error of about 5 to 9%.

9.4 Other Software

AGIProfile was quite useful for many first generation injection schemes, but is probably not sufficient for the injection wells for larger projects. Other software has been developed such as *GLEWPro*. Wang and Carroll (2006) give many examples of the application of this software.

In addition there is other software available for modeling well flow but the user of these packages should ensure that they are applicable to acid gas mixtures. As we have seen, acid gas tends to have high density when compared to natural gas.

9.5 In Summary

One of the most important process parameters in acid gas injection is the wellhead pressure. Ultimately, this dictates the size of the compressor required. Methods were presented in this chapter to calculate the injection pressure. Note the density of the acid gas is an important parameter in these calculations.

References

Carroll, J.J. and D.W. Lui. 1997. Density, phase behavior keys to acid gas injection. *Oil & Gas J.* 95(25):63–72.

Keushnig, H. 1995. Hydrogen sulphide – If you don't like it put it back. *J. Can. Petrol. Tech.* 34(6):19–20.

Lock, B.W. 1997. Acid gas disposal a field perspective. 76th Annual GPA Convention, San Antonio, TX.

Peng, D.-Y. and D.B. Robinson. 1976. A new two-constant equation of state. *Ind. Eng. Chem. Fundment.* 15:59–64.

Wang. S. and J.J. Carroll. 2006. Model calculates acid gas injection profiles. *Oil & Gas J.* Sept. 4.

Appendix 9A Additional Examples

9A.1 Assuming that the Mix 1 in Example 9.4 is injected at a rate of 0.5 MMSCFD into a 27/9-inch tubing string (ID = 1.995 in). Estimate the pressure drop per unit length of pipe and estimate the effect of this pressure drop on the injection pressure.

Answer: The procedure follows that given in Chapter 7 for horizontal flow. First convert the volumetric flow rate to a molar flow rate:

$$\begin{aligned} n &= (0.5)(1.195 \times 106) \text{ this conversion is from Chapter 1} \\ &= 597\,500 \text{ mol/d} \\ &= 6.91551 \text{ mol/s} \end{aligned}$$

The molar mass of the mixture is:

$$\begin{aligned} M &= 0.20(34.082) + 0.80(44.101) \quad \text{Molar masses from} \\ &= 42.024 \text{ g/mol} \qquad\qquad\qquad\quad \text{Chapter 2} \end{aligned}$$

Using the mixture molar mass, convert to a mass flow rate:

$$\begin{aligned} m = (6.91551)(42.024) &= 290.62 \text{ g/s} \\ &= 0.29062 \text{ kg/s} \end{aligned}$$

Convert to the actual volumetric flow rate:

$$Q_{act} = 0.29062/370.2 = 7.850 \times 0^{-4} \text{ m}^3\text{/s}$$

Convert the ID from inches to meters: 1.995 in = 0.050673 m and then calculate the fluid velocity:

$$\begin{aligned} v &= 4Q_{act}/\pi D^2 = 4(7.850 \times 10^{-4})/\pi/(0.050673)^2 \\ &= 0.38925 \text{ m/s} \end{aligned}$$

Calculate the Reynolds number (note 0.031 cp = 0.031×10^{-3} Pa.s)

$$\begin{aligned} Re &= vD\rho/\mu \\ &= (0.38225)(370.2)(0.050673)/(0.031 \times 10^{-3}) \\ &= 231312 = 2.31312 \times 10^{+5} \end{aligned}$$

Calculate the relative roughness of the pipe using an absolute roughness of 0.045 mm:

$$\frac{\varepsilon}{D} = \frac{0.045 \times 10^{-3}}{0.050673} = 0.000\,888$$

From the friction factor chart, the estimated friction factor is 0.0052. Finally the pressure drop per unit length is

$$\frac{\Delta P}{\rho} = \frac{2\langle v\rangle^2 L f}{D}$$

$$= \frac{2(0.38925)^2(370.2)(0.0052)}{0.050673} = 11.5 \text{ Pa/m}$$

$$= 0.0115 \text{ kPa/m}$$

Substituting this into *AGIProfile* (output below) and the estimated injection pressure is 9449 kPa. This compares to 9438 kPa for the calculation without including friction. So in this case the frictional effect is negligible.

```
*****************************************
*              AGI Profile              *
* ACID GAS INJECTION PRESSURE CALCULATION *
*              Version 1.4              *
*            Copyright 1997             *
*      Gas Liquids Engineering Ltd.     *
*       #300, 2749 - 39 Avenue NE       *
*   Calgary, Alberta  CANADA   T1Y 4T8  *
* J.J. Carroll                 May  1999 *
*****************************************

RUN DATE: Oct. 28, 2004
---------

PROJECT: Example 9.1A
--------

WELL PROFILE:
-------------

        Depth       Pressure    Temperature      Density
         (m)         (kPa)        (deg C)      (kg/m**3)
        ------    ----------    -----------    ----------
        1525.0    1.5000E+04     8.8000E+01    3.7417E+02
        1448.8    1.4721E+04     8.6100E+01    3.7406E+02
        1372.5    1.4442E+04     8.4200E+01    3.7383E+02
        1296.3    1.4164E+04     8.2300E+01    3.7361E+02
        1220.0    1.3885E+04     8.0400E+01    3.7339E+02
        1143.8    1.3607E+04     7.8500E+01    3.7317E+02
        1067.5    1.3329E+04     7.6600E+01    3.7296E+02
         991.3    1.3051E+04     7.4700E+01    3.7275E+02
         915.0    1.2773E+04     7.2800E+01    3.7254E+02
         838.8    1.2496E+04     7.0900E+01    3.7235E+02
         762.5    1.2218E+04     6.9000E+01    3.7215E+02
         686.3    1.1941E+04     6.7100E+01    3.7197E+02
         610.0    1.1663E+04     6.5200E+01    3.7179E+02
```

533.8	1.1386E+04	6.3300E+01	3.7162E+02
457.5	1.1109E+04	6.1400E+01	3.7147E+02
381.3	1.0833E+04	5.9500E+01	3.7133E+02
305.0	1.0556E+04	5.7600E+01	3.7120E+02
228.8	1.0279E+04	5.5700E+01	3.7110E+02
152.5	1.0002E+04	5.3800E+01	3.7102E+02
76.3	9.7258E+03	5.1900E+01	3.7097E+02
.0	9.4491E+03	5.0000E+01	3.7097E+02

Estimated injection pressure = 9.4491E+03 kPa

Frictional pressure drop = 1.150E-02 kPa/m - input by user

STREAM DIAGNOSTICS:

DENSITY CORRELATION: Peng-Robinson equation of state - volume shifted (SiPPS Version 2.0 - (C) J.J. Carroll, 1993)

SPECIFIED PHASE: gas - ** User should verify **

MIXTURE MOLAR MASS: 42.024 kg/kmol

ESTIMATED VISCOSITY:

Bottom hole conditions:	3.168E-05	Pa.s
	3.168E-02	centipoise
Surface conditions:	2.974E-05	Pa.s
	2.974E-02	centipoise
Approximate average:	3.071E-05	Pa.s
	3.071E-02	centipoise

DENSITY RANGE:

Maximum Density:	3.742E+02	kg/m**3
Minimum Density:	3.710E+02	kg/m**3
Approx. Average:	3.726E+02	kg/m**3

STREAM COMPOSITION	(mole %)	(wt %)
CARBON DIOXIDE	80.000	83.781
HYDROGEN SULFIDE	20.000	16.219

INTEGRATION DIAGNOSTICS:

Maximum integration error: 1.988E-05 kPa/m
Number of integration steps: 20
Initial step size: 7.625E+01 m
Maximum step size: 7.625E+01 m
Minimum step size: 7.625E+01 m
Step size halved 0 times
Step size doubled 0 times

Integration completed without step-size modification

9A.2 Repeat example 9.4 for Mix 1 assuming an ideal gas.

Answer: First assume an average temperature (88 + 50)/2 = 69°C and take the molar mass from the previous example.

$$
\begin{aligned}
ln\,P_{inj} &= ln\,P_{res} - \frac{Mg}{RT}h_{res} \\
&= ln(15000) - \frac{(42.024)(9.81)}{(8314)(273.15+69)}(1525) \\
&= 9.615805 - 0.221009 \\
&= 9.394797 \\
P_{inj} &= 12\,025\ \text{kPa}
\end{aligned}
$$

This is significantly larger than the estimate from *AGIProfile,* which was 9 439 kPa. In this case the assumption of an ideal gas is inadequate.

This Page Intentionally Left Blank

10

Selection of Disposal Zone

The first step in the design of an acid gas injection scheme is probably the selection of a suitable reservoir for injection the acid gas. The selection of an appropriate injection zone is influenced by many factors.

There are three important considerations in the selection of an injection zone. They are: 1. Containment, 2. Injectivity, and 3. Interactions. A suitable injection zone should also be within a reasonable and economic distance from the compressor location. Large aquifers, depleted reservoirs, and zones that produce sour fluids can be suitable for use as an injection zone.

A depleted zone is particularly attractive because the main reservoir parameters, namely size and original pressure, are known. Thus, one can easily estimate how much gas can safely be injected.

If no suitable depleted zone or large aquifer is readily available near the sour gas plant, then disposal into a producing horizon is feasible because the amount of gas returned to the zone is usually a small fraction of the total gas in place.

10.1 Containment

The basic criterion for containment is that the injected fluid remains in the formation and does not seep to other formations,

or worse, to the surface. There are several sub-criteria in the selection of the injection zone and these are discussed in the section that follows.

The reservoir must contain the fluid for longer than the life of the project. However, it is unrealistic to expect that the gas will remain there forever.

10.1.1 Reservoir Capacity

Perhaps the first concern is the volume of the selected reservoir. Does it have the capacity to store the acid gas for the life of the project? The size of the potential disposal zone must be such to ensure that it will hold the injected gas over the life of the project.

In order to estimate the capacity of a selected reservoir, one needs to know the thickness and extent of the formation and its porosity. From the physical dimensions of the reservoir, one can calculate the volume of the rock, and multiplying this by the porosity gives the pore space, which is where the acid gas will be stored.

The gas is stored not only in the pore volume. Much of the gas will dissolve in the formation fluids, both hydrocarbon and water. Some of the CO_2 and H_2S will react with components in the reservoir and form new minerals – the so-called mineralization.

The most common cation in reservoir water is sodium (Na^+). Both sodium sulfide and sodium carbonate are soluble in water and thus do not provide a mechanism for sequestering the acid gas. Perhaps the next most common cation in the reservoir is calcium (Ca^{2+}). Carbon dioxide can react with the calcium ion and form one of many calcium carbonate minerals including calcite ($CaCO_3$). Calcium sulfide is not a very stable compound and readily decomposes and thus is not common on the earth. However, H_2S can react with other cations in the reservoir water and produce several sulfide minerals including pyrite.

In addition, the CO_2 and H_2S can react with minerals in the formation and transform them into different minerals.

10.1.2 Caprock

The caprock should be impermeable, which means it should have a permeability of about 1 nanodarcy (1×10^{-9} darcy) or less. In addition, one must examine the thickness, potential fracturing, and extent of the caprock to see if it will contain the acid gas.

One simple approach to verifying the caprock integrity is to inject into a formation that has held pressure for geological time.

10.1.3 Other Wells

In addition, it is important to know the integrity of all of the other wells that pass through the proposed injection zone. There may be dozens of wells that penetrate the zone and may be of unknown age and quality. These wells may provide a channel for the injected fluid to rise to higher zones or worse – to the surface.

In addition, common cement can be attacked by carbon dioxide. Thus all wells though the zone should be completed and, if necessary, abandoned using CO_2-resistant cement.

10.2 Injectivity

Another important factor in the selection of a disposal zone is the injectivity. Can the desired rate of acid gas be injected at down hole conditions? The injection rate is a function of the properties of the reservoir, notably the permeability, and the properties of the fluid, notably the viscosity. The injectivity can be estimated by doing an injection test.

The flow through the reservoir begins with Darcy's law, which is described in detail in many books on reservoir engineering (such as Craft and Hawkins, 1959). Clearly the results presented in this section are simplified, but they provide insights into the injection modeling for acid gas injection projects.

10.2.1 Liquid Phase

If the acid gas is injected in the liquid phase at injection conditions, then the injection of a test liquid, typically water, can be compared with that for the acid gas. This can be done using Darcy's law for an incompressible fluid in cylindrical coordinates.

$$q = C_1 \frac{2\pi k h (P_e - P_w)}{\mu \, ln(r_e/r_w)} \tag{10.1}$$

where: q – flow rate, Sm^3/day
C_1 – conversion factor
π – 3.141 59
k – permeability, darcies
h – thickness of the formation, m
P_e – pressure at external radius, kPa
P_w – pressure at wellbore, kPa
μ – fluid viscosity, cp
r_e – radial extent of reservoir, m
r_w – radius of wellbore, m

The conversion factor, C_1, is included to ensure that the units agree given the units specified for all of the other quantities in the equation and for the units specified above, C_1 = 14 700. By convention, r_e is usually set to 201 m or 600 ft for 16.2 hectare or 40 acre well spacing.

Comparing two fluids using Darcy's law and assuming the permeability is independent of the fluid, gives:

$$\frac{q_{AG}}{q_{test}} = \left(\frac{\mu_{test}}{\mu_{AG}}\right)\left(\frac{P_e - P_{w,AG}}{P_e - P_{w,test}}\right) \tag{10.2}$$

where the subscripts test refers to the test fluid and AG refers to the acid gas. Note, when the ratio of the flows is used, the r_e is eliminated from the relation.

Thus given the injection rate of the test fluid, say water, and its viscosity, and the bottom hole pressure, one can estimate the injection rate for the acid gas at a given bottom hole pressure, given the viscosity of the acid gas. Methods for calculating the viscosity of acid gas were given earlier, and the viscosity of water as a function of pressure and temperature is well known.

When water is used as the test fluid, the injectivity of acid gas will always be greater than the test fluid for a given pressure drop. The reason for this is that the viscosity of acid gas is less than that of water at the same conditions. Alternatively, for a given pressure drop, the injection rate for acid gas will always be great then the injection rate for water.

Example

10.1 An injection test is run using water as a test fluid. At a wellhead pressure of 700 kPa (100 psia), a water injection rate of 16 m^3/day

(100 bpd) is achieved. The reservoir is at a depth of 2500 m and has a pressure of 24.5 MPa and a temperature of 100°C. We wish to estimate the pressure drop from the well to the reservoir if we are to inject acid gas into this formation at a rate of 2850 Sm^3/day of hydrogen sulfide.

Answer: If the surface pressure for the water column is 700 kPa, or 0.7 MPa, then we can estimate the bottom hole pressure using the hydrostatic head equation (see Chapter 8). First, assume the density of water is 1000 kg/m^3.

$$\begin{aligned} P_w &= P_{inj} + \rho_{test}\, g\, h \\ &= 0.7 + (1000)(9.81)(2500)/10^6 \\ &= 25.225 \text{ MPa} \end{aligned}$$

the 10^6 in the denominator of the second term is to convert from Pa to MPa. At bottom hole conditions (100°C and 25.225 MPa), the density of water is 970 kg/m^3, so the average density is 985 kg/m^3 (Parry et al. 2000). Updating the bottom hole pressure calculation:

$$\begin{aligned} P_w &= P_{inj} + \rho_{test}\, g\, h \\ &= 0.7 + (985)(9.81)(2500)/10^6 \\ &= 24.857 \text{ MPa} \end{aligned}$$

Neglect this small change in pressure on the density and use this as the bottom hole pressure.

At reservoir conditions the viscosity of water is 0.290 cp (Parry et al. 2000). From figure 2.6 the viscosity of H_2S at reservoir conditions is 0.08 cp. From equation (10.2):

$$\frac{q_{AG}}{q_{test}} = \left(\frac{\mu_{test}}{\mu_{AG}}\right)\left(\frac{P_e - P_{w,AG}}{P_e - P_{w,test}}\right)$$

rearranging this equation slightly yields:

$$P_e - P_{w,AG} = \left(\frac{\mu_{AG}}{\mu_{test}}\right)\left(\frac{q_{AG}}{q_{test}}\right)\left(P_e - P_{w,test}\right)$$

$$P_e - P_{w,AG} = \left(\frac{0.08}{0.290}\right)\left(\frac{5.12}{16}\right)(24.5 - 24.857)$$
$$= -0.032 \text{ MPa}$$
$$= -32 \text{ kPa}$$

Therefore, the pressure drop from the well bore to the formation due to the flow through the porous media is 32 kPa (4.6 psia).

10.2.2 Gas Injection

If the acid gas is injected in the gas phase, then a gas injection test can be used. For the flow of a gas in a porous media in cylindrical coordinates, Darcy's law becomes:

$$q = C_2 \frac{2\pi k h T_b \left(P_e^2 - P_w^2\right)}{\mu z T_f P_b \ ln(r_e/r_w)} \tag{10.3}$$

where: q – flow rate in Sm^3/d
C_2 – conversion factor
z – average compressibility factor, unitless
T_f – average fluid temperature, K
T_b – standard temperature, 288.7 K
P_b – standard pressure, 101.325 kPa

All other symbols are the same as equation (10.1). As with equation (10.1), the values of C_2 are such that the units given in the above equation cancel out and for the units given, $C_2 = 23.145 \times 10^4$.

Next, comparing the injection of a test fluid to the injection of an acid gas mixture yields the following relation – if both injected fluids are in the gas phase.

$$\frac{q_{AG}}{q_{test}} = \left(\frac{\mu_{test}}{\mu_{AG}}\right)\left(\frac{z_{test}}{z_{AG}}\right)\left(\frac{P_e^2 - P_{w,AG}^2}{P_e^2 - P_{w,test}^2}\right) \tag{10.4}$$

Again, when the ratio of the flows is used, the r_e is eliminated from the relation. Therefore, given the injection rate for the test gas and the bottom hole pressure, we can estimate the injection rate for the acid gas mixture, in the gas phase, given the properties of the acid gas at

injection conditions. Nitrogen makes a good test fluid because the physical properties are well known over a wide range of temperatures and pressures.

Note there is a difference between the Darcy's law for a gas (a compressible fluid) and that for a liquid (an incompressible fluid). Thus, before doing an injection test, it is important to know whether the injected acid gas mixture is in the gas phase or in the liquid phase.

10.2.3 Fracturing

If very high pressure is required to inject the fluid, then the reservoir rock may fracture. Although this will improve the injectivity, it may result in containment issues (including fracturing the caprock). Fracturing the injection reservoir is prohibited by law in Alberta and probably in other jurisdictions as well.

10.2.4 Horizontal Wells

Most simple injection wells are vertical. If the injection rate is high, it may be necessary to use a horizontal well in order to improve the injectivity. The injection scheme at Sleipner in the North Sea, where 50 MMSCFD of CO_2 are injected, uses only a single horizontal injection well.

10.3 Interactions With Acid Gas

Tests will be conducted to ensure the acid gas is compatible with the reservoir rock and reservoir fluids. Adverse reactions could reduce injectivity with time, as the acid gas reacts with the formation rocks or the original fluid in the reservoir.

In general, this is not a significant problem for acid gas injection. One possible problem might arise if the reservoir fluid contains significant amounts of iron. The iron would react with the hydrogen sulfide to form sulfides of iron. The iron sulfide might then precipitate and plug the injection formation ultimately inhibiting the injection of the fluid.

As was noted earlier, mineralization of the acid gas components is not necessarily a bad thing. On the contrary, it may be an excellent mechanism to sequester the acid gas safely and permanently.

It is only a problem if the resulting reaction plugs the formation, particularly in the near-wellbore region and thus inhibits the injection process.

10.4 In Summary

The selection of an injection zone is probably the first stage in the design of an injection project. Without an acceptable reservoir, acid gas injection is not feasible. The selected zone must contain the injected fluid – the acid gas must not leak through the caprock, or via other wells that penetrate the zone. Furthermore, injection must be achieved without an excess injection pressure. Fracturing the reservoir may aid injection, but it probably should be avoided because of containment issues.

References

Craft, B.C. and M.F. Hawkins. 1959. *Applied Petroleum Reservoir Engineering*. Englewood Cliffs, NJ: Prentice-Hall.

Parry, W.T., J.C. Bellows, J.S. Gallagher, and A.H. Harvey. 2000. *ASME International Steam Tables for Industrial Use*. New York: ASME Press.

11

Health, Safety and The Environment

Clearly, one of the most important considerations in the design of an acid gas injection scheme is the safety of those operating the facility and the general public. Perhaps not less important is the protection of the environment.

Acid gas injection is promoted as a near-zero emission process that is environmentally friendly. And during steady operation that is in general the case. However, accidents can occur with the associated release of both hydrogen sulfide and carbon dioxide. It is important to understand the effects of these releases and to develop a plan to deal with them.

Much of the determination of HSE is dictated by local laws, and such laws vary from place to place. Thus what is presented in this chapter is often only guidelines, and the reader should consult local regulations for the most precise approach to emergency planning.

11.1 Hydrogen Sulfide

Hydrogen sulfide is a highly dangerous substance, and it deserves respect. Workers in an area with hydrogen sulfide present should

be trained to handle emergency situations – intuition is often a poor guide as to how to respond to an emergency.

11.1.1 Physiological Properties

At room conditions, hydrogen sulfide is a colorless gas that has a highly offensive odor. It has a density of about 1.33 kg/m^3, which is slightly larger than air. Thus it tends to accumulate in such low areas as ditches and the bottom of vessels.

Hydrogen sulfide has a characteristic "rotten egg" smell. The human olfactory is capable of detecting the presence of only a few parts per million (ppm) in the air, although some individuals can detect less than 1 ppm. Most humans can detect H_2S at levels much less than 10 ppm.

The primary route of exposure to H_2S is inhalation. Hydrogen sulfide is classified as a chemical asphyxiant. A single breath of H_2S at a concentration of 1000 ppm is sufficient to kill an individual. Prolonged exposure at 250 ppm levels can cause pulmonary edema (the lungs filling with fluid), which can lead to death. However, even at low concentrations (less than 10 ppm), H_2S may cause irritation of the eye and respiratory system (including the nose, mouth, and bronchial tubes). The effect of hydrogen sulfide can be exacerbated if the individual already suffers from such a pulmonary disease as asthma.

Although H_2S has a strong offensive odor, this should not be used as a guide to expose to this toxin. The olfactory quickly deadens to the smell of H_2S, making smell a somewhat unreliable test for exposure.

Hydrogen sulfide can also affect the eyes of an individual exposed to this toxin. Exposure to only 20 to 50 ppm for one hour may cause damage to the eye. Thus exposure to the eyes is to be avoided.

Typically, H_2S is not absorbed through the skin. However, contact with liquid H_2S may cause freeze burns due the heat loss with the rapid vaporization of the liquid. A similar, although not as large, effect can be obtained by wetting the skin with alcohol. The cooling felt is due to the absorption of heat during the vaporization of the alcohol.

11.1.2 Regulations

In Alberta, Canada, by law, workers may not be exposed to levels of H_2S which average more than 10 ppm over an eight-hour period. In addition, they may not be exposed to 15 ppm over any fifteen-minute

period during the working day. Finally, at no time should they be exposed to levels that exceed 20 ppm.

The US Occupational Safety and Health Administration (OSHA) permissible exposure limits for hydrogen sulfide is 10 ppm (time weighted average) for an eight-hour exposure and 15 ppm (short-term exposure limit). The transitional limits are 20 ppm (ceiling) and 50 ppm (peak – ten-minute exposure).

If work must be performed in an atmosphere high in H_2S, then the worker must wear breathing equipment. Air must be supplied, and the worker must wear a mask that covers the mouth, nose, and eyes. The mask must be under positive pressure such that any leak is from the mask to the atmosphere and not vice versa.

11.1.3 Other Considerations

Another potential problem with hydrogen sulfide is that it is combustible. The explosive limits for hydrogen sulfide are 4.3% to 46%. Within this range of concentration, ignition of the gas will cause an explosion.

11.2 Carbon Dioxide

The other significant component in the acid gas mixture, carbon dioxide, is more benign than hydrogen sulfide, but it is not without concern.

11.2.1 Physiological Properties

At room conditions, carbon dioxide is a colorless, odorless gas. At room conditions, it has a density of 1.84 kg/m^3, which is more dense than air.

In general, it is non-toxic, but if the concentrations reach levels beyond 2% it can cause physiological problems. Those of you familiar with the plight of the Apollo 13 space mission will recall that a build-up of carbon dioxide was making the astronauts ill and threatened to kill them. The chemical filtration system in the spacecraft was not removing a sufficient amount of CO_2. One of the many challenges of this flight was to repair the system for removing CO_2 from the space craft (see Lovell and Kluger, 1994).

Such conditions are rarely important in the production and processing of natural gas. However, precautions should be taken

when working in a confined space with an enriched CO_2 atmosphere, regardless of the source of the CO_2.

Carbon dioxide is included in the OSHA list of air contaminants. The OSHA permissible exposure limits for CO_2 are 5000 ppm or 9000 mg/m^3 TWA for an eight-hour exposure.

11.2.2 Climate Change

Carbon dioxide, and in particular emissions from man-made sources, has been implicated in the global climate change. This book is not the place to debate whether or not CO_2 is actually causing a change in the climate. However, the processes described in this book provide a potential solution to the CO_2 emission problem.

11.2.3 Other Considerations

Unlike H_2S, or natural gas for that matter, carbon dioxide is noncombustible. Therefore it poses neither a fire nor explosion hazard.

11.3 Emergency Planning

It is worth repeating that emergency planning and development is the subject of local legislation. What is provided here are some guidelines based on the Canadian experience. They do not represent the laws of any jurisdiction.

11.3.1 Accidental Releases

As was mentioned early, the biggest potential problem is the accidental release of acid gas due to equipment failure. This could be the release of acid gas from a ruptured pipeline or the blowout of an injection well. We can define two types of accidental releases: 1. Continuous leak and 2. A fixed volume leak.

A continuous leak is one where the leak is without bound. An example of this is a well blowout. The flow from the well continues unrestricted until the well is brought under control and shut in. In petroleum engineering terms this is absolute open flow (AOF). Thus the planning zones should be based on the AOF.

It is common for a well to blow out during the drilling of said well. However, this is not the problem for an acid gas injection well,

unless it has been drilled into a sour zone. The problem is a blow-out after injection has begun with the associated release.

Unfortunately, it is difficult to do a well flow test on an injection well and thus the standard test to estimate AOF is difficult to perform. A suitable well flow model should be used to model the AOF of the injection well. Some safety factor can be used to increase this flow rate based on the uncertainty of the available models.

GLEWPro, which was discussed briefly in Chapter 9, can be used to model the AOF for acid gas injection wells. In this case, the surface pressure is set to atmospheric and the flow rate can be calculated. Furthermore, as a worst case scenario, the flow can be assumed to be isothermal at the reservoir temperature.

A fixed volume leak, on the other hand, is where only a certain amount of fluid is released and then the leak can be contained.

An example of a fixed-volume leak is a ruptured pipeline. Once the pipeline breaks, it must be isolated using emergency shut down valves. Thus, only the volume contained in the pipeline will leak, perhaps slightly more until the emergency procedures are activated and completed.

When specifying potential leaks, once should always consider the worst case. For example, when calculating the volume of fluid contained in a pipeline one should use the design pressure, which is always larger than the normal operating pressure, and the ambient temperature (i.e., the lowest temperature experienced by the pipeline). Also, one should assume that the entire pipeline is at these conditions. The high pressure and low temperature will result in the calculations of the largest mass in the pipeline, which in turn translates into the largest potential leak.

11.3.2 Planning Zones

There are two planning zones:

1. Exclusion Zone: No human habitation is permitted within this zone. This would typically be 100 to 1000 m on either side of the equipment but may be larger depending upon the jurisdiction.
2. Emergency Planning Zone (EPZ): People are allowed to reside in this zone, but a emergency plan must be established to handle an accidental release.

People can live within the EPZ, but they must be well informed of the situation and this begins with the initiation of the project – the public should be informed from the outset. From that point, there must be continual consultation with the public. This may include emergency drills. Furthermore, there must be a system for contacting them in case of an emergency. This would include an automated phone call out system, which must log the result (i) answered by human, (ii) answered by machine, or (iii) no answer.

There are several considerations when establishing the planning zones. The most important consideration is the type of human habitation. These may be broken down simply as follows: 1. Uninhabited, 2. Rural (family farms with limited number of inhabitants and possibly livestock), 3. Town or village (limited number of residents and permanent structures, say 500), and 4. City (more inhabitants than a town or village).

Once the potential leak has been established, these levels of human habitation are used to establish the two planning zones. Based on the design of the injection scheme, the design engineer should then establish the exclusion and the planning zones.

Example release levels may be as follows:

Level 1:

- Release volume of less than 300 Sm^3 of H_2S
- Release rate of less than 0.3 Sm^3/s of H_2S

Level 2:

- Release volume between 300 and 2000 Sm^3 of H_2S
- Release rate between 0.3 and 2.0 Sm^3/s of H_2S

Level 3:

- Release volume between 2000 and 6000 Sm^3 of H_2S
- Release rate between 2.0 and 6.0 Sm^3/s of H_2S

Level 4:

- Release volume greater than 6000 Sm^3 of H_2S
- Release rate greater than 6.0 Sm^3/s of H_2S

Note there is a release rate based on a fixed volume leak and a continuous leak.

Thus, based on these release levels we can further establish the planning zones. Example exclusion zones may be as follows:

Level 1: 100 m

Level 2: 100 m for individual buildings, 500 m for urban center

Level 3: 100 m for individual buildings, 1000 m for rural development, and 1500 m for urban center

Level 4: By written agreement with those within the planning zone (minimum Level 3)

The size of the planning zones is also established based on the potential leak and may be several kilometers from the equipment depending upon the size of the leak and the level of human habitation.

Example

11.1 For an acid gas injection well with 4.5 inch tubing and wall thickness of 0.271 in, estimate the AOF. The well has a depth of 4000 m and the temperature is 120°C and the pressure is 550 bar. Assume the flow is isothermal. The composition of the acid gas is: H_2S: 70.71%, CO_2: 28.29%, and methane: 1.00%.

Answer: Using the *GLEWPro* software, the full output is given below. The AOF is 4.792 MMSCFD (136×10^3 Sm^3/d). Converting this to the values given in the text yields:

$$136 \times 10^3 \text{ Sm/d} \times \frac{\text{day}}{24\,\text{hour}} \times \frac{\text{hour}}{60\,\text{min}} \times \frac{\text{min}}{60\,\text{sec}} = 1.57\ \text{Sm}^3/\text{s}$$

Thus the AOF is 1.57 Sm^3/s, which would put this in a Level 2 category.

Note that in much of the tubing string the acid gas remains in the liquid phase, but at the surface it flashes to the gas phase.

AOF

Calculation Routine

Flow rate and Profiles

Data and Calculation Requirements

Fluid Component Fractions

Component Name	Mole Fraction
H_2S	0.7071
CO_2	0.2829
Methane	0.0100

Size of Well Tube

Data Name	Value	Unit
Depth	4	km
Outer Diameter	4.5	inch
Wall Thickness	0.271	inch
Wall Roughness	0.0018	inch

Flowing Setpoints

Data Name	Value	Unit
Well Head Pressure	1.01325	bar
Bottom Hole Pressure	550	bar

Temperature Profile of Flowing Fluid

Data Name	Value	Unit
Well Head Flowing Temperature	120	C
Bottom Hole Flowing Temperature	120	C

Calculation Results and Profile

Result Summary

Data Name	Value	Unit
Flow Direction	Production; Flow up	
Flow Rate	4.792	MMSCFD
Well Head Pressure	1.01325	bar
Bottom Hole Pressure	550	bar
Well Head Flowing Temperature	248	F
Bottom Hole Flowing Temperature	248	F

Well Profile

No	Depth m	Pres bar	Temp C	Dens kg/m^3	Visco cP	Speed m/s	Vapor Mass %	Water Mass %	Cond Mass %
1	0.00	1.01	120.0	1.14	0.01743	82.029	100.00	0.00	0.00
2	200.00	298.62	120.0	587.21	0.05923	0.159	0.00	0.00	100.00
3	400.00	310.28	120.0	598.41	0.06099	0.156	0.00	0.00	100.00
4	600.00	322.15	120.0	609.14	0.06271	0.154	0.00	0.00	100.00
5	800.00	334.22	120.0	619.42	0.0644	0.151	0.00	0.00	100.00
6	1000.00	346.50	120.0	629.30	0.06606	0.149	0.00	0.00	100.00
7	1200.00	358.96	120.0	638.79	0.06769	0.147	0.00	0.00	100.00
8	1400.00	371.60	120.0	647.93	0.06929	0.145	0.00	0.00	100.00
9	1600.00	384.42	120.0	656.73	0.07086	0.143	0.00	0.00	100.00
10	1800.00	397.41	120.0	665.22	0.0724	0.141	0.00	0.00	100.00
11	2000.00	410.56	120.0	673.42	0.07391	0.139	0.00	0.00	100.00
12	2200.00	423.87	120.0	681.34	0.0754	0.137	0.00	0.00	100.00
13	2400.00	437.34	120.0	689.01	0.07686	0.136	0.00	0.00	100.00
14	2600.00	450.95	120.0	696.43	0.0783	0.134	0.00	0.00	100.00
15	2800.00	464.70	120.0	703.62	0.07971	0.133	0.00	0.00	100.00
16	3000.00	478.59	120.0	710.60	0.0811	0.132	0.00	0.00	100.00
17	3200.00	492.62	120.0	717.36	0.08247	0.131	0.00	0.00	100.00
18	3400.00	506.78	120.0	723.94	0.08382	0.129	0.00	0.00	100.00
19	3600.00	521.06	120.0	730.32	0.08514	0.128	0.00	0.00	100.00
20	3800.00	535.47	120.0	736.54	0.08644	0.127	0.00	0.00	100.00
21	4000.00	550.00	120.0	742.58	0.08773	0.126	0.00	0.00	100.00

Example

11.2 Estimate the leak volume for a 4 inch Schedule 80 pipeline (ID = 1.939 in = 49.251 mm) with a length of 2 km. The conditions within the pipeline are 5°C and 7000 kPa (70 bar). The composition of the acid gas is: 25% H_2S, 74% CO_2, 1% methane

Answer: The properties of the fluid are calculated using *AQUAlibrium* and are as follows: density: 903 kg/m^3 and molar mass: 41.248 kg/kmol. Use simple geometry to calculate the volume of the pipe:

$$V = \frac{\pi}{4} d^2 L = \frac{\pi}{4}\left(\frac{49.251}{1000}\right)^2 (2 \times 2000) = 7.62\ \text{m}^3$$

Next estimate the mass of gas in the pipe:

$$m = 901\ \text{kg/m}^3 \times 7.62\ \text{m}^3 = 6866\ \text{kg}$$

Convert this mass to moles:

$$n = \frac{6866\ \text{kg}}{41.248\ \text{kg/kmol}} = 166.5\ \text{kmol}$$

And from the composition, the moles of H_2S are

$$n_{H_2S} = 166.5\ \text{kmol} \times 0.25 = 41.6\ \text{kmol}\ H_2S$$

Finally, convert this to standard volume using the conversion factor given in Chapter 1:

$$Q_{H_2S} = \frac{41.6\ \text{kmol}\ H_2S}{42.21\text{kmol}/1000\ \text{Sm}^3} = 0.99 \times 1000\ \text{Sm}^3 = 990\ \text{Sm}^3\ H_2S$$

So the leak volume is 990 Sm of H_2S would be in the Level 2 category given above.

11.3.3 Other Considerations

In addition to those factors noted above, there are some other factors that are important if a leak occurs. These are discussed briefly in this section.

11.3.3.1 Sour vs. Acid Gas

As discussed above, the release volumes and rates were based on the amount of hydrogen sulfide released. It matters not whether the H_2S is from sour gas or acid gas. Perhaps some special consideration should be given to the release of acid gas.

11.3.3.2 Wind

None of the discussion above mentioned either the prevailing winds or the current winds. Clearly, the winds have an effect on the direction of the dispersion of the leak and perhaps should have some effect on designating the planning zones.

Perhaps some consideration should be given to an urban center that lies outside the standard planning zones, but is downwind based on the prevailing winds in the area.

11.3.3.3 Carbon Dioxide

Again, all of the discussion of planning zones above are based on H_2S release. A release of carbon dioxide can have significant consequences as well.

First, CO_2 is heavier than air and thus any leak will tend to settle near the earth until it has had the time to diffuse away. Since molecular diffusion is a relatively slow process, this may take some time to occur.

An important example of the consequences of a large CO_2 release occurred in 1986. Lake Nyos is a crater lake in Cameroon in west central Africa. In 1986, this lake belched a large cloud of carbon dioxide that settle in the region around the lake. More than 1500 people and 3000 head of livestock were killed in the CO_2 blanket.

11.3.3.4 Sensitive Areas

Once again, in the above discussion there is no mention of such sensitive environmental areas as World Heritage Sites, national parks, habitat for endangered species, etc. Clearly, all of these locations deserve special consideration in the environmental design of an injection scheme.

References

Lovell, J. and J. Kluger. 1994. *Apollo 13*. New York: Simon & Schuster, Inc. (Orig. pub. as *Lost Moon*.)

OSHA. *Occupational Safety and Health Standards. Z Toxic and Hazardous Substances*. 2009. http://www.osha.gov/pls/oshaweb/owadisp.show_document?p_table=STANDARDS&p_id=9991

12

Capital Costs

In this chapter some approximate capital costs are presented in order to make a preliminary analysis of the cost of an acid gas injection scheme. The information in this chapter comes from a combination of the author's experience and published cost data [such as Ulrich and Vasudevan (2004)]. Some additional cost information was taken from Louie (2009). The cost data presented in this chapter are budget costs, ±25% (and perhaps not even that accurate).

Many factors affect the capital cost of equipment. These include: 1. Location (and in particular variation in labor costs), 2. Onshore vs. offshore, 3. Materials. None of these factors are included in the cost information presented here. Furthermore, costs presented here are in 2009 dollars.

12.1 Compression

Depending upon the size of the injection scheme, the compressor may be a reciprocating or centrifugal compressor. The approach

to costing these machines is slightly different. However, we begin with the scaling law for cost estimates. Mathematically, this is:

$$\frac{\text{cost}_2}{\text{cost}_1} = \left(\frac{\text{size}_2}{\text{size}_1}\right)^n \tag{12.1}$$

where n is the scaling factor and, for compressors, the size is the compression power.

Why use the power as the scaling factor? Why not use flow rate or discharge pressure or compression ratio? From equation (6.8) it can be seen that the power best embodies all of the design parameters for a compressor.

12.1.1 Reciprocating Compressor

There is plenty of experience with small reciprocating compressors for this service. Therefore, we have a pretty good understanding of the cost of these machines. The common rule of thumb for the cost of a reciprocating compressor is $1000 per hp for carbon steel construction. This can be multiplied by a material factor of between 3 and 4 to account for the use of 316L stainless steel. A larger factor is required if more exotic material is specified.

This rule of thumb translates into n = 1 in equation (12.1). Furthermore, from my personal files, table 12.1 presents the cost of a small reciprocating compressor. Substituting this into equation (12.1) gives the following scaling equation:

$$\text{cost}_2 = \$3{,}750{,}000\left(\frac{\text{power}_2}{750}\right) \tag{12.2}$$

where: cost_2 – US dollars (2007)
power_2 – kW

or equivalently:

$$\text{cost}_2 = \$3{,}750{,}000\left(\frac{\text{power}_2}{1000}\right) \tag{12.3}$$

where: cost_2 – US dollars (2007)
power_2 – horsepower

Table 12.1 Comparison between a small reciprocating compression and a larger centrifugal compressor.

Small Reciprocating	**Large Centrifugal**
• 1000 hp (750 kW)	• 10 MW (13,500 hp)
• 3.5 MMSCFD	• 100 MMSCFD
• electric drive	• gas turbine drive
• appropriate materials	• appropriate materials
$3.75 million (2007)	**$27.5 million (2007)**

12.1.2 Centrifugal

There are only a few centrifugal acid gas compressors installed in the world today (and note acid gas is the key word). Therefore, there is significantly less confidence in the prediction for centrifugal machines than for the reciprocating machines.

Experience with reciprocating machines for other applications (sweet gas for example) indicates that the scaling factor is about 0.9. Thus, these machine do not quite scale directly with the required power. Table 12.1 lists an example centrifugal compressor. This is an estimate from one of the projects in my files. Using the scaling factor and this cost estimate gives:

$$\text{cost}_2 = \$27,500,000\left(\frac{\text{power}_2}{10}\right)^{0.9} \tag{12.4}$$

where: cost_2 – US dollars (2007)
power_2 – MW

12.2 Pipeline

The scaling factor for pipeline cost is a combination of the diameter of the pipe and then length of the line.

Pipeline costs are approximately $2000 to $3000 per diameter mm per kilometer in length ($80,000 to $125,000 per diameter inch per mile). Shorter pipeline lengths tend to be on the higher end and longer lines on the lower end (Louie, 2009).

12.3 Wells

The cost of drilling and completing injection wells depends on many factors, including the depth of the well, the location, etc. However, the cost of drilling most wells in North America is approximate $1000 (US) per m. However, this can range from $500 to $3000 or more.

Another factor in the costing of an injection well is the choice to use an existing well versus drilling a new well. It may be cheaper to work over an existing well and recomplete in the target zone than to drill a new well. However, it is very important that the re-used well is suitable for high sour service.

Example

12.1 Estimate the cost for an acid gas injection scheme with the following characteristics:

Acid Gas:	1 MMSCFD 49.8% H_2S, 48.2% CO_2, balance hydrocarbons
Compressor:	250 hp = 185 kW
Pipeline:	Length: 1.75 km
	Diameter: 2 inch (50.8 mm)
Well:	Depth: 2500 m

Answer: The estimated costs break down as follows:

Compressor:	$\text{cost}_2 = \$3,750,000\left(\frac{185}{750}\right) = \$925,000$
Pipeline:	cost = $3000/mm/km × 1.75 km × 50.8 mm = $267,000
Well:	cost = 2500 m × $1000/m = $2,500,000

The total cost of this scheme is about $3.7 million.

If necessary a small sour dehydration unit for this application would cost approximately an additional $250,000.

The costing of sulfur recovery units is outside the scope of this book. However, the acid gas injection scheme described would produce approximately 20 tonne/d of sulfur and the capital cost of such a sulfur plant (including tail gas clean up) would be about $8 million.

Note, if the acid gas contain only 30% H_2S, this would be equivalent to about 11 tonne/d. The cost of the injection scheme would remain unchanged to an order of magnitude approximation (the required horsepower for the compressor would change a little and hence the cost would change). However, the cost of the sulfur plant would be less, because it would be processing tones of sulfur.

In addition, there are many factors to be considered. For example, transport of the sulfur, storage of the sulfur, and H_2S enrichment (if needed). Thus it is difficult to make a simple comparison between AGI and a sulfur plant.

12.4 In Summary

In this section some techniques are presented to estimate the capital cost associated with an acid gas injection scheme. The author provides no guarantees for the cost data presented. These values are very approximate and should be used with some caution.

References

Louie, J. 2009. Learnings from CO_2 miscible floods provides design guidelines for CO_2 sequestration. 1st International Acid Gas Injection Symposium, Calgary, AB.

Ulrich, G.D. and Vasudevan, P.T. 2004 edition. *Chemical Engineering Process Design and Economics. A Practical Guide.* Durham, NH: Process Publishing.

This Page Intentionally Left Blank

13

Additional Topics

This chapter presents some miscellaneous topics and some summary of the previous chapters in the book. Some of these topics would be appended to other chapters, but they cover more than a single topic.

13.1 Rules of Thumb

In the preceding chapters, details were presented for estimating the physical properties of acid gas, and procedures were presented for designing the equipment required. Note that in this section some of the conversions are not exact because of the approximate nature of the information presented. Although some of the rules of thumb presented in this section are general in nature, the reader is wise to apply them only to acid gas systems.

13.1.1 Physical Properties

The following are some rules of thumb for the physical properties of compressed acid gas:

1. Pure CO_2 at 10°C and 7 MPa (50°F and 1000 psia) has a density of 900 kg/m^3 (56 lb/ft^3) and a viscosity 0.09 mPa•s (0.09 cp)

2. Acid gas at (50°F and 1000 psia) has a density of about 800 kg/m^3 (50 lb/ft^3) and a viscosity 0.1 mPa•s (0.1 cp)
3. The properties of acid gas are sensitive to the pressure and temperature
4. For comparison, water at (50°F and 1000 psia) is 1000 kg/m^3 and 1.3 mPa•s (62.6 lb/ft^3 and 1.3 cp)

Using these rules of thumb, the standard flow rates can be converted in to actual flow rates. For example, a flow rate of 28 × 10^3 Sm^3/d (1 MMSCFD) of acid gas is equivalent to about 40 L[act]/min (10 USgal[act]/min) at 10°C and 7 MPa (50°F and 1000 psia).

13.1.2 Water Content

The water content diagram of an acid gas mixture has two characteristic shapes: 1. A minimum in the water content, and 2. Liquefaction of the acid gas – the liquefied acid gas holds more water than the gas at similar pressures. Both can be used to reduce the water content of an acid gas stream using compression and cooling alone.

The presence of a liquid water phase leads to concerns about corrosion. Acid gas without free water is not corrosive to common carbon steels.

13.1.3 Hydrates

As for hydrates in mixtures of acid gas, we have the following rules of thumb:

1. When operating at temperatures greater than 30°C (85°F) hydrates are not a problem.
2. Below 30°C (85°F) hydrate pressure is a function of the temperature, composition, and water content.
3. For water content greater than about 250 lb/MMSCF, hydrate pressure is independent of the water content.

13.1.4 Compression

The following rules of thumb apply to acid gas mixtures. However, some of them are based on general rules for any compressor design.

1. Avoid condensation of the acid gas on the inter-stage. Use a minimum 5°C (9°F) offset from the acid gas dew point
2. If possible, design for maximum water knock-out using compression and cooling alone. At 50°C (120°F) inter-stage this corresponds to about (500 to 900 pisa) for the penultimate stage discharge (note the previous point)
3. Interstage cooling with air at 50°C (120°F) in North American and up to 65°C (150°F) in warmer climates
   a. Cooling with water can reduce the interstage temperature, but be wary of hydrate formation and acid gas condensation
4. Maximum discharge temperature of 150°C (300°F), but in some cases it can be up to 180°C (350°F) – never greater than 180°C
5. For acid gas k, the ratio of the heat capacities ranges from about 1.28 to 1.32 at 50°C (120°F).
6. Small reciprocating compressors have efficiencies of about 85%.

It is important to operate the compressor the way it was designed. Deviating from the design can result in operating problems including: 1. Condensation of acid gas on the interstage, 2. Hydrate formation, and 3. Not achieving optimum water knockout, which may result in the formation of a corrosive water phase.

13.1.5 Pipelines

The following provide quick estimates of the pressure drop for acid gas flow. In both of these cases the acid gas in the pipeline is in the liquid phase and thus has a relatively high density. The properties used for these calculations are those given in the previous section.

> Acid gas at a flow rate of 28×10^3 Sm^3/d (1 MMSCFD) compressed to 7 MPa (1000 psia) and cooled to 10°C (50°F) the pressure drop is about 0.08 psi/100 ft for 2-in Schedule 80
>
> By comparison, acid gas with a flow of 2.8×10^6 Sm^3/d (100 MMSCFD) compressed to 7 MPa (1000 psia) and cooled

to 10°C (50°F) the pressure drop is about 0.6 psi/100 ft for 8-in Schedule 80

For 1.6 km (1 mile) of pipeline:

- 2-in schedule 80 contains 108 ft^3[act]
- 4-in schedule 80 contains ft^3[act]
- 8-in schedule 80 contains 1621 ft^3[act]

13.1.6 Reservoir

The general guidelines for selecting a zone into which the acid gas is to be injected are:

1. Containment
   a. Volume to hold injected fluid
   b. Caprock to seal reservoir
   c. Integrity of all wells penetrating the zone
2. Injectivity
3. Negative interactions

Details for each of these three criteria are given in Chapter 10.

13.2 Graphical Summary

The detailed approached to designing an injection scheme was presented in this book. Here an example is presented in a graphical manner showing all of the pieces of the injection scheme and how they fit in the pressure-temperature plane and on the water content diagram.

13.2.1 Pressure-Temperature

Figure 13.1 shows the process summary for an acid gas injection scheme on a pressure-temperature plot. The composition of the acid gas used to generate this and the next plot is: H_2S 75 mol% and CO_2 25% (on a water-free basis).

The first step in the design of an AGI scheme is to build the phase envelope, which is shown in figure 13.1. For this case the pressure at the sandface (approximately the reservoir pressure) is 24 MPa

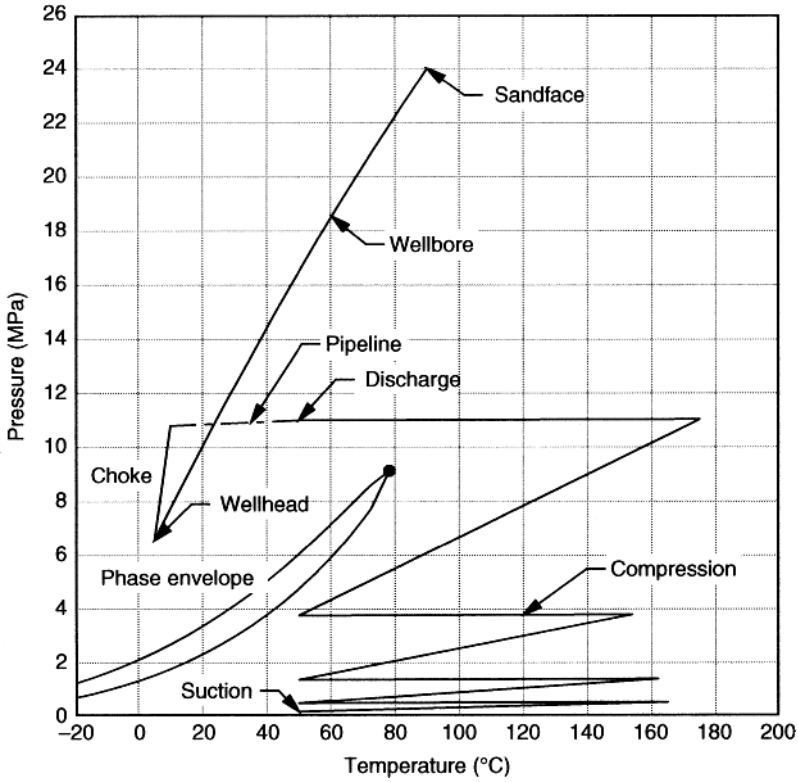

Figure 13.1 Acid gas injection summary on a pressure-temperature plot.

and the temperature is 90°C. The ground temperature at the surface is 5°C. The well profile was calculated using these inputs and the methods described in Chapter 9. From this analysis the estimated wellhead pressure is about 6.6 MPa.

Next comes the design of the compressor. Using a target discharge pressure of 8 MPa (6.6 MPa plus a 20% margin of safety) and examining the water knockout, which will be discussed next, we arrive at a discharge pressure of 11 MPa. It may seem unusual to design to 11 MPa when the well calculation indicates that only 6.6 MPa is required. This is done to ensure that we can achieve injection – it would be dreadful if the designed scheme cannot achieve the actual injection pressure. Also, over compression can be used to reduce the water content to a sufficient level that a dehydration unit is not required.

For this case, the compressor is four stage with interstage cooling to 50°C. Note that for each stage there is sufficient offset from the phase envelop ensuring that the acid gas will not liquefy in the interstage coolers. The discharge temperatures exceed the 150°C guideline, but are never greater than 175°C.

Next, the compressed acid gas is transported via pipeline to the injection well. Figure 13.1 shows the fluid cooling to ground temperature and a small amount of pressure drop.

At the wellhead there is a choke valve, and the fluid pressure drops to the actual injection pressure. There is a Joule-Thomson temperature drop associated with this pressure drop, but because the acid gas is in the liquid phase, the temperature drop is quite small.

Finally, the fluid enters the well where it warms because of the geothermal gradient, and the pressure increases largely because of the hydrostatic head of the fluid.

The entire process is shown graphically in figure 13.1. This plot looks complicated at first glance, but by following the various process paths, the reader should be able to understand the process.

13.2.2 Water Content

Next, consider the water content of the acid gas, which is shown in figure 13.2. Also shown on this plot is the compression of the acid gas and the changing water content as it is compressed. Examining the water content curve, in order to minimize the water in the stream the pressure should be between about 3 to 4.5 MPa. In this range of pressures the water content will be less than 4 g/Sm^3. In this design the third stage discharge pressure is set to about 3.75 MPa.

At the suction conditions, 50°C and 200 kPa, the water content is about 48 g/Sm^3. Through the first stage of compression and cooling, the water content is reduced to slightly less than 20 g/Sm^3. Thus for every standard cubic meter of gas compressed, about 28 g of water is produced. For example, compressing 50×10^3 Sm^3/d results in a water flow of about 0.97 kg/min.

Similarly, compression and cooling through the second stage knocks out about 12 g of water per Sm^3 and the third stage about 4 g/Sm^3.

Through the final stage of compression and the after cooler, the water content remains unchanged, about 3.65 g/Sm^3, and liquid water does not form and there is no need for a scrubber on the discharge. At 50°C and 11 MPa the stream can hold 13.5 g/Sm^3 and thus is well under saturated.

13.2.3 Operation

Plant operators are trained to operate the plant in an efficient manner. Typically, they are not engineers and thus may not understand all of the subtle behavior just described. However, it is important to operate an injection scheme the way it was designed.

On cool days, particularly in the winter, it may be possible to cool the interstage to temperatures lower than 50°C. However, if the interstage is cooled to 40°C or less than condensation of the acid gas will occur on the discharge from the third stage. This can be seen from figure 13.1. This liquid acid gas will be sent with the condensed water and will cause problems with the system.

From figure 13.2 it can be demonstrated why adjusting the compressor can affect the operation. The operator in the field may conclude that since only 7 MPa is required to achieve injection, why

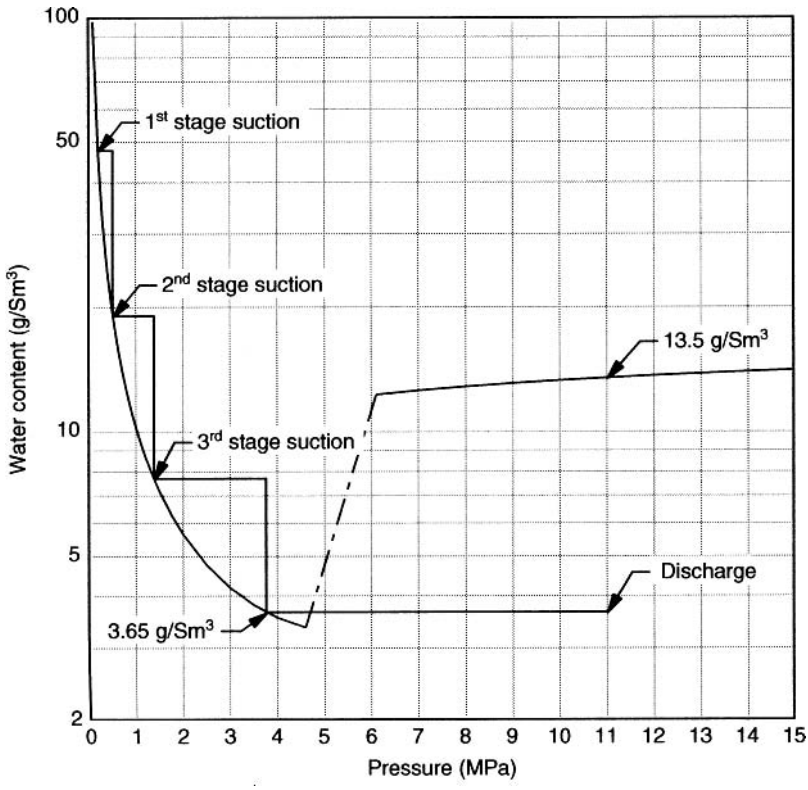

Figure 13.2 Water content of an acid gas mixture at 50°C showing the water knockout.

compress to 11 MPa? The cost of compression can be reduced if the gas is only compressed to 7 MPa. This will result in lower pressures through the compression. The discharge pressure might be reduced to between 2 and 3 MPa. This will result in significantly less water knockout and may ultimate result in the formation of a liquid water phase or hydrates.

These examples demonstrate why it is important to operate the compressor the way it is designed. Otherwise, process problems may result.

13.2.4 Summary

These two plots give an excellent graphical representation of the injection process and are quite useful in building the final design.

The complete design of the compressor is an exchange between the two figures. However, the ultimate design comes in conjunction with the compressor manufacturer and its ability to supply a machine that best fits the optimum design.

13.3 The Three Types of Gas

In the introduction to this book, three types of gas were presented: sweet, sour, and acid gas. The definitions for these types were presented in chapter 1 and will not be repeated here. However, differences in the behavior of these three types of gases will be presented and in addition an example will be presented.

Table 13.1 provides a brief comparison of the three types of gases.

13.3.1 Example Gases

Table 13.2 gives the composition for four gas mixture 1. Sweet (and, in this case, CO_2-free), 2. Sour, 3. Very Sour (the combined H_2S plus CO_2 is 40 mol%), and 4. Acid Gas. When the terms are capitalized, then they refer to the gas mixtures listed in table 13.2. When they are not capitalized, they refer to these types of gases in the general sense.

First consider the non-aqueous phase equilibria for the four mixtures. The phase envelopes for the Very Sour Gas and the Acid Gas are shown in figure 13.3.

The estimated critical points for the four mixtures are listed in table 13.3. These critical points are specifically for the mixtures in

Table 13.1 A qualitative comparison of sweet, sour, and acid gases.

	Sweet Gas	**Sour Gas**	**Acid Gas**
Flammability	Very High	Very High	H_2S – High CO_2 – Non-flam.
Toxicity	Low	High	H_2S – Very High CO_2 – Very Low
Corrosivity (in the presence of water)	CO_2-free – Low CO_2 present – High	High	High
Odor	None	Rotten Eggs	H_2S – Rotten Eggs CO_2 – None
Color	Colorless	Colorless	Colorless

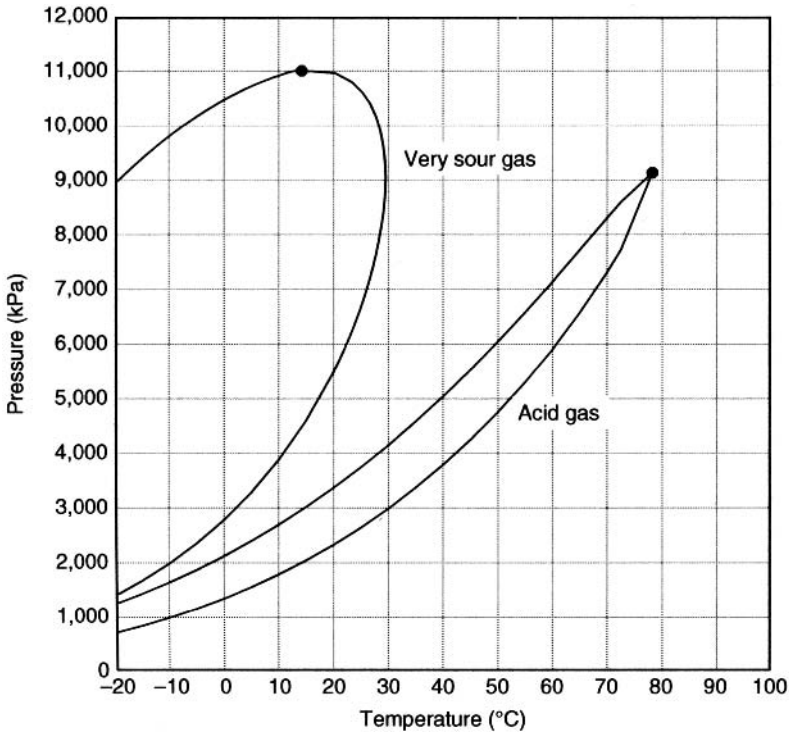

Figure 13.3 Phase envelopes for an acid gas mixture and a sour gas mixture (compositions given in table 13.2).

Table 13.2 The composition of four gases: sweet (CO_2-free), sour, very sour, and acid gas (mole fraction).

	Sweet	Sour	Very Sour	Acid Gas
H_2S	0.0000	0.0375	0.3750	0.7500
CO_2	0.0000	0.0125	0.1250	0.2500
Methane	0.9000	0.8550	0.4500	0.0000
Ethane	0.0500	0.0475	0.0250	0.0000
Propane	0.0250	0.0238	0.0125	0.0000
Isobutane	0.0130	0.0124	0.0065	0.0000
n-Butane	0.0120	0.0113	0.0060	0.0000

Table 13.3 Estimated critical points for the four mixtures in table 13.2.

Mixture	Critical Temperature (°C)	Critical Pressure (kPa)
Sweet	–53.5	7207
Sour	–47.5	7574
Very Sour	14.2	11003
Acid Gas	78.2	9135

table 13.2 and are not general for all mixtures of this type. Note that the critical points for the Sweet and Sour Gas are significantly less than –20°C and thus are off scale in figure 13.2.

Figure 13.4 shows the water content at 50°C for the four gas mixtures with compositions given in table 13.2. The Acid Gas mixture shows one of the two characteristic shapes; in this case, the acid gas liquefies and there is an increase in the water cornet from the gas phase to the liquids phase. The other three mixtures do not liquefy at this temperature and thus are continuous curves.

On the scale shown in figure 13.4 there is very little difference between the Sweet gas and the Sour gas. Both show a continual decrease in the water content with increasing pressure (at least up

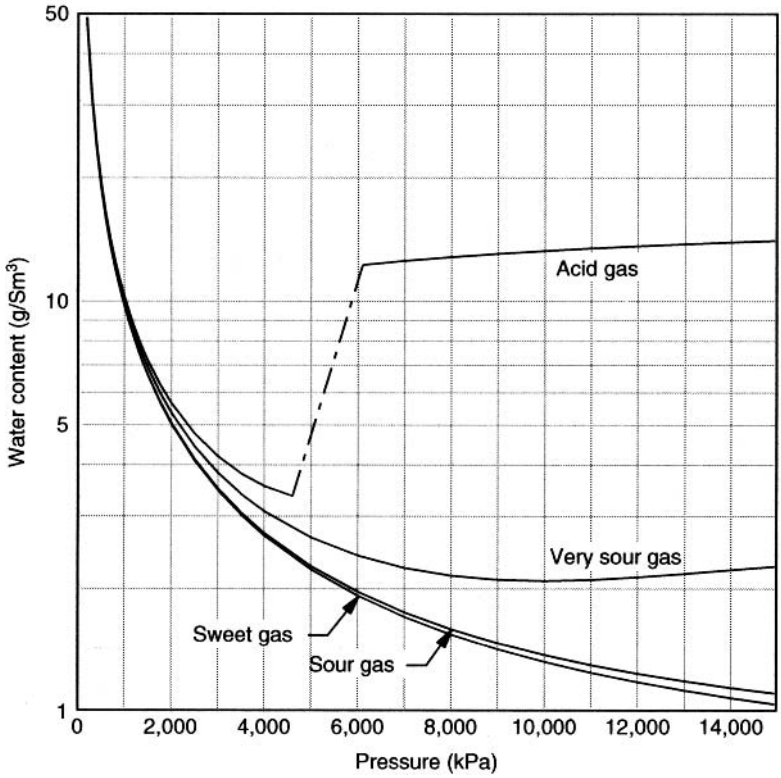

Figure 13.4 Water content of four mixtures at 50°C (compositions given in table 13.2).

to 15 000 kPa). Even at 15 000 kPa, the difference is only about 10%. The Very Sour gas mixture begins to show significant differences from the Sweet and Sour streams at about 2500 kPa (roughly 350 psia). At this pressure the difference is about 10%. As the pressure increases from that point the differences become larger.

The Very Sour gas mixture shows a very shallow minimum at about 10 000 kPa. Unfortunately, this minimum is too shallow to use compression and cooling aloe to dehydrate this stream – a technique which is very useful for acid gas mixtures.

This Page Intentionally Left Blank

Index

This Page Intentionally Left Blank

Also of Interest

Check out these forthcoming related titles coming soon from Scrivener Publishing

Advanced Petroleum Reservoir Simulation, by Rafiqul Islam, S. Hossein Mousavizadegan, Shabbir Mustafiz, and Jamal Abou-Kassem, April 2010, ISBN 9780470625811. The most up-to-date practices, processes, and technologies for petroleum reservoir simulations.

The Greening of Petroleum Operations, by Rafiqul Islam, June 2010, ISBN 9780470625903. A breakthrough treatment of one of the most difficult and sought-after subjects of the modern era: sustainable energy.

Energy Storage: A New Approach, by Ralph Zito, July 2010, ISBN 9780470625910. Exploring the potential of reversible concentrations cells, the author of this groundbreaking volume reveals new technologies to solve the global crisis of energy storage.

Formulas and Calculations for Drilling Engineers, by Robello Samuel, September 2010, ISBN 9780470625996. The only book every drilling engineer must have, with all of the formulas and calculations that the engineer uses in the field.

Ethics in Engineering, by James Speight and Russell Foote, December 2010, ISBN 9780470626023. Covers the most thought-provoking ethical questions in engineering.

Zero-Waste Engineering, by Rafiqul Islam, February 2011, ISBN 9780470626047. In this controvercial new volume, the author explores the question of zero-waste engineering and how it can be done, efficiently and profitably.

Fundamentals of LNG Plant Design, by Saeid Mokhatab, David Messersmith, Walter Sonne, and Kamal Shah, August 2011. The only book of its kind, detailing LNG plant design, as the world turns more and more to LNG for its energy needs.

Flow Assurance, by Boyun Guo and Rafiqul Islam, September 2011, ISBN 9780470626085. Comprehensive and state-of-the-art guide to flow assurance in the petroleum industry.